Carbon, nitrogen and phosphorus cycling in a tropical montane forest in Ecuador under environmental change: Isotopic and stoichiometric assessments

Zur Erlangung des akademischen Grades eines
DOKTORS DER NATURWISSENSCHAFTEN (Dr. rer. nat.)
von der KIT-Fakultät für
Bauingenieur-, Geo- und Umweltwissenschaften des
Karlsruher Instituts für Technologie (KIT)
genehmigte

DISSERTATION

von

Pablo Armando Alvarez Figueroa

Tag der mündlichen Prüfung: 11.11.2026

Referent: Prof. Dr. Wolfgang Wilcke
Korreferent: Prof. Dr. Karsten Kalbitz

Karlsruhe (2026)

Contents

Contents II
Acknowledgments V
Summary VI
Zusammenfassung VII
List of tables VIII
List of figures XI
List of abbreviations XIX
A. Summarizing overview 1
1. Introduction 1
2. Materials and methods 4
2.1. Study area and field sampling 4
2.2. Chemical analyses 7
2.3. Stable isotope measurements 7
2.4. Calculations and statistical analysis 8
3. Results and discussion 10
3.1. Carbon isotope composition of DOM (Section B) 10
3.2. Nitrogen isotope composition of TDN (Section C) 10
3.3. Long-term DOM composition and stoichiometry (Section D) 11
3.4. Synthesis: bringing the three approaches together 12
3.5. Uncertainties or limitations 13
4. General conclusions 15
5. Author contributions 17
6. References 18
B. $\delta^{13}C$ values of DOM 25
1. Abstract 26
2. Introduction 27
3. Material and methods 29
3.1. Study Area 29
3.2. Field sampling 30
3.3. Chemical Analyses 32
3.4. Calculations and statistical evaluation 33
4. Results 34
5. Discussion 41
5.1. Seasonality of the $\delta^{13}C$ values of DOM 41

5.2. $\delta^{13}C$ values of DOM in aboveground ecosystem solutions 42
5.3. $\delta^{13}C$ values of DOM in belowground ecosystem solutions 43
5.4. $\delta^{13}C$ values of DOM in streamflow 45
5.5. Relationship between $\delta^{13}C$ values and TOC/DON ratios of DOM 46
5.6. Environmental Implications 46
6. Acknowledgments 47
7. Supporting information 48
8. References 51
C. $\delta^{15}N$ values of total dissolved nitrogen 60
1. Abstract 61
2. Introduction 63
3. Material and methods 66
3.1. Study Site 66
3.2. Field sampling 66
3.3. Chemical Analyses 68
3.4. Calculations and statistical evaluation 69
4. Results 70
5. Discussion 77
5.1. Temporal variation in the $\delta^{15}N$ values of total dissolved nitrogen in rainfall 77
5.2. Change in the $\delta^{15}N$ values of total dissolved nitrogen from rainfall to litter leachate 78
5.3. Change of the $\delta^{15}N$ values of total dissolved nitrogen from litter leachate to topsoil solution 81
5.4. Change in the $\delta^{15}N$ values of total dissolved nitrogen from topsoil solution to streamflow 82
5.5. Temporal variation in the $\delta^{15}N$ values of ecosystem solutions 83
6. Conclusions 84
7. Acknowledgments 85
8. Supporting Information 86
9. References 90
D. Long-term trends of DOM and its stoichiometric ratios 100
1. Abstract 101
2. Introduction 102
3. Materials and methods 105
3.1. Study site 105
3.2. Field sampling 105
3.3. Chemical analyses 106

3.4. Stable isotope ratios 107
3.5. Calculations and statistical evaluation 107
4. Results 108
5. Discussion 117
5.1. Temporal trends in DON and DOP concentrations and fluxes and DOC/DON and DOC/DOP ratios of DOM 117
5.2. Temporal trend in DON/DOP ratios of DOM in ecosystem solutions 119
5.3. Relationship between the $\delta^{13}C$ and $\delta^{15}N$ values in solid phases of the ecosystem and dissolved organic matter 120
6. Conclusions 121
7. Acknowledgments 122
8. Supporting information 124
9. References 140
E. Appendix 148

Acknowledgments

I would like to express my gratitude to everyone who accompanied and supported me throughout this work.

First, I am deeply indebted to Wolfgang Wilcke for his guidance, his continuous feedback, and his steady support and confidence in me during all these years. I am equally grateful to my co-authors, Andre Velescu, Kerstin Pierick, and Jürgen Homeier, for sharing their knowledge and their data and for their careful reading of the manuscripts.

I gratefully acknowledge the funding that made this research possible. I thank the German Research Foundation (DFG) for funding the long-term research in Ecuador (FOR 402, FOR 816, PAK 823-825, and the Research Unit FOR 2730, RESPECT). I received a four-year doctoral scholarship from the Secretary of Higher Education, Science, Technology and Innovation of Ecuador (SENESCYT, Grant No. CA07-000439-2018), which I gratefully acknowledge.

I thank the Ecuadorian Ministry of the Environment for granting the research permits, and Naturaleza y Cultura Internacional (NCI) in Loja for providing access to the study area and to the research station. I am grateful to Felix Matt and Jörg Zeilinger for their support at the research station, and to José Luis Peña and Jimmy Alexander Villalta for their dedicated work as field technicians.

This thesis rests on a long-term record built by many hands. I thank J. Boy, K. Fleischbein, R. Goller, M. Meyer-Grünefeldt, M. Sequeira, H. Wullaert, S. Yasin, and the many undergraduate students who contributed to the data acquisition during parts of the observation period. I also thank Tobias Fabian and Lukas Lorenz for their support in the laboratory, and Uli Hensler, Martin Schwarz, and Jaime García for their help during the field sampling campaigns.

I am thankful to all my colleagues in the Soil Science Group of the Institute of Geography and Geoecology for the shared work, the discussions, and the good moments. I thank in particular Bastian Bayer, Stefan Merseburger, José Ledesma, Sophia Leimer, Svenja Stock, Sara Kimmig, and above all Nuria Basdediós, from whom I learned so much. I am also grateful to the administrative staff for their kind help with every task.

My thanks also go to the friends I made in Karlsruhe during my stay, for their encouragement and for making these years brighter.

Finally, my deepest gratitude goes to my family for their unconditional support, and above all to my mother. Without them, none of this would have been possible.

Summary

Dissolved organic matter (DOM) couples the carbon (C), nitrogen (N), and phosphorus (P) cycles of forest ecosystems and contributes to the export of these elements with the stream. As a mobile and partly bioavailable fraction of soil organic matter, DOM is highly susceptible to environmental change, yet its element and isotope composition and its response to environmental change remain little studied in tropical montane forests. The forests on the rim of the Amazon basin in south Ecuador have been exposed to rising atmospheric N deposition from Amazonian biomass burning, a continuous dust-derived P input, more frequent warm days, and drier conditions over the past 25 years.

I assessed DOM along the water path through a tropical montane forest, from rainfall via throughfall, stemflow, litter leachate, and mineral soil solutions to streamflow, with three complementary approaches: the C isotope composition of DOM, the N isotope composition of the total dissolved N (TDN), both during four years (2013-2016), and the trends of the dissolved organic N (DON) and dissolved organic P (DOP) concentrations, fluxes, and stoichiometric DOC, DON and DOP ratios during 25 years (1998-2023).

The $\delta^{13}C$ values of DOM were highest in rainfall and decreased via throughfall and stemflow to litter leachate, because isotopically light hydrophobic compounds were leached from the leaves and the bark. The $\delta^{13}C$ values of DOM increased in the mineral soil solutions, where roots and root exudates contributed DOM and the isotopically light fraction was preferentially sorbed and mineralized. Because the $\delta^{13}C$ values and the C/N ratios of DOM were not consistently related, these two measures provided independent information.

The $\delta^{15}N$ values of TDN identified the N sources and sinks. The canopy retained isotopically heavy N and leached isotopically lighter nitrate and DON. Consequently, throughfall was N-isotopically lighter than rainfall. The $\delta^{15}N$ values of TDN then increased toward litter leachate because of the leaching of isotopically heavy DON. In the mineral topsoil solution the $\delta^{15}N$ values of TDN decreased relative to the litter leachate because DON and ammonium were retained and nitrate added. With increasing soil depth toward streamflow the $\delta^{15}N$ values of TDN increased again because of the loss of isotopically light N by denitrification.

Over the 25 years, the DON and DOP concentrations and fluxes increased and the DOC/DON and DOC/DOP ratios decreased in all ecosystem solutions but DOP was not detected in rainfall, the mineral soil solutions and streamflow with our method. This indicated a progressive enrichment of N and P in DOM. Nitrogen was increasingly exported with streamflow, while P was retained within the forest. The $\delta^{13}C$ and $\delta^{15}N$ values increased in parallel in the solid-phase organic matter, reflecting a coupled C and N turnover, but varied independently in DOM.

Taken together, the three approaches elucidated the sources, sinks and transformations of DOC and TDN along the water path through the forest and reflected the environmental change of the past 25 years. The C and N cycles were less closely coupled in the dissolved phase than in the solid phase. The forest appeared to be drifting toward an emerging N saturation, with N increasingly exported and P retained. I found that combining the three approaches revealed a development that no single tracer could have shown alone.

Zusammenfassung

Gelöste organische Substanz (DOM) koppelt den Kohlenstoff- (C), Stickstoff- (N) und Phosphorkreislauf von Waldökosystemen und trägt sie mit dem Abfluss aus. Als mobiler, teilweise bioverfügbarer Anteil der organischen Bodensubstanz reagiert DOM sensibel auf Umweltveränderungen. Dennoch sind Zusammensetzung und Verhalten in tropischen Bergwäldern kaum erforscht. Die Wälder am Rande des Amazonasbeckens im Süden Ecuadors waren einem steigenden Stickstoffeintrag aus dem Verbrennen von Amazonas-Biomasse, einem stetigen Phosphoreintrag durch Staub, häufigeren warmen Tagen und zunehmend trockenen Bedingungen ausgesetzt.

Ich untersuchte DOM entlang des Wasserpfads vom Freilandniederschlag über Kronendurchlass, Stammabfluss, Streusickerwasser und die Bodenlösung des Mineralbodens bis zum Bachabfluss mittels dreier komplementärer Ansätze: der Kohlenstoffisotopenzusammensetzung der DOM und der Stickstoffisotopenzusammensetzung des gesamten gelösten Stickstoffs (TDN), jeweils über vier Jahre (2013–2016), sowie der zeitlichen Entwicklung der Konzentrationen, Frachten und stöchiometrischen Verhältnisse von DOC, gelöstem organischem N (DON) und gelöstem organischem P (DOP) über 25 Jahre (1998–2023).

Die $\delta^{13}C$-Werte waren im Freilandniederschlag am höchsten und nahmen zum Streusickerwasser ab, da isotopisch leichte Verbindungen aus Blättern und Rinde gelöst wurden. Sie nahmen in der Bodenlösung des Mineralbodens zu, wo Wurzeln und Wurzelexsudate zur DOM beitrugen, während die isotopisch leichtere Fraktion bevorzugt sorbiert und mineralisiert wurde. Da $\delta^{13}C$-Werte und C/N-Verhältnisse der DOM nicht konsistent zusammenhingen, lieferten beide Messungen unabhängige Informationen.

Die $\delta^{15}N$-Werte des TDN identifizierten Stickstoffquellen und -senken. Das Kronendach hielt isotopisch schweren N zurück und gab isotopisch leichteres Nitrat und DON ab, sodass der Kronendurchlass leichter war als der Freilandniederschlag. Die $\delta^{15}N$-Werte stiegen dann zum Streusickerwasser an, aufgrund der Auswaschung isotopisch schweren DONs, und nahmen im mineralischen Oberboden ab, da DOM und Ammonium zurückgehalten und Nitrat ausgewaschen wurde. Mit zunehmender Bodentiefe zum Bachabfluss stiegen sie erneut, aufgrund der Denitrifikation isotopisch leichten Stickstoffs.

Über die 25 Jahre stiegen die Konzentrationen und Frachten von DON und DOP an, während die DOC/DON- und DOC/DOP-Verhältnisse abnahmen. DOP war jedoch im Freilandniederschlag, in der Bodenlösung und im Bachabfluss nicht nachweisbar. Die $\delta^{13}C$- und $\delta^{15}N$-Werte stiegen in der Festphase parallel an, was einen gekoppelten C- und N-Umsatz widerspiegelt, variierten jedoch unabhängig in der DOM.

Insgesamt beleuchteten die drei Ansätze die Quellen, Senken und Transformationen von DOC und TDN. Kohlenstoff- und Stickstoffkreislauf waren in der gelösten Phase weniger eng gekoppelt als in der Festphase, und das Waldökosystem schien auf eine Stickstoffsättigung zuzusteuern, bei der N zunehmend ausgetragen und P zurückgehalten wird. Die Kombination der drei Ansätze machte Entwicklungen sichtbar, die mit keinem einzelnen Tracer nachweisbar gewesen wären.

List of tables

Table B-1. Volume-weighted mean (±standard deviation) of total organic carbon (TOC) and dissolved organic nitrogen (DON) concentrations, and TOC/DON ratios of the ecosystem solutions along the water path through the ecosystem from 2013 to 2016. For litter leachate and soil solutions no volume-weighting was possible and therefore arithmetic monthly means of electrical conductivity (EC) and H^+ activities of the solutions were calculated from the values measured in the weekly collected samples. H^+ activities of the solutions were thereafter converted to pH values. Lower case letters indicate significant differences ($p < 0.05$) among the ecosystem solutions based on Tukey's HSD post-hoc test following one-way ANOVA. **35**

Table B-S1. Range of pH values and mean (±standard deviation) thickness, organic carbon (C_{org}), C/N ratios, oxalate-extractable iron (Fe_o) and exchangeable aluminum (Al_{exc}) concentrations, effective (CEC_{eff}) and potential cation-exchange capacity (CEC_{pot}) in the soils at three transects (at approximately 1900, 1950 and 2000 m above sea level). For each transect, data was collected from three soil profiles. Lower case letters indicate significant differences ($p < 0.05$) among soil horizons based on Tukey's HSD post-hoc test following one-way ANOVA. **48**

Table B-S2. List of common tree species in the San Francisco Reserve in south Ecuador for which leaf and root samples were collected **48**

Table C-1. Mean pH, total carbon (TC), total nitrogen (TN), and TC/TN concentration ratios of leaves (n=10), roots (n=10), and soil horizons (n=20); and quarterly mean TOC, TOC/DON and nitrate/ammonium concentration ratios (±standard deviations) in ecosystem solutions during the period 2013-2016 (n=16). Different lowercase letters indicate significant differences among the plant and soil samples or the ecosystem solutions according to Tukey's HSD post-hoc test.....**71**

Table C-S1. List of the most abundant tree species in the San Francisco Biological Reserve in south Ecuador, ordered according to their abundance and number (#) of leaf and root samples collected from these trees **86**

Table D-S1. Mean (± standard deviation, n = 20 yr for DOP, n = 24 yr for DON and n = 25 yr for DOC) annual dissolved organic carbon (DOC), nitrogen (DON), and phosphorus (DOP) concentrations, and DOC/DON and DOC/DOP ratios in dissolved organic matter of ecosystem solutions along the water path through the ecosystem. Lowercase

letters indicate significant differences ($p < .05$) among the ecosystem solutions according to a Tukey's HSD post hoc test following two-factor analysis of variance (ANOVA) with year and solution type as fixed factors and sequential (Type I) sum of squares. n.d., not detected with our method. **124**

Table D-S2. Kendall's τ, p values, and Sen's slopes of the seasonal Mann-Kendall trend test for the mean monthly dissolved organic carbon (DOC) concentrations and fluxes from April 1998 to March 2023 and DOC/DON ratios in dissolved organic matter (DOM) from April 1999 to March 2023 in ecosystem solutions (related to Figures D-S2, D-S3, and D-S6). Trends were assessed with the seasonal Mann-Kendall test (Hirsch et al., 1982), implemented in the function kendallSeasonalTrendTest of the EnvStats package (Millard, 2013). Significant trends are shown in bold. The seasonal Sen's slopes are referred to the overall median concentrations of the whole observation period. RF, rainfall; TF, throughfall; SF, stemflow; LL, litter leachate; SS15 and SS30, soil solution at the 0.15 and 0.3 m mineral soil depth, respectively; ST, streamflow. **125**

Table D-S3. Kendall's τ, p values, and Sen's slopes of the seasonal Mann-Kendall trend test for the mean monthly dissolved organic nitrogen (DON) and dissolved organic phosphorus (DOP) concentrations and fluxes and DOC/DOP and DON/DOP ratios in dissolved organic matter (DOM) in ecosystem solutions from April 1999 for DON and April 2003 for DOP to March 2023 (related to Figures D-1 to D-4, D-S4, and D-S7). Trends were assessed with the seasonal Mann-Kendall test (Hirsch et al., 1982), implemented in the function kendallSeasonalTrendTest of the EnvStats package (Millard, 2013). Significant trends are shown in bold. The seasonal Sen's slopes are referred to the overall median concentrations of the whole observation period. RF, rainfall; TF, throughfall; SF, stemflow; LL, litter leachate; SS15 and SS30, soil solution at the 0.15 and 0.3 m mineral soil depth, respectively; ST, streamflow; n.a. is not applicable, because if the trend was not significant, we did not calculate a seasonal Sen's slope. **126**

Table D-S4. Kendall's τ, p-values, and Sen's slopes of the seasonal Mann-Kendall trend test for the dissolved organic nitrogen (DON) contribution to total dissolved nitrogen (TDN) in ecosystem solutions from April 1999 to March 2023 (related to Figure D-S5) and dissolved organic phosphorus (DOP) contributions to total dissolved P (TDP) from April 2003 to March 2023. DOP was not detected in rainfall, the mineral soil

solutions, and streamflow. Trends were assessed with the seasonal Mann-Kendall test (Hirsch et al., 1982), implemented in the function kendallSeasonalTrendTest of the EnvStats package (Millard, 2013). Significant trends are shown in bold. The seasonal Sen's slopes are referred to the overall median concentrations of the whole observation period. RF, rainfall; TF, throughfall; SF, stemflow; LL, litter leachate; SS15 and SS30, soil solution at the 0.15 and 0.3 m mineral soil depth, respectively; ST, streamflow; n.a. is not applicable, because if the trend was not significant, we did not calculate a seasonal Sen's slope.....**127**

List of figures

Figure A-1. Location of the study area in the San Francisco Biological Reserve at south Ecuador. Catchment refers to the microcatchment 2 (MC2), T2.1, T2.2 and T2.3 are the transects stated in the experimental design. Rainfall measurement station 1 was operational from May 2000 to December 2005, station 2 from April 1998 to March 2023, station 3 from May 2000 to March 2023, and station 4 from June 2004 to June 2009. The weir and the meteorological station operated from April 1998 to March 2023. ..... **4**

Figure A-2. a) General view of the tropical montane forest, b) San Francisco River valley, c) view inside the forest, and d) typical soil profile in the study area. Photo a) was provided by Martin Schwarz, b) by Wolfgang Wilcke, c) by Jürgen Homeier, and d) by Andre Velescu. **5**

Figure A-3. Instrumentation of the study forest. a) Rain gauge, b) rainfall and c) throughfall collectors, d) zero-tension lysimeter for litter leachate, e) suction cups, f) gauging weir at the catchment outlet, where streamflow was sampled, and g) sampling design. Photos a)–c) and f) were provided by Wolfgang Wilcke, and d) and e) by Andre Velescu. **6**

Figure A-4. a) Elemental analyzer in liquid mode, coupled through b) a low-concentration module (LCM) to c) an isotope ratio mass spectrometer (TOC-LCM-IRMS), and d) scheme of the coupled system. Photos a) to c) were taken from Elementar Analysensysteme GmbH, and d) was taken from Federherr et al. (2016). **8**

Figure B-1. Course of monthly $\delta^{13}C$ values from January 2013 to December 2016. RF is rainfall, TF throughfall, SF stemflow, LL litter leachate, SS15 and SS30 mineral soil solutions at 0.15 and 0.30 m depth, respectively and ST streamflow. For TF, LL, S15, and SS30, the error bars represent the standard deviation among the three study transects at ca. 1900, 1950, and 2000 m a.s.l. SF was measured in a single composite sample collected from five separate trees. There was only one stream draining the study catchment. **36**

Figure B-2. Mean $\delta^{13}C$ values of sunlight-exposed leaves and fine roots of 10 common canopy-forming tree species in the forest of the San Francisco Biological Reserve. The error bars represent the standard deviations (n=4 for leaves and n=3 for roots). The

species were ordered from left to right according to their decreasing contribution to the total tree number. **37**

Figure B-3. Comparison of the mean $\delta^{13}C$ values in potential solid-phase sources of DOM and in DOM along the water path through the forest ecosystem. RF is rainfall, TF throughfall, SF stemflow, LL litter leachate, SS15 and SS30 mineral soil solutions at the 0.15 and 0.30 m soil depths, respectively, ST streamflow. OL organic layer (thickness-weighted mean $\delta^{13}C$ value of the three increasingly decomposed organic horizons Oi, Oe and Oa), and A and B are the soil mineral horizons. The $\delta^{13}C$ value of the bark (-28.5 ± 0.2‰) was taken from Cernusak and Hutley (2011). Error bars indicate standard errors. **39**

Figure B-4. Relationship between the mean TOC/DON ratios and the $\delta^{13}C$ values of DOM in ecosystem solutions (n=48 for each solution type). RF is rainfall, TF throughfall, SF stemflow, LL litter leachate, SS15 and SS30 mineral soil solutions at the 0.15 and 0.30 m depths, respectively and ST streamflow. The error bars indicate standard errors. .**40**

Figure B-S1. Mean monthly precipitation from April 1998 to December 2016 in the San Francisco Biological Reserve, south Ecuador. **49**

Figure B-S2. Mean monthly temperature from April 1998 to December 2016 in the San Francisco Biological Reserve, south Ecuador. **49**

Figure B-S3. Annual mean $\delta^{13}C$ values in leaves of *Graffenrieda emarginata* Triana from 2005 to 2015. The error bars indicate the standard deviations of up to five trees (except in 2009 when no replicates were sampled). **50**

Figure B-S4. Relationship between total organic carbon (TOC) concentrations filtered <1-7 µm and dissolved organic carbon (DOC) concentrations (<0.45 µm) in ecosystem solutions sampled in the San Francisco Biological Reserve in South Ecuador. RF is rainfall, TF throughfall, SF stemflow, LL litter leachate, SS15 and SS30 mineral soil solutions at 0.15 and 0.30 m depth, respectively and ST stream water flow (n=70). .**50**

Figure C-1. Mean quarterly concentrations of DON, NH_4^+-N, and NO_3^--N from 2013 to 2016 in a tropical montane forest in south Ecuador. Error bars represent standard deviations. RF is rainfall, TF throughfall, SF stemflow, LL litter leachate, SS15 and SS30 mineral soil solutions at the 0.15 and 0.30 m depths, respectively, and ST streamflow. **72**

Figure C-2. Mean annual N flux with bulk deposition (BD), dry deposition (DD, Eq. 3), throughfall (TF), stemflow (SF), the resulting canopy budget (CB, Eq. 1), litter leachate (LL), mineral soil solution at the 0.15 m (SS15) and 0.30 m depths (SS30), and streamflow (ST) from 2013 to 2016. The DD is based on the deposition ratio of Cl^- assuming negligible Cl^- leaching from the canopy and does not include the gaseous N exchange between the canopy and the atmosphere. The error bars represent standard deviations to illustrate temporal variation among the four study years. **73**

Figure C-3. Bulk deposition of N (a) and course of the quarterly $\delta^{15}N$ values in ecosystem solutions along the water path through the forest ecosystem from January 2013 to December 2016 (b-g). Error bars represent the standard deviation of three study transects at approximately 1900, 1950, and 2000 m a.s.l. RF is rainfall, TF throughfall, SF stemflow, LL litter leachate, SS15 and SS30 mineral soil solutions at the 0.15 and 0.30 m depths respectively, and ST streamflow. The $\delta^{15}N$ values in rainfall and streamflow could only be measured in individual weeks when the TDN concentrations were sufficiently high. Oblique hatching indicates the periods with the lowest rainfall and extended dry spells (the "veranillo") (Figure C-S4). Mind the different Y axis scaling in (b) than in all other subfigures showing $\delta^{15}N$ values. **75**

Figure C-4. Mean $\delta^{15}N$ values of TDN (rhombi) and dissolved NO_3^- (squares) taken from Schwarz et al. (2011) in ecosystem solutions along the water path through the forestand in solid materials (circles) that could serve as source or sink of N. RF is rainfall, TF throughfall, SF stemflow, LL litter leachate, SS15 and SS30 mineral soil solutions at the 0.15 and 0.30 m depths, respectively, and ST stream flow. Leaves are live canopy leaves, OL is the organic layer, Oi, Oe, Oa are the three differently decomposed organic horizons, A and B are the mineral top- and subsoil horizons. Error bars represent standard errors refering to the means of quarterly samples of the ecosystem solutions (averaged for the three transects, n=16 for TDN and n=4 for NO_3), 20 Oi, Oe, Oa, A, and B horizons from the whole catchment, 20 horizon thickness-weighted organic layer means (OL), and 10 samples of each of fresh leaves and roots from 10 different tree species. The mean $\delta^{15}N$ value of NO_3 in litter leachate was -7.43 ± 1.98 and is not shown to scale. To avoid the overlap of error bars, data points that should appear on the same level were slightly offset on the Y axis. **76**

Figure C-S1. Mean monthly precipitation from April 1998 to December 2016 in the San Francisco Biological Reserve, south Ecuador. Error bars represent standard deviations. **86**

Figure C-S2. Mean $\delta^{15}N$ values of leaves and roots of 10 canopy-forming tree species in the forest of the San Francisco Biological Reserve. Error bars represent standard deviations for leaves (n=1-3 individuals, Table C-S1) and roots (n=3 individuals). The species were ordered from left to right according to their decreasing contribution to the total tree number on the study plots. **87**

Figure C-S3. Temporal variation of the $\delta^{15}N$ values in leaves of a) *Graffenrieda emarginata* Triana and b) *Myrcia myrtiformis* Naudin in the San Francisco Reserve from 2005 to 2015. Error bars represent standard deviations (n=5 individual trees per species and sampling date). Temporal trends were statistically evaluated with the Mann-Kendall test. Regression lines are shown to illustrate significant trends but do not necessarily imply that the trend is linear. **88**

Figure C-S4. Mean contribution of DON, NH_4^+-N, and NO_3^--N to the total dissolved nitrogen (TDN) concentrations in each ecosystem solution, based on monthly mean concentrations from 2013-2016. RF is rainfall, TF throughfall, SF stemflow, LL litter leachate, SS15 and SS30 mineral soil solutions at the 0.15 and 0.30 m mineral soil depths, respectively, and ST streamflow. **89**

Figure C-S5. Course of the monthly precipitation in the San Francisco Reserve from January 2013 to December 2016 measured at two gaging stations on clear-cut areas. **89**

Figure D-1. Temporal course of the mean monthly dissolved organic nitrogen (DON) concentrations in ecosystem solutions from April 1998 to March 2023. RF is rainfall, TF throughfall, SF stemflow, LL litter leachate, SS15 and SS30 mineral soil solutions at the 0.15 and 0.30 m depths, respectively, and ST streamflow. Error bars represent the standard deviations among one to four gauging stations for RF and three study transects for TF, LL, SS15, and SS30; there was only one measurement station for each of SF and ST. Temporal trends in monthly data were statistically evaluated with the Seasonal Mann-Kendall test (Hirsch et al., 1982). Regression lines are shown when there was a significant temporal trend for illustration purposes. **111**

Figure D-2. Temporal course of the dissolved organic phosphorus (DOP) concentrations in throughfall (TF), stemflow (SF) and litter leachate (LL) from April 2003 to March

2023. Error bars represent the standard deviations among three study transects. There was only one measurement station for SF. Temporal trends in monthly data were statistically evaluated with the Seasonal Mann-Kendall test (Hirsch et al., 1982). Regression lines are shown when there was a significant temporal trend for illustration purposes. **112**

Figure D-3. Temporal course of the dissolved organic carbon to phosphorus concentrations ratio (DOC/DOP) in throughfall (TF), stemflow (SF) and litter leachate (LL) from April 2003 to March 2023. Error bars represent the standard deviations among three study transects. There was only one measurement station for SF. Temporal trends in monthly data were statistically evaluated with the Seasonal Mann-Kendall test (Hirsch et al., 1982). Regression lines are shown when there was a significant temporal trend for illustration purposes..... **113**

Figure D-4. Temporal course of dissolved organic nitrogen to dissolved organic phosphorus concentrations ratio (DON/DOP) in ecosystem solutions from April 2003 to March 2023. TF is throughfall, SF stemflow and LL litter leachate. Error bars represent the standard deviations from three study transects for TF and LL. There was only one measurement station for SF. Temporal trends in monthly data were statistically evaluated with the Seasonal Mann-Kendall test (Hirsch et al., 1982). Regression lines are shown when there was a significant temporal trend for illustration purposes. .. **114**

Figure D-5. Relationship between a) C and N stable isotope ratios ($\delta^{13}C$ and $\delta^{15}N$ values) in litterfall (n=48), organic and mineral soil horizons (n=21 soil profiles) from Microcatchment (MC) 2. Oi, Oe, and Oa are the three increasingly decomposed organic horizons, and A and B are the mineral soil horizons; and b) relationship between $\delta^{13}C$ and $\delta^{15}N$ values in dissolved organic matter. RF is rainfall, TF throughfall, SF stemflow, LL litter leachate, SS15 and SS30 mineral soil solutions at the 0.15 and 0.30 m depths, respectively, and ST streamflow (n = 48 monthly values for $\delta^{13}C$ and n = 16 quarterly values for $\delta^{15}N$). Error bars indicate the standard error. The $\delta^{13}C$ values are taken from Alvarez et al. (2023) and the $\delta^{15}N$ values from Alvarez et al. (2024a, 2024b)..... **115**

Figure D-6. Relationship between the mean DOC/DON ratios and the $\delta^{15}N$ values of DOM in ecosystem solutions, n = 48 monthly values for DOC and DON concentrations, n = 16 quarterly values for $\delta^{15}N$ values. RF is rainfall, TF throughfall, SF stemflow, LL litter leachate, SS15 and SS30 mineral soil solutions at the 0.15 and 0.30 m depths,

respectively and ST streamflow. The error bars indicate standard errors. The $\delta^{15}N$ values of DOM are taken from Alvarez et al. (2024a). **116**

Figure D-S1. Vertical distribution of the a) dissolved organic nitrogen (DON) contribution to the total dissolved nitrogen (TDN) concentrations and b) dissolved organic phosphorus (DOP) contribution to total dissolved phosphorus (TDP) concentrations, based on mean monthly concentrations from April 1999 to March 2023 for DON and April 2003 to March 2023 for DOP. RF is rainfall, TF throughfall, SF stemflow, LL litter leachate, SS15 and SS30 mineral soil solutions at the 0.15 and 0.30 m depths, respectively, and ST streamflow. Error bars represent the standard deviations among 24 years for DON (1999-2023) and 20 years for DOP (2003-2023). Lower case letters indicate significant differences ($p < .05$) among the ecosystem solutions according to a Tukey's HSD post hoc test following two-factor analysis of variance (ANOVA) with year and solution type as fixed factors.....**128**

Figure D-S2. Course of mean monthly dissolved organic carbon (DOC) concentrations in ecosystem solutions from April 1998 to March 2023. RF is rainfall, TF throughfall, SF stemflow, LL litter leachate, SS15 and SS30 mineral soil solutions at the 0.15 and 0.30 m depths, respectively, and ST streamflow. Error bars represent the standard deviations from two to four gauging stations for RF and from three study transects for TF, LL, SS15, and SS30, whereas there was only one measurement station for each of SF and ST. The regression lines are shown only to illustrate significant trends. Please note the different y-axis scaling for SF, ST and LL. Temporal trends in monthly data were statistically evaluated with the Seasonal Mann-Kendall test (Hirsch et al., 1982). Regression lines are shown when there was a significant temporal trend for illustration purposes. **130**

Figure D-S3. Course of mean monthly dissolved organic carbon (DOC) fluxes in ecosystem solutions from April 1998 to March 2023. RF is rainfall, TF throughfall, SF stemflow, LL litter leachate, SS15 and SS30 mineral soil solutions at the 0.15 and 0.30 m depths, respectively, and ST streamflow. Error bars represent the standard deviations from two to four gauging stations for RF and from three study transects for TF, LL, SS15, and SS30, whereas there was only one measurement station for each of SF and ST. The regression lines are shown only to illustrate significant trends. Please note the different y-axis scaling for SF, ST and LL. Temporal trends in monthly data were statistically

evaluated with the Seasonal Mann-Kendall test (Hirsch et al., 1982). Regression lines are shown when there was a significant temporal trend for illustration purposes. .. **132**

Figure D-S4. Course of mean monthly dissolved organic nitrogen (DON) fluxes in ecosystem solutions from April 1999 to March 2023. RF is rainfall, TF throughfall, SF stemflow, LL litter leachate, SS15 and SS30 mineral soil solutions at the 0.15 and 0.30 m depths, respectively, and ST streamflow. Error bars represent the standard deviations from two to four gauging stations for RF and from three study transects for TF, LL, SS15, and SS30, whereas there was only one measurement station for each of SF and ST. The regression lines are shown only to illustrate significant trends. Temporal trends in monthly data were statistically evaluated with the Seasonal Mann-Kendall test (Hirsch et al., 1982). Regression lines are shown when there was a significant temporal trend for illustration purposes. Please note the different y-axis scaling for SF, LL and ST. **134**

Figure D-S5. Temporal course of dissolved organic nitrogen (DON) contributions to total dissolved nitrogen (TDN) in ecosystem solutions from April 1999 to March 2023. RF is rainfall, TF throughfall, SF stemflow, LL litter leachate, SS15 and SS30 mineral soil solutions at the 0.15 and 0.30 m depths, respectively, and ST streamflow. Error bars represent the standard deviations from two to four gauging stations for RF and from three study transects for TF, LL, SS15, and SS30, whereas there was only one measurement station for each of SF and ST. The regression lines are shown only to illustrate significant trends. Temporal trends in monthly data were statistically evaluated with the Seasonal Mann-Kendall test (Hirsch et al., 1982). Regression lines are shown when there was a significant temporal trend for illustration purposes. Mean monthly trends of the relative DON contributions to TDN from 1998 to 2013 (Wilcke et al. (2013) were extended and evaluated until March 2023. ..... **136**

Figure D-S6. Course of mean monthly dissolved organic carbon (DOC) to dissolved organic nitrogen (DON) ratios in ecosystem solutions from April 1999 to March 2023. RF is rainfall, TF throughfall, SF stemflow, LL litter leachate, SS15 and SS30 mineral soil solutions at the 0.15 and 0.30 m depths, respectively, and ST streamflow. Error bars represent the standard deviations from two to four gauging stations for RF and from three study transects for TF, LL, SS15, and SS30, whereas one weekly sample was collected for SF and ST. The regression lines are shown only to illustrate significant trends. Temporal trends in monthly data were statistically evaluated with the Seasonal

Mann-Kendall test (Hirsch et al., 1982). Regression lines are shown when there was a significant temporal trend for illustration purposes. Please note the different y-axis scaling for SF, ST and LL. **138**

Figure D-S7. Course of the mean dissolved organic phosphorus (DOP) fluxes in ecosystem solutions from April 2003 to March 2023. TF throughfall, SF stemflow, and LL litter leachate. Error bars represent the standard deviations of three study transects for TF and LL. There was only one measurement station for SF. Temporal trends in monthly data were statistically evaluated with the Seasonal Mann-Kendall test (Hirsch et al., 1982). Regression lines are shown when there was a significant temporal trend for illustration purposes. Please note the different y-axis scaling for SF. **138**

Figure D-S8. Temporal course of dissolved organic phosphorus (DOP) contribution to total dissolved phosphorus (TDP) in ecosystem solutions from April 2003 to March 2023. TF throughfall, SF stemflow and LL litter leachate. Error bars represent the standard deviations from three study transects for TF and LL, whereas there was only one measurement station for SF. Temporal trends in monthly data were statistically evaluated with the Seasonal Mann-Kendall test (Hirsch et al., 1982). Regression lines are shown when there was a significant temporal trend for illustration purposes. ... **139**

List of abbreviations

a.s.l.	above sea level
ANOVA	analysis of variance
C_3	plants using the C_3 photosynthetic pathway
C/N	carbon to nitrogen ratio
C/P	carbon to phosphorus ratio
CFA	continuous flow analysis
DD	dry deposition
DFG	Deutsche Forschungsgemeinschaft (German Research Foundation)
DIN	dissolved inorganic nitrogen
DOC	dissolved organic carbon
DOC/DON	dissolved organic carbon to dissolved organic nitrogen ratio
DOC/DOP	dissolved organic carbon to dissolved organic phosphorus ratio
DOM	dissolved organic matter
DON	dissolved organic nitrogen
DON/DOP	dissolved organic nitrogen to dissolved organic phosphorus ratio
DOP	dissolved organic phosphorus
DVWK	Deutscher Verband für Wasserwirtschaft und Kulturbau (now part of the German Association for Water, Wastewater and Waste)
EA-IRMS	elemental analyzer-isotope ratio mass spectrometer
ECSF	Estación Científica San Francisco (San Francisco Research Station)
HSD	honestly significant difference (according to Tukey's post-hoc test)
IRMS	isotope ratio mass spectrometer
IUSS	International Union of Soil Sciences
LL	litter leachate
N/P	nitrogen to phosphorus ratio
NH_4^+	ammonium
NO_3^-	nitrate
RF	rainfall
SF	stemflow

SOM	soil organic matter
SS15	mineral soil solution at the 0.15 m soil depth
SS30	mineral soil solution at the 0.30 m soil depth
ST	streamflow
TC	total carbon
TDN	total dissolved nitrogen
TDP	total dissolved phosphorus
TF	throughfall
TN	total nitrogen
TOC	total organic carbon
TOC-LCM-IRMS	total organic carbon analyzer (liquid mode) coupled via a low concentration module to an isotope ratio mass spectrometer
USGS-61, -62, -64	reference materials from the U.S. Geological Survey
VPDB	Vienna Pee Dee Belemnite ($\delta^{13}C$ reference standard)
WRB	World Reference Base for Soil Resources
$\delta^{13}C$	difference between the carbon stable isotope ratio of a sample and VPDB times 1000 [‰]
$\delta^{15}N$	difference between the nitrogen stable isotope ratio of a sample and air times 1000 [‰]

A. Summarizing overview

1. Introduction

Dissolved organic matter (DOM) couples the carbon (C), nitrogen (N), and phosphorus (P) cycles of forest ecosystems and links the terrestrial and aquatic components of these cycles. The DOM that leaves forests with the draining water contributes a substantial part of the C that rivers transport to the ocean (Camino-Serrano et al. 2014; Dai et al. 2012; Regnier et al. 2013). Tropical montane forests store large amounts of C and regulate regional water and nutrient cycles, but they remain understudied relative to temperate and tropical lowland forests, particularly with regard to the long-term dynamics of DOM (Lange et al. 2024; Leuschner et al. 2013; Wilcke et al. 2002, 2020). As a mobile and partly bioavailable component of soil organic matter, DOM is highly susceptible to environmental change (Evans et al. 2008; Michalzik et al. 2001).

The tropical montane forests on the rim of the Amazon basin, including my study site, a 9.1 ha catchment under evergreen tropical lower montane forest (Bruijnzeel and Hamilton 2000) in the San Francisco Biological Reserve, are exposed to several environmental drivers that act simultaneously. Atmospheric N deposition has increased, driven mainly by Amazonian biomass burning (Boy et al. 2008a; Wilcke et al. 2013), while Saharan and African savanna dust reaches the study area (Boy & Wilcke 2008) and supplies a continuous input of P (Barkley et al. 2019; Van Langenhove et al. 2020; Wilcke et al. 2019). More frequent warm days, longer dry spells, and a decreasing soil water content enhance microbial decomposition and consequently soil organic matter mineralization in organic and mineral soil horizons (Wilcke et al. 2020). The increasing N deposition raises the C/P and N/P ratios of plants, soils, and microbial biomass and pushes the ecosystems toward or enhances P limitation (Jiang et al. 2024; Wang et al. 2017).

The concentrations, sources, and transformations of DOM change along the water path through the forest canopy, the bark surfaces, the organic layer, and the mineral soil (Kalbitz et al. 2000; Michalzik et al. 2001; Qualls et al. 1991). The concentrations of dissolved organic N (DON) and dissolved organic P (DOP) usually increase from rainfall via throughfall and stemflow to litter leachate, and then decrease in the mineral soil as the organic forms are retained, mineralized, or transformed into inorganic species (Goller et al. 2006; Michalzik et al. 2001; Schrumpf et al. 2006). Reports of how DOM responds to

environmental change come mostly from temperate ecosystems, where the long-term DOM trends were largely attributed to the recovery from acid deposition. Tropical forests, which lack that history of acid rain and its recovery, remain little studied (Borken et al. 2011; Camino-Serrano et al. 2014).

The ratio of the stable C isotopes, expressed as the $\delta^{13}C$ value, i.e., the difference between the carbon stable isotope ratio of a sample and Vienna Pee Dee Belemnite times 1000 [‰], is a widely used tool in ecology (Bowling et al. 2008). It is routinely measured on solid samples such as leaves, litterfall, roots, and soil organic matter (Gerschlauer et al. 2019; Lorenz et al. 2020). In C_3 plants, it is species-specific and reflects the response to light, nutrients, water availability, and other environmental conditions (Brüggemann et al. 2011; Kohn 2010). The $\delta^{13}C$ values of DOM, in contrast, have rarely been reported from terrestrial ecosystems, mainly because the technology to measure them directly in solution has only become available in the past decade and is not yet widespread (Federherr et al. 2014; Kirkels et al. 2014). The direct measurement of the $\delta^{13}C$ values of DOM with a TOC-IRMS avoids the freeze-drying of the large sample volumes that the conventional collection of DOM as a solid for elemental analyzer isotope ratio mass spectrometry (EA-IRMS) requires, and can therefore be applied to the large number of small-volume samples that long-term ecosystem studies collect (Alvarez et al. 2023). This direct approach allows the $\delta^{13}C$ value to trace the sources and transformations of DOM and to add information that more easily accessible properties such as the C/N ratio do not provide. However, the interpretation of the $\delta^{13}C$ values of DOM requires knowledge of the $\delta^{13}C$ values of the potential solid-phase sources and of the size and age of the C pools (Gandois et al. 2014; Hood et al. 2005).

The globally increasing richness in reactive N affects even remote ecosystems such as the tropical montane forests in Ecuador (Galloway et al. 2004, 2008; Lamarque et al. 2013; Wilcke et al. 2013). Along the water path, several N sources and sinks, including the exchange of N in the canopy, the retention of dissolved organic N and ammonium, mineralization, nitrification, and denitrification, are expected to change the $\delta^{15}N$ value, i.e., the difference between the nitrogen stable isotope ratio of a sample and atmospheric N_2 times 1000 [‰], of the total dissolved N (Schwarz et al. 2011; Wilcke et al. 2013). Measured directly in solution, the $\delta^{15}N$ value could identify the nature and the scale of these sources and sinks and could serve as a comparatively simple tool to monitor the N cycle on large sample numbers. Whether the $\delta^{15}N$ value of the total dissolved N can fulfil this role along the water path through a tropical montane forest had not yet been assessed.

The concentrations of DON and DOP and their stoichiometric ratios DOC/DON, DOC/DOP, and DON/DOP indicate the quality of DOM and the balance between the N and P cycles, and they provide complementary signals of the processes that govern the production, transformation, and retention of organic matter in the ecosystem compartments (Cleveland and Liptzin 2007; Neff et al. 2000; Saunders et al. 2006). The stable C and N isotopes add a complementary tool to trace sources, sinks, and transformations of DOM (Alvarez et al. 2023, 2024). In solid-phase organic matter, the $\delta^{13}C$ and $\delta^{15}N$ values increase together with depth and degree of decomposition, because microbial processing preferentially removes the isotopically light C and N (Gerschlauer et al. 2019; Lorenz et al. 2020; Nel et al. 2018). However, whether the same coupling holds for DOM along the water path remains open. This gap limits the understanding of how global environmental change is reorganizing the coupled C, N, and P cycles of tropical montane forests. The combination of measurements of the C isotope ratios of DOM, the N isotope ratios of TDN, and the long-term response of the stoichiometric C:N:P ratios in DOM to environmental change is a promising novel approach to assess whether the long-term environmental change altered the composition and the source and sink dynamics of DOM in the studied tropical montane forest in south Ecuador.

The overall goal of this thesis was therefore to assess the vertical transformations of the DOM and TDN composition along the water path through the ecosystem and how the environmental change of the past 25 years altered the composition and the source and sink dynamics of DOM in a tropical montane forest. To this end, I addressed the following research questions in my cumulative dissertation:

(1) Can the $\delta^{13}C$ values of DOM be used to identify the sources and transformations of DOM along the water path through the forest? (Section B).

(2) Can the $\delta^{15}N$ values of the total dissolved N be used to identify the sources and sinks of N along the water path and to monitor the N cycle? (Section C).

(3) How did the environmental change of the past 25 years alter the elemental composition and the stoichiometry of DOM, and does the coupling between the C and N cycles that is reported for the solid phases also hold for DOM along the water path? (Section D).

2. Materials and methods

2.1. Study area and field sampling

The study site is a ca. 9.1 ha-large catchment under evergreen lower tropical montane forest (Bruijnzeel and Hamilton 2000) on a 38 to 70° steep slope between about 1850 and 2200 m a.s.l. in the San Francisco Biological Reserve, on the east-exposed slope of the Andean cordillera in south Ecuador, i.e., on the rim of the Amazon basin (**Figure A-1 and A-2**; Wilcke et al. 2017, 2020). The climate is perhumid, with a mean annual rainfall of about 2340 mm and a mean annual temperature of about 15 °C from 1998 to 2023 (Bendix et al. 2018; Bendix 2020, updated in May 2026).

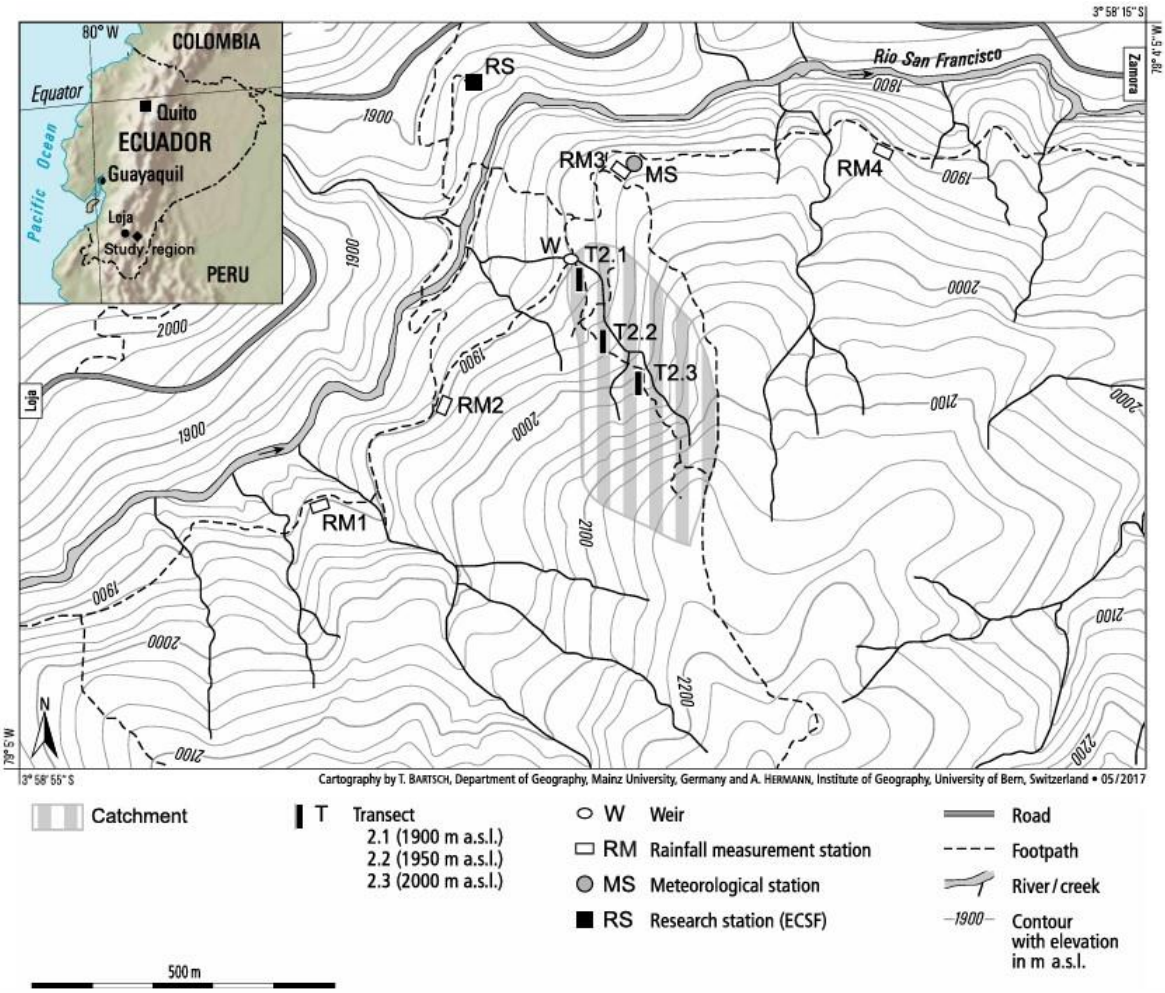


Figure A-1. Location of the study area in the San Francisco Biological Reserve at south Ecuador. Catchment refers to the microcatchment 2 (MC2), T2.1, T2.2 and T2.3 are the transects stated in the experimental design. Rainfall measurement station 1 was operational from May 2000 to December 2005, station 2 from April 1998 to March 2023, station 3 from

May 2000 to March 2023, and station 4 from June 2004 to June 2009. The weir and the meteorological station operated from April 1998 to March 2023.

The soils are shallow Dystric Cambisols developed from phyllite and quartzite, with thick organic layers and clay fractions dominated by three-layer clay minerals together with kaolinite and pedogenic chlorite (**Figure A-2d**; Schrumpf et al. 2001). During the study period, the site experienced increasing atmospheric deposition of N, a continuous input of P, and a warmer and drier climate (Wilcke et al. 2013, 2019, 2020).

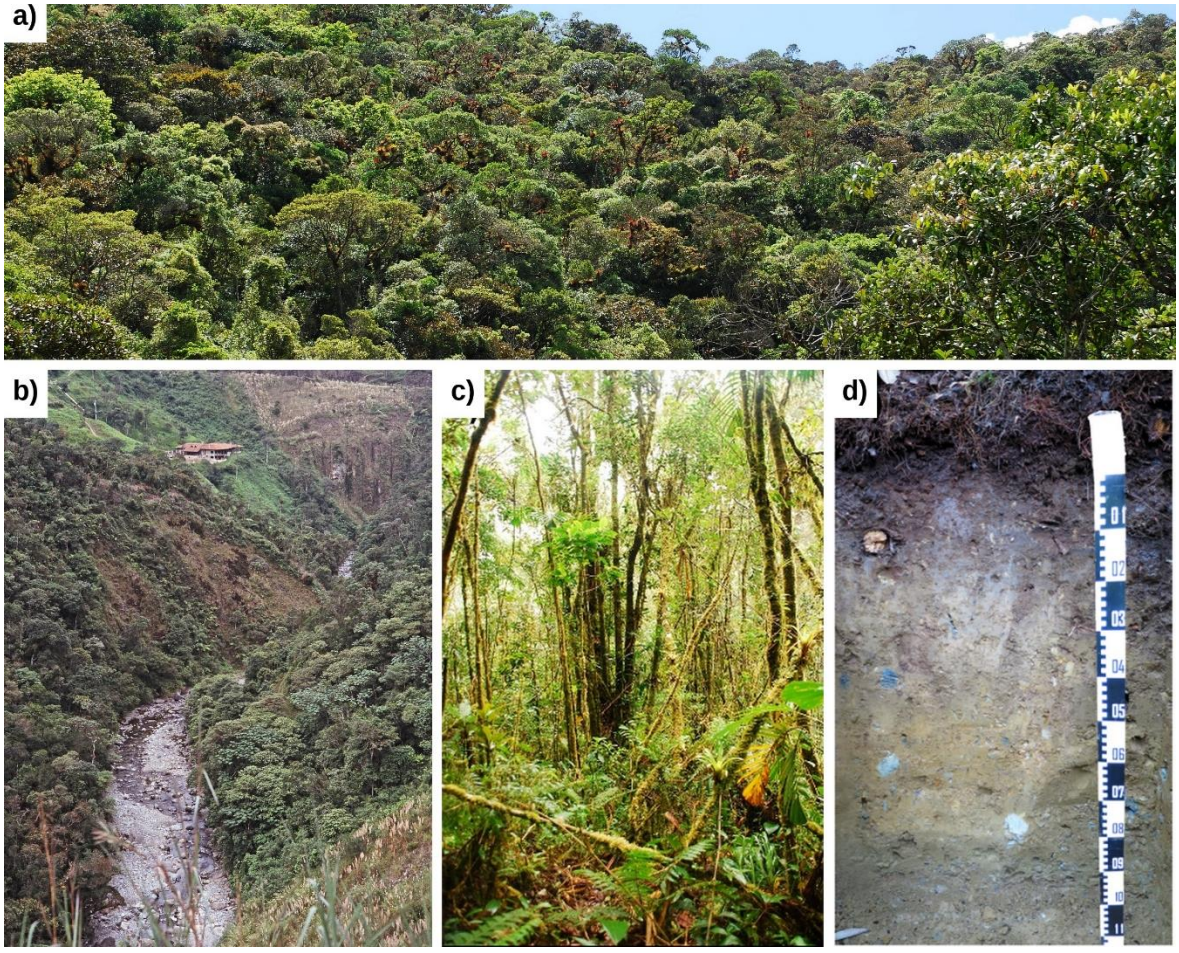


Figure A-2. a) General view of the tropical montane forest, b) San Francisco River valley, c) view inside the forest, and d) typical soil profile in the study area. Photo a) was provided by Martin Schwarz, b) by Wolfgang Wilcke, c) by Jürgen Homeier, and d) by Andre Velescu.

The ecosystem solutions were collected weekly along the water path (**Figure A-3**). Rainfall (RF) was sampled in clear-cut areas (RM in **Figure A-1**). Throughfall (TF) was collected under the canopy with 20 fixed-position funnel collectors along each of three transects (T2.1-2.3 in **Figure A-1**), litter leachate (LL) was sampled below the organic layer

with zero-tension lysimeters and the mineral soil solutions at 0.15 and 0.30 m depth (SS15, SS30) with ceramic suction cups also at each transect. Stemflow (SF) was sampled with collars on five trees and extrapolated to the whole forest from the number of trees per hectare, and streamflow (ST) was sampled at a single station above a weir (W in **Figure A-1**). The volumes of RF, TF, SF, and LL were measured and bulked into volume-weighted composite samples per sample type, transect, and collection date. For the solid phase, sunlit leaves of the ten most abundant tree species, litterfall, fine roots, the organic horizons (Oi, Oe, Oa), and the mineral soil horizons were sampled for the analyses of total C and N concentrations, and their $\delta^{13}C$ and $\delta^{15}N$ values (Alvarez et al. 2023, 2024).

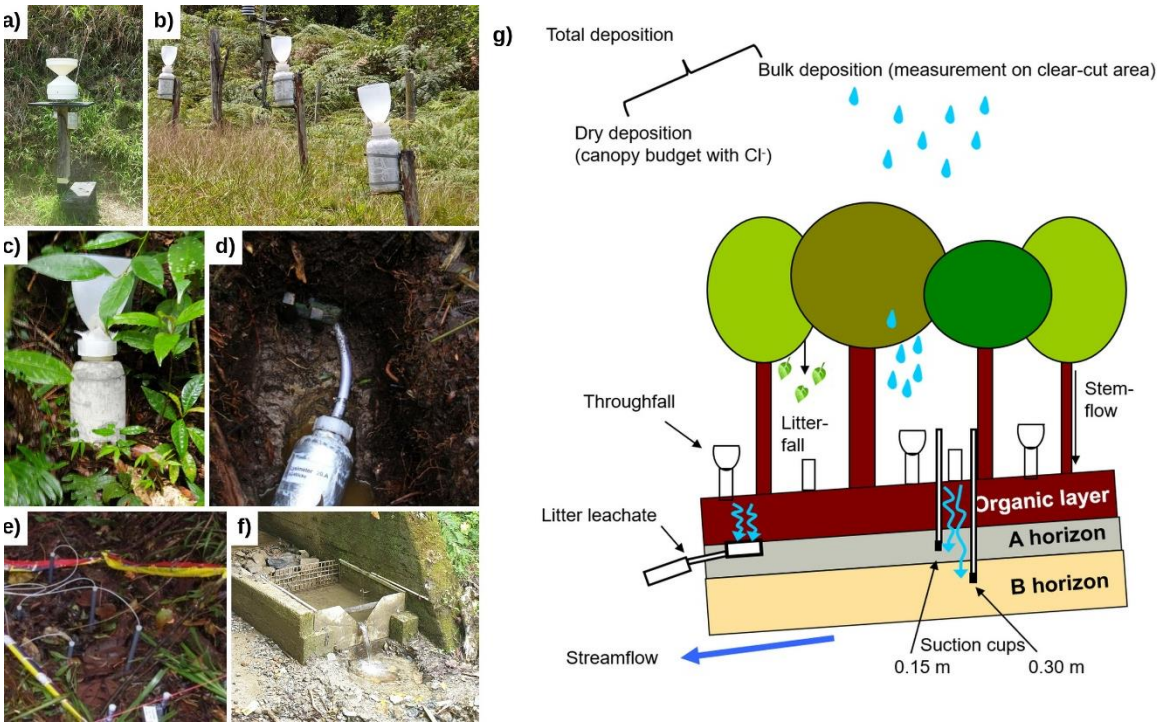


Figure A-3. Instrumentation of the study forest. a) Rain gauge, b) rainfall and c) throughfall collectors, d) zero-tension lysimeter for litter leachate, e) suction cups, f) gauging weir at the catchment outlet, where streamflow was sampled, and g) sampling design. Photos a)–c) and f) were provided by Wolfgang Wilcke, and d) and e) by Andre Velescu.

The solutions were collected along the water path from 1998 to 2023, and the analyses compiled here relied on different subperiods of this record. The $\delta^{13}C$ values of DOM (**Section B**, Alvarez et al. 2023) were measured on volume-weighted monthly composite samples and the $\delta^{15}N$ values of TDN (**Section C**, Alvarez et al. 2024) in quarterly resolution from January 2013 to December 2016. The DON, DOP, and DOC concentrations and fluxes and their stoichiometric ratios were analyzed for the 25-year record from April 1998 to

March 2023 (**Section D**). For the evaluation of the relationship between the stable C and N isotope ratios and the stoichiometric ratios of DOM, the $\delta^{13}C$ and $\delta^{15}N$ values of Alvarez et al. (2023, 2024) were used covering the period January 2013 to December 2016.

2.2. Chemical analyses

The ecosystem solutions were filtered in the field laboratory through ashless folded filters of 4 to 7 µm pore size, except the mineral soil solutions, which were collected through ceramic suction cups of 1 ± 0.1 µm pore size. All samples were exported in frozen state from Ecuador to Europe for the chemical analysis. The dissolved organic carbon (DOC) concentrations were determined as total organic carbon with an elemental analyzer (varioTOC cube, Elementar Analysensysteme GmbH, Langenselbold, Germany) after acidification to remove inorganic carbon. A comparison of 70 samples, ten of each solution type, showed no detectable difference between these TOC concentrations and the DOC concentrations obtained by conventional filtration to below 0.45 µm, so that the TOC is reported here as DOC (Alvarez et al. 2023). The total dissolved N (TDN), nitrate, and ammonium were measured by high-resolution colorimetry with a continuous flow analyzer (CFA San++, Skalar, Breda, The Netherlands). The dissolved inorganic N (DIN) concentration was calculated as the sum of the ammonium and nitrate concentrations, and the DON concentrations as the difference between those of TDN and DIN (Alvarez et al. 2024). The total dissolved P (TDP) and phosphate concentrations were also measured with the CFA, and the DOP concentration was calculated as the difference between those of TDP and phosphate. For the solid phase, the total C and N concentrations and the C/N ratios of the leaf, litterfall, root, organic layer, and mineral soil samples were determined by elemental analysis.

2.3. Stable isotope measurements

In the ecosystem solutions, the $\delta^{13}C$ values of DOM and the $\delta^{15}N$ values of TDN were measured directly in the liquid samples with an elemental analyzer optimized for stable isotope analysis in liquid mode coupled through a low-concentration module for peak focusing to an isotope ratio mass spectrometer (TOC-LCM-IRMS**, Figure A-4**) (Alvarez et al. 2023, 2024). The $\delta^{13}C$ values were referenced to the Vienna Pee Dee Belemnite (VPDB) scale and the $\delta^{15}N$ values to the atmospheric N_2 scale with certified reference materials and a linear calibration. The $\delta^{13}C$ values were measured on volume-weighted monthly composite

samples and the $\delta^{15}N$ values on volume-weighted quarterly composite samples, mixed from the weekly samples proportional to the water fluxes when these were measured in the field (RF, TF, SF) and in equal parts when they were not (LL, SS15, SS30, ST). In the solid phase, the $\delta^{13}C$ and $\delta^{15}N$ values, together with the total C and N concentrations of the leaf, root, organic layer, and mineral soil samples were measured with an elemental analyzer coupled to an isotope ratio mass spectrometer (EA-IRMS), calibrated with certified reference materials (Alvarez et al. 2024).

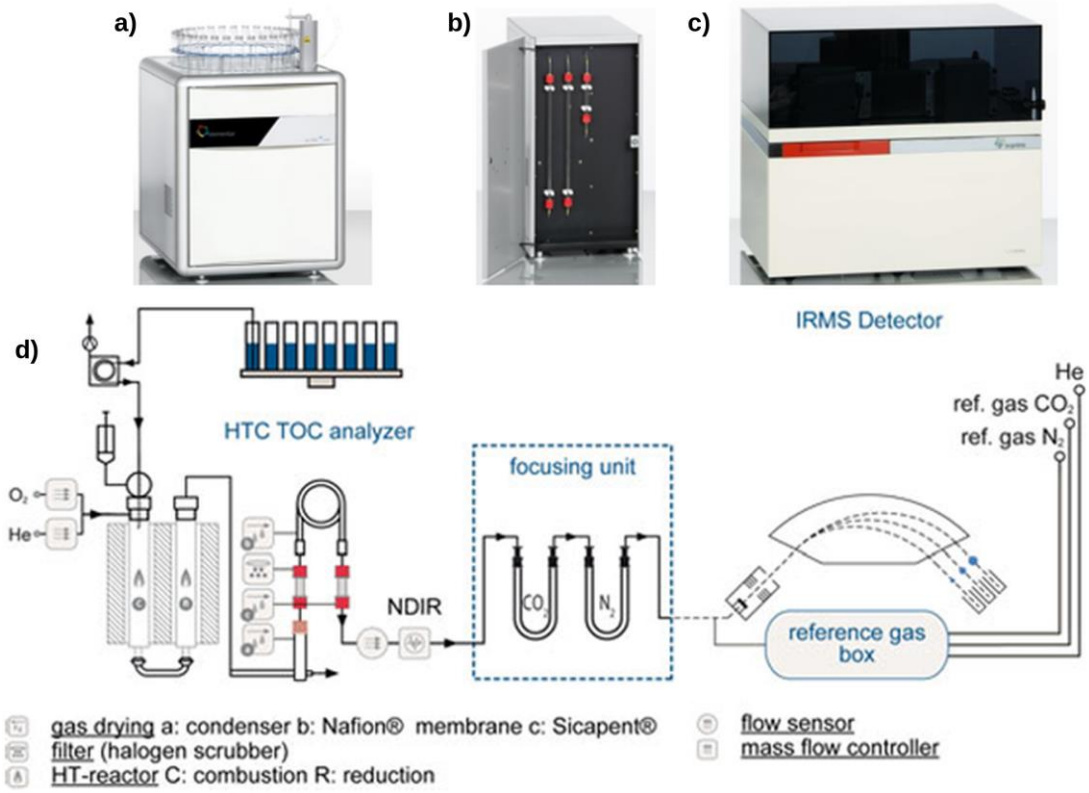


Figure A-4. a) Elemental analyzer in liquid mode, coupled through b) a low-concentration module (LCM) to c) an isotope ratio mass spectrometer (TOC-LCM-IRMS), and d) scheme of the coupled system. Photos a) to c) were taken from Elementar Analysensysteme GmbH, and d) was taken from Federherr et al. (2016).

2.4. Calculations and statistical analysis

The water fluxes of rainfall, throughfall, and stemflow were calculated from the measured volumes and the known collector areas. The stemflow flux was extrapolated via the average number of trees per hectare, i.e. 1000 trees with a diameter at breast height (dbh) > 0.1 m and 4000 trees with a dbh < 0.1 m which were considered to deliver 50% of the stemflow of the larger trees. The water fluxes of litter leachate and the mineral soil solutions

were derived from a Soil Water Balance Model (DVWK 1996) using available data from 1999 to 2003 and extended to the full study period by a regression equation described by Wilcke et al. (2020) for litter leachate and by Schwarz et al. (2011) for the mineral soil solutions. The element fluxes were obtained by multiplying the concentrations by the corresponding water fluxes. The stoichiometric ratios DOC/DON, DOC/DOP, and DON/DOP were calculated from the respective concentrations in mg L^{-1}, i.e., they are mass-related.

The temporal trends of the monthly mean concentrations, fluxes, and stoichiometric ratios from 1998 to 2023 were assessed with the Seasonal Mann-Kendall trend test, which accounts for seasonal autocorrelation, and the strength and direction of each trend were expressed by Kendall's τ (Hirsch et al. 1982). Differences among the ecosystem solutions were tested on the arithmetic annual means from 1998 to 2023 with a bifactorial ANOVA, with the year fitted before the ecosystem solution as factors, followed by a Tukey's HSD post-hoc test. The coupling between the C and N cycles was examined through the correlations among the $\delta^{13}C$ and $\delta^{15}N$ values, the total C to total N ratios of the solid phase, and the DOC/DON ratios of the ecosystem solutions. The level of significance was set at $p < 0.05$.

3. Results and discussion

3.1. Carbon isotope composition of DOM (Section B)

The $\delta^{13}C$ values of DOM did not vary seasonally and decreased along the aboveground water path, from rainfall via throughfall and stemflow to litter leachate. This decrease reflected the selective leaching of C-isotopically light, hydrophobic compounds from the leaves and the bark, because this DOM fraction is C-isotopically lighter than the hydrophilic compounds (Alvarez et al. 2023). The $\delta^{13}C$ values of DOM in throughfall and stemflow fell at the lower end of the range of the fresh leaves, and those in litter leachate resembled the least decomposed organic horizon, i.e., the Oi horizon. In the mineral soil solutions, the $\delta^{13}C$ values were higher than in litter leachate, pointing to roots and root exudates as the main belowground DOM sources, together with the preferential sorption of the isotopically light hydrophobic DOM onto the mineral surfaces and the preferential mineralization of isotopically light compounds during the passage through the mineral soil (Alvarez et al. 2023; Kalbitz et al. 2000; Wilcke et al. 2020). In the streamflow, the $\delta^{13}C$ values reflected a mixture of DOM, combining older and isotopically heavier compounds released by the mineralization of old soil organic matter with younger and isotopically lighter compounds delivered by fast lateral flow through the soil when it became saturated (Alvarez et al. 2023; Boy et al. 2008b; Wilcke et al. 2020). A single event of high $\delta^{13}C$ values was attributed to black carbon inputs from local pasture fires. The $\delta^{13}C$ values and the C/N ratios of DOM were not closely related, so that the $\delta^{13}C$ values and C/N ratios of DOM provided largely independent tools to assess the sources and transformations of DOM (Section B).

3.2. Nitrogen isotope composition of TDN (Section C)

The $\delta^{15}N$ values of TDN showed no seasonality and were not related to the monthly rainfall. The $\delta^{15}N$ values varied most strongly in rainfall, which pointed at temporally variable N sources. Throughfall was ^{15}N-depleted relative to rainfall, because the canopy retained isotopically heavy N, mainly ammonium, while isotopically lighter nitrate was leached. From throughfall via stemflow to litter leachate, the $\delta^{15}N$ values of TDN increased with the increasing contribution of DON, suggesting that DON was N-isotopically heavier than DIN. In the mineral topsoil solution, the $\delta^{15}N$ values were lower than in the litter leachate, because the likely N-isotopically heavy DON and ammonium were retained and isotopically lighter nitrate was added from mineralization and nitrification. From the topsoil

solution via the subsoil solution to the streamflow, the $\delta^{15}N$ values of TDN increased again, which indicated the loss of isotopically light gaseous N by an increasing denitrification with depth. The $\delta^{15}N$ values of TDN thus identified the nature and the size of the N sources and sinks along the water path (Section C).

3.3. Long-term DOM composition and stoichiometry (Section D)

The DON concentrations increased from rainfall via throughfall and stemflow to litter leachate, were much lower in mineral soil solutions, and decreased towards streamflow paralleling a similar vertical change of the DOC concentrations, while the DOP concentrations were highest in stemflow and were near or below the detection limit in rainfall, mineral soil solutions, and streamflow. During the 25 observation years, the DOC concentrations decreased in most solutions but increased in stemflow and litter leachate, so that the trends reported for the first 15 years continued (Wilcke et al. 2020). The DON concentrations increased in stemflow, litter leachate, and streamflow, driven by an enhanced mobilization of organic N from bark surfaces, epiphytes, and the organic layer, but decreased in mineral soil solutions, where DON was increasingly lost by mineralization and sorption. The DOP concentrations increased in throughfall, stemflow, and litter leachate, consistent with the progressive enrichment of the canopy and organic layer P pool by the sustained P deposition (Wilcke et al. 2019). DOP was almost completely retained in the mineral soil. The DOC/DON ratios decreased in all solutions and the DOC/DOP ratios decreased in throughfall and stemflow, which reflected a progressive enrichment in N and P. The DON/DOP ratios decreased in throughfall, because of the stronger leaching of DOP than DON from the canopy, but increased in litter leachate, where P was more tightly retained than N.

The $\delta^{13}C$ and $\delta^{15}N$ values of the solid-phase organic matter increased together from litterfall via the organic horizons to the mineral soil horizons and correlated closely, which reflected the coupled fractionation of C and N during the microbial decomposition (Lorenz et al. 2020; Nel et al. 2018). In the ecosystem solutions, the $\delta^{13}C$ and $\delta^{15}N$ values instead formed an aboveground and a belowground cluster, which reflected the mixing of sources and the transformation of DOM rather than a coupled C and N turnover. The $\delta^{15}N$ values increased along the water path within both clusters, governed by the increasing leaching of isotopically heavy DON in the aboveground cluster and by the increasing denitrification with depth in the belowground cluster, rather than by the coupled fractionation seen in the solid phase. The $\delta^{15}N$ values of DOM were not related to the DOC/DON ratios, so that the C/N

stoichiometry and the N isotope composition of DOM carried different and complementary information, as had been found for the $\delta^{13}C$ values and the C/N ratios (Alvarez et al. 2023). After 25 years of environmental change, the coupled C, N, and P cycles of the forest thus appeared to drift towards a new state, with N increasingly exported and P retained, as is typical of an emerging N saturation (Section D).

3.4. Synthesis: bringing the three approaches together

Combined, the three approaches describe the development of DOM concentrations and composition under the environmental change of the past 25 years. The $\delta^{13}C$ values located the sources and transformations of the organic C, the $\delta^{15}N$ values located the sources and sinks of the N, and the DOM composition and stoichiometry tracked how both, together with the P, changed over time. Each approach on its own resolved one part of the DOM dynamics along the water path, but only their combination revealed the direction of the change.

The solid-phase organic matter showed a tight coupling of the C and N cycles, with the $\delta^{13}C$ and $\delta^{15}N$ values increasing together along the decomposition gradient. The DOM along the water path did not inherit this coupling. The $\delta^{13}C$ values were shaped by the leaching of isotopically light hydrophobic compounds and by the root-derived inputs and the sorption in the mineral soil. The $\delta^{15}N$ values were shaped by the increasing leaching of isotopically heavy DON aboveground and by the increasing denitrification with depth belowground. The composition and stoichiometry of DOM showed a progressive enrichment of N and P over the 25 years, with N increasingly exported in the draining water while P was retained in the soil. Whereas the $\delta^{13}C$ and $\delta^{15}N$ values increased in parallel in the solid phase, pointing to a coupled C and N turnover during decomposition, they varied independently in DOM, where each isotope ratio followed its own set of processes along the water path. The C and N cycles were therefore tightly linked in the solid organic matter but became decoupled in DOM.

Thus, the three approaches converged on the same conclusion. The sustained N deposition, the continuous P input, and the warmer and drier climate moved the forest towards an emerging N saturation, in which the N was increasingly mobilized and exported with the draining water while the P was retained within the ecosystem. This integrated reading, which no single tracer could provide on its own, is the central result of the thesis.

3.5. Uncertainties or limitations

The three approaches in Sections A-C relied on different subperiods and sample sets, the $\delta^{13}C$ values on monthly composite samples and the $\delta^{15}N$ values on quarterly composite samples from 2013 to 2016, and the long-term trends of the concentrations, fluxes, and stoichiometric ratios on the full record from 1998 to 2023. The water fluxes of the litter leachate and the mineral soil solutions were modeled, with a higher uncertainty in the mineral soil and particularly at greater depth. The DOP data were available only from 2003 onward and were near or below the detection limit in several solutions. The stemflow and the streamflow were each sampled at a single station, which limited their spatial representativeness.

As is generally the case when stable isotope ratios are interpreted in natural ecosystems, the complete understanding of the $\delta^{13}C$ and $\delta^{15}N$ values of DOM requires their combination with further DOM properties. Part of this information was measured in this study, such as the C, N and P concentrations and fluxes and the stoichiometric ratios, while the radiocarbon age of DOM had been determined earlier at the site (Wilcke et al. 2020). Future studies could assess more DOM properties e.g., the contributions of hydrophobic and hydrophilic fractions or detailed chemical properties measured with UV-vis absorption, fluorescence spectroscopy combined with parallel factor analysis (PARAFAC) or Fourier transform ion cyclotron resonance mass spectrometry (FT-ICR-MS) as in the study of Thieme et al. (2019).

With the measurement of the $\delta^{15}N$ values of TDN, I only obtained a bulk information for all different chemical N species together. The compound-specific analysis of the major N species including ammonium, nitrate and DON could deliver even more detailed information about the N turnover in the study forest. The study of Schwarz et al. (2011) indicated, for instance, an influence of the soil moisture content on the degree of stable N isotope fractionation in nitrate in the ecosystem solutions along the water path in the same study forest in Ecuador. Thus, the compound-specific isotope analysis might help in elucidating more details of the responses of N turnover processes to the changing environmental conditions, which include rising DIN inputs and increasingly less waterlogging.

A particular gap concerns the P cycle, which we could not trace isotopically as we did for the C and N cycles. Phosphorus has only one stable isotope, so it cannot be analyzed

through its own isotopic composition. The established alternative is the oxygen isotope composition of phosphate ($\delta^{18}O\text{-}PO_4$), as a proxy for the P cycle, because phosphate is strongly bonded to oxygen, and the P-O bond is broken mainly by biological, enzyme-mediated reactions that exchange oxygen with the ambient water (Blake et al. 1997). The $\delta^{18}O\text{-}PO_4$ values have been used to identify P sources, to distinguish source-derived from biologically cycled phosphate, and to follow P transformation and uptake in soils and waters (Gross and Angert 2015; Tamburini et al. 2014). Such values were not determined here, because their analysis requires the extraction, purification, and precipitation of the phosphate as silver phosphate before measurement (McLaughlin et al. 2004; Tamburini et al. 2010), and the methods remain demanding and are not yet fully standardized, particularly for solutions with low phosphate concentrations (Davies et al. 2014) found at our study site. Their determination could have located the P sources and sinks along the water path, distinguished the signatures of the inorganic phosphate and the phosphate bound in DOP, and resolved which P forms were preferentially retained in the canopy and the organic layer and which were leached, just as the $\delta^{13}C$ and $\delta^{15}N$ values helped to understand the C and N dynamics. Among the C, N, and P cycles, the P cycle thus remained the least isotopically constrained, and its characterization with the help $\delta^{18}O\text{-}PO_4$ is a promising direction for future work.

4. General conclusions

The $\delta^{13}C$ values of DOM traced the sources and transformations of the organic C along the water path. They decreased aboveground because isotopically light hydrophobic compounds were leached from the leaves and the bark, and increased in mineral soil solutions, where roots and root exudates contributed belowground DOM and the isotopically light fraction was preferentially sorbed and mineralized. In streamflow, they reflected a mixture of older DOM from the mineralization of old soil organic matter and younger DOM delivered by fast lateral flow. Because the $\delta^{13}C$ values and the C/N ratios were not consistently related, the $\delta^{13}C$ value provided additional information that the C/N ratio did not include (**Section B**).

The $\delta^{15}N$ values of TDN identified the N sources and sinks along the water path. The canopy retained isotopically heavy N and isotopically lighter nitrate and DON were leached, so that throughfall had lower $\delta^{15}N$ values than rainfall. The $\delta^{15}N$ values of TDN then increased toward litter leachate with the increasing leaching of isotopically heavy DON. In the mineral topsoil, where DON and ammonium were retained and nitrate was added from mineralization and nitrification, the $\delta^{15}N$ values of TDN decreased but increased again toward streamflow with the loss of isotopically light N by an increasing denitrification with depth (**Section C**).

During the observation period of 25 years from 1998 to 2023, DON and DOP concentrations and fluxes increased and the DOC/DON and DOC/DOP ratios decreased, which indicated a progressive enrichment of N and P in DOM. DON concentrations increased in stemflow, litter leachate, and streamflow but decreased in mineral soil solutions, whereas DOP concentrations increased in throughfall, stemflow, and litter leachate, reflecting the progressive enrichment of the canopy and the organic layer with P from sustained atmospheric deposition. The DOP cycling remained restricted to the aboveground ecosystem, with concentrations near or below the detection limit in the mineral soil and streamflow. The N was increasingly mobilized and exported with streamflow, whereas the P was retained within the ecosystem (**Section D**). Overall, the observed changes in the stoichiometry of DOM indicated that the study ecosystem approached N saturation with an increasing importance of P as growth-limiting element. Thus, the studied remote tropical forest clearly drifted to another state only because of global environmental change in spite of the absence of strong direct anthropogenic impacts.

In my thesis, I found that assessing DOM and TDN through the C and N isotope compositions, respectively, together with the elemental composition of DOM revealed a spatial and temporal development of DOM that no single tracer could have shown, that is, the partial decoupling of the dissolved C, N, and P cycles under environmental change. However, my findings are based on the measurement of stable isotope ratios that contributed to a better understanding of the C and N cycles but not the P cycle, and that could yield even more value in combination with an isotopic characterization of the major chemical N species (ammonium, nitrate and DON) and further properties of DOM. Therefore, future research should try to trace the P cycle with the oxygen isotopes of phosphate, determine the N isotope composition of the N species and further characterize the chemical composition of DOM.

5. Author contributions

I prepared the samples, generated the isotope data, and carried out the laboratory measurements of the carbon and nitrogen isotope studies together with Andre Velescu (Sections B and C). I implemented the stable isotope measurements of DOM, by TOC-LCM-IRMS for the liquid phase and EA-IRMS for the solid phase, and performed the formal analysis, the visualization, and all statistical analyses (Sections B to D). I wrote the original drafts of all chapters (Sections A to D). I conducted this work with a four-year doctoral scholarship from the Secretary of Higher Education, Science, Technology and Innovation of Ecuador (SENESCYT).

Andre Velescu prepared the instruments for the measurement of the TOC concentrations, the DOM properties, and the stable isotope ratios, organized the collection of the samples in Ecuador with the help of local field helpers, particularly José Luis Peña Caivinagua, and the transport of the samples to Germany, contributed to the measurement and the data collection, and commented on the manuscript drafts (Sections B to D).

Kerstin Pierick provided root samples and contributed to the root sampling methodology. She helped with suggestions to improve the first and second drafts (Sections B and C).

Jürgen Homeier provided root and leaf samples as well as stable isotope data from several tree species, which helped address some reviewer comments. He helped with the project administration and the funding acquisition (DFG) and contributed with suggestions to improve the first and second drafts (Sections B and C).

Wolfgang Wilcke contributed the conceptualization, the methodology, the project administration, the funding acquisition (DFG), the resources, participated in the investigation, and supervised this thesis and its manuscripts (Sections A to D).

6. References

Alvarez, P., Velescu, A., Pierick, K., Homeier, J., & Wilcke, W. (2023). Carbon stable isotope ratio of dissolved organic matter as a tool to identify its sources and transformations in a tropical montane forest in Ecuador. *Environmental Science & Technology, 57*, 14983-14993. https://doi.org/10.1021/acs.est.3c01623

Alvarez, P., Velescu, A., Pierick, K., Homeier, J., & Wilcke, W. (2024). Sources and sinks of N in ecosystem solutions along the water path through a tropical montane forest in Ecuador assessed with $\delta^{15}N$ values of total dissolved nitrogen. *Journal of Geophysical Research: Biogeosciences, 129*, e2024JG008043. https://doi.org/10.1029/2024JG008043

Barkley, A. E., Prospero, J. M., Mahowald, N., Hamilton, D. S., Popendorf, K. J., Oehlert, A. M., et al. (2019). African biomass burning is a substantial source of phosphorus deposition to the Amazon, Tropical Atlantic Ocean, and Southern Ocean. Proceedings of the National Academy of Sciences, 116(33), 16216-16221. https://doi.org/10.1073/pnas.1906091116

Bendix, J., Dobbermann, M., & Werner, N. (2018). Climate station data from ECSF Thies station. Updated on 2026-05-22. Retrieved from: http://www.tropicalmountainforest.org/data_pre.do?citid=1713

Bendix, J. (2020). ECSF climate station best estimate Ver. 3 1998-2020. Retrieved from: http://www.tropicalmountainforest.org/data_pre.do?citid=1876

Blake, R. E., O'Neil, J. R., & Garcia, G. A. (1997). Oxygen isotope systematics of biologically mediated reactions of phosphate: I. Microbial degradation of organophosphorus compounds. *Geochimica et Cosmochimica Acta, 61*, 4411-4422. https://doi.org/10.1016/S0016-7037(97)00272-X

Borken, W., Ahrens, B., Schulz, C., & Zimmermann, L. (2011). Site-to-site variability and temporal trends of DOC concentrations and fluxes in temperate forest soils. *Global Change Biology, 17*, 2428-2443. https://doi.org/10.1111/j.1365-2486.2011.02390.x

Bowling, D. R., Pataki, D. E., & Randerson, J. T. (2008). Carbon isotopes in terrestrial ecosystem pools and CO2 fluxes. *New Phytologist, 178*, 24-40. https://doi.org/10.1111/j.1469-8137.2007.02342.x

Boy, J., Rollenbeck, R., Valarezo, C., & Wilcke, W. (2008a). Amazonian biomass burning-derived acid and nutrient deposition in the north Andean montane forest of Ecuador. *Global Biogeochemical Cycles, 22*, GB4011. https://doi.org/10.1029/2007GB003158

Boy, J., Valarezo, C., & Wilcke, W. (2008b). Water flow paths in soil control element exports in an Andean tropical montane forest. *European Journal of Soil Science, 59*(6), 1209-1227. https://doi.org/10.1111/j.1365-2389.2008.01063.x

Boy, J., & Wilcke, W. (2008). Tropical Andean forest derives calcium and magnesium from Saharan dust. *Global Biogeochemical Cycles, 22*, GB1027. https://doi.org/10.1029/2007GB002960

Brüggemann, N., Gessler, A., Kayler, Z., Keel, S. G., Badeck, F., et al. (2011). Carbon allocation and carbon isotope fluxes in the plant-soil-atmosphere continuum: a review. *Biogeosciences, 8*, 3457-3489. https://doi.org/10.5194/bg-8-3457-2011

Bruijnzeel, L. A., & Hamilton, L. S. (2000). *Decision time for cloud forests. IHP Humid Tropics Programme Series, vol 13*. IHP-UNESCO, IUCN and WWF, Paris, France.

Camino-Serrano, M., Gielen, B., Luyssaert, S., Ciais, P., Vicca, S., Guenet, B., et al. (2014). Linking variability in soil solution dissolved organic carbon to climate, soil type, and vegetation type. *Global Biogeochemical Cycles, 28*, 497-509. https://doi.org/10.1002/2013GB004726

Cleveland, C. C., & Liptzin, D. (2007). C:N:P stoichiometry in soil: is there a Redfield ratio for the microbial biomass? *Biogeochemistry, 85*, 235-252. https://doi.org/10.1007/s10533-007-9132-0

Dai, M., Yin, Z., Meng, F., Liu, Q., & Cai, W.-J. (2012). Spatial distribution of riverine DOC inputs to the ocean: an updated global synthesis. *Current Opinion in Environmental Sustainability, 4*, 170-178. https://doi.org/10.1016/j.cosust.2012.03.003

Davies, C. L., Surridge, B. W. J., & Gooddy, D. C. (2014). Phosphate oxygen isotopes within aquatic ecosystems: global data synthesis and reproducibility assessment. *Science of the Total Environment, 496*, 563-575. https://doi.org/10.1016/j.scitotenv.2014.07.057

DVWK. (1996). *Ermittlung der Verdunstung von Land-und Wasserflächen*. Retrieved from Bonn, Germany.

Evans, C. D., Goodale, C. L., Caporn, S. J. M., Dise, N. B., Emmett, B. A., Fernandez, I. J., et al. (2008). Does elevated nitrogen deposition or ecosystem recovery from acidification drive increased dissolved organic carbon loss from upland soil? A review of evidence from field nitrogen addition experiments. *Biogeochemistry, 91*, 13-35. https://doi.org/10.1007/s10533-008-9256-x

Federherr, E., Cerli, C., Kirkels, F. M. S. A., Kalbitz, K., Kupka, H. J., Dunsbach, R., et al. (2014). A novel high-temperature combustion based system for stable isotope analysis of dissolved organic carbon in aqueous samples. I: development and validation. *Rapid Communications in Mass Spectrometry, 28*, 2559-2573. https://doi.org/10.1002/rcm.7051

Federherr, E., Kupka, H. J., Cerli, C., Kalbitz, K., Dunsbach, R., Loos, A., et al. (2016). A novel tool for stable nitrogen isotope analysis in aqueous samples. Rapid Communications in Mass Spectrometry, 30(23), 2537-2544. https://doi.org/10.1002/rcm.7740

Galloway, J. N., Dentener, F. J., Capone, D. G., Boyer, E. W., Howarth, R. W., Seitzinger, S. P., et al. (2004). Nitrogen cycles: past, present, and future. *Biogeochemistry, 70*, 153-226. https://doi.org/10.1007/s10533-004-0370-0

Galloway, J. N., Townsend, A. R., Erisman, J. W., Bekunda, M., Cai, Z., Freney, J. R., et al. (2008). Transformation of the nitrogen cycle: recent trends, questions, and potential solutions. *Science, 320*, 889-892. https://doi.org/10.1126/science.1136674

Gandois, L., Teisserenc, R., Cobb, A. R., Chieng, H. I., Lim, L. B. L., Kamariah, A. S., et al. (2014). Origin, composition, and transformation of dissolved organic matter in tropical peatlands. *Geochimica et Cosmochimica Acta, 137*, 35-47. https://doi.org/10.1016/j.gca.2014.03.012

Gerschlauer, F., Saiz, G., Schellenberger Costa, D., Kleyer, M., Dannenmann, M., & Kiese, R. (2019). Stable carbon and nitrogen isotopic composition of leaves, litter, and soils of various ecosystems along an elevational and land-use gradient at Mount Kilimanjaro, Tanzania. *Biogeosciences, 16*, 409-424. https://doi.org/10.5194/bg-16-409-2019

Goller, R., Wilcke, W., Fleischbein, K., Valarezo, C., & Zech, W. (2006). Dissolved nitrogen, phosphorus, and sulfur forms in the ecosystem fluxes of a montane forest in Ecuador. *Biogeochemistry, 77*, 57-89. https://doi.org/10.1007/s10533-005-1061-1

Gross, A., & Angert, A. (2015). What processes control the oxygen isotopes of soil bioavailable phosphate? *Geochimica et Cosmochimica Acta, 159*, 100-111. https://doi.org/10.1016/j.gca.2015.03.023

Hirsch, R. M., Slack, J. R., & Smith, R. A. (1982). Techniques of trend analysis for monthly water quality data. *Water Resources Research, 18*, 107-121. https://doi.org/10.1029/WR018i001p00107

Hood, E., Williams, M., & McKnight, D. (2005). Sources of dissolved organic matter (DOM) in a Rocky Mountain stream using chemical fractionation and stable isotopes. *Biogeochemistry, 74*, 231-255. https://doi.org/10.1007/s10533-004-4322-5

Jiang, X., Wang, X., Qiao, Y., Cao, Y., Jiao, Y., Yang, A., et al. (2024). Atmospheric nitrogen deposition affects forest plant and soil system carbon:nitrogen:phosphorus stoichiometric flexibility: A meta-analysis. Forest Ecosystems, 11, 100192. https://doi.org/10.1016/j.fecs.2024.100192

Kalbitz, K., Solinger, S., Park, J.-H., Michalzik, B., & Matzner, E. (2000). Controls on the dynamics of dissolved organic matter in soils: a review. *Soil Science, 165*, 277-304. https://doi.org/10.1097/00010694-200004000-00001

Kirkels, F. M. S. A., Cerli, C., Federherr, E., Gao, J., & Kalbitz, K. (2014). A novel high-temperature combustion based system for stable isotope analysis of dissolved organic carbon in aqueous samples. II: optimization and assessment of analytical performance. *Rapid Communications in Mass Spectrometry, 28*, 2574-2586. https://doi.org/10.1002/rcm.7053

Kohn, M. J. (2010). Carbon isotope compositions of terrestrial C3 plants as indicators of (paleo)ecology and (paleo)climate. *Proceedings of the National Academy of Sciences, 107*, 19691-19695. https://doi.org/10.1073/pnas.1004933107

Lamarque, J. F., Dentener, F., McConnell, J., Ro, C. U., Shaw, M., Vet, R., et al. (2013). Multi-model mean nitrogen and sulfur deposition from the Atmospheric Chemistry and Climate Model Intercomparison Project (ACCMIP): evaluation of historical and projected future changes. *Atmos. Chem. Phys., 13*(16), 7997-8018. https://doi.org/10.5194/acp-13-7997-2013

Lange, D. F., Schröter, S. A., da Luz, F. M., Pires, E., Santos, Y. R., da Silva, J. S., et al. (2024). Cycling of dissolved organic nutrients and indications for nutrient limitations in contrasting Amazon rainforest ecosystems. Biogeochemistry, 167(12), 1567-1588. https://doi.org/10.1007/s10533-024-01187-3

Leuschner, C., Zach, A., Moser, G., Homeier, J., Graefe, S., Hertel, D., et al. (2013). The carbon balance of tropical mountain forests along an altitudinal transect. In J. Bendix, E. Beck, A. Bräuning, F. Makeschin, R. Mosandl, S. Scheu, & W. Wilcke (Eds.), *Ecosystem services, biodiversity and environmental change in a tropical mountain ecosystem of south Ecuador* (pp. 117-139). Springer, Berlin, Heidelberg. https://doi.org/10.1007/978-3-642-38137-9_10

Lorenz, M., Derrien, D., Zeller, B., Udelhoven, T., Werner, W., & Thiele-Bruhn, S. (2020). The linkage of ^{13}C and ^{15}N soil depth gradients with C/N and O/C stoichiometry reveals tree species effects on organic matter turnover in soil. *Biogeochemistry, 151*, 203-220. https://doi.org/10.1007/s10533-020-00721-3

McLaughlin, K., Silva, S., Kendall, C., Stuart-Williams, H., & Paytan, A. (2004). A precise method for the analysis of $\delta^{18}O$ of dissolved inorganic phosphate in seawater. *Limnology and Oceanography: Methods, 2*, 202-212. https://doi.org/10.4319/lom.2004.2.202

Michalzik, B., Kalbitz, K., Park, J.-H., Solinger, S., & Matzner, E. (2001). Fluxes and concentrations of dissolved organic carbon and nitrogen: a synthesis for temperate forests. *Biogeochemistry, 52*, 173-205. https://doi.org/10.1023/A:1006441620810

Neff, J. C., Hobbie, S. E., & Vitousek, P. M. (2000). Nutrient and mineralogical control on dissolved organic C, N and P fluxes and stoichiometry in Hawaiian soils. *Biogeochemistry, 51*, 283-302. https://doi.org/10.1023/A:1006414517212

Nel, J. A., Craine, J. M., & Cramer, M. D. (2018). Correspondence between ^{13}C and ^{15}N in soils suggests coordinated fractionation processes for soil C and N. *Plant and Soil, 423*, 257-271. https://doi.org/10.1007/s11104-017-3500-x

Qualls, R. G., & Haines, B. L. (1991). Geochemistry of dissolved organic nutrients in water percolating through a forest ecosystem. *Soil Science Society of America Journal, 55*, 1112-1123. https://doi.org/10.2136/sssaj1991.03615995005500040036x

Regnier, P., Friedlingstein, P., Ciais, P., Mackenzie, F. T., Gruber, N., et al. (2013). Anthropogenic perturbation of the carbon fluxes from land to ocean. *Nature Geoscience, 6*, 597-607. https://doi.org/10.1038/ngeo1830

Saunders, T. J., McClain, M. E., & Llerena, C. A. (2006). The biogeochemistry of dissolved nitrogen, phosphorus, and organic carbon along terrestrial-aquatic flowpaths of a montane headwater catchment in the Peruvian Amazon. Hydrological processes, 20(12), 2549-2562. https://doi.org/10.1002/hyp.6215

Schrumpf, M., Guggenberger, G., Valarezo, C., & Zech, W. (2001). Tropical montane rain forest soils: development and nutrient status along an altitudinal gradient in the South Ecuadorian Andes. *Erde, 132*, 43-59.

Schrumpf, M., Zech, W., Lehmann, J., & Lyaruu, H. V. C. (2006). TOC, TON, TOS and TOP in rainfall, throughfall, litter percolate and soil solution of a montane rainforest succession at Mt. Kilimanjaro, Tanzania. *Biogeochemistry, 78*, 361-387. https://doi.org/10.1007/s10533-005-4428-4

Schwarz, M. T., Oelmann, Y., & Wilcke, W. (2011). Stable N isotope composition of nitrate reflects N transformations during the passage of water through a montane rain forest in Ecuador. *Biogeochemistry, 102*, 195-208. https://doi.org/10.1007/s10533-010-9434-5

Tamburini, F., Bernasconi, S. M., Angert, A., Weiner, T., & Frossard, E. (2010). A method for the analysis of the $\delta^{18}O$ of inorganic phosphate extracted from soils with HCl. *European Journal of Soil Science, 61*, 1025-1032. https://doi.org/10.1111/j.1365-2389.2010.01290.x

Tamburini, F., Pfahler, V., von Sperber, C., Frossard, E., & Bernasconi, S. M. (2014). Oxygen isotopes for unraveling phosphorus transformations in the soil-plant system: a review. *Soil Science Society of America Journal, 78*, 38-46. https://doi.org/10.2136/sssaj2013.05.0186dgs

Thieme, L., Graeber, D., Hofmann, D., Bischoff, S., Schwarz, M. T., Steffen, B., et al. (2019). Dissolved organic matter characteristics of deciduous and coniferous forests with variable management: different at the source, aligned in the soil. *Biogeosciences, 16*(7), 1411-1432. https://doi.org/10.5194/bg-16-1411-2019

Van Langenhove, L., Verryckt, L. T., Bréchet, L., Courtois, E. A., Stahl, C., Hofhansl, F., et al. (2020). Atmospheric deposition of elements and its relevance for nutrient budgets of tropical forests. Biogeochemistry, 149(2), 175-193. https://doi.org/10.1007/s10533-020-00673-8

Wang, R., Goll, D., Balkanski, Y., Hauglustaine, D., Boucher, O., Ciais, P., et al. (2017). Global forest carbon uptake due to nitrogen and phosphorus deposition from 1850 to 2100. *Global Change Biology, 23*(11), 4854-4872. https://doi.org/10.1111/gcb.13766

Wilcke, W., Yasin, S., Abramowski, U., Valarezo, C., & Zech, W. (2002). Nutrient storage and turnover in organic layers under tropical montane rain forest in Ecuador. *European Journal of Soil Science, 53*, 15-27. https://doi.org/10.1046/j.1365-2389.2002.00411.x

Wilcke, W., Leimer, S., Peters, T., Emck, P., Rollenbeck, R., Trachte, K., Valarezo, C., & Bendix, J. (2013). The nitrogen cycle of tropical montane forest in Ecuador turns inorganic under environmental change. Global Biogeochemical Cycles, 27(4), 1194-1204. https://doi.org/10.1002/2012GB004471

Wilcke, W., Velescu, A., Leimer, S., Bigalke, M., Boy, J., & Valarezo, C. (2017). Biological versus geochemical control and environmental change drivers of the base

metal budgets of a tropical montane forest in Ecuador during 15 years. *Biogeochemistry, 136*, 167-189. https://doi.org/10.1007/s10533-017-0386-x

Wilcke, W., Velescu, A., Leimer, S., Bigalke, M., Boy, J., & Valarezo, C. (2019). Temporal trends of phosphorus cycling in a tropical montane forest in Ecuador during 14 years. *Journal of Geophysical Research: Biogeosciences, 124*, 1370-1386. https://doi.org/10.1029/2018JG004942

Wilcke, W., Velescu, A., Leimer, S., Blotevogel, S., Alvarez, P., & Valarezo, C. (2020). Total organic carbon concentrations in ecosystem solutions of a remote tropical montane forest respond to global environmental change. *Global Change Biology, 26*, 6989-7005. https://doi.org/10.1111/gcb.15351

B. $\delta^{13}C$ values of DOM

The carbon stable isotope ratio of dissolved organic matter as a tool to identify its sources and transformations in a tropical montane forest in Ecuador

Pablo Alvarez[1,2], Andre Velescu[1], Kerstin Pierick[3], Jürgen Homeier[4,5] & Wolfgang Wilcke[1]

[1] Institute of Geography and Geoecology, Karlsruhe Institute of Technology (KIT), Reinhard-Baumeister-Platz 1, 76131 Karlsruhe, Germany

[2] Faculty of Agricultural Sciences, National University of Loja, Ciudadela Universitaria Guillermo Falcone, 110103 Loja, Ecuador

[3] Spatial Structures and Digitization of Forests / Silviculture and Forest Ecology of the Temperate Zones, Georg August University Göttingen, 37077 Göttingen, Germany

[4] Faculty of Resource Management, University of Applied Sciences and Arts, 37077 Göttingen, Germany

[5] Department of Plant Ecology and Ecosystem Research, Georg August University Göttingen, 37073 Göttingen, Germany

Environmental Science & Technology (2023): 57, 14983–14993:

https://doi.org/10.1021/acs.est.3c01623

1. Abstract

Dissolved organic matter (DOM) contributes to forest C cycling. We assessed temporal variability, sources, and transformations of DOM during four years in a tropical montane forest with the help of stable C isotope ratios ($\delta^{13}C$ values). We measured $\delta^{13}C$ values of DOM in rainfall (RF), *throughfall* (TF), stemflow (SF), litter leachate (LL), soil solutions at the 0.15 and 0.30 m depths (SS15, SS30), and streamflow (ST) with TOC-IRMS. The $\delta^{13}C$ values of DOM did not vary seasonally. We detected an event with a high $\delta^{13}C$ value, likely attributable to black carbon from local pasture fires. The mean $\delta^{13}C$ values of DOM outside the event decreased in the order, RF (-26.0±1.3‰) > TF (-28.7±0.3‰) > SF (-29.2±0.2‰) > LL (-29.6±0.2‰) because of increasing leaching of C-isotopically light compounds. The higher $\delta^{13}C$ values of DOM in SS15 (-27.8±1.0‰), SS30 (-27.6±1.1‰), and ST (-27.9±1.1‰) than in the aboveground solutions suggested that roots and root exudates are major belowground DOM sources. Although in DOM the C/N ratios correlated with the $\delta^{13}C$ values when all solutions were considered, this was not the case for SS15, SS30, and ST alone. Thus, the $\delta^{13}C$ values of DOM provide an additional tool to assess sources and turnover of DOM.

Keywords: atmospheric deposition event, C/N ratios of dissolved organic matter, $\delta^{13}C$ values of dissolved organic matter, ecosystem solutions, water path

Synopsis: Carbon stable isotope ratios of dissolved organic matter in forest ecosystem solutions inform about its sources and transformations.

2. Introduction

Dissolved organic matter (DOM) is a complex mixture of organic molecules. The DOM sources include leached compounds from aboveground organism biomass, plant litter, soil organic matter, root exudates and microbial metabolites (Kalbitz et al., 2000). The ratio of the natural abundance of the two stable C isotopes (^{12}C and ^{13}C), usually expressed as a difference to that of the international standard Pee Dee Belemnite as $\delta^{13}C$ value, is a widely used tool in ecology (Michener & Lajtha, 2008), which could also help trace sources and transformations of DOM. However, $\delta^{13}C$ values of DOM from terrestrial ecosystems have rarely been reported, likely because routine technology to run such measurements directly in solution has only become available in the past decade and is still not widespread (Federherr et al., 2014; Kirkels et al., 2014). The direct measurement of the $\delta^{13}C$ values of DOM with the novel TOC-IRMS device avoids freeze-drying of usually large sample volumes to collect DOM as solid-state sample for subsequent EA-IRMS measurements and can therefore be more easily applied to the large number of small-volume samples collected in long-term ecosystem studies. The $\delta^{13}C$ value of DOM from forest ecosystem solutions can be used to assess sources and transformations of DOM possibly adding information that more easily accessible DOM properties like the C/N ratio do not include. Source identification of DOM with the help of $\delta^{13}C$ values requires the knowledge of the $\delta^{13}C$ values of the solid-phase organic matter in ecosystems (e.g., leaves, litter, soil organic matter, roots), which are potential DOM sources. Moreover, the $\delta^{13}C$ values of DOM resulting from a multitude of sources and transformations in forest ecosystems might only be interpreted with the help of additional information such as the size of the C fluxes, the age of the C pools, or other chemical DOM properties including C/N ratios (Gandois et al., 2014; Hood et al., 2005; Solinger et al., 2001).

By far, most forest trees use the C_3 photosynthetic pathway resulting in $\delta^{13}C$ values of -22‰ to -30‰ (Kohn, 2010). The $\delta^{13}C$ value of plant tissue is species-specific and responds to competition for light and nutrients (Heaton, 1999), temperature, air humidity, CO_2 concentrations, and soil moisture (Dawson et al., 2002). Water stress causes the stomata of the leaves to close for longer times, which results in a more exhaustive depletion of the CO_2 in the stomata, reducing the isotopic fractionation and thus causing a higher $\delta^{13}C$ value than during wet phases when the stomata are open for longer times (Damesin et al., 1998). For tropical montane forest ecosystems on shallow soils without clear climate seasonality, but

with short dry periods, it is unknown if the $\delta^{13}C$ values of trees respond to the soil moisture conditions.

The chemical composition of DOM in throughfall and stemflow is determined by the input of organic compounds leached from the canopy and bark resulting in higher DOM concentrations in throughfall and stemflow relative to rainfall (Van Stan & Stubbins, 2018). In temperate and tropical coniferous forests, throughfall contained more hydrophobic DOM than rainfall, which was attributed to an enrichment of microbial degradation products of aromatic lignin leached from the tree surfaces (Ciglasch et al., 2004; Guggenberger & Zech, 1993, 1994). The literature suggests that part of the DOM in throughfall originates from freshly produced plant and microbial metabolites (Guggenberger et al., 1994), for which it can be assumed that they show a lower $\delta^{13}C$ value than DOM leached from more degraded organic matter in which ^{13}C accumulates (Guggenberger et al., 1998; Sanderman et al., 2008).

In the solutions of the organic layer (i.e., litter leachate) and of the mineral soil, additionally to the fresh plant and microbial metabolites, DOM with high $\delta^{13}C$ values might be released from the C-isotopically heavier aged soil organic matter (SOM). In an experiment with ^{13}C-labeled Norway spruce litter, Fröberg et al. (2007) observed that the fresh litter only contributed ca. 5% to the DOM in litter leachate and concluded that most of the DOM in litter leachate originated from the O horizon. The latter coincides with the finding that in a tropical montane forest, the $\Delta^{14}C$-dated ages (i.e., dated with the help of the radioactive ^{14}C fallout) of the organic layer and the DOM in litter leachate were with approximately one decade similar (Wilcke et al., 2020). Because $\delta^{13}C$ values of roots are reported to be 1.0-2.3‰ higher than those of leaves (Badeck et al., 2005; Bowling et al., 2008), an alternative explanation for the possibly higher $\delta^{13}C$ values of DOM in the mineral soil solution than in throughfall, stemflow, and litter leachate might also be a larger contribution of root organic matter to DOM (Tückmantel et al., 2017). Moreover, microbial biomass is reported to be C-isotopically heavier than bulk SOM and thus could also contribute to higher $\delta^{13}C$ values of DOM in soils (Blagodatskaya et al., 2011; Dijkstra et al., 2006).

The DOM concentrations, fluxes, and composition in stream water are regulated by rainfall intensity and seasonality, preceding soil water content (Xu et al., 2012), and leaching from the soil (Xu & Saiers, 2010). In sloping water catchments, a high rainfall intensity on wet soil can result in fast surface-near lateral flow through soil layers with high

concentrations of comparatively young organic matter (Boy et al., 2008b; Goller et al., 2005). Thus, fast lateral flow might contribute younger and C-isotopically lighter DOM. Conversely, mineralization of aged SOM in the deeper soil layers e.g., by rhizosphere microorganisms associated with deep roots (Shahzad et al., 2018), may contribute C-isotopically heavier DOM. For a headwater stream in a tropical montane forest, Wilcke et al. (2020) suggested that DOM might be a mixture of old SOM and recalcitrant younger, C-isotopically lighter compounds that percolated rapidly through the soil profile by preferential flow, because they found a $\Delta^{14}C$-dated age of approximately 50 years, which was younger than that of the solid phase organic matter in the subsoil (approximately 115 years).

Our overall goal was to assess the potential of the $\delta^{13}C$ values of DOM to elucidate the sources and turnover of DOM in a tropical montane forest of Ecuador, for which Wilcke et al. (2020) had shown that DOM concentrations and TOC/DON ratios had decreased in most ecosystem solutions from 1998-2013. The results of Wilcke et al. (2020) reflected global change consisting of decreasing soil moisture in an otherwise very wet ecosystem and N deposition. A better understanding of DOM sources and turnover will therefore help assess the effect of global change on the dissolved C cycle in forest ecosystems. We hypothesized that (i) there is a seasonal pattern of the $\delta^{13}C$ values of DOM in all ecosystem fluxes, because the more efficient photosynthetic use of atmospheric CO_2 during a short dry phase at the end of the year could be reflected by higher $\delta^{13}C$ values of DOM than during the wetter phase. (ii) In the aboveground ecosystem fluxes throughfall and stemflow, the $\delta^{13}C$ values of the DOM are determined by the leaching of fresh plant and microbial metabolites from leaves and bark with low $\delta^{13}C$ values. In the belowground ecosystem fluxes, DOM shows similar $\delta^{13}C$ values (iiia) in the litter leachate as in its main source, the bulk organic layer and (iiib) in the mineral soil solutions as the roots of C_3 plants and microbial biomass. (iv) The DOM in streamflow is a mixture of C-isotopically heavy SOM and recalcitrant C-isotopically light compounds of young age that originate from the aboveground ecosystem and are hardly retained in the soil.

3. Material and methods

3.1. Study Area

We studied a 9.1-ha catchment in a tropical montane rain forest between 1850 and 2200 m above sea level (a.s.l.) on the east-exposed slope of the eastern Andean cordillera, located in the San Francisco Biological Reserve in southern Ecuador. The same catchment

has been described in previous work as Microcatchment 2 (Boy et al., 2008b; Wilcke et al., 2017, 2020). During the period from April 1998 to March 2013, the average annual precipitation was 2320±238 mm and the mean annual temperature 14.9°C (Wilcke et al., 2020). In spite of a short dry spell, the "veranillo", at the end of the year (Figure B-S1), the study area was consistently humid with only a small variation in temperature (Figure B-S2). The studied forest is a lower montane forest (Homeier et al., 2008) further described in Homeier et al. (2010). Soils are mainly shallow Folic Dystric Cambisols (IUSS Working Group WRB, 2014) developed from metamorphic rock (phyllite and quartzite). Table B-S1 summarizes selected soil properties that drive DOM concentrations.

3.2. Field sampling

Young sunlight-exposed leaves of the 10 most abundant tree species of the study forest were sampled monthly from November 2005 to February 2006 (**Table B-S2**). Species-specific tree fine root segments (diameter ≤ 2 mm, length >10 cm) were sampled in 2016, washed with tap-water and dried at 60 °C. More details of the root analysis can be found in Pierick et al. (2021) To test whether the $\delta^{13}C$ values of the leaves have changed between the sampling in 2005/2006 and our observation period from 2013-2016, we analyzed leaves of one of the locally most abundant species, i.e., *Graffenrieda emarginata* Triana, from 2005 to 2015 and did not observe a systematic temporal variation (**Figure B-S3**). Litterfall, soil, and soil solution samples were collected along three transects located at ca. 1900, ca. 1950, and ca. 2000 m a.s.l. Litterfall was collected weekly from January 2013 to December 2016 with three 0.25 m^2 traps per transect, which consisted of PE nets with a mesh width of 0.5 mm held by PVC frames. The litterfall collection was considered representative of the whole forest canopy. Samples of the slightly (Oi), moderately (Oe), and highly decomposed (Oa) organic horizons and of the A, B, and C mineral horizons of 21 soil profiles near the three transects were collected in the years 2006 and 2016. We did not remove roots from the organic layer samples. All solid phase samples were dried to a constant mass at 40 °C in a drying oven. Litterfall samples were monthly bulked. Leaf, root, litterfall, and O horizon samples were subsequently ground with a knife mill (Grindomix GM 200, Retsch, Haan, Germany) and a planetary ball mill (PM 200, Retsch, Haan, Germany). Mineral soil samples were sieved <2 mm and aliquots ground with the planetary ball mill.

At each transect, we collected weekly samples of throughfall, litter leachate, and soil solution from the 0.15 m and 0.30 m mineral soil depths, while for streamflow one instantaneous sample from the single stream draining the whole catchment was collected per

week. Rainfall was collected at two gaging stations, each consisting of five Hellmann-type collectors, placed on clear-cut areas. Those collectors were permanently open and sampled bulk deposition. Throughfall was collected with 20 fixed-position funnel collectors which were placed randomly along the transect. The 20 samples were combined into one sample per transect and collection date which we considered as representative for the canopy tree composition of this highly biodiverse tropical montane forest further described in Homeier et al. (2010). Litter leachate percolating through the organic layer was collected with three zero-tension lysimeters per transect made of plastic boxes covered with a polyethylene net. The lysimeters had a collecting surface area of 0.15 m x 0.15 m and were laterally installed below the organic layer from a small soil pit. Mineral soil solutions were sampled with suction cups (mullite, 1 µm±0.1 µm pore size) at each of the 15- and 30-cm soil depths and installed into an auger-drilled hole in the dimension and depth of the suction cups. To improve the contact of the suction cup with the mineral soil, we poured a suspension made of local soil and throughfall into the remaining space left after installation of the suction cup. The sampling of the solutions analyzed in this study took place >10 yr after the installation in the years 1998 (lysimeters) and 2000 (suction cups). Lysimeters and suction cups at the two soil depths were installed in triplicate at random positions along each of the three transects to collect a sample that we considered representative for each transect and collection date. Stemflow was collected with polyurethane collars at five trees in the lower part of the catchment. The five samples were bulked into a single stemflow sample per collection date, which we considered as representative for the forest. Wilcke et al. (2017). Streamflow was sampled from the middle of the undisturbed flowing stream above a weir, which was used to gage streamflow (Fleischbein et al., 2006). The volumes of rainfall, throughfall, stemflow, and litter leachate were measured with a graduated cylinder and bulked to result in one volume-weighted, composite sample per sample type, transect, and collection date in the field. Mineral soil solutions from the three suction cups per soil depth were bulked into one collection vessel per transect, depth, and collection date. For the analysis of the $\delta^{13}C$ values of DOM, the weekly samples were combined to monthly samples in a volume-weighted way, except for the soil solution samples (lysimeters and suction cups), which included the same volume from each week in the considered month, because the samplers did not collect the solutions quantitatively. Except for soil solutions, all liquid samples were filtered in the field laboratory with ashless folded filters of 4–7 µm pore size, Type 392 (Sartorius-Stedim GmbH, Göttingen, Germany). The filters were conditioned with an aliquot of the collected ecosystem solutions, which was discarded before final filtration

of the sample. DOM was approximated as TOC in solutions filtered <1-7 µm. We used a set of 70 samples (ten samples of each solution type) that were passed through 0.45 µm syringe filters (regenerated cellulose, Minisart RC-25, Sartorius-Stedim GmbH, Göttingen, Germany) to determine whether there are differences between our TOC and conventional DOC concentrations. The syringe filters were rinsed with ultrapure water until no DOC was detected in the filtrate before using them for the ecosystem solutions. We found no significant differences ($p<0.05$) between mean TOC and DOC concentrations in the ecosystem solutions after a paired t-test. Moreover, the regression line of TOC on DOC showed a slope near 1 (0.98) and an R^2 value of 0.99 illustrating that our TOC measurements represented the conventional DOC well (**Figure B-S4**).

3.3. Chemical Analyses

The C concentrations and $\delta^{13}C$ values of leaf, root, litterfall, and soil samples were measured with an Elemental Analyzer (Thermo Scientific, Flash 2000 HT Plus, Bremen, Germany) coupled to an Isotope Ratio Mass Spectrometer (IRMS, Thermo Scientific, Delta V Advantage, Bremen, Germany) via a Conflo IV interface using the ISODAT 3.0 software. We used acetanilide as calibration standard for C concentrations, a high organic concentration sediment (OAS, IVA Analysentechnik, Meerbusch, Germany) as IRMS working standard, and an aromatic polyimide (EMA-P2, Elemental Microanalysis Ltd, Okehampton, UK) for drift correction. USGS-64 ($\delta^{13}C$: -40.81‰), USGS-62 ($\delta^{13}C$: -14.79‰), and IAEA-CO-8 ($\delta^{13}C$: -5.76‰) were used to reference the results to the Vienna Pee Dee Belemnite (VPDB) scale by linear regression. The precision of the $\delta^{13}C$ values determined by routinely performed, repeated measurements of the working standards was 0.10‰ (SD).

TOC concentrations in ecosystem solutions were measured with an elemental analyzer (varioTOC cube, Elementar Analysensysteme GmbH, Langenselbold, Germany) after acidification with HCl. The $\delta^{13}C$ values of DOM were determined with an elemental analyzer optimized for stable isotope measurements (isoTOC cube, Elementar Analysensysteme GmbH, Langenselbold, Germany), which was coupled via a thermoelectric purge and trap, low concentration focusing module (LCM) to an IRMS (Vision, Isoprime Ltd, Stockport, UK). We applied a linear calibration function to reference the measured $\delta^{13}C$ values to the VPDB scale using the international reference materials USGS-64, USGS-61 ($\delta^{13}C$: -35.05‰), IAEA-600 ($\delta^{13}C$: -27.77‰), and USGS-62. We used repeated measurements of benzoic acid (IAEA-601) for drift correction. For blank and

linearity corrections, we followed Federherr et al. (2014). The precision of the measurement was determined by triplicate measurements of the reference materials at the beginning, in the middle, and at the end of each sequence. The standard uncertainty of the $\delta^{13}C$ values calculated according to Federherr (2016) in samples with TOC concentrations ≥5 mg L^{-1} was 0.10‰ and in samples with TOC concentrations <5 mg L^{-1} 0.25‰. The mean differences between the certified mean value and our measurements ranged from -0.05‰ for IAEA-600 to +0.12‰ for USGS-61.

Dissolved organic nitrogen (DON) concentrations were calculated as the difference between total dissolved nitrogen (TDN) and dissolved inorganic nitrogen (DIN = NH_4-N + NO_3-N). The NH_4-N and NO_3-N concentrations were measured with high resolution colorimetry and photometric detection in a continuous flow analyzer (CFA San++, Skalar, Breda, The Netherlands). Concentrations of Cl^- were also measured by CFA using an ion-selective electrode (Orion Ionplus, Thermo Scientific, Beverly, USA). The concentrations of Ca, K, and S in the ecosystem solutions were measured with an Inductively-Coupled Plasma Optical Emission Spectrometer (5100 VDV ICP-OES, Agilent, Waldbronn, Germany). Immediately after sampling, we determined electrical conductivity and then pH with a glass electrode (Sentix HWS; WTW GmbH) in an aliquot of the sample which was discarded afterwards.

3.4. Calculations and statistical evaluation

Monthly chemical solution properties except for $\delta^{13}C$ values of DOM concentrations, which were measured in bulked monthly samples, were calculated as volume-weighted means of weekly measurements, except for litter leachate and the soil solutions, where no volume-weighting was possible, because the used lysimeters and suction cups collected an incomplete aliquot of the fluxes of unknown size. Rainfall and throughfall water fluxes were directly measured in the field. The stemflow volume was recorded in the field and extrapolated to the forest area via the assumption that the measured stemflow was representative for trees with a diameter at breast height (dbh) ≥0.1 m and that there were 1000 large trees ha^{-1} with a dbh ≥0.1 and another 2000 small trees with a dbh <0.1 (Homeier et al., 2008, 2010), which yielded 50% of the stemflow of the large trees. The water fluxes with litter leachate and in the mineral soil were modeled with the Soil Water Balance Model (DVWK, 1996) described in Boy et al. (2008a), using available data from 1999 to 2003 and then calculated for our study period (2013-2016) with regression equations described in Wilcke et al. (2020) for the litter leachate and in Schwarz et al. (2011) for the mineral soil.

The coefficients of determination of these regressions were lower for the mineral soil solutions (0.51-0.79) than for the litter leachate (0.85), implying a higher uncertainty of the water flux estimates in the mineral soil, particularly at greater soil depth. Weekly measurements of the water level at the weir were used to calculate streamflow fluxes based on a calibration function determined with a bucket and stop watch at different water levels assuming a constant flux between two water level measurements (Boy et al., 2008a; Fleischbein et al., 2006; Wilcke et al., 2019). To compare means among ecosystem solutions, we used ANOVA followed by Tukey's HSD post-hoc test. Homoscedasticity was assessed with the Levene's test. Normality of residuals was checked by visual inspection. Data handling, analysis and visualizations were performed in R version 4.1.1 (R Core Team, 2025).

4. Results

The pH values increased from strongly acidic rainfall via throughfall to slightly acidic values in stemflow, while the litter leachate and mineral soil solutions were again strongly acidic and the streamflow neutral. The high pH of the streamflow is related with the strong acid buffering of the mineral subsoil, which is still little weathered and provides a high buffer capacity resulting into the release of base cations into the stream (Wilcke et al., 2017). The electrical conductivity (EC) increased in the order, rainfall < throughfall < stemflow < litter leachate and was lower and similar in the mineral soil solutions and streamflow. The TOC and DON concentrations correlated with the EC in all ecosystem solutions except in streamflow, where EC was similar to soil solutions, but TOC and DON concentrations were lower. The TOC/DON ratios increased from rainfall to litter leachate and decreased from litter leachate to streamflow (**Table B-1**).

From February to April 2014, we observed an event during which the $\delta^{13}C$ values of DOM in rainfall, soil solutions and streamflow were markedly higher than in the remaining period (**Figure B-1**). During this event, the TOC/DON ratio of DOM in rainfall was also markedly higher (18.9±0.8) than on average of the time outside the event (9.7±2.3). The same pattern was observed for the mean monthly concentrations of the Ca, K, S, and Cl^- concentrations in rainfall, which increased from 0.10±0.09, 0.15±0.11, 0.13±0.08 and 0.35±0.19 mg L^{-1}, respectively, outside the event to 0.24±0.10, 0.34±0.11, 0.64±0.47 and 2.45±2.17 mg L^{-1}, respectively, during the event. The monthly concentrations of NH_4-N and

NO_3-N decreased during the event from 0.43±0.22 and 0.39±0.21 mg L^{-1}, respectively, to 0.10±0.04 and 0.25±0.07 mg L^{-1}, respectively.

Disregarding the event, the $\delta^{13}C$ values of DOM did not show a seasonal pattern in any ecosystem solution, i.e., there were no significant differences between the driest (October to December) and the wettest quarter (April to June, **Figure B-1**). Outside the event, the mean $\delta^{13}C$ value of DOM in rainfall (-26.0 ± 1.3‰) was higher than those of throughfall (-28.7 ± 0.3‰) and stemflow (-29.2 ± 0.2‰). The lowest mean $\delta^{13}C$ value of DOM occurred in litter leachate (-29.6 ± 0.2‰). In the mineral soil solutions, the mean $\delta^{13}C$ values of DOM were higher than that in litter leachate and lower than that in rainfall. There were no significant differences in the mean $\delta^{13}C$ values of DOM between the 0.15 m (-27.8 ± 1.0‰) and 0.30 m (-27.6 ± 1.1‰) mineral soil depths. In streamflow, the mean $\delta^{13}C$ value of DOM (-27.9 ± 1.1‰) was similar to those in the soil solutions.

Table B-1. Volume-weighted mean (±standard deviation) of total organic carbon (TOC) and dissolved organic nitrogen (DON) concentrations, and TOC/DON ratios of the ecosystem solutions along the water path through the ecosystem from 2013 to 2016. For litter leachate and soil solutions no volume-weighting was possible and therefore arithmetic monthly means of electrical conductivity (EC) and H^+ activities of the solutions were calculated from the values measured in the weekly collected samples. H^+ activities of the solutions were thereafter converted to pH values. Lower case letters indicate significant differences ($p < 0.05$) among the ecosystem solutions based on Tukey's HSD post-hoc test following one-way ANOVA.

	pH	EC µS cm^{-1}	TOC mg L^{-1}	DON mg L^{-1}
Rainfall	4.7 (±0.2) ab	13 (±7) a	2.5 (±1.1) a	0.25 (±0.09) ab
Throughfall	6.2 (±0.3) c	42 (±13) c	13.3 (±5.6) c	0.82 (±0.22) c
Stemflow	6.7 (±0.3) d	72 (±19) e	26.8 (±11.5) d	1.38 (±0.42) d
Litter leachate	4.8 (±0.2) b	58 (±14) d	49.6 (±14.7) e	2.34 (±0.68) e
Soil solution at 0.15 m	4.6 (±0.1) a	26 (±7) b	7.6 (±1.2) b	0.42 (±0.09) b
Soil solution at 0.30 m	4.7 (±0.1) a	21 (±5) b	5.9 (±0.9) ab	0.33 (±0.07) ab
Streamflow	7.0 (±0.3) e	21 (±2) b	2.8 (±2.5) a	0.17 (±0.08) a

To support the interpretation of the $\delta^{13}C$ values of DOM in ecosystem solutions, we also determined the $\delta^{13}C$ values of the major DOM sources including leaves and fine roots (diameter <2mm) of 10 common tree species (**Table B-S2**). There was a large variation in

the $\delta^{13}C$ values of the leaves among the different species from -25.7 to -30.2‰ (**Figure B-2**), with a mean of -28.3‰. There were no significant differences in the $\delta^{13}C$ values of the leaves collected in dry and wet periods. The $\delta^{13}C$ values of the fine roots (-26.0 to -29.1‰) varied less than those of the leaves. With a mean $\delta^{13}C$ value of -27.2‰, the fine roots had on average a by 1.2‰ higher $\delta^{13}C$ value than the leaves (**Figure B-2**).

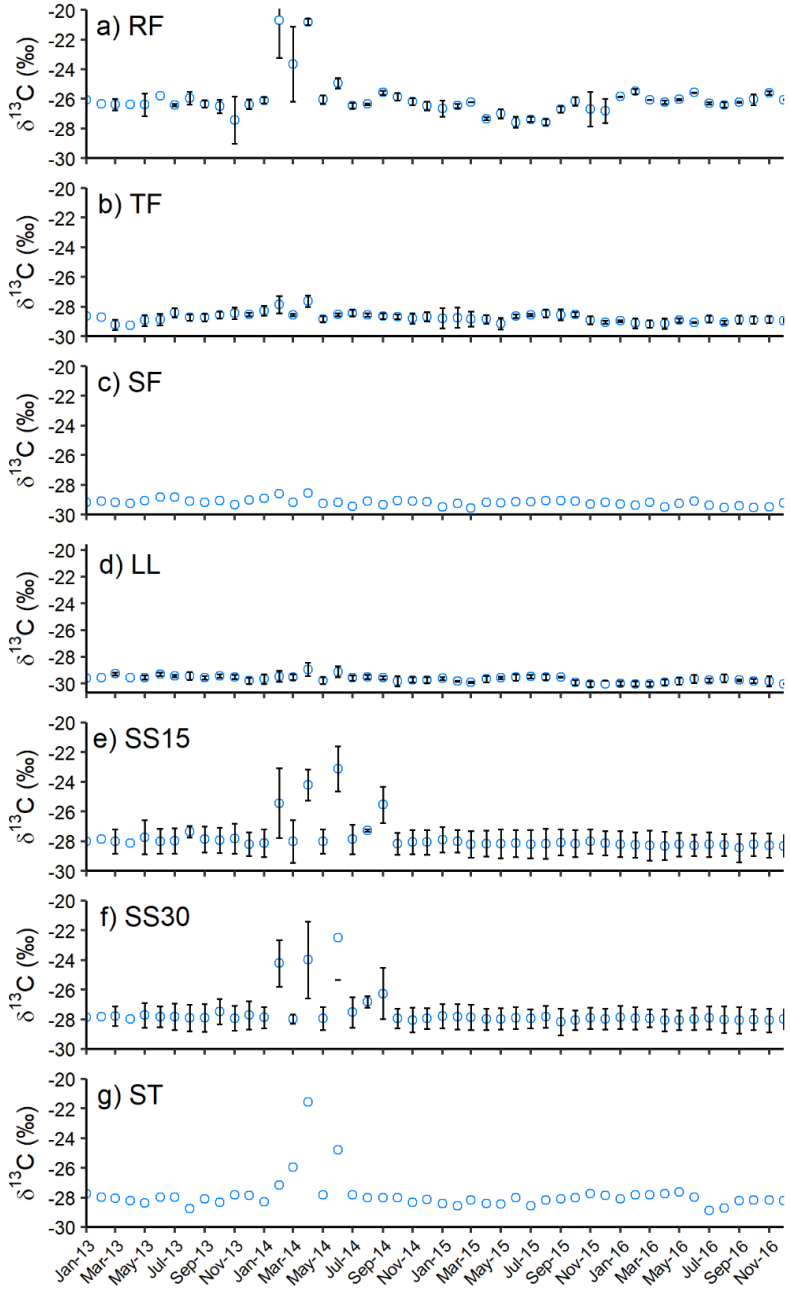


Figure B-1. Course of monthly $\delta^{13}C$ values from January 2013 to December 2016. RF is rainfall, TF throughfall, SF stemflow, LL litter leachate, SS15 and SS30 mineral soil solutions at 0.15 and 0.30 m depth, respectively and ST streamflow. For TF, LL, S15, and SS30, the error bars represent the standard deviation among the three study transects at ca.

1900, 1950, and 2000 m a.s.l. SF was measured in a single composite sample collected from five separate trees. There was only one stream draining the study catchment.

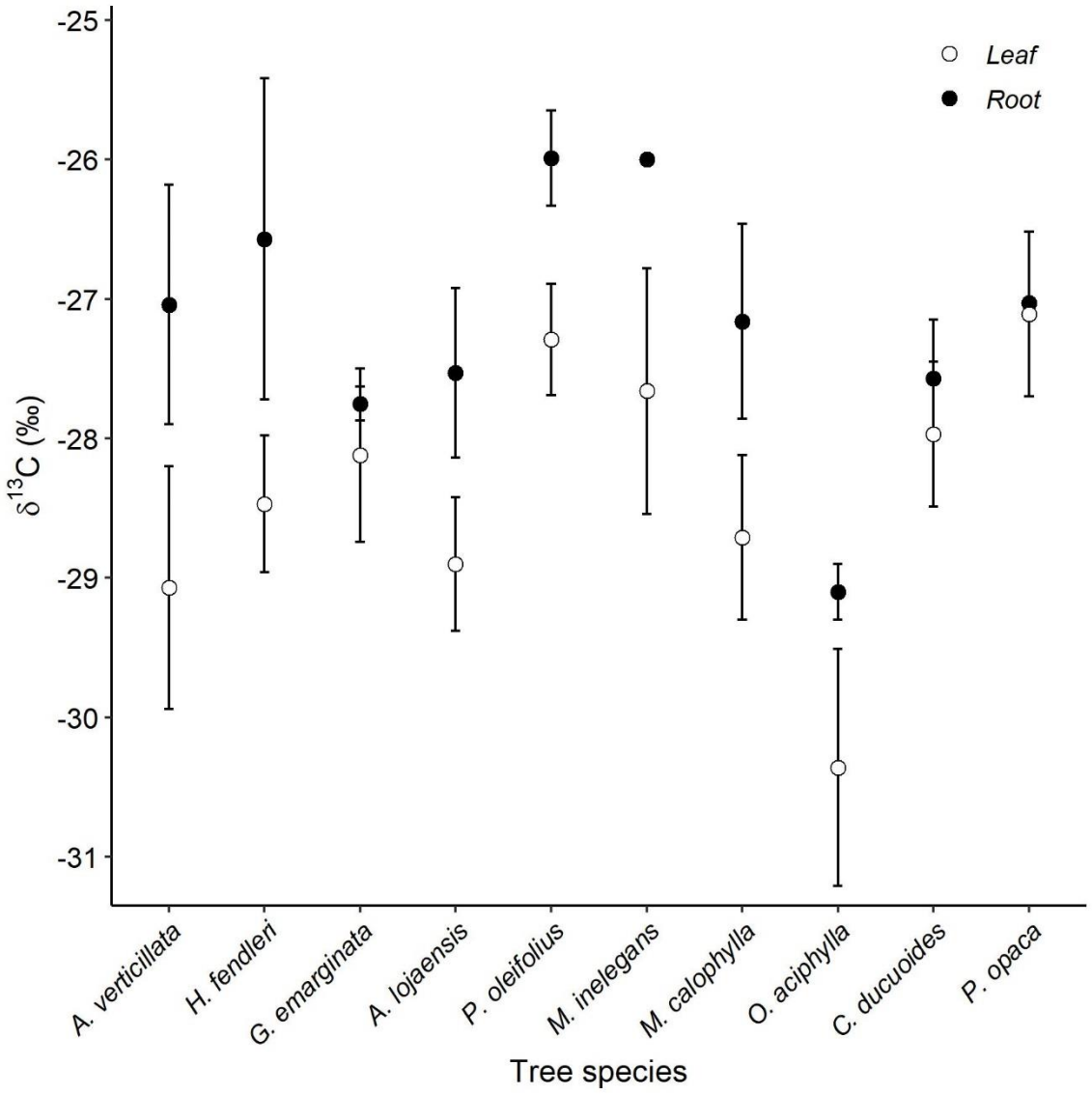


Figure B-2. Mean $\delta^{13}C$ values of sunlight-exposed leaves and fine roots of 10 common canopy-forming tree species in the forest of the San Francisco Biological Reserve. The error bars represent the standard deviations (n=4 for leaves and n=3 for roots). The species were ordered from left to right according to their decreasing contribution to the total tree number.

For the period outside the event, **Figure B-3** compares the mean $\delta^{13}C$ values of the potential solid phase sources which may contribute to DOM with the mean $\delta^{13}C$ values of the DOM in the various ecosystem solutions. The $\delta^{13}C$ values of DOM in throughfall and stemflow were at the lower end of the range of the weighted mean $\delta^{13}C$ values of fresh leaves, while the $\delta^{13}C$ values of DOM in litter leachate were lower than in litterfall but similar to the $\delta^{13}C$ values of the Oi horizon. The $\delta^{13}C$ values of DOM in the mineral soil solutions and streamflow were similar to those in the Oa horizon but lower than those in the A and B horizons. Generally, the $\delta^{13}C$ values of DOM were lower than their possible direct solid phase sources.

To determine if the $\delta^{13}C$ values of DOM bear additional information to the TOC/DON ratios, we plotted the TOC/DON ratio vs. the $\delta^{13}C$ values of DOM (**Figure B-4**). When all ecosystem solutions were considered, there was a significant, negative correlation between the TOC/DON ratios and the $\delta^{13}C$ values of DOM. However, the mineral soil solutions at the 0.15 and 0.30 m depths and the streamflow had different C/N ratios, but similar $\delta^{13}C$ values, while throughfall and streamflow and stemflow and the mineral soil solutions, respectively, had similar C/N ratios but different $\delta^{13}C$ values.

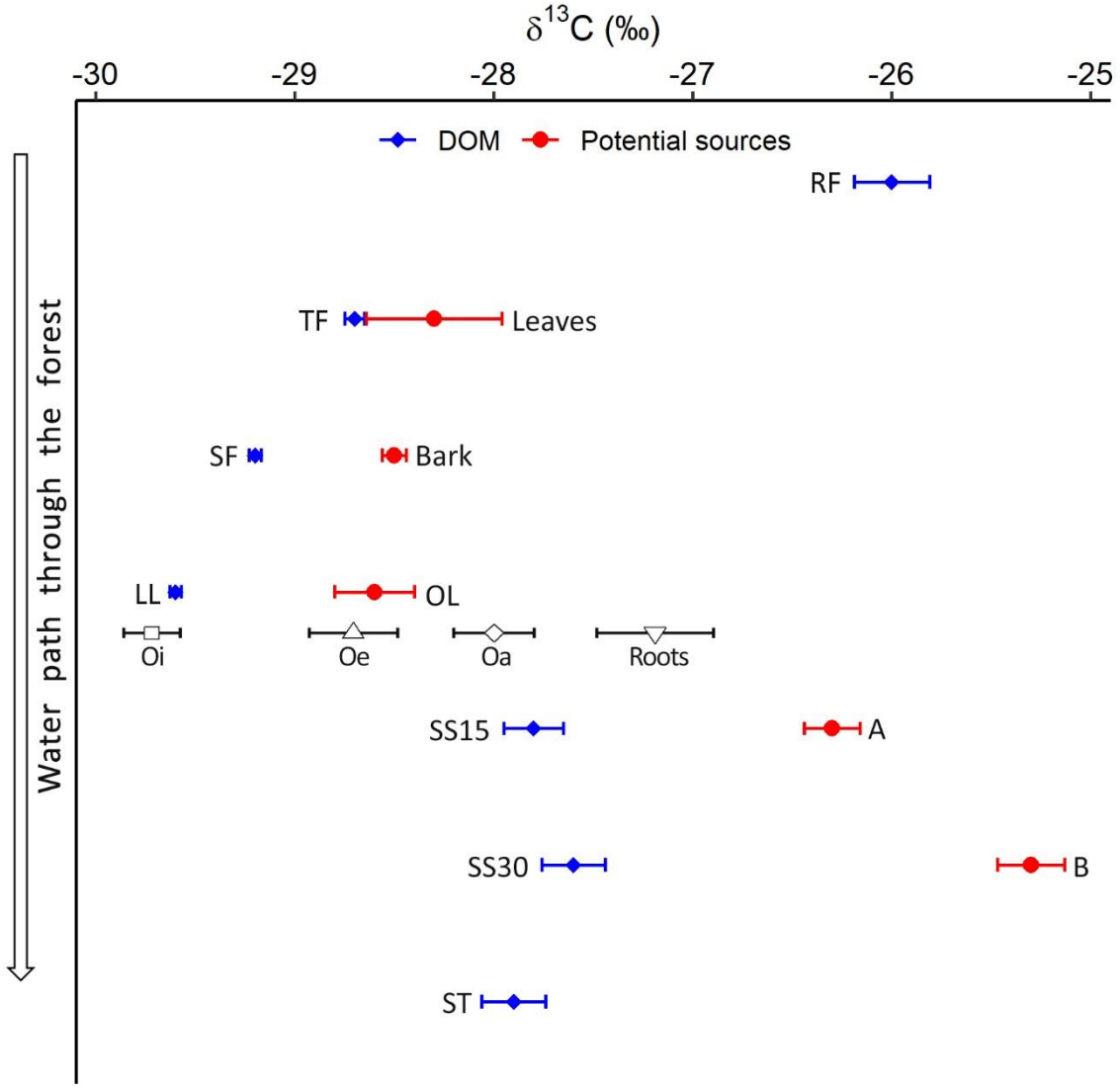


Figure B-3. Comparison of the mean $\delta^{13}C$ values in potential solid-phase sources of DOM and in DOM along the water path through the forest ecosystem. RF is rainfall, TF throughfall, SF stemflow, LL litter leachate, SS15 and SS30 mineral soil solutions at the 0.15 and 0.30 m soil depths, respectively, ST streamflow. OL organic layer (thickness-weighted mean $\delta^{13}C$ value of the three increasingly decomposed organic horizons Oi, Oe and Oa), and A and B are the soil mineral horizons. The $\delta^{13}C$ value of the bark (-28.5 ± 0.2‰) was taken from Cernusak and Hutley (2011). Error bars indicate standard errors.

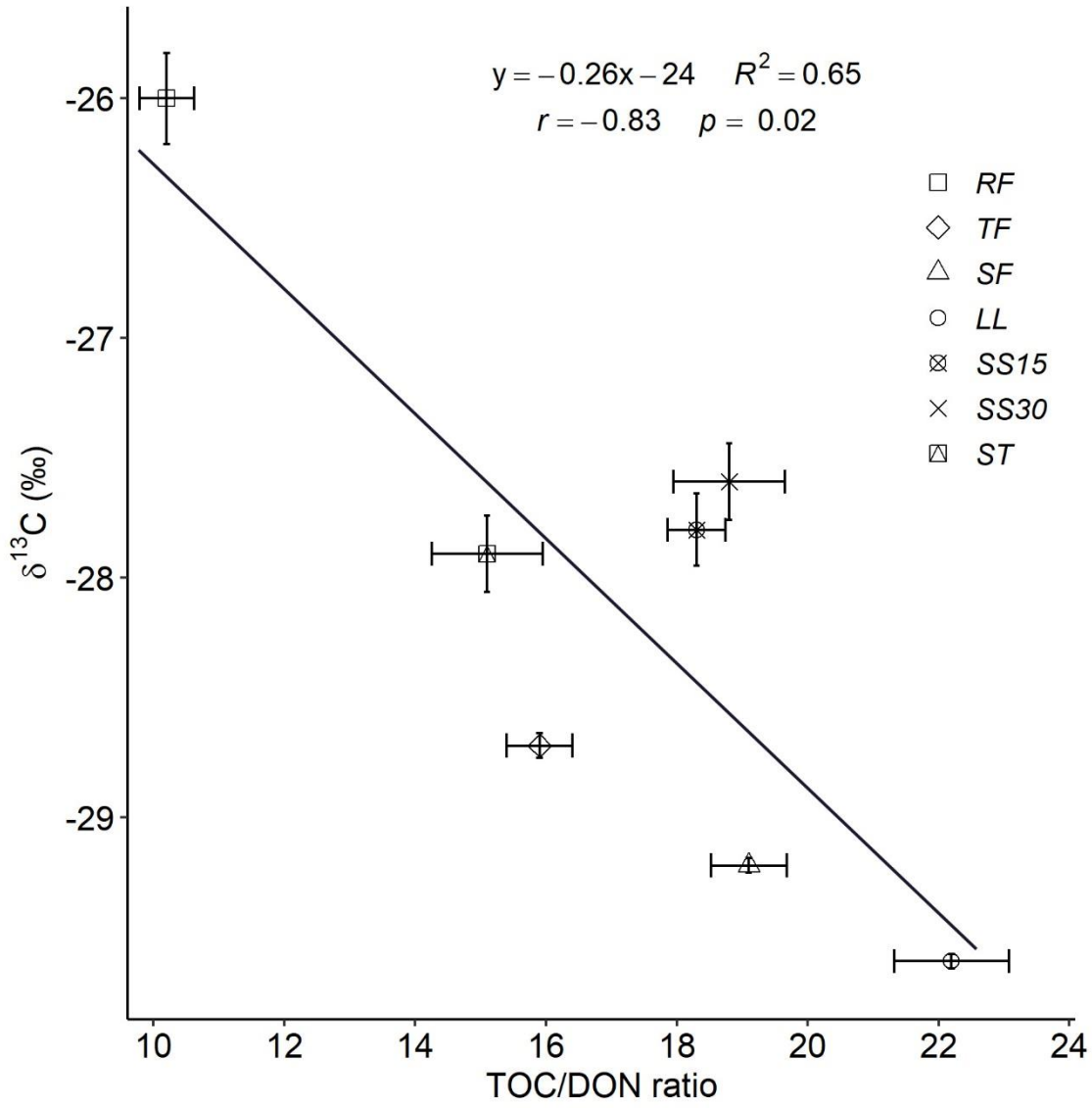


Figure B-4. Relationship between the mean TOC/DON ratios and the $\delta^{13}C$ values of DOM in ecosystem solutions (n=48 for each solution type). RF is rainfall, TF throughfall, SF stemflow, LL litter leachate, SS15 and SS30 mineral soil solutions at the 0.15 and 0.30 m depths, respectively and ST streamflow. The error bars indicate standard errors.

5. Discussion

5.1. Seasonality of the $\delta^{13}C$ values of DOM

In spite of a pronounced dry phase at the end of the year (**Figures B-S1 and B-S2**), the "veranillo" during which the soil water content decreased considerably (Wilcke et al., 2013), there was no seasonal variation in the $\delta^{13}C$ values of tree leaves and of the DOM in all studied ecosystem solutions (**Figure B-1**), so that we have to reject our first hypothesis. Our findings for the leaves contrast the results of several studies from temperate forests, which reported a seasonal variation in the $\delta^{13}C$ values of leaves (Cao et al., 2020; Rascher et al., 2010; Scartazza et al., 2004). Obviously, at our study site the water availability in the soil was always high enough to satisfy the plant requirements even during the dry periods so that the extent of C isotope fractionation by photosynthesis remained unaffected. The same lack of seasonality was observed by Wang et al. (2021) for $\delta^{13}C$ values of DOM in soil solutions of tropical tree plantations in Guangdong, China.

Instead of seasonality, an event with higher $\delta^{13}C$ values of DOM in rainfall was observed from February to April 2014 (**Figure B-1**). We suggest that this event was related to vegetation fires in the proximity of the study area, which emitted C-isotopically heavy black carbon. Higher $\delta^{13}C$ values than in C_3 plants have been reported for biomass-derived soot and char (Han et al., 2010). In line with these findings, Song et al. (2012) reported $\delta^{13}C$ values of wood, soot, and char of -26.4‰ and -26.0‰, respectively, and of grass soot and char of -21‰ and -20.4‰ after thermal oxidation. Considering that the higher $\delta^{13}C$ values during the event (-21‰) persisted after filtering the solutions <0.45 µm, we suggest that atmospheric deposition of colloidal soot and soot-derived dissolved black carbon (Yamashita et al., 2021), resulting from fires of adjacent woody plants (invasive shrubs), ferns (CAM photosynthesis with similar $\delta^{13}C$ values as C_3 plants) and planted C_4 grasses (Roos et al., 2013), can be transported by throughfall, stemflow, and soil solutions (Wagner et al., 2019) reaching the rivers (Wang et al., 2016; Yamashita et al., 2021), which is in line with the elevated $\delta^{13}C$ values in streamflow from February to June 2014 (**Figure B-1**). The elevated TOC/DON ratio and concentrations of Ca, K, total S, and Cl^- observed during the event are also in line with a local fire, which, besides elemental C, also emits HNO_3, H_2SO_4, and fly ashes including alkaline and earth alkaline cations. While long-range transport of forest fire emissions from the Amazon basin was associated with elevated H^+ and NO_3^- concentrations in rainfall (Boy et al., 2008a), this was not the case for our assumed fire event

during which the concentrations of NH_4^+ and NO_3^- even decreased relative to the period outside the event and the pH did not change. This suggests that the fire-produced acids were neutralized by fly ash, which usually only occurs at short transport distances of the fire emissions (Bodí et al., 2014). Moreover, the fire source was N-poor, which is typical of the mostly degraded infertile local pastures (Günter et al., 2009).

5.2. $\delta^{13}C$ values of DOM in aboveground ecosystem solutions

The small spatial and temporal variation in $\delta^{13}C$ values of DOM in throughfall and stemflow (**Figure B-1**) is surprising given the large heterogeneity of the $\delta^{13}C$ values of tree leaves **(Figure B-2**). Moreover, distinct differences in DOM quality of throughfall were reported between coniferous and deciduous forest in a temperate ecosystem, which became less heterogeneous belowground (Thieme et al., 2019). We attribute the small spatial and temporal variation in the $\delta^{13}C$ values of DOM in throughfall and stemflow to the restricted occurrence of the individual tree species driven by elevational and topographic gradients (Homeier et al., 2008; Werner & Homeier, 2015). To explain the decreasing $\delta^{13}C$ values in the order, rainfall > throughfall > stemflow (**Figure B-3**) by plant and microbial metabolites of freshly assimilated C would be in line with the $\Delta^{14}C$ dating of throughfall in a temperate forest that revealed that DOM consisted of predominantly recently fixed biogenic C (Brüggemann et al., 2011). However, the C isotopic composition of plant and microbial metabolites is complex and plant metabolites can be both lighter or heavier than the bulk plant tissue (Brüggemann et al., 2011). The fact that microbial biomass is usually C-isotopically heavier than SOM and DOM (Blagodatskaya et al., 2011; Dijkstra et al., 2006) suggests that is more likely that microbial metabolites would shift the C-isotopic composition of DOM towards higher $\delta^{13}C$ values, which contrasts our observation (**Figure B3**). However, microbial transformation of DOM is reported to decrease the concentrations of the protein-like and increase those of the fulvic- and humic-like compounds and also the molecular weight of the residual DOM (Hur et al., 2009), which reduces hydrophilic and increases hydrophobic contributions to DOM. Because the hydrophobic DOM was reported to be C-isotopically lighter than the hydrophilic DOM (Kaiser et al., 2001), this compositional change of DOM could indeed contribute to the decreasing $\delta^{13}C$ values of DOM in throughfall and stemflow relative to rainfall. In the Brazilian savanna region, Ciglasch et al. (2004) similarly observed a higher contribution of hydrophobic DOC to total DOC in throughfall and stemflow (only in the second half of the rainy season) of native Cerrado and Caribbean pine (*Pinus caribaea* Morelet) plantations, which they explained by

leaching of hydrophobic compounds from the surface tissue of leaves and bark and of lipophilic plant excreta. Therefore, we suggest that at our study site selective leaching of C-isotopically light hydrophobic DOM from leaves and bark explains the increasingly ^{13}C-depleted DOM from rainfall to throughfall. Thus, our second hypothesis is not fully supported, because microbial metabolites are unlikely to contribute to DOM in throughfall and stemflow while leaching of freshly assimilated plant components could well play a role in the change of the $\delta^{13}C$ values from rainfall to stemflow.

5.3. $\delta^{13}C$ values of DOM in belowground ecosystem solutions

The lower $\delta^{13}C$ value of the DOM in litter leachate than the mean $\delta^{13}C$ value of the solid organic layer (**Figure B-3**) suggested that litter leachate consisted of C-isotopically lighter compounds than the organic layer on average, so that we have to reject the first part of our third hypothesis that the C-isotopic composition of the DOM in litter leachate was similar to that of the Oa horizon. The fact that the age of DOM in litter leachate was with approximately 10 yr similar to that of the Oa horizon (Wilcke et al., 2020) suggests that either the soluble part of the Oa horizon had a C-isotopically light composition or that the DOM in litter leachate contains freshly produced microbial degradation products of the Oa horizon, which are C-isotopically light such as lignin degradation products (Kaiser et al., 2001).

The finding that the $\delta^{13}C$ values of DOM in the mineral soil were C-isotopically heavier than those of aboveground ecosystem fluxes and litter leachate indicated a change in DOM composition between litter leachate and the mineral soil solutions (**Figure B-3**). The observation that the $\delta^{13}C$ values of DOM were not different between the two mineral soil depths suggested that the change in DOM quality occurred in the mineral soil above 0.15 m depth. Because Wilcke et al. (2020) reported that the DOM in the mineral soil solutions was younger (approximately 1 yr old) than in the litter leachate, the vertically changing DOM quality was related with the retention of old DOM from the Oa horizon (Schulze et al., 2011), while young DOM passed through from the organic layer to the mineral soil. At the same time, it is unlikely that dissolution of solid-state organic matter from the A and B horizons contributed to the DOM in the soil solutions at the 0.15 to the 0.3 m soil depths because the A and B horizons in the study area were reported to be 50 and 115 years old, respectively and thus much older than the DOM in the mineral soil solution (approximately 1 yr) (Wilcke et al., 2020).

Obviously, the young DOM that passed through from the litter leachate to the mineral soil solution had a higher $\delta^{13}C$ value than the soluble part of the Oa horizon or its degradation products dominating the DOM of litter leachate. One explanation of this change in the C isotope composition between litter leachate and the mineral soil solutions may be the preferential consumption of C-isotopically light compounds during mineralization resulting in higher $\delta^{13}C$ values (Garten et al., 2000). Another explanation for the marked increase in the $\delta^{13}C$ values of DOM from litter leachate to the mineral soil solutions could be the preferential sorption of C-isotopically light DOM components to the solid soil. It has been shown that the hydrophobic fraction of the DOM is preferentially adsorbed in the mineral soil (Guggenberger & Zech, 1993; Kaiser & Zech, 1997) and that this DOM fraction is C-isotopically light (Kaiser et al., 2001) so that the remaining DOM becomes C-isotopically heavier in line with our observation (**Figure B-3**).

As a possible third explanation, Wilcke et al. (2020) suggested that root exudates and root litter might have been sources of DOM in the mineral soil. Soethe et al. (2007) reported that the soil in our study area contained 890 g m^{-2} of fine root biomass (< 2 mm) of which 44% were located in the organic layer, and 16 and 29% in the 0-0.1 m and 0.1-0.3 m layers of the mineral soil, respectively. Thus, there was enough root biomass as potential source of DOM in the mineral soil. The fact that the bulk roots of the studied 10 tree species had on average a slightly higher $\delta^{13}C$ value than the DOM of the mineral soil solutions and the streamflow (**Figure B-3**) suggested that particularly root exudates, which are likely C-isotopically lighter than the root biomass might have contributed to DOM. In a riparian forest, $\delta^{13}C$ values of -32 to -28‰ for water-soluble root exudates were reported (Gougherty et al., 2018), which is ^{13}C-depleted relative to our bulk fine roots.

However, a $^{14}CO_2$ pulse-labeling experiment in microcosms showed that the immediate leaching of ^{14}C was negligible although roots released a significant proportion of the assimilated CO_2 into the soil, suggesting a rapid incorporation of released C into microbial biomass (Paterson et al., 1999). Similarly, Kramer et al. (2010) reported that more than 60% of the C used by microbes in the mineral soil was root-derived. Thus, a large part of root exudates and root litter were possibly first microbially processed before they could potentially be released as DOM into the mineral soil solution. Dijkstra et al. (2006) observed that microbial biomass was ^{13}C-enriched (by 1.6‰) relative to SOM in the first 0.1 m of the mineral soil under C_3 trees, which is line with the finding of Blagodatskaya et al. (2011) who reported that microbial C was ^{13}C-enriched relative to SOM and DOC (by 0.9 and 0.4‰,

respectively). Thus, the $\delta^{13}C$ value of microbial biomass is even farther away from that of DOM in the mineral soil solutions than that of bulk SOM, rendering contributions of bulk microbial biomass to the DOM unlikely. However, Kohl et al. (2015) reported that fungal phospholipid fatty acids (PLFA) are ^{13}C-depleted relative to bacterial PLFA, so that it cannot be ruled out that individual microbially produced organic substances might have contributed to the lower $\delta^{13}C$ values of DOM in the mineral soil solutions and streamflow than in the bulk SOM. While a contribution of C-isotopically light microbial metabolites to the DOM in mineral soil solutions is possible, their influence on the $\delta^{13}C$ values of DOM in the mineral soil must be smaller than in throughfall, stemflow, and litter leachate, which are C-isotopically lighter than the mineral soil solutions.

Overall, it seems possible that the increase in the $\delta^{13}C$ values of DOM in the mineral soil solutions relative to litter leachate is partly attributable to organic substances derived from root exudates and root litter decomposition, because bulk roots had a $\delta^{13}C$ value that was closer to that of DOM in the mineral soil solutions than SOM and microbial biomass. If true, this would support the second part of our third hypothesis, although we cannot rule out that some C-isotopically light DOM was preferentially degraded and that there were differential sorption/desorption processes with C isotope effects and additional contributions of microbial transformation products.

5.4. $\delta^{13}C$ values of DOM in streamflow

The $\delta^{13}C$ values of DOM in streamflow were similar to those of the mineral soil solutions (**Figure B3**), but the DOM in streamflow was with ca. 50 yr much older than in the mineral soil solutions (Wilcke et al., 2020). Thus, there must have been a change in DOM sources between the soil solution at the 0.3 m mineral soil depth and streamflow. The fact that the DOM in streamflow tended to be slightly C-isotopically lighter than in the mineral soil (**Figure B-3**) indicated that it might contain contributions of isotopically light microbial degradation products of old SOM in the deeper subsoil (Boström et al., 2007). However, such contributions would not explain the younger age of the DOM in streamflow (ca. 50 yr) than the SOM in the subsoil (>100 yr, Wilcke et al., 2020). Therefore, we suggest that the younger age of the DOM in streamflow can be attributed to an addition of young DOM originating from the organic layer, which is flushed during strong rain events on wet soil into the streamflow (Boy et al., 2008b; Goller et al., 2006; Goller et al., 2005). Such events contributed 36% to the total DOM export in only 3.4% of the time (Boy et al., 2008b) and would besides the age also decrease the $\delta^{13}C$ values, because of the C-isotopically lighter

DOM of the litter leachate (**Figure B-3**). Together, these results support our fourth hypothesis that DOM in streamflow is a mixture of microbial degradation products of SOM in the deep soil and some younger DOM.

5.5. Relationship between $\delta^{13}C$ values and TOC/DON ratios of DOM

In spite of the overall correlation between the C/N ratios and $\delta^{13}C$ values of DOM, there was considerable variation in $\delta^{13}C$ values when the C/N ratio was similar and vice versa, illustrating that C/N ratios and $\delta^{13}C$ values of DOM bear independent information (**Figure B-4**). While C/N ratios are a widely used tool to infer SOM turnover and to explain changes in $\delta^{13}C$ values with soil depth in solid-state soil organic matter (Boström et al., 2007; Garten et al., 2000; Lorenz et al., 2020), this does not seem to be possible for DOM in soil solution. Further work is necessary to determine potential relationships between the $\delta^{13}C$ values of DOM and other chemical properties than the C/N ratio such as assessed with the help of UV-vis absorption, fluorescence spectroscopy combined with parallel factor analysis (PARAFAC), or Fourier transform ion cyclotron resonance mass spectrometry (FT-ICR-MS).

5.6. Environmental Implications

There is still little literature about $\delta^{13}C$ values of DOM addressing the whole water path through the forest, likely because the approach to collect DOM as solid sample by freeze-drying used up to now (Fry et al., 1996; Peterson et al., 1994) is cumbersome and requires high water volumes. It is thus not easily applicable to common ecosystem studies with regular sampling of small water volumes. Moreover, freeze-drying can result in incomplete C recovery because of the loss of volatile compounds which subsequently changes the $\delta^{13}C$ values and suffers from a contamination risk (Federherr et al., 2014; de Lecea et al., 2011; Fry et al., 1993; Fry et al., 1998). The sample contamination can result in high blanks, which are particularly problematic at low C concentrations (Peterson et al., 1994). The use of TOC-IRMS allowing for the direct measurement of $\delta^{13}C$ values of DOM in small sample volumes of < 20 mL avoids these problems and provides comparatively easy access to the $\delta^{13}C$ values of DOM. These data can be used to assess sources and transformations of DOM adding information that other DOM properties like the C/N ratio does not include. However, as likely always when stable isotope ratios in natural ecosystems are to be interpreted, the complete understanding of the $\delta^{13}C$ values of DOM requires further

information such as C concentrations and fluxes, accompanying element concentrations, chemical DOM properties, or age dating.

6. Acknowledgments

We thank the Ecuadorian Ministry of the Environment for the research permits and Naturaleza y Cultura Internacional (NCI) in Loja for providing the study area and the research station. We thank José Luis Peña and Jimmy Villalta for their support as field technicians, Tobias Fabian for his support in the field and the laboratory, and Uli Hensler, Martin Schwarz, and Jaime García for their contributions to the field sampling campaigns. Pablo Alvarez received a four-years scholarship from the Secretary of Higher Education, Science, Technology and Innovation of Ecuador (SENESCYT), Grant No. CA07-000439-2018, which is gratefully acknowledged.

7. Supporting information

Table B-S1. Range of pH values and mean (±standard deviation) thickness, organic carbon (C_{org}), C/N ratios, oxalate-extractable iron (Fe_o) and exchangeable aluminum (Al_{exc}) concentrations, effective (CEC_{eff}) and potential cation-exchange capacity (CEC_{pot}) in the soils at three transects (at approximately 1900, 1950 and 2000 m above sea level). For each transect, data was collected from three soil profiles. Lower case letters indicate significant differences ($p < 0.05$) among soil horizons based on Tukey's HSD post-hoc test following one-way ANOVA.

	Thickness mm	**pH** (H2O)	**C_{org}** mg g^{-1}	**C/N**	**Fe_o** mg g^{-1}	**Al_{exc}** $mmol_c$ kg^{-1}	**CEC_{eff}** $mmol_c$ kg^{-1}	**CEC_{pot}** $mmol_c$ kg^{-1}
Oi	14 (±3)	5.2 -7.0	471 (±7) c	25.5 (±1.3) c				
Oe	56 (±11)	4.5 – 5.1	389 (±39) bc	16.8 (±1.4) b				
Oa	31 (±3)	3.8 – 4.2	320 (±108) b	14.9 (±1.4) ab				
A	111 (±7)	3.9 – 4.7	43 (±20) a	11.6 (±2.1) a	3.7 (±1.3)	59 (±34)	75 (±23)	225 (±103)
B	186 (±54)	4.4 – 4.8	23 (±13) a	10.6 (±2.6) a	3.1 (±1)	71 (±53)	80 (±50)	150 (±75)

Table B-S2. List of common tree species in the San Francisco Reserve in south Ecuador for which leaf and root samples were collected**.**

Species	**Observations**
Alchornea lojaensis Secco	3*
Graffenrieda emarginata Triana	3*
Podocarpus oleifolius D. Don	3*
Alzatea verticilata Ruiz & Pav.	1
Clusia ducoides Engl.	1
Hyeronima fendleri Briq.	1
Matayba inelegans Radlk.	1
Miconia calophylla (D. Don) Triana	1
Ocotea aciphylla (Nees) Mez	1
Prunus opaca Walp	1

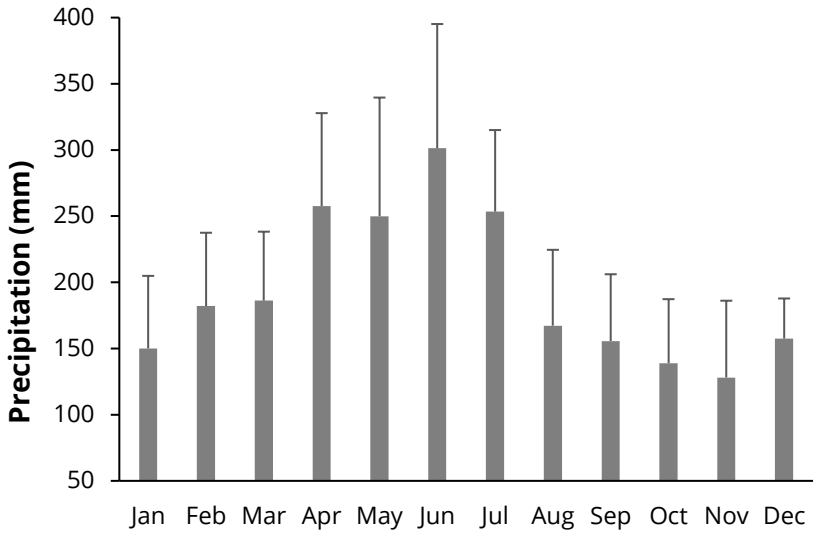


Figure B-S1. Mean monthly precipitation from April 1998 to December 2016 in the San Francisco Biological Reserve, south Ecuador.

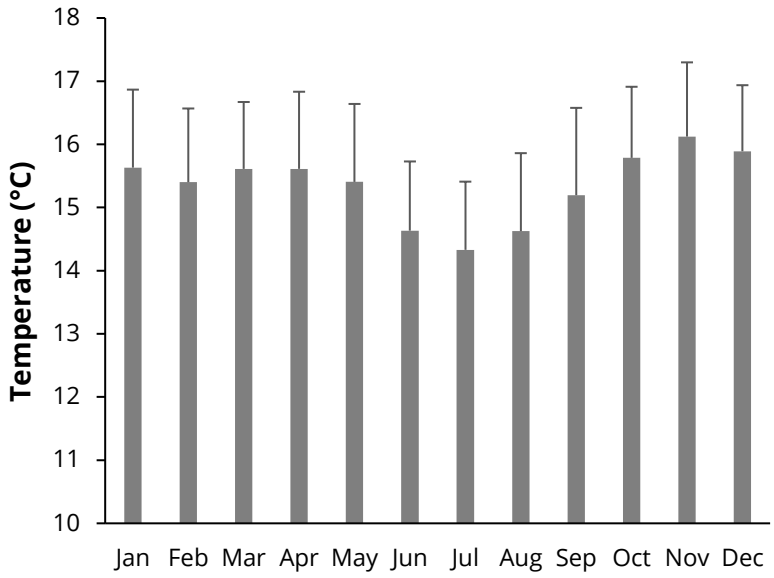


Figure B-S2. Mean monthly temperature from April 1998 to December 2016 in the San Francisco Biological Reserve, south Ecuador.

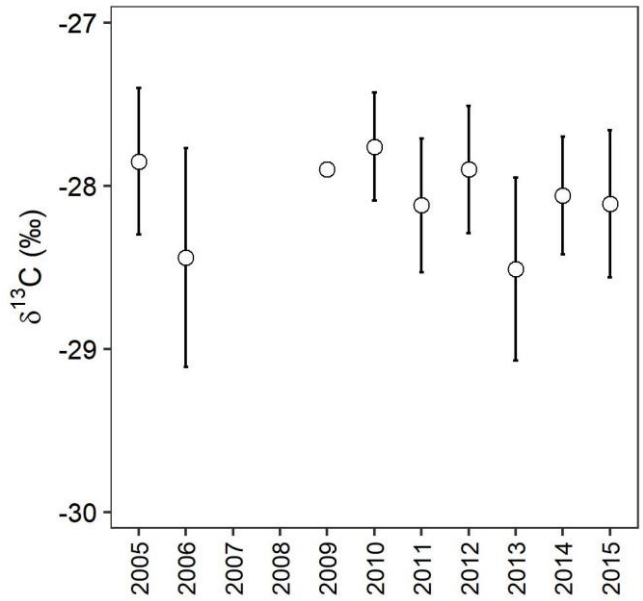


Figure B-S3. Annual mean $\delta^{13}C$ values in leaves of *Graffenrieda emarginata* Triana from 2005 to 2015. The error bars indicate the standard deviations of up to five trees (except in 2009 when no replicates were sampled).

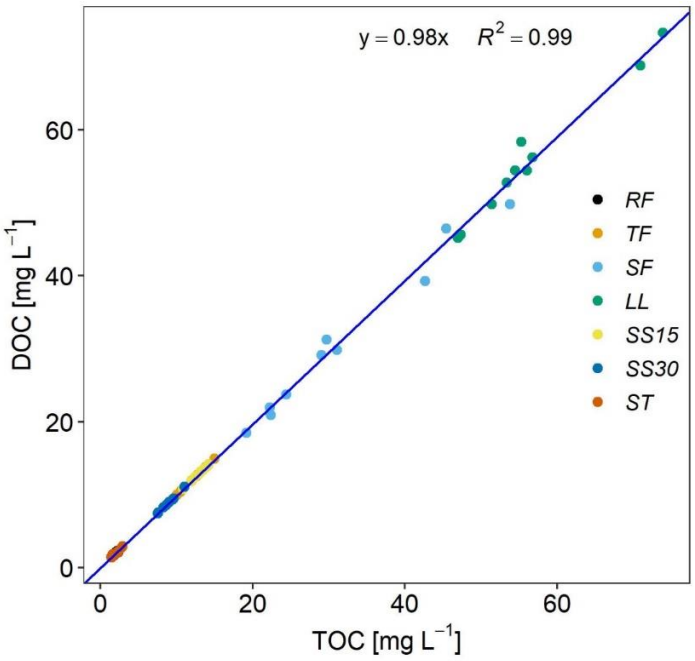


Figure B-S4. Relationship between total organic carbon (TOC) concentrations filtered <1-7 µm and dissolved organic carbon (DOC) concentrations (<0.45 µm) in ecosystem solutions sampled in the San Francisco Biological Reserve in South Ecuador. RF is rainfall, TF throughfall, SF stemflow, LL litter leachate, SS15 and SS30 mineral soil solutions at 0.15 and 0.30 m depth, respectively and ST stream water flow (n=70).

8. References

Badeck, F.-W., Tcherkez, G., Nogués, S., Piel, C., & Ghashghaie, J. (2005). Post-photosynthetic fractionation of stable carbon isotopes between plant organs—a widespread phenomenon. *Rapid Communications in Mass Spectrometry, 19*(11), 1381-1391. https://doi.org/10.1002/rcm.1912

Blagodatskaya, E., Yuyukina, T., Blagodatsky, S., & Kuzyakov, Y. (2011). Turnover of soil organic matter and of microbial biomass under C_3–C_4 vegetation change: Consideration of ^{13}C fractionation and preferential substrate utilization. *Soil Biology and Biochemistry, 43*(1), 159-166. https://doi.org/10.1016/j.soilbio.2010.09.028

Bodí, M. B., Martin, D. A., Balfour, V. N., Santín, C., Doerr, S. H., Pereira, P., Cerdà, A., & Mataix-Solera, J. (2014). Wildland fire ash: Production, composition and eco-hydro-geomorphic effects. *Earth-Science Reviews, 130*, 103-127. https://doi.org/10.1016/j.earscirev.2013.12.007

Boström, B., Comstedt, D., & Ekblad, A. (2007). Isotope fractionation and ^{13}C enrichment in soil profiles during the decomposition of soil organic matter. *Oecologia, 153*(1), 89-98. https://doi.org/10.1007/s00442-007-0700-8

Bowling, D. R., Pataki, D. E., & Randerson, J. T. (2008). Carbon isotopes in terrestrial ecosystem pools and CO_2 fluxes. *New Phytologist, 178*(1), 24-40. https://doi.org/10.1111/j.1469-8137.2007.02342.x

Boy, J., Rollenbeck, R., Valarezo, C., & Wilcke, W. (2008a). Amazonian biomass burning-derived acid and nutrient deposition in the north Andean montane forest of Ecuador. *Global Biogeochemical Cycles, 22*, GB4011. https://doi.org/10.1029/2007GB003158

Boy, J., Valarezo, C., & Wilcke, W. (2008b). Water flow paths in soil control element exports in an Andean tropical montane forest. *European Journal of Soil Science, 59*(6), 1209-1227. https://doi.org/10.1111/j.1365-2389.2008.01063.x

Brüggemann, N., Gessler, A., Kayler, Z., Keel, S. G., Badeck, F., Barthel, M., et al. (2011). Carbon allocation and carbon isotope fluxes in the plant-soil-atmosphere continuum: a review. *Biogeosciences, 8*(11), 3457-3489. https://doi.org/10.5194/bg-8-3457-2011

Cao, M., Wu, C., Liu, J., & Jiang, Y. (2020). Increasing leaf $\delta^{13}C$ values of woody plants in response to water stress induced by tunnel excavation in a karst trough valley:

implication for improving water-use efficiency. *Journal of Hydrology, 586*, 124895. https://doi.org/10.1016/j.jhydrol.2020.124895

Cernusak, L. A., & Hutley, L. B. (2011). Stable isotopes reveal the contribution of corticular photosynthesis to growth in branches of *Eucalyptus miniata*. *Plant Physiology, 155*(1), 515-523. https://doi.org/10.1104/pp.110.163337

Ciglasch, H., Lilienfein, J., Kaiser, K., & Wilcke, W. (2004). Dissolved organic matter under native Cerrado and *Pinus caribaea* plantations in the Brazilian savanna. *Biogeochemistry, 67*(2), 157-182. https://doi.org/10.1023/B:BIOG.0000015281.74705.f8

Damesin, C., Rambal, S., & Joffre, R. (1998). Seasonal and annual changes in leaf $\delta^{13}C$ in two co-occurring Mediterranean oaks: relations to leaf growth and drought progression. *Functional Ecology, 12*(5), 778-785. https://doi.org/10.1046/j.1365-2435.1998.00259.x

Dawson, T. E., Mambelli, S., Plamboeck, A. H., Templer, P. H., & Tu, K. P. (2002). Stable isotopes in plant ecology. *Annual review of ecology and systematics, 33*(1), 507-559. https://doi.org/10.1146/annurev.ecolsys.33.020602.095451

de Lecea, A. M.; Smit, A. J.; Fennessy, S. T. The effects of freeze/thaw periods and drying methods on isotopic and elemental carbon and nitrogen in marine organisms, raising questions on sample preparation, *Rapid Communications in Mass Spectrometry* **2011**, *25*(23), 3640-3649. https://doi.org/10.1002/rcm.5265.

Dijkstra, P., Ishizu, A., Doucett, R., Hart, S. C., Schwartz, E., Menyailo, O. V., & Hungate, B. A. (2006). ^{13}C and ^{15}N natural abundance of the soil microbial biomass. *Soil Biology and Biochemistry, 38*(11), 3257-3266. https://doi.org/10.1016/j.soilbio.2006.04.005

DVWK. (1996). *Ermittlung der Verdunstung von Land-und Wasserflächen*. Retrieved from Bonn, Germany:

Federherr, E. (2016). *Stable carbon and nitrogen isotope analysis in aqueous samples–method development, validation and application.* (Ph.D. Ph.D. Thesis), Universität Duisburg-Essen, Essen, Germany.

Federherr, E., Cerli, C., Kirkels, F. M. S. A., Kalbitz, K., Kupka, H. J., Dunsbach, R., Lange, L., & Schmidt, T. C. (2014). A novel high-temperature combustion based system for stable isotope analysis of dissolved organic carbon in aqueous samples. I:

development and validation. *Rapid Communications in Mass Spectrometry, 28*(23), 2559-2573. https://doi.org/10.1002/rcm.7052

Fleischbein, K., Wilcke, W., Valarezo, C., Zech, W., & Knoblich, K. (2006). Water budgets of three small catchments under montane forest in Ecuador: experimental and modelling approach. *Hydrological processes, 20*(12), 2491-2507. https://doi.org/10.1002/hyp.6212

Fröberg, M., Jardine, P. M., Hanson, P. J., Swanston, C., Todd, D., Tarver, J., & Garten, C. (2007). Low dissolved organic carbon input from fresh litter to deep mineral soils. *Soil Science Society of America Journal, 71*(2), 347-354. https://doi.org/10.2136/sssaj2006.0188

Fry, B.; Saupe, S.; Hullar, M.; Peterson, B. J. (1993). Platinum-catalyzed combustion of DOC in sealed tubes for stable isotopic analysis, *Marine Chemistry* **1993**, *41*(1), 187-193. https://doi.org/10.1016/0304-4203(93)90118-8.

Fry, B., Peltzer, E. T., Hopkinson, C. S., Nolin, A., & Redmond, L. (1996). Analysis of marine DOC using a dry combustion method. *Marine Chemistry, 54*(3), 191-201. https://doi.org/10.1016/0304-4203(96)00031-X

Fry, B.; Hopkinson, C. S.; Nolin, A.; Wainright, S. C. (1998). $^{13}C/1^{2}C$ composition of marine dissolved organic carbon, *Chemical Geology* **1998**, *152*(1), 113-118. https://doi.org/10.1016/S0009-2541(98)00100-4.

Gandois, L., Teisserenc, R., Cobb, A. R., Chieng, H. I., Lim, L. B. L., Kamariah, A. S., Hoyt, A., & Harvey, C. F. (2014). Origin, composition, and transformation of dissolved organic matter in tropical peatlands. *Geochimica et Cosmochimica Acta, 137*, 35-47. https://doi.org/10.1016/j.gca.2014.03.012

Garten, C., Cooper, L., Post, W., & Hanson, P. (2000). Climate controls on forest soil C isotope ratios in the southern Appalachian Mountains. *Ecology, 81*(4), 1108-1119. https://doi.org/10.1890/0012-9658(2000)081[1108:CCOFSC]2.0.CO;2

Goller, R., Wilcke, W., Fleischbein, K., Valarezo, C., & Zech, W. (2006). Dissolved nitrogen, phosphorus, and sulfur forms in the ecosystem fluxes of a montane forest in Ecuador. *Biogeochemistry, 77*(1), 57-89. https://doi.org/10.1007/s10533-005-1061-1

Goller, R., Wilcke, W., Leng, M. J., Tobschall, H. J., Wagner, K., Valarezo, C., & Zech, W. (2005). Tracing water paths through small catchments under a tropical montane rain forest in south Ecuador by an oxygen isotope approach. *Journal of Hydrology, 308*(1), 67-80. https://doi.org/10.1016/j.jhydrol.2004.10.022

Gougherty, S. W., Bauer, J. E., & Pohlman, J. W. (2018). Exudation rates and δ13C signatures of tree root soluble organic carbon in a riparian forest. *Biogeochemistry, 137*(1), 235-252. https://doi.org/10.1007/s10533-017-0415-9

Guggenberger, G., Kaiser, K., & Zech, W. (1998). Mobilization and immobilization of dissolved organic matter in forest soils. *Zeitschrift für Pflanzenernährung und Bodenkunde, 161*(4), 401-408. https://doi.org/10.1002/jpln.1998.3581610408

Guggenberger, G., & Zech, W. (1993). Dissolved organic carbon control in acid forest soils of the Fichtelgebirge (Germany) as revealed by distribution patterns and structural composition analyses. *Geoderma, 59*(1-4), 109-129. https://doi.org/10.1016/0016-7061(93)90065-S

Guggenberger, G., & Zech, W. (1994). Composition and dynamics of dissolved carbohydrates and lignin-degradation products in two coniferous forests, NE Bavaria, Germany. *Soil Biology and Biochemistry, 26*(1), 19-27. https://doi.org/10.1016/0038-0717(94)90191-0

Guggenberger, G., Zech, W., & Schulten, H.-R. (1994). Formation and mobilization pathways of dissolved organic matter: evidence from chemical structural studies of organic matter fractions in acid forest floor solutions. *Organic Geochemistry, 21*(1), 51-66. https://doi.org/10.1016/0146-6380(94)90087-6

Günter, S., Gonzalez, P., Álvarez, G., Aguirre, N., Palomeque, X., Haubrich, F., & Weber, M. (2009). Determinants for successful reforestation of abandoned pastures in the Andes: Soil conditions and vegetation cover. *Forest Ecology and Management, 258*(2), 81-91. https://doi.org/10.1016/j.foreco.2009.03.042

Han, Y. M., Cao, J. J., Lee, S. C., Ho, K. F., & An, Z. S. (2010). Different characteristics of char and soot in the atmosphere and their ratio as an indicator for source identification in Xi'an, China. *Atmos. Chem. Phys., 10*(2), 595-607. https://doi.org/10.5194/acp-10-595-2010

Heaton, T. H. (1999). Spatial, species, and temporal variations in the $^{13}C/^{12}C$ ratios of C_3 plants: implications for palaeodiet studies. *Journal of Archaeological Science, 26*(6), 637-649. https://doi.org/10.1006/jasc.1998.0381

Homeier, J., Breckle, S.-W., Günter, S., Rollenbeck, R. T., & Leuschner, C. (2010). Tree diversity, forest structure and productivity along altitudinal and topographical gradients in a species-rich Ecuadorian montane rain forest. *Biotropica, 42*(2), 140-148. https://doi.org/10.1111/j.1744-7429.2009.00547.x

Homeier, J., Werner, F. A., Gradstein, S. R., Breckle, S. W., & Richter, M. (2008). Potential vegetation and floristic composition of Andean forests in south Ecuador, with a focus on the RBSF. In E. Beck, J. Bendix, I. Kottke, F. Makeschin, & R. Mosandl (Eds.), *Gradients in a Tropical Mountain Ecosystem of Ecuador* (pp. 87-100). Berlin, Heidelberg: Springer-Verlag. https://doi.org/10.1007/978-3-540-73526-7_10

Hood, E., Williams, M., & McKnight, D. (2005). Sources of dissolved organic matter (DOM) in a Rocky Mountain stream using chemical fractionation and stable isotopes. *Biogeochemistry, 74*(2), 231-255. https://doi.org/10.1007/s10533-004-4322-5

Hur, J., Park, M.-H., & Schlautman, M. A. (2009). Microbial Transformation of Dissolved Leaf Litter Organic Matter and Its Effects on Selected Organic Matter Operational Descriptors. *Environmental science & technology, 43*(7), 2315-2321. https://doi.org/10.1021/es802773b

IUSS Working Group WRB. (2014). *World Reference Base for Soil Resources 2014. International soil classification system for naming soils and creating legends for soil maps.*

Kaiser, K., Guggenberger, G., & Zech, W. (2001). Isotopic fractionation of dissolved organic carbon in shallow forest soils as affected by sorption. *European Journal of Soil Science, 52*(4), 585-597.

Kaiser, K., & Zech, W. (1997). Competitive sorption of dissolved organic matter fractions to soils and related mineral phases. *Soil Science Society of America Journal, 61*(1), 64-69.

Kalbitz, K., Solinger, S., Park, J.-H., Michalzik, B., & Matzner, E. (2000). Controls on the dynamics of dissolved organic matter in soils: a review. *Soil Science, 165*(4), 277-304. https://doi.org/10.1097/00010694-200004000-00001

Kirkels, F. M. S. A., Cerli, C., Federherr, E., Gao, J., & Kalbitz, K. (2014). A novel high-temperature combustion based system for stable isotope analysis of dissolved organic carbon in aqueous samples. II: optimization and assessment of analytical performance. *Rapid Communications in Mass Spectrometry, 28*(23), 2574-2586. https://doi.org/10.1002/rcm.7053

Kohl, L., Laganière, J., Edwards, K. A., Billings, S. A., Morrill, P. L., Van Biesen, G., & Ziegler, S. E. (2015). Distinct fungal and bacterial δ13C signatures as potential drivers of increasing δ13C of soil organic matter with depth. *Biogeochemistry, 124*(1), 13-26. https://doi.org/10.1007/s10533-015-0107-2

Kohn, M. J. (2010). Carbon isotope compositions of terrestrial C_3 plants as indicators of (paleo) ecology and (paleo) climate. *Proceedings of the National Academy of Sciences, 107*(46), 19691-19695. https://doi.org/10.1073/pnas.1004933107

Kramer, C., Trumbore, S., Fröberg, M., Cisneros Dozal, L. M., Zhang, D., Xu, X., Santos, G. M., & Hanson, P. J. (2010). Recent (<4 year old) leaf litter is not a major source of microbial carbon in a temperate forest mineral soil. *Soil Biology and Biochemistry, 42*(7), 1028-1037. https://doi.org/10.1016/j.soilbio.2010.02.021

Lorenz, M., Derrien, D., Zeller, B., Udelhoven, T., Werner, W., & Thiele-Bruhn, S. (2020). The linkage of ^{13}C and ^{15}N soil depth gradients with C:N and O:C stoichiometry reveals tree species effects on organic matter turnover in soil. *Biogeochemistry, 151*(2), 203-220. https://doi.org/10.1007/s10533-020-00721-3

Michener, R., & Lajtha, K. (2008). *Stable isotopes in ecology and environmental science* (2 ed.). Oxford, UK. Blackwell Scientific Publications.p.

Paterson, E., Hodge, A., Thornton, B., Millard, P., & Killham, K. (1999). Carbon partitioning and rhizosphere C-flow in *Lolium perenne* as affected by CO_2 concentration, irradiance and below-ground conditions. *Global Change Biology, 5*(6), 669-678. https://doi.org/10.1046/j.1365-2486.1999.00267.x

Peterson, B., Fry, B., Hullar, M., Saupe, S., & Wright, R. (1994). The distribution and stable carbon isotopic composition of dissolved organic carbon in estuaries. *Estuaries, 17*(1), 111-121. https://doi.org/10.2307/1352560

Pierick, K., Leuschner, C., & Homeier, J. (2021). Topography as a factor driving small-scale variation in tree fine root traits and root functional diversity in a species-rich tropical montane forest. *New Phytologist, 230*(1), 129-138. https://doi.org/10.1111/nph.17136

R Core Team. (2025). R: A language and environment for statistical computing. R Foundation for Statistical Computing. Vienna, Austria. Retrieved from https://www.r-project.org/

Rascher, K., Máguas, C., & Werner, C. (2010). On the use of phloem sap $\delta^{13}C$ as an indicator of canopy carbon discrimination. *Tree Physiology, 30*(12), 1499-1514. https://doi.org/10.1093/treephys/tpq092

Roos, K., Bendix, J., Curatola, G. F., Gawlik, J., Gerique, A., Hamer, U., et al. (2013). Current provisioning services: pasture development and use, weeds (bracken) and management. In J. Bendix, E. Beck, A. Bräuning, F. Makeschin, R. Mosandl, S. Scheu, & W. Wilcke (Eds.), *Ecosystem services, biodiversity and environmental*

change in a tropical mountain ecosystem of south Ecuador. (pp. 205-217). Germany: Springer. https://doi.org/10.1007/978-3-642-38137-9_15

Sanderman, J., Baldock, J. A., & Amundson, R. (2008). Dissolved organic carbon chemistry and dynamics in contrasting forest and grassland soils. *Biogeochemistry, 89*(2), 181-198. https://doi.org/10.1007/s10533-008-9211-x

Scartazza, A., Mata, C., Matteucci, G., Yakir, D., Moscatello, S., & Brugnoli, E. (2004). Comparisons of $\delta^{13}C$ of photosynthetic products and ecosystem respiratory CO_2 and their responses to seasonal climate variability. *Oecologia, 140*(2), 340-351. https://doi.org/10.1007/s00442-004-1588-1

Schulze, K., Borken, W., & Matzner, E. (2011). Dynamics of dissolved organic ^{14}C in throughfall and soil solution of a Norway spruce forest. *Biogeochemistry, 106*(3), 461-473. https://doi.org/10.1007/s10533-010-9526-2

Schwarz, M. T., Oelmann, Y., & Wilcke, W. (2011). Stable N isotope composition of nitrate reflects N transformations during the passage of water through a montane rain forest in Ecuador. *Biogeochemistry, 102*(1), 195-208. https://doi.org/10.1007/s10533-010-9434-5

Shahzad, T., Rashid, M. I., Maire, V., Barot, S., Perveen, N., Alvarez, G., Mougin, C., & Fontaine, S. (2018). Root penetration in deep soil layers stimulates mineralization of millennia-old organic carbon. *Soil Biology and Biochemistry, 124*, 150-160. https://doi.org/10.1016/j.soilbio.2018.06.010

Soethe, N., Lehmann, J., & Engels, C. (2007). Carbon and nutrient stocks in roots of forests at different altitudes in the Ecuadorian Andes. *Journal of Tropical Ecology, 23*(3), 319-328. https://doi.org/10.1017/S0266467407004002

Solinger, S., Kalbitz, K., & Matzner, E. (2001). Controls on the dynamics of dissolved organic carbon and nitrogen in a Central European deciduous forest. *Biogeochemistry, 55*(3), 327-349. https://doi.org/10.1023/A:1011848326013

Song, J., Huang, W., & Peng, P. (2012). Stability and carbon isotope changes of soot and char materials during thermal oxidation: implication for quantification and source appointment. *Chemical Geology, 330-331*, 159-164. https://doi.org/10.1016/j.chemgeo.2012.08.003

Thieme, L., Graeber, D., Hofmann, D., Bischoff, S., Schwarz, M. T., Steffen, B., et al. (2019). Dissolved organic matter characteristics of deciduous and coniferous forests with variable management: different at the source, aligned in the soil. *Biogeosciences, 16*(7), 1411-1432. https://doi.org/10.5194/bg-16-1411-2019

Tückmantel, T., Leuschner, C., Preusser, S., Kandeler, E., Angst, G., Mueller, C. W., & Meier, I. C. (2017). Root exudation patterns in a beech forest: dependence on soil depth, root morphology, and environment. *Soil Biology and Biochemistry, 107*, 188-197. https://doi.org/10.1016/j.soilbio.2017.01.006

Van Stan, J. T., & Stubbins, A. (2018). Tree-DOM: dissolved organic matter in throughfall and stemflow. *Limnology and Oceanography Letters, 3*(3), 199-214. https://doi.org/10.1002/lol2.10059

Wagner, S., Brantley, S., Stuber, S., Van Stan, J., Whitetree, A., & Stubbins, A. (2019). Dissolved black carbon in throughfall and stemflow in a fire-managed longleaf pine woodland. *Biogeochemistry, 146*(2), 191-207. https://doi.org/10.1007/s10533-019-00620-2

Wang, M., Zhang, Z., Wang, Y., Mo, X., Zhang, Q., Zhang, P., et al. (2021). Characteristics of dissolved organic matter and dissolved lignin phenols in tropical forest soil solutions during rainy seasons and their responses to nitrogen deposition. *ACS Earth and Space Chemistry, 5*(11), 3150-3158. https://doi.org/10.1021/acsearthspacechem.1c00243

Wang, X., Xu, C., Druffel, E. M., Xue, Y., & Qi, Y. (2016). Two black carbon pools transported by the Changjiang and Huanghe Rivers in China. *Global Biogeochemical Cycles, 30*(12), 1778-1790. https://doi.org/10.1002/2016GB005509

Werner, F. A., & Homeier, J. (2015). Is tropical montane forest heterogeneity promoted by a resource-driven feedback cycle? Evidence from nutrient relations, herbivory and litter decomposition along a topographical gradient. *Functional Ecology, 29*(3), 430-440. https://doi.org/10.1111/1365-2435.12351

Wilcke, W., Leimer, S., Peters, T., Emck, P., Rollenbeck, R., Trachte, K., Valarezo, C., & Bendix, J. (2013). The nitrogen cycle of tropical montane forest in Ecuador turns inorganic under environmental change. *Global Biogeochemical Cycles, 27*(4), 1194-1204. https://doi.org/10.1002/2012GB004471

Wilcke, W., Velescu, A., Leimer, S., Bigalke, M., Boy, J., & Valarezo, C. (2017). Biological versus geochemical control and environmental change drivers of the base metal budgets of a tropical montane forest in Ecuador during 15 years. *Biogeochemistry, 136*(2), 167-189. https://doi.org/10.1007/s10533-017-0386-x

Wilcke, W., Velescu, A., Leimer, S., Bigalke, M., Boy, J., & Valarezo, C. (2019). Temporal trends of phosphorus cycling in a tropical montane forest in Ecuador during 14 years.

Journal of Geophysical Research: Biogeosciences, 124(5), 1370-1386. https://doi.org/10.1029/2018JG004942

Wilcke, W., Velescu, A., Leimer, S., Blotevogel, S., Alvarez, P., & Valarezo, C. (2020). Total organic carbon concentrations in ecosystem solutions of a remote tropical montane forest respond to global environmental change. *Global Change Biology, 26*(12), 6989-7005. https://doi.org/10.1111/gcb.15351

Xu, N., & Saiers, J. E. (2010). Temperature and hydrologic controls on dissolved organic matter mobilization and transport within a forest topsoil. *Environmental science & technology, 44*(14), 5423-5429. https://doi.org/10.1021/es1002296

Xu, N., Saiers, J. E., Wilson, H. F., & Raymond, P. A. (2012). Simulating streamflow and dissolved organic matter export from a forested watershed. *Water Resources Research, 48*, W05519. https://doi.org/10.1029/2011WR011423

Yamashita, Y., Kojima, D., Yoshida, N., & Shibata, H. (2021). Relationships between dissolved black carbon and dissolved organic matter in streams. *Chemosphere, 271*, 129824. https://doi.org/10.1016/j.chemosphere.2021.129824

C. $\delta^{15}N$ values of total dissolved nitrogen

Sources and sinks of N in ecosystem solutions along the water path through a tropical montane forest in Ecuador assessed with $\delta^{15}N$ values of total dissolved nitrogen

Pablo Alvarez[1,2], Andre Velescu[1], Kerstin Pierick[3], Jürgen Homeier[4,5], and Wolfgang Wilcke[1]

[1] Institute of Geography and Geoecology, Karlsruhe Institute of Technology (KIT), Reinhard-Baumeister-Platz 1, 76131 Karlsruhe, Germany

[2] Faculty of Agriculture and Renewable Natural Resources, Universidad Nacional de Loja, Avenida Reinaldo Espinoza s/n, 110103 Loja, Ecuador

[3] Spatial Structures and Digitization of Forests/Silviculture and Forest Ecology of the Temperate Zones, Georg August University Göttingen, 37077 Göttingen, Germany

[4] Faculty of Resource Management, University of Applied Sciences and Arts, 37077 Göttingen, Germany

[5] Department of Plant Ecology and Ecosystem Research, Georg August University Göttingen, 37073 Göttingen, Germany

Journal of Geophysical Research: Biogeosciences (2024): 129, e2024JG008043.

https://doi.org/10.1029/2024JG008043

1. Abstract

The globally increasing reactive N richness affects even remote ecosystems such as the tropical montane forests in Ecuador. We tested whether the $\delta^{15}N$ values of total dissolved N (TDN), measured directly in solution with a TOC-IRMS, can be used to help elucidate N sources and sinks along the water path and thus might be suitable for ecosystem monitoring. From 2013-2016, the $\delta^{15}N$ values of TDN in bulk deposition showed the most pronounced temporal variation of all ecosystem solutions ($\delta^{15}N$ values: 1.9-5.9‰). In throughfall (TF), TDN was on average ^{15}N-depleted (-1.8±s.d. 0.4‰) relative to rainfall (3.4±0.9‰), resulting from net retention of isotopically heavy N, mainly as NH_4^+. Simultaneously, N-isotopically light NO_3^--N and dissolved organic nitrogen (DON) with a $\delta^{15}N$ value between NO_3^--N and NH_4^+-N were leached from the canopy (leaves: -3.5±0.5‰). The increasing $\delta^{15}N$ values in the order, TF<stemflow (SF, 0.1±0.6‰)<litter leachate (LL, 1.3±0.7‰) concurred with an increasing DON contribution to TDN reflecting the $\delta^{15}N$ value of the organic layer (1.9±0.9‰). The lower $\delta^{15}N$ value of the mineral soil solution at the 0.15 m soil depth (SS15, -1.5±0.3‰) than in LL can be explained by the retention of DON and NH_4^+ and the addition of NO_3^- from mineralization and nitrification. The increasing $\delta^{15}N$ values in the order, SS15<SS30 (-0.6±0.2‰)<streamflow (ST, 0.5±0.6‰) suggested gaseous N losses because of increasing denitrification. There was no seasonality of the $\delta^{15}N$ values. Our results demonstrate that the $\delta^{15}N$ values of TDN in ecosystem solutions help identify N sources and sinks in forest ecosystems.

Keywords: Nitrogen stable isotope ratio, dissolved organic matter, dissolved organic nitrogen, total dissolved nitrogen, ecosystem solution.

Key Points:

- Increasing $\delta^{15}N$ values in total dissolved nitrogen from throughfall to litter leachate correlated with an increasing organic contribution.
- The retention of N-isotopically heavy dissolved organic nitrogen in the mineral topsoil decreased the $\delta^{15}N$ values in mineral soil solutions.
- Increasing $\delta^{15}N$ values from the topsoil solution via the subsoil to the streamflow suggested gaseous N losses because of denitrification.

Plain Language Summary

Many ecosystems experience increasing nitrogen availability because of nitrogen deposition from the atmosphere caused by human activities. The deposited nitrogen can produce a growth boost or be leached into groundwater and surface water. The stable isotope ratios of nitrogen ($\delta^{15}N$ values) provide a tool to investigate into the consequences of increasing nitrogen availability. Here, we applied a new direct measurement method of $\delta^{15}N$ values in total dissolved nitrogen of ecosystem solutions to follow sources and sinks of nitrogen in a tropical montane rain forest in Ecuador. We found that the isotopically heavy nitrogen input via rainfall is enriched by isotopically lighter nitrogen from plants and nitrogen turnover in the canopy during the water passage through the canopy. Once, the solutions reach the mineral soil, dissolved organic nitrogen, which is comparatively rich in the heavy nitrogen isotope, is retained rendering the remaining nitrogen isotopically lighter. This process is reversed deeper in the soil by conversion of the nitrate to nitrogen gasses, which are depleted in the heavy nitrogen isotope and leave the ecosystem to the atmosphere. The direct measurement of $\delta^{15}N$ values provides a tool to monitor the changing nitrogen cycle in ecosystems.

2. Introduction

Tropical forests are generally described as nutrient-limited ecosystems. Lowland tropical forests are frequently considered P-limited (Aragão et al., 2009; Vitousek, 1984) and tropical montane forests N- or N+P-co-limited (Fisher et al., 2013; Turner & Wright, 2014). As a consequence, tropical forests are susceptible to N and/or P deposition, which can increase their biomass production and threaten their frequently high biodiversity (Barthlott et al., 1996; Sala et al., 2000; Wassen et al., 2005).

Currently, N deposition increases the N availability in many global forest ecosystems (Galloway et al., 2004; Galloway et al., 2008; Lamarque et al., 2013). At the same time, many forest ecosystems receive a low but constant input of P from the atmosphere (Bol et al., 2016; Sohrt et al., 2017; Tipping et al., 2014; Wilcke et al., 2019). In addition to the nutrient inputs, increasing dry phases in otherwise wet tropical montane forests enhance soil organic matter mineralization and result in an additional nutrient release (Peters et al., 2013; Wilcke et al., 2013). Thus, the availability of N and P is on the rise in many tropical forests. To assess the redistribution of increasingly available nutrients in forest ecosystems new methods that can be applied to monitoring efforts are helpful. For N, the recently developed direct measurement of the stable N isotope ratio ($\delta^{15}N$ values) of total dissolved N (TDN) in ecosystem solutions with a Total Organic Carbon Analyzer coupled to an Isotope Ratio Mass Spectrometer (TOC-IRMS), which allows for the measurement of stable C and N isotope ratios may provide such a method (Alvarez et al., 2023; Federherr et al., 2014; Kirkels et al., 2014).

Because transformations among different chemical species in the soil solution such as between NH_4^+ and NO_3^- do not change the $\delta^{15}N$ value of TDN in ecosystem solutions, observed changes of the $\delta^{15}N$ value of TDN can only be attributed to the addition or the loss of N with a $\delta^{15}N$ value deviating from the mean $\delta^{15}N$ value of the original TDN, i.e., the TDN in the preceding ecosystem solution along the water path through the forest. Following the flow path of water through a forest ecosystem, the first source of N is the deposition from the atmosphere. It has been shown that the $\delta^{15}N$ values of NH_4^+ and NO_3^- in deposition from the atmosphere show a considerable temporal variation likely reflecting different sources of inorganic N (Felix et al., 2017; Garten, 1996; Schwarz et al., 2011). We are not aware of studies addressing the $\delta^{15}N$ values of total N in deposition. The deposited N comes first into contact with the forest canopy and thus could be influenced by the $\delta^{15}N$ values of leaves widely ranging from -7.8‰ to 8.7‰ (Craine et al., 2009; Craine et al., 2012). If N_2 fixation

from the atmosphere is a major source of plant N, the $\delta^{15}N$ values of plant tissue are close to 0‰, i.e., similar to that of the atmospheric N_2 serving as international standard for $\delta^{15}N$ values and thus showing by definition a $\delta^{15}N$ value of 0‰ (Craine et al., 2015). As a consequence, throughfall and stemflow might be influenced by the $\delta^{15}N$ values of the leaves, because of N leaching, particularly in organic form (Goller et al., 2006; Schwarz et al., 2014; Wilcke et al., 2013). However, if ecosystems are N-limited, N is on balance retained in the canopy (Harrison et al., 2000; Lovett & Lindberg, 1993; Schwarz et al., 2014). Because the retention of inorganic N and leaching of organic N may fractionate N isotopes, the canopy interaction of the deposited N is likely to result in changed $\delta^{15}N$ values in throughfall and stemflow.

When throughfall and stemflow reach the soil surface, they first come into contact with the soil organic layer on top of the mineral soil, where N can be retained or leached (Schwarz et al., 2016; Solinger et al., 2001; Wilcke et al., 2013). For a tropical montane forest in Ecuador Goller et al. (2006) and Wilcke et al. (2013) have shown that the N concentration in the litter leachate is higher than in throughfall and stemflow pointing at a net enrichment of N because of organic matter mineralization. The NH_4^+ released by mineralization is N-isotopically lighter than the N in bulk organic matter (Högberg, 1997). If enough N is released into soil solution to activate nitrification, NH_4^+ becomes increasingly heavier while the produced NO_3^- is isotopically lighter than NH_4^+ (Craine et al., 2015; Högberg, 1997). Moreover, in a tropical montane forest, dissolved organic N (DON) was increasingly enriched from bulk deposition via throughfall and stemflow to litter leachate, indicating DON leaching from the vegetation and the organic layer (Goller et al., 2006; Wilcke et al., 2013). A preferential retention of NH_4^+ by cation-exchange sites or plant uptake and the leaching of DON and NO_3^- will likely be reflected by the $\delta^{15}N$ values of TDN in litter leachate. Temporally changing contributions of NO_3^- and DON leaching to the TDN in litter leachate can possibly be detected by determining $\delta^{15}N$ values in time series.

In the mineral soil, DON is adsorbed resulting in decreasing DON concentrations and fluxes (Goller et al., 2006; Michalzik et al., 2001; Wilcke et al., 2013). In the same tropical montane forest as in our study, the NO_3^--N/NH_4^+-N ratio increased strongly from litter leachate to mineral soil solution (Wilcke et al., 2013), suggesting the further production of NO_3^- by nitrification and/or a NH_4^+ retention in the mineral soil at cation-exchange sites or by fixation in clay minerals such as illites. The retention of DON and possibly also NH_4^+ will again likely change the $\delta^{15}N$ values of TDN in the soil solutions. Wilcke et al. (2020)

and Alvarez et al. (2023) reported that root exudates and decomposing roots contribute to the dissolved organic matter concentrations in the mineral soil, which would also be a possible source of N for the mineral soil solutions. Because it has been reported that leaves show a lower $\delta^{15}N$ value than roots by 0.3 to <1‰ (Craine et al., 2005; Dijkstra et al., 2003), root-derived N might increase the $\delta^{15}N$ value of TDN in mineral soil solutions. Finally, denitrification favoring N-isotopically light NO_3^- will result in a higher $\delta^{15}N$ value of TDN in mineral soil solutions and stream water fed by mineral soil solutions. For the same tropical montane forest as studied here, Schwarz et al. (2011) observed an increasing $\delta^{15}N$ value of NO_3^- with increasing mineral soil depth and in the stream water relative to the soil solutions indicating that denitrification indeed occurred in this ecosystem. In line with the assumption of a positive relationship between denitrification and soil depth, Castellano-Hinojosa et al. (2018), reported an increasing abundance of the denitrification genes with increasing soil depth which paralleled the decrease in dissolved oxygen concentrations. Dissolved organic C (DOC)-rich ecosystems such as the tropical montane forests with their thick organic layers (Wilcke et al., 2002) might favor denitrification, because Barrett et al. (2016) observed that DOC amendments to the soil resulted in larger denitrifier populations and N_2 emissions. Moreover, a high supply of NO_3^- to the subsoil as reported for the tropical montane forest in Ecuador (Wilcke et al., 2013) likely further enhances denitrification particularly under wet conditions (Arango & Tank, 2008). In summary, the multiple sources and sinks of TDN in ecosystem solutions along the water path from rainfall through the ecosystem to the stream water are expected to change the $\delta^{15}N$ values, which in turn could be used to identify the kind and size of these sinks and sources. Moreover, the direct measurement of $\delta^{15}N$ values could be used as a comparatively simple tool to monitor changes in the N cycle of ecosystems that can be applied to large sample numbers.

We studied the change in $\delta^{15}N$ values of TDN in ecosystem solutions along the water path from above-canopy rainfall through the forest ecosystem to streamflow during four years in quarterly resolution to test whether there are temporal changes in the N sources and sinks of ecosystem solutions. We hypothesized that the $\delta^{15}N$ values of TDN (i) in rainfall are temporally most variable of all ecosystem solutions reflecting changing N sources, (ii) decrease from rainfall via throughfall and stemflow to litter leachate, because of increasing contributions of N-isotopically lighter N leached from the canopy, (iii) decrease from litter leachate to the mineral soil, because of the retention of DON and NH_4^+ with higher $\delta^{15}N$ values than NO_3^-, and (iv) increase from mineral topsoil solution via subsoil solution to

stream water, because of increasing denitrification. Moreover, (v) we expected that the changes in the $\delta^{15}N$ values of TDN in ecosystem solutions showed a temporal variation reflecting temporally variable strengths of the various N sources and sinks.

3. Material and methods

3.1. Study Site

We studied a 9.1-ha catchment at 1850-2150 m above sea level (a.s.l.) under evergreen lower tropical montane forest (Bruijnzeel & Hamilton, 2000) in the San Francisco Biological Reserve on the east-exposed slope of the Andean cordillera in south Ecuador (Beck et al., 2019). This catchment has been described in previous studies as Microcatchment (MC) 2 (Alvarez et al., 2023; Boy et al., 2008b; Wilcke et al., 2020).

The mean annual temperature during 1998-2013 was 14.9 °C and the mean annual precipitation 2320 mm. The study ecosystem is perhumid with always >100 mm of monthly precipitation (Figure C-S1). November and October have the lowest monthly precipitation and June has the highest. Particularly, in the period October-November, there can be extended dry spells of up to several weeks, called “veranillo”. From 1998 to 2010, it has been reported that throughfall, relative humidity, and the soil moisture content decreased, while interception loss from the forest canopy increased (Wilcke et al., 2020). Soils are mainly shallow, loamy Folic Dystric Cambisols (IUSS Working Group WRB, 2014) developed from phyllite with some interlayering of metasandstone. The soils are covered by partly thick organic layers (Wilcke et al., 2002). The clay mineralogy of the mineral soil is dominated by illite, vermiculite, and kaolinite (Schrumpf et al., 2001). The mean pH value of the mineral topsoil is 4.4, the mean effective cation-exchange capacity 63±standard deviation 26 $mmol_c\ kg^{-1}$, the mean organic C concentration 32±19 $g\ kg^{-1}$, and the mean C/N ratio 11±2.8 (Wilcke et al., 2017). The vegetation growth was reported to be N+P co-limited (Homeier et al., 2012).

3.2. Field sampling

Leaves of ten common tree species of the study forest were sampled from October to December 2016 (see species names in Table C-S1 and Figure C-S2). Additionally, leaves of two common tree species were sampled during the period 2005–2015 to determine the temporal variation (Figure C-S3). Species-specific fine roots segments (diameter ≤ 2 mm, length >10 cm) were sampled from individuals of the same 10 common tree species from

which leaves were sampled from October to December 2016. Further details of root sampling and processing are described in Pierick et al. (2021). Samples of the Oi, Oe, Oa, A, and B horizons of 20 soil profiles were collected during two campaigns in 2006 and 2016. Leaf, root, Oi, Oe, and Oa samples were subsequently ground with a knife mill (Grindomix GM 200, Retsch, Haan, Germany) and a planetary ball mill (PM 200, Retsch, Haan, Germany). Mineral soil samples were sieved <2 mm and ground with the planetary ball mill.

The Long-term Ecosystem study was set up in April 1998 and since then continuously run with the same field sampling methods. Here, we considered ecosystem solution samples from the period 2013-2016 that were collected weekly. Rainfall was collected at two gaging stations, consisting of five Hellmann-type collectors, placed on clear-cut areas. Those collectors were permanently open and sampled bulk deposition, i.e., wet deposition and the soluble part of coarse particulate dry deposition that sediments into the collectors (Wilcke et al., 2013; Wilcke et al., 2017; Wilcke et al., 2020). Throughfall was collected with 20 fixed-position hand-made funnel collectors which were placed randomly along three 20-m long transects at the lower to middle slope at each of approximately 1900, 1950, and 2000 m a.s.l. Stemflow was collected with polyurethane collars at five trees in the lower part of the catchment. Litter leachate was collected with three zero-tension lysimeters per transect installed laterally below the organic layer. Mineral soil solutions were sampled with three suction cups (mullite, 1 µm±0.1 µm pore size) installed at the 0.15 and 0.3 m mineral soil depths, respectively (Wilcke et al., 2020). Streamflow was sampled weekly from the middle of the undisturbed flowing stream above a weir (Fleischbein et al., 2006).

Rainfall, throughfall, and stemflow water volumes were measured in the field and converted to water fluxes based on the collection surface of the samplers (RF, TF) or extrapolated according to the number of trees ha^{-1} (SF) (Wilcke et al., 2017). Water fluxes of litter leachate and soil solutions were estimated with the Soil Water Balance Model (DVWK, 1996) using data from 1999-2003 and then calculated for our study period by regression equations described in Wilcke et al. (2020) and (Schwarz et al., 2011), respectively. We combined the weekly samples into volume-weighted quarterly samples, except for litter leachate and mineral soil solutions from which we composited the same volume of each weekly sample, because the samplers do not collect the solutions in a way that is representative for the fluxes. All ecosystem solutions were filtered in the field laboratory with ashless folded filters of 4–7 µm pore size, Type 392 (Sartorius-Stedim GmbH, Göttingen, Germany), except the mineral soil solutions. Alvarez et al. (2023) tested

whether the TOC concentrations in our samples differed from dissolved organic carbon (DOC), which is conventionally filtered to <0.45 µm and did not detect a difference.

3.3. Chemical Analyses

The pH of the organic and mineral horizons was determined in a suspension of 10 and 40 g of soil in 100 mL of deionized water for organic and mineral horizons, respectively, using a pH glass electrode (Orion U402-S7, Thermo Scientific, Waltham, USA) after equilibration overnight. In the ecosystem solutions, the pH was measured directly with the same electrode type in an aliquot that was afterwards discarded.

The $\delta^{15}N$ values and N concentrations of leaf, root, and soil samples were measured with an elemental analyzer (Thermo Scientific, Flash 2000 HT Plus, Bremen, Germany) coupled to an IRMS (Thermo Scientific, Delta V Advantage, Bremen, Germany) through a Conflo IV interface. We used acetanilide as calibration standard for N concentrations, an organic-rich sediment (OAS, IVA Analysentechnik, Meerbusch, Germany) as IRMS working standard, and an aromatic polyimide (EMA-P2, Elemental Microanalysis Ltd, Okehampton, UK) for drift correction. IAEA-N-1 ($\delta^{15}N$: +0.40‰), IAEA-N-2 ($\delta^{15}N$: +20.30‰) and USGS-61 ($\delta^{15}N$: -2.87‰) were used to reference the results to the N_2 in air scale by linear regression. The precision of the $\delta^{15}N$ values determined by routinely performed, repeated measurements of the working standard was 0.20‰.

Total dissolved nitrogen (TDN) and dissolved inorganic nitrogen (DIN = NH_4-N+NO_3-N) were measured using high resolution colorimetry and photometric detection with a continuous flow analyzer (CFA San++, Skalar, Breda, The Netherlands). Dissolved organic nitrogen (DON) was calculated as the difference between TDN and DIN. Cl^- concentrations were also measured by CFA using an ion-selective electrode (Orion Ionplus, Thermo Scientific, Beverly, USA).

The $\delta^{15}N$ values of TDN were determined with an elemental analyzer for liquid samples optimized for stable isotope measurements (isoTOC cube, Elementar Analysensysteme GmbH, Langenselbold, Germany), which was coupled via a low concentration module for peak focusing (LCM) to an IRMS (Vision, Isoprime Ltd, Stockport, UK). A volume of 1-2.5 mL of sample was injected via a four-way valve into the combustion tube. The combustion occurred at 850 °C in a He flow on a Pt catalyst, while O_2 was introduced as reaction gas by a mass-flow controler. Excess O_2 was removed and NO_x compounds were reduced to N_2 by elemental Cu in a reduction tube at 500 °C. Water was

removed by a condenser, a trap filled with phosphorus pentoxide and a membrane dryer. Volatile halogen compounds were bound on silver wool. The background caused by dissolved atmospheric N_2 was reduced during sample uptake by a membrane degasser. N_2 was focused by an adsorption column at -38°C in the LCM and then rapidly desorbed at 100°C and transported by the carrier gas to the open split of the IRMS.

We applied a linear calibration function to reference the measured $\delta^{15}N$ values to the N_2 in air scale using the reference materials USGS-25 ($\delta^{15}N$: -30.4‰), IAEA-N-1, USGS-64 ($\delta^{15}N$: +1.76‰), IAEA-600 ($\delta^{15}N$: +1.0‰) and USGS-62 ($\delta^{15}N$: +20.17). We used repeated measurements of caffeine (USGS-61, $\delta^{15}N$: -2.87‰) for drift correction. Linearity corrections followed the procedure suggested by Federherr et al. (2014) for $\delta^{13}C$ measurements. The precision of the measurement was determined by triplicate measurements of the reference materials at the beginning and at the end of each sequence. The standard uncertainty of the $\delta^{15}N$ values according to (Federherr et al., 2016) in the TDN concentration range of 1.4-6 mg L^{-1} was ~0.4‰. It was not possible to measure $\delta^{15}N$ values in all the quarterly composited samples of RF and ST because of TDN concentrations <1.4 mg L^{-1}. In such cases, we based the quarterly values on selected weekly samples that contained a TDN concentration of at least 1.4 mg L^{-1}.

3.4. Calculations and statistical evaluation

We calculated the canopy budget CB_N for total nitrogen to determine if N is leached or retained in the canopy (Eq. 1) according to Ulrich (1984). Negative CB_N indicates retention and positive leaching. Because dry gaseous N deposition is unknown, the CB_N might be overestimated.

$$CB_N = (TF_N + SF_N) - TD_N \qquad (1)$$

where TF_N is the N flux with throughfall, SF_N is the N flux with stemflow and TD_N is total deposition. TD_N was calculated with Eq. 2.

$$TD_N = BD_N + DD_N \qquad (2)$$

where BD_N is the TN flux with rainfall and DD_N is the particulate dry deposition estimated with Eq. 3 assuming that Cl^- is an inert tracer in the forest canopy and thus only reflects the dry deposition but no leaching from the canopy.

$$DD_N = \left(\frac{TF_{Cl}+SF_{Cl}}{BD_{Cl}} \times BD_N\right) - BD_N \qquad (3)$$

where TF_{Cl} and SF_{Cl} are the Cl^- fluxes with TF and SF; BD_{Cl} is the Cl^- flux with rainfall; $\frac{TF_{Cl}+SF_{Cl}}{BD_{Cl}}$ is the deposition ratio of Cl^-. Because of time delays between dry deposition to the canopy and wash down into the throughfall and stemflow collectors, the deposition ratio of Cl^- is only stable and meaningful if it integrates longer time periods. We therefore calculated the annual dry deposition of N. Our estimate of dry deposition includes particulate but not gaseous N deposition.

To compare mean properties among the solid samples and among the solution samples, we used ANOVA followed by Tukey's Honest Significant Difference post-hoc test. Homoscedasticity was assessed with the Levene's test. Normality of residuals was checked by visual inspection. To compare differences between leaves and roots, we conducted a paired t-test for connected datasets, in which the normal distribution of the differences between each pair of values was checked using the Shapiro-Wilk test. The level of significance in both cases was set at $p<0.05$. We used R, version 4.1.1 for data handling, analysis, and graphs (R Core Team, 2025).

4. Results

The pH of the soil horizons was acidic, except for the uppermost organic soil horizon (Oi) which mainly consists of the little decomposed litterfall (**Table C-1**). The total carbon (TC) and total nitrogen (TN) concentrations and the TC/TN concentration ratios decreased markedly with increasing soil depth from the organic to the mineral horizons. The highest TC/TN ratios occurred in leaves followed by roots.

The solution pH increased from RF via TF to SF, decreased in the soil solutions (LL, SS15, SS30), and increased from SS30 to ST (**Table C-1**). The TOC concentrations and TOC/DON ratios increased from RF via TF and SF to LL and then decreased from LL via SS15 and SS30 to ST. The NO_3^--N/NH_4^+-N concentration ratios slightly increased from RF to LL, markedly in SS15 and SS30, and finally decreased markedly between SS30 and ST (**Table C-1**).

The mean $\delta^{15}N$ values of the 10 considered tree species varied from -6.0 to -1.9‰ in leaves and from -3.6 to 1.6‰ in roots (**Figure C-S2**). The roots were N-isotopically heavier than the leaves by 2.2‰ and the difference was statistically significant according to a paired t-test. *Prunus opaca* Walp showed the lowest $\delta^{15}N$ value for leaves (-6.0‰) and *Matayba inelegans* Radlk. the highest value for roots (1.6‰). The $\delta^{15}N$ values in leaves of

Graffenrieda emarginata Triana increased significantly from 2005 to 2015, while those of *Myrcia myrtiformis* Naudin. did not change (**Figure C-S3**).

Table C-1. Mean pH, total carbon (TC), total nitrogen (TN), and TC/TN concentration ratios of leaves (n=10), roots (n=10), and soil horizons (n=20); and quarterly mean TOC, TOC/DON and nitrate/ammonium concentration ratios (±standard deviations) in ecosystem solutions during the period 2013-2016 (n=16). Different lowercase letters indicate significant differences among the plant and soil samples or the ecosystem solutions according to Tukey's HSD post-hoc test.

Solid samples	pH	TC mg g^{-1}	TN mg g^{-1}	TC/TN	Ecosystem solutions	pH	TOC mg L^{-1}	TOC/ DON	NO_3^--N/ NH_4^+-N
Leaves		481 (±16.7) e	12.4 (±3.5) b	41.4 (±8.6) e	Rainfall (RF)	4.8 (±0.2) ab	2.5 (±1.1) a	10.2 (±2.0) a	1.4 (±1.2) a
Roots		493 (±8.6) e	12.5 (±5.3) b	44.2 (±16.7) e	Throughfall (TF)	6.2 (±0.3) c	13.3 (±5.6) c	15.9 (±2.5) bc	1.6 (±0.7) a
Oi	6.1 (±0.7) b	436 (±29.5) d	17.0 (±4.2) b	24.1 (±3.7) c	Stemflow (SF)	6.7 (±0.3) d	26.8 (±11.5) d	19.1 (±2.8) d	1.3 (±1.2) a
Oe	4.8 (±0.3) a	373 (±67.6) c	22.2 (±3.6) c	17.3 (±4.6) b	Litter leachate (LL)	4.9 (±0.2) b	49.6 (±14.7) e	22.2 (±3.8) e	2.7 (±1.6) a
Oa	4.0 (±0.2) a	295 (±124) b	33.9 (±34) d	13.7 (±3.8) a	Soil solution at the 0.15 m depth (SS15)	4.7 (±0.1) a	7.6 (±1.2) b	18.3 (±2.1) cd	33.1 (±9.1) c
A	4.3 (±0.4) a	32.8 (±13.3) a	2.6 (±0.9) a	12.7 (±2.0) a	Soil solution at the 0.30 m depth (SS30)	4.7 (±0.1) a	5.9 (±0.9) ab	18.8 (±3.8) d	24 (±7.0) b
B	4.7 (±0.2) a	12.7 (±8.8) a	1.2 (±0.6) a	10.3 (±2.7) a	Streamflow (ST)	7.0 (±0.3) e	2.8 (±2.5) a	15.1 (±4.1) b	0.40 (±0.20) a

Quarterly mean TDN, NH_4^+-N, and DON concentrations increased in the order, RF<TF<SF<LL and then decreased in the order, SS15>SS30>ST (**Figure C-1**). The highest mean quarterly NO_3^--N concentration was found in LL, which decreased slightly with increasing soil depth and strongly in ST. Aboveground, TF had the highest mean quarterly NO_3^--N concentration followed by stemflow and rainfall (**Figure C-1**). The contribution of DON to TDN increased from 35 to 52% in the order TF<SF<LL and was lower in RF, SS15, SS30, and ST with a range of 21-24%. The NH_4^+-N contribution decreased from RF to LL (39-17%), with the highest contribution in ST (59%) and the lowest in the mineral soil solutions (4%). The highest NO_3^--N contribution to TDN was found in soil solutions with 76% and the lowest in streamflow with 17% (**Figure C-S4**).

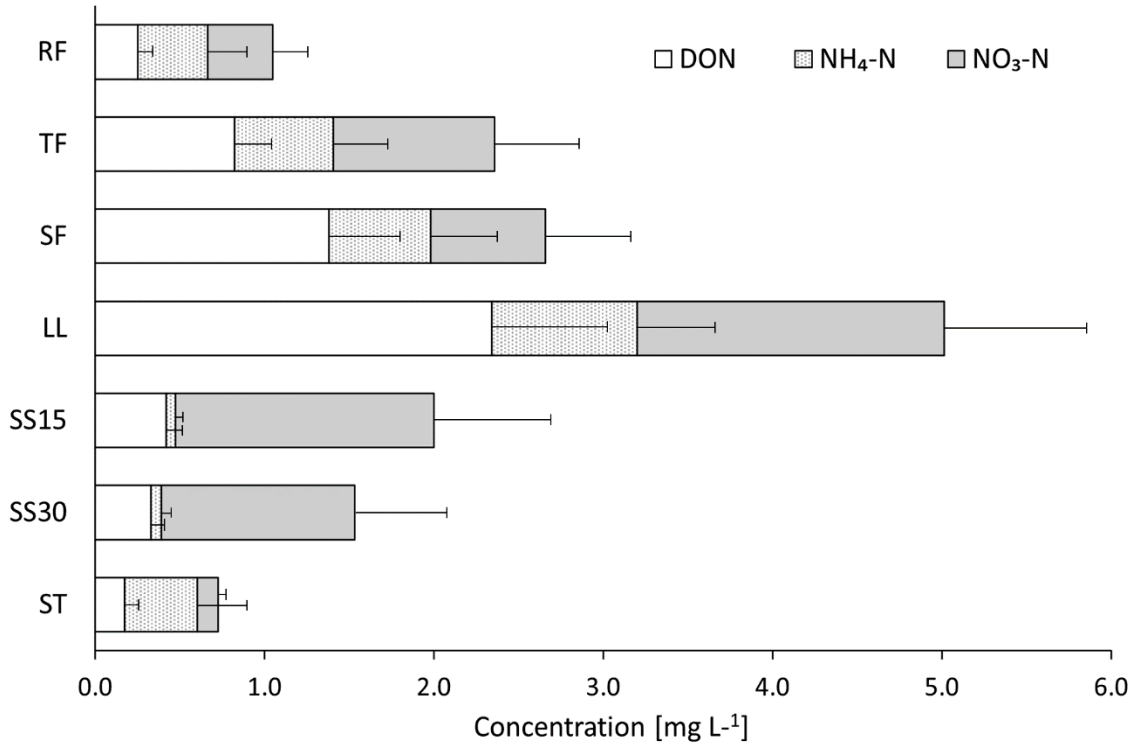


Figure C-1. Mean quarterly concentrations of DON, NH_4^+-N, and NO_3^--N from 2013 to 2016 in a tropical montane forest in south Ecuador. Error bars represent standard deviations. RF is rainfall, TF throughfall, SF stemflow, LL litter leachate, SS15 and SS30 mineral soil solutions at the 0.15 and 0.30 m depths, respectively, and ST streamflow.

The bulk deposition, i.e., the mass flux with RF, of N in **Figure C-2** was higher than the 5.2-11 kg ha^{-1} at other tropical forest sites compiled by Boy et al. (2008a). The estimated mean fine particulate dry deposition of N without gaseous exchange, based on the mean annual Cl^- deposition ratio, was 1.7 times the bulk deposition. The high dry deposition may in part be related with the fact that in spite of the high precipitation at the study sites, there are frequent dry spells, which can even extend over several weeks during the veranillo in October/November (Peters et al., 2013; Wilcke et al., 2013). The N fluxes with TF had a similar size as the bulk N deposition, while the N fluxes with SF were negligibly small (**Figure C-2**). The canopy budget of N was negative in all four study years indicating N retention by the canopy organisms (**Figure C-2**).

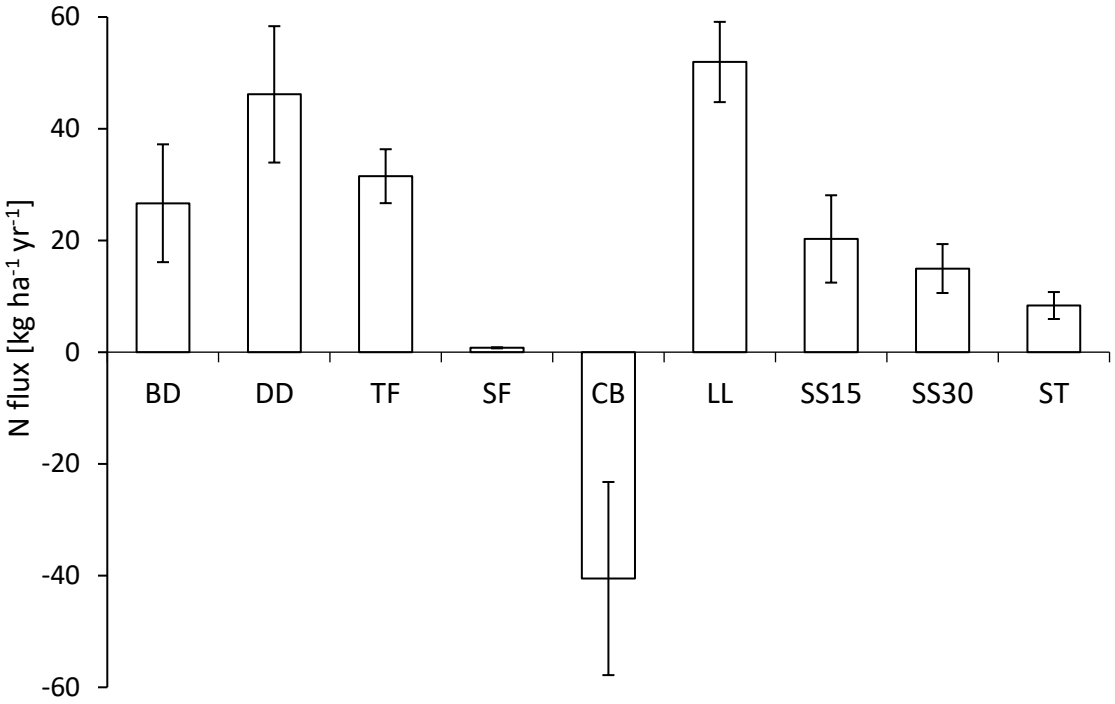


Figure C-2. Mean annual N flux with bulk deposition (BD), dry deposition (DD, Eq. 3), throughfall (TF), stemflow (SF), the resulting canopy budget (CB, Eq. 1), litter leachate (LL), mineral soil solution at the 0.15 m (SS15) and 0.30 m depths (SS30), and streamflow (ST) from 2013 to 2016. The DD is based on the deposition ratio of Cl^- assuming negligible Cl^- leaching from the canopy and does not include the gaseous N exchange between the canopy and the atmosphere. The error bars represent standard deviations to illustrate temporal variation among the four study years.

The temporal variation in the $\delta^{15}N$ values of TDN were not related with the variation in monthly rainfall (**Figures C-3, C-S1**). The $\delta^{15}N$ values of TDN in RF, which were determined in selected weeks with sufficiently high N concentrations for isotopic analysis, showed the highest variation from 1.9 to 5.9‰ pointing at different N sources. The $\delta^{15}N$ value of TDN in TF varied from -2.6 to -1.0‰ reflecting the high variability in the $\delta^{15}N$ values of TDN in rainfall and in the leaves (**Figure C-S2**). The $\delta^{15}N$ values of SF varied from -1.2 to +1.0‰ with a mean value near 0‰, typical of N_2 fixation. Throughfall, SF, and LL showed a similar temporal pattern. The solutions at the 0.15 and 0.30 m mineral soil depths exhibited the lowest temporal variation. The $\delta^{15}N$ values of ST, again determined in selected weeks with sufficiently high N concentrations, varied from -0.1 to 1.5‰ which was higher than in the soil solutions but lower than in RF (**Figure C-3**).

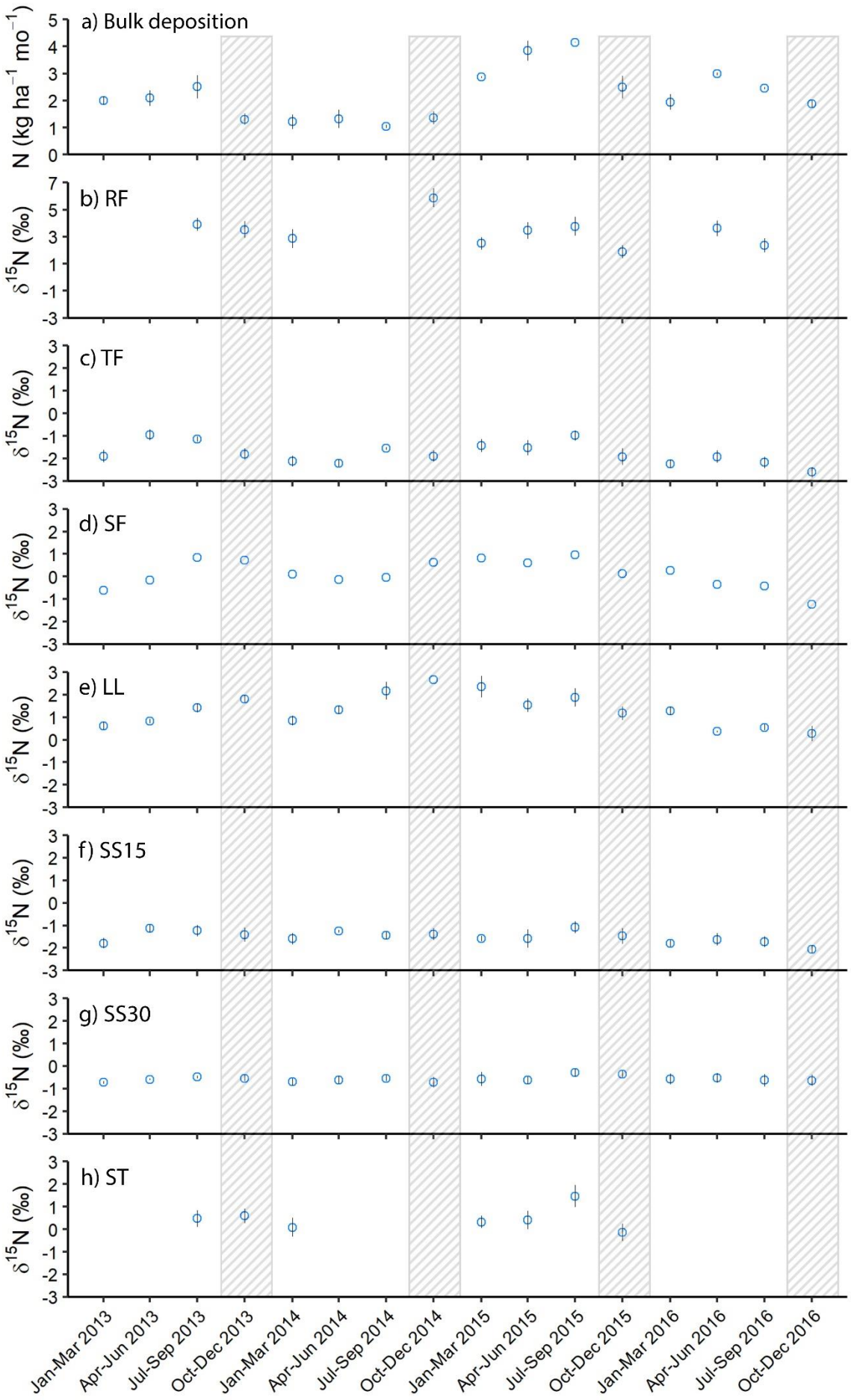

a) Bulk deposition
N (kg ha^{-1} mo^{-1})
b) RF
c) TF
d) SF
e) LL
f) SS15
g) SS30
h) ST
$\delta^{15}N$ (‰)
Jan-Mar 2013
Apr-Jun 2013
Jul-Sep 2013
Oct-Dec 2013
Jan-Mar 2014
Apr-Jun 2014
Jul-Sep 2014
Oct-Dec 2014
Jan-Mar 2015
Apr-Jun 2015
Jul-Sep 2015
Oct-Dec 2015
Jan-Mar 2016
Apr-Jun 2016
Jul-Sep 2016
Oct-Dec 2016

Figure C-3. Bulk deposition of N (a) and course of the quarterly $\delta^{15}N$ values in ecosystem solutions along the water path through the forest ecosystem from January 2013 to December 2016 (b-g). Error bars represent the standard deviation of three study transects at approximately 1900, 1950, and 2000 m a.s.l. RF is rainfall, TF throughfall, SF stemflow, LL litter leachate, SS15 and SS30 mineral soil solutions at the 0.15 and 0.30 m depths respectively, and ST streamflow. The $\delta^{15}N$ values in rainfall and streamflow could only be measured in individual weeks when the TDN concentrations were sufficiently high. Oblique hatching indicates the periods with the lowest rainfall and extended dry spells (the "veranillo") (Figure C-S4). Mind the different Y axis scaling in (b) than in all other subfigures showing $\delta^{15}N$ values.

The mean $\delta^{15}N$ value of TDN in RF was the highest of all ecosystem solutions (**Figure C-4**). The TDN in TF was N-isotopically lighter than in RF but heavier than in the leaves. The mean $\delta^{15}N$ values of TDN increased in the order, TF<SF<LL. The mean $\delta^{15}N$ value of TDN in LL was similar to the thickness-weighted mean $\delta^{15}N$ value of the whole organic layer. The $\delta^{15}N$ value of the organic horizons increased with increasing depth (i.e., Oi<Oe<Oa). Fine roots, a large part of which occurred in the organic layer, were N-isotopically lighter than the organic horizons but heavier than the leaves. The TDN in SS15 was N-isotopically lighter than in LL. Belowground, the $\delta^{15}N$ values of TDN increased in the order, SS15<SS30<ST. The $\delta^{15}N$ values of the mineral A and B horizons were similar and N-isotopically heavier than the soil solutions (**Figure C-4**).

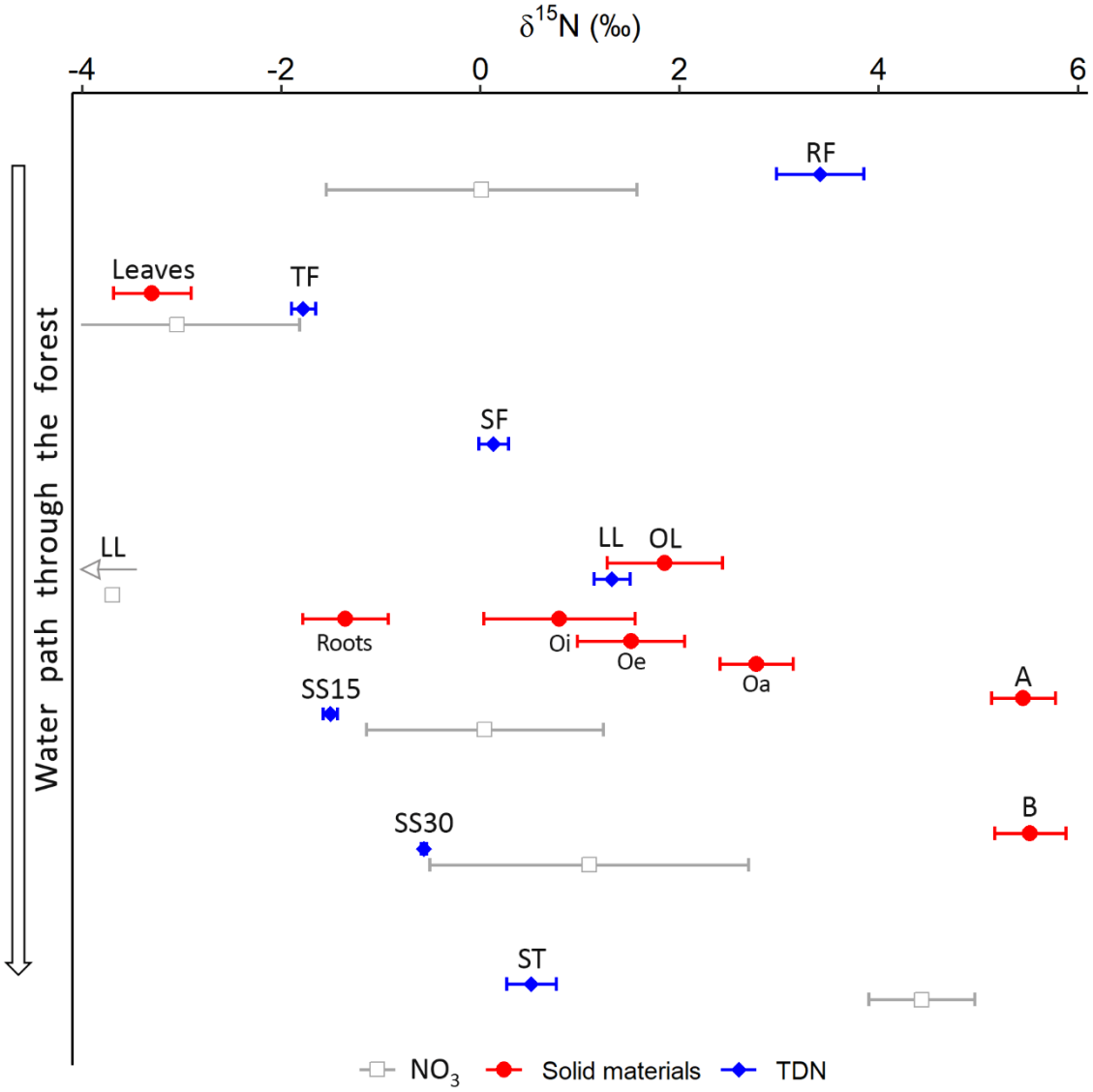


Figure C-4. Mean $\delta^{15}N$ values of TDN (rhombi) and dissolved NO_3^- (squares) taken from Schwarz et al. (2011) in ecosystem solutions along the water path through the forestand in solid materials (circles) that could serve as source or sink of N. RF is rainfall, TF throughfall, SF stemflow, LL litter leachate, SS15 and SS30 mineral soil solutions at the 0.15 and 0.30 m depths, respectively, and ST stream flow. Leaves are live canopy leaves, OL is the organic layer, Oi, Oe, Oa are the three differently decomposed organic horizons, A and B are the mineral top- and subsoil horizons. Error bars represent standard errors refering to the means of quarterly samples of the ecosystem solutions (averaged for the three transects, n=16 for TDN and n=4 for NO_3), 20 Oi, Oe, Oa, A, and B horizons from the whole catchment, 20 horizon thickness-weighted organic layer means (OL), and 10 samples of each of fresh leaves and roots from 10 different tree species. The mean $\delta^{15}N$ value of NO_3 in litter leachate

was -7.43 ± 1.98 and is not shown to scale. To avoid the overlap of error bars, data points that should appear on the same level were slightly offset on the Y axis.

5. Discussion

5.1. Temporal variation in the $\delta^{15}N$ values of total dissolved nitrogen in rainfall

The $\delta^{15}N$ values of TDN in RF showed the strongest temporal variation of all ecosystem solutions in line with our first hypothesis that TDN in RF reflects temporally changing N sources (**Figure C-3**). Similarly, Knapp et al. (2010) and Rolff et al. (2008) reported that the $\delta^{15}N$ values of TDN in rainfall in Bermuda and the Baltic Sea region varied strongly from -8.0 to +12.3‰. The $\delta^{15}N$ values of NO_3^--N and NH_4^+-N in RF, which are more frequently reported than those of TDN, showed a minimum of -7.7‰ for NH_4^+-N and a maximum of +5.3‰ for NO_3^--N at a south Chinese subtropical forest site (Koba et al., 2012). A wide variation in $\delta^{15}N$ values (from -4.9‰ for NH_4^+-N to 0.5‰ for NO_3^--N) in RF was also reported by Lee et al. (2012) in a Korean agricultural area. At our study site in Ecuador, Schwarz et al. (2011) found a variation from -2.64‰ to 2.76‰ for the $\delta^{15}N$ values of NO_3^- in RF during differently wet quarters of one study year further confirming different sources of the N deposition to the study forest. Boy et al. (2008a) have shown that the forest fires of the Amazon basin were a major source of N deposition at our study site. These authors used a satellite-based fire pixel count to define “fire” and “no fire” periods in the Amazon basin and demonstrated that during the “fire” periods, both bulk and dry deposition of NO_3^--N, DON and total N were significantly higher than during “no fire” periods, because the emitted N is transported to the study area by the northeasterly trade winds that dominate during most of the year. The fact that the dry deposition of TOC was also significantly higher during “fire” than “no fire” periods in the Amazon basin points at a strong contribution of organic aerosols to dry deposition (Boy et al., 2008a). However, during a short period at the end of the year, westerly winds dominated and might have carried some N from anthropogenic emissions in the densely settled inter-Andean depression to our study site, although both bulk and dry deposition of N were lower than during the Amazonian “fire” periods (Wilcke et al., 2013). Moreover, Alvarez et al. (2023) observed indications that occasional pasture fires in the near surroundings of the study site can also contribute to the N input at our study site, with likely a strong dry deposition component. Moreover, there might be some N emissions from the connection road between the provincial capitals of Loja

and Zamora-Chinchipe, which passes nearby the study area and from local animal grazing. We suggest that the different sources of N (Amazonian and local vegetation fires, local and inner-Andean agriculture) explain the strong variation in the $\delta^{15}N$ values of TDN in rainfall.

5.2. Change in the $\delta^{15}N$ values of total dissolved nitrogen from rainfall to litter leachate

The finding that the $\delta^{15}N$ value of TDN decreased substantially from RF to TF partly supported our second hypothesis that expected decreasing $\delta^{15}N$ values from rainfall via throughfall and stemflow to litter leachate, because of increasing contributions of N-isotopically lighter N leached from the vegetation. However, against this hypothesis, the $\delta^{15}N$ values of TDN increased again in the order TF<SF<LL. The N-isotopically lighter TF than RF (**Figure C-4**) concurred with a net N retention in the leaves as indicated by the negative canopy budget (**Figure C-2**). The net retention of N in the canopy is in line with the reported N+P colimitation of the vegetation growth at our study site (*Homeier et al.*, 2012; *Velescu et al.*, 2016). Similarly, *Boy et al.* (2008a) observed net N retention in the forest canopy during the Amazonian "fire" period. *Wullaert et al*. (2010) and *Velescu et al.* (2016) reported that N was still retained in the canopy after the amendment of N as urea to the soil of the study forest in and accompanying fertilizer experiment next to our study site indicating that the study ecosystem has not yet reached N saturation. Still prevailing N limitation in spite of the on-going high N deposition is further suggested by a ratio of bulk deposition to N export with the stream of 3.2 during the study period (2013-2016; mean bulk deposition of 26.7 kg ha^{-1} yr^{-1} divided by the dissolved N export with ST of 8.4 kg ha^{-1} yr^{-1}, **Figure C-2**), particularly because *Martinson et al.* (2013) reported that even after the addition of 100 kg ha^{-1} of N as urea in the accompanying fertilization experiment, gaseous N_2O emission were still small (0.1-0.2 kg ha^{-1} N_2O-N in the unfertilized controls and up to 1.4 kg ha^{-1} in the N+P-fertilized treatments) so that gaseous N losses little influenced the catchment budget. If the estimated dry deposition of 46.2 kg ha^{-1} yr^{-1} was considered the input/output ratio would even increase to 8.7.

The N-isotopically lighter TF than RF can be explained by the preferred retention of isotopically heavy N in the deposition. Alternatively, N-isotopically light dry deposition could be dissolved in TF. Unfortunately, we don't know the $\delta^{15}N$ value of the dry deposition so that we cannot explore this possibility further. It is well known that mineral N deposited from the atmosphere can be taken up by the plants via leaf surfaces and by canopy-dwelling

organisms (Bourgeois et al., 2019; Dail et al., 2009; Guerrieri et al., 2015; Houle et al., 2015). In a mesocosm experiment, 40% of ^{15}N-labeled NH_4^+ sprayed on seedlings of *Populus euramericana* Neva was taken up by the leaves (Wang et al., 2021). However, a net N retention in the canopy does not mean that all N species are retained to the same degree so that a differential retention of different N species with different $\delta^{15}N$ values could help explain the change in the $\delta^{15}N$ values of TDN between RF and TF. Garten and Hanson (1990) reported that from the applied ^{15}N-labeled NH_4^+ and NO_3^- to the leaves of white oak and red maple via artificial rainfall, NH_4^+ was strongly retained (84 and 58%) while most of the NO_3^- was leached (73 and 87%, respectively). The apparent preferential retention of NH_4^+ might also be related with nitrification in the canopy as has been inferred by Schwarz et al. (2011) for our study region based on the N-isotopically lighter NO_3^- in TF than in RF (**Figure C-4**).

Another possible reason for lower $\delta^{15}N$ values of TDN in TF than in RF would be the leaching of N-isotopically light N as DON. Although the $\delta^{15}N$ values in leaves of 10 common tree species varied considerably (-5.9 to -1.9‰, **Figure C-S2**), which can in part be attributed to the species-specific uptake of different N species (Wittich et al., 2015), they were consistently N-isotopically lighter than the TDN (**Figure C-4**). However, the fact that with increasing DON concentrations, the $\delta^{15}N$ values of TDN increased from TF via SF to LL rather pointed at a comparatively heavy N isotope ratio in the increasingly leached DON (**Figures C-1**). Thus, the decreasing $\delta^{15}N$ values of TDN in TF relative to RF can probably be explained by the preferential retention of N-isotopically heavy N in the canopy, presumably mainly as NH_4^+, and the leaching of N-isotopically light NO_3^-, partly produced by nitrification in the canopy.

A representative leaching of N from the bark or bark-associated lichens might not explain the higher $\delta^{15}N$ values of TDN in SF than in TF (**Figure C-4**), because Feng et al. (2008) reported that the outer bole bark of old Norway spruce trees (*Picea abies* (L.) Karst) with a $\delta^{15}N$ value of -4.8‰ was even N-isotopically lighter than other tree tissues. Moreover, lichens growing on the bark of a Norway spruce forest were N-isotopically lighter than the bark itself (-8.7 to -3.5‰; Potapov et al. (2018)). In a study of 665 samples of lichen, moss, and bark samples, the $\delta^{15}N$ values ranged from -15.2 to -1.5‰ (Boltersdorf et al., 2014). Most of the $\delta^{15}N$ values in bark and bark-associated lichens or mosses in the literature have been reported from the temperate zone and it is unclear if these findings can be transferred to the tropics. In the only study of a tropical forest, we found, the $\delta^{15}N$ values of bark were

around 0‰ and thus had a similar $\delta^{15}N$ value than the TDN in our SF (Wang et al., 2018). Moreover, leaching of N originating from N_2-fixing organisms like cyanobacteria living on the bark which should show a $\delta^{15}N$ value close to 0‰ could contribute to explain the $\delta^{15}N$ values of TDN in our SF. In a forest in south Chile dominated by *Nothofagus* and *Araucaria* trees, the cyanolichens *Pseudocyphellaria berberina* (G. Forster) D. Galloway & P. James and *Pseudocyphellaria coriifolia* (Müll. Arg.) Malme sampled from the tree barks (both including *Nostoc* sp.) had a $\delta^{15}N$ value of -3.1 and -2.8‰ (Pérez et al., 2017) and were enriched in ^{15}N relative to the bark, but showed lower $\delta^{15}N$ values than the TDN in our SF. Additionally, SF might also contain more unchanged rainfall-N than TF, because of a faster flow of RF water along the trunks of the trees than during the partly cascading passage through the canopy and thus include more of the N-isotopically heavier RF-N than TF. Therefore, leaching of isotopically heavy compounds from the bark and/or a higher contribution of unchanged RF could explain the $\delta^{15}N$ values in SF in contrast to our second hypothesis.

Again in contrast to our second hypothesis, the $\delta^{15}N$ values of TDN in the LL were higher than in TF and SF (**Figure C-4**). The similar $\delta^{15}N$ values of TDN in the LL and total N in the organic layer and the highest N concentration of all ecosystem solutions suggested a strong role of DON leaching from the organic layer (**Figures C-1 and C-4**). This assumption is corroborated by the highest DON contribution to total N in LL of all ecosystem solutions (**Figure C-S4**). Because the dissolved organic matter (DOM) in litter leachate was dated at approximately 10 years (Wilcke et al., 2020), which corresponds to the mean residence time of the organic layer at our study site (Wilcke et al., 2020), it can be concluded that the increase in DON concentrations originated mainly from the leaching of the Oa horizon and that the resulting $\delta^{15}N$ value of TDN represents a mixture of DON leached from the Oa horizon and N from TF and SF. The many roots in the organic layer (Soethe et al., 2007) showed a much lower $\delta^{15}N$ value than TDN in LL and are therefore unlikely to contribute to the TDN in the LL (**Figure C-4**). Similarly, the nitrification that had been observed by Schwarz et al. (2011) in the organic layer and subsequent stronger leaching of N-isotopically light NO_3^- supported by the strong increase in the NO_3^--N/NH_4^+-N ratio between TF/SF and LL (Wilcke et al., 2013, **Table C-1**) cannot have markedly contributed to the $\delta^{15}N$ value of TDN in LL, because it would have shifted the $\delta^{15}N$ to lower values.

5.3. Change of the $\delta^{15}N$ values of total dissolved nitrogen from litter leachate to topsoil solution

The abrupt decrease in the $\delta^{15}N$ values of TDN from LL to SS15 indicated strong sorption of N-isotopically heavy DON in the upper mineral soil (**Figure C-4**). The assumed DON sorption is in line with the strongly decreasing DON contribution to total N in the mineral soil solutions (**Figures C-1 and C-S4**). These results support our third hypothesis which expected decreasing $\delta^{15}N$ values from litter leachate to the mineral soil because of the strong retention of N-isotopically heavy DON and NH_4^+ with respect to the role of DON. In line with our interpretation, Michalzik et al. (2001) explained the decreasing DON concentrations with increasing depth by either strong selective sorption on mineral surfaces or decomposition. Sorption has been shown in the field and in laboratory experiments to be more important than decomposition in mineral soil horizons (Qualls & Haines, 1991, 1992; Vandenbruwane et al., 2007). Another explanation for lower $\delta^{15}N$ values of TDN in SS15 than in LL could be an addition of N-isotopically light inorganic N from mineralization and nitrification. However, Schwarz et al. (2011) had shown that NO_3^- in SS15 was N-isotopically heavier than in LL (**Figure C-4**), so that this NO_3^- would increase the $\delta^{15}N$ values of TDN in SS15, while we observed the opposite. Dissolution of N from the A horizon or contributions of N-isotopically heavy microbial N compounds can be largely ruled out because of their much higher $\delta^{15}N$ values than in the TDN of SS15 (**Figure C-4**; Dijkstra et al., 2006). On the contrary, some contributions of N from the N-isotopically similar roots to SS15 seem possible and can also contribute to explain the shift between LL and SS15. The latter would be similar to the likely contribution of roots to the DOM in mineral soil solutions suggested by Wilcke et al. (2020) and Alvarez et al. (2023). The decrease in NH_4^+ concentrations from LL to SS15 (**Figure C-1**) suggests that the sorption of isotopically heavy NH_4^+ to clay minerals such as the illites that occur in the study soils (Schrumpf et al., 2001) contributed to the shift in $\delta^{15}N$ values of TDN from LL to SS15, which would support our third hypothesis also with respect to NH_4^+. Finally, the similar $\delta^{15}N$ values of TF and SS15 suggest that some direct leaching of throughfall into the mineral soil without changing the $\delta^{15}N$ values of TDN could also have contributed to the $\delta^{15}N$ value of TDN in SS15. The latter had already been suggested by Wilcke et al. (2020) based on the young age of DOM in SS15 of only approximately 1 yr.

5.4. Change in the $\delta^{15}N$ values of total dissolved nitrogen from topsoil solution to streamflow

The $\delta^{15}N$ values of TDN increased in the order, SS15< SS30< ST (**Figure C-4**), supporting our fourth hypothesis that the $\delta^{15}N$ values of TDN increase from mineral topsoil via subsoil solution to stream water because of increasing denitrification. In line with similar findings for the $\delta^{15}N$ values of NO_3^- of Schwarz et al. (2011) (**Figure C-4**), N-isotopically light gaseous N losses by increasing denitrification with increasing depth seem to be the most likely explanation. Denitrification in the subsoil is further supported by the fact that the NO_3^-concentrations decreased strongly from the soil solutions to the streamflow suggesting that a large part of NO_3^- was consumed by denitrification (**Figure C-1**). The total loss of NO_3^--N between SS15 and ST amounted to 13.8 kg ha^{-1} yr^{-1}, of which 9.8 kg ha^{-1} yr^{-1} were lost between SS30 and ST. While in the topsoil there is likely still considerable uptake of NO_3^- by soil organisms and plants, in the deeper soil most of this loss is more likely attributable to denitrification which thus results in a total gaseous N loss in the range of a few kg. This is higher than reported by Martinson et al. (2013), who, however, only measured N_2O-N losses but not N losses as other N gases like NO and N_2. Moreover, the measurements of Martinson et al. (2013) date back to the years 2008-2009, while until our observation period (2013-2016) the N deposition has further increased. Interestingly, there must have been a source of NH_4^+ to the stream because the NH_4^+ concentrations increased strongly in streamflow relative to the mineral soil solutions. This NH_4^+ might have been flushed from the organic layers directly into the stream as was observed during strong rain events by Boy et al. (2008b), because of a fast responsiveness of the shallow catchment to rainfall events at the scale of hours to days (Goller et al., 2005). Alternatively, the NH_4^+ in ST might originate from mineralization of subsoil organic matter. Both the organic layer and the subsoil organic matter showed markedly higher $\delta^{15}N$ values than the mineral soil solutions so that the NH_4^+ released by mineralization possibly also showed a high $\delta^{15}N$ value (Figure C-4). The NH_4^+ in streamflow could also have been released from sequestered NH_4^+ in clay minerals or the phyllite by weathering. In line with this assumption, (Steffens & Sparks, 1997) reported the release of nonexchangeable NH_4^+ from clay minerals and (Smith et al., 1994) showed that this release only occurred at low NH_4^+ concentrations in soil solutions, which was indeed the case for the mineral soil solutions at our study site (**Figure C-1**). To explain why NH_4^+ only seems to be released by weathering in the deeper soil and the riparian zone, we speculate that at the 0.3 m soil depth the conditions were still sufficiently aerobic

so that any potentially released NH_4^+ was quickly immobilized or nitrified, while the riparian zone was sufficiently anaerobic to reduce organismic uptake and prevent nitrification so that the weathered NH_4^+ could be released into the stream water. Unfortunately, we don't know the $\delta^{15}N$ value of the NH_4^+ sequestered in soil clay minerals or parent rock. Moreover, some N-isotopically heavy NH_4^+ might have been released from dying microorganisms which are usually enriched in ^{15}N relative to extractable and total N in soil (Coyle et al., 2009; Dijkstra et al., 2006; Dijkstra et al., 2008). Our finding of elevated NH_4^+ concentrations in ST relative to the soil solutions is in line with reports that the soil solution in riparian zones and groundwater are frequently rich in ammonium (Hill, 1990; Young & Briggs, 2005).

5.5. Temporal variation in the $\delta^{15}N$ values of ecosystem solutions

The $\delta^{15}N$ values of TDN in all ecosystem solutions showed a considerable temporal variation, which roughly paralleled that of the $\delta^{15}N$ values of TDN in RF and TF and was increasingly delayed and dampened along the water path through the ecosystem, particularly in the mineral soil (**Figure C-3**). Thus, the input signal of deposited N, as reflected by TF which includes bulk and dry deposition, was passed through the ecosystem. In addition to the input signal, there are additional processes that further modify the $\delta^{15}N$ values of TDN in ecosystem solutions. In several studies, leaf $\delta^{15}N$ values were negatively correlated with mean annual rainfall and water availability, i.e., during moist conditions leaves were N-isotopically lighter than during dry conditions (Handley et al., 1999; Roa-Fuentes et al., 2015). This pattern was also confirmed by a modeling approach that showed that water availability was the main driver of leaf $\delta^{15}N$ values (Vitousek et al., 2021). As a consequence, the TDN leached from leaves, bark, and the Oi horizon (containing newly fallen leaves) should show lower $\delta^{15}N$ values during wet than during dry phases. In our study area, TF, SF, and LL showed the lowest $\delta^{15}N$ values of TDN from April to December 2016 (**Figure C-3**), which is in line with the increasing precipitation from 2013 to 2016 (from 2075 to 2586 mm, **Figure C-S5**). The highest $\delta^{15}N$ values of TDN were observed during October-December 2013 and 2014. This is in line with the fact that during the observation period from 2013-2016 the last quarter of the year showed the lowest mean precipitation (412±13 mm) of all quarters (Quarters 1-3: 565-795 mm) in the San Francisco Biological Reserve (**Figure C-S5**).

In the soil solution at the 0.15 cm depth (SS15), the $\delta^{15}N$ values were slightly higher in July-September 2015 (**Figure C-3**), which is consistent with a low precipitation period (**Figure C-S5**). Lower $\delta^{15}N$ values of TDN were observed from January to December 2016,

a period with high precipitation (**Figure C-S5**). Soil water content and temperature together have been reported as main drivers of mineralization (Curtin et al., 2012; Glass et al., 2023). Under aerobic conditions, mineralization rates increase with increasing temperature and soil moisture (Jin et al., 2013). Therefore, higher mineralization rates in the least moist periods could have released more N-isotopically heavy N from the solid phase organic matter than during wetter periods in this perhumid forest, where water logging occurs frequently. During wet phases, denitrification should be enhanced because of the lower redox potential, which would drive the $\delta^{15}N$ of TDN to higher values as a consequence of the enhanced release of N-isotopically light N gases. However, in SS30, we did not observe such a change and in ST we lack $\delta^{15}N$ values of TDN for the wet period (**Figure C-3**). In summary, our fifth hypothesis that expected that the changes in the $\delta^{15}N$ values of TDN in ecosystem solutions showed a temporal variation reflecting temporally variable strengths of the various N sources and sinks is largely not supported, because ecosystem processes apparently contributed little to the observed temporal variation of the $\delta^{15}N$ values of TDN in ecosystem solutions, which were mainly inherited from RF.

6. Conclusions

Our results confirmed the first hypothesis that the highest variation in the $\delta^{15}N$ values of TDN of all studied solution types occurred in RF. We attribute this to varying contributions of N from different sources. The $\delta^{15}N$ value of TDN decreased strongly in TF relative to RF. The reasons included a net N retention, particularly of the likely N-isotopically heavy NH_4^+, and leaching of N-isotopically light NO_3^-. This partly confirmed our second hypothesis. However, against our second hypothesis, the $\delta^{15}N$ values in TDN increased in the order TF<SF<LL, along with increasing contributions of likely N-isotopically comparatively heavy DON to the TDN. The abrupt decrease in the $\delta^{15}N$ value of TDN between LL and SS15 can be attributed to the sorption of DON in the first centimeters of the mineral soil. Moreover, N-isotopically light NO_3^- from nitrification and N from TF, that was flushed unchanged through the organic layer might have contributed to the TDN in SS15. Together, this supported our third hypothesis. The increasing $\delta^{15}N$ values in the order SS15< SS30<ST can mainly be explained by gaseous N losses because of increasing denitrification with increasing soil depth which is in line with our fourth hypothesis. However, we had to largely reject our fifth hypothesis, because most of the variation in the $\delta^{15}N$ value of TDN in all ecosystem solutions was inherited from RF, while in-situ processes in the ecosystem were still detectable but seemed to play a smaller role than

the variation in the $\delta^{15}N$ values of TDN in the atmospheric input. Our results demonstrate that the $\delta^{15}N$ values of TDN in ecosystem solutions indeed provide information about N sources and sinks in forest ecosystems and thus offer a novel straight-forward approach to explore the fate of N in forest ecosystems. This approach is particularly suitable for long-term observations in high temporal resolution.

7. Acknowledgments

We thank the German Research Foundation (DFG) for funding our research in Ecuador (FOR 402, FOR 816, PAK 823-825), Naturaleza y Cultura Internacional (NCI) in Loja for providing access to the study area and to the research station, and the Ecuadorian Ministry of Environment for the research permits. We thank José Luis Peña and Jimmy Villalta for their support as field technicians, Tobias Fabian for his support in the laboratory, and Jaime García and Uli Hensler for their help in the field campaigns. Pablo Alvarez received a four-year scholarship from the Secretary of Higher Education, Science, Technology and Innovation of Ecuador (SENESCYT), Grant No. CA07-000439-2018.

Global Research Collaboration

The first draft of this manuscript was written by an Ecuadorian Ph.D. student from the Universidad Nacional de Loja, Ecuador who is the first author and who has conducted most of the analytical work at the Karlsruhe Institute of Technology in Germany, where he is enrolled as a doctoral student. The study was realized in the frame of a long-term German-Ecuadorian cooperation since 1997, resulting in a multitude of international scientific publications with shared German-Ecuadorian authorships, extensive capacity building of Ecuadorian scientists at the level of university certificates and doctoral studies, several information booklets in Spanish language on the research results, a long-standing cooperation with the nongovernmental organization Nature and Culture International who provided the study area, and regular public scientific symposia hosted by the Ecuadorian partner universities in Ecuador. All work was realized in compliance with the national laws of Ecuador under a repeatedly renewed research permit.

8. Supporting Information

Table C-S1. List of the most abundant tree species in the San Francisco Biological Reserve in south Ecuador, ordered according to their abundance and number (#) of leaf and root samples collected from these trees**.**

Tree species	# Root samples	# Leaf samples
Alzatea verticillata Ruiz & Pav.	3	1
Hyeronima fendleri Briq.	3	1
Graffenrieda emarginata Triana	3	3
Alchornea lojaensis Secco	3	3
Podocarpus oleifolius D. Don	3	3
Matayba inelegans Radlk.	3	1
Miconia myrtiformis Naudin	3	1
Ocotea aciphylla (Nees & Mart.) Mez	3	1
Clusia ducuoides Engl.	3	1
Prunus opaca Walp.	3	1

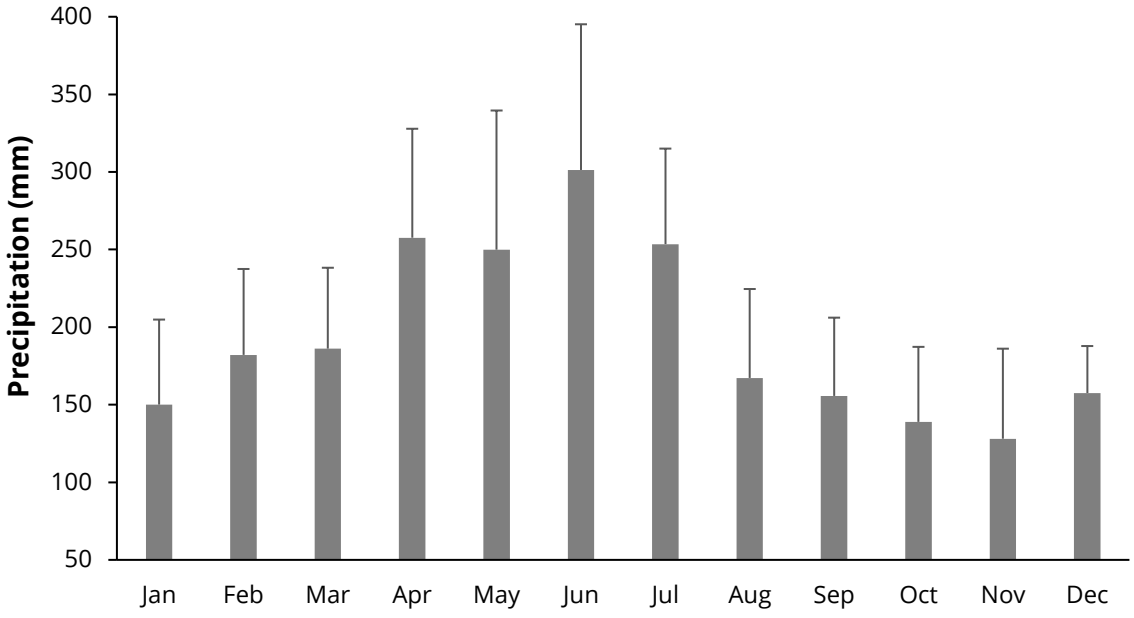


Figure C-S1. Mean monthly precipitation from April 1998 to December 2016 in the San Francisco Biological Reserve, south Ecuador. Error bars represent standard deviations.

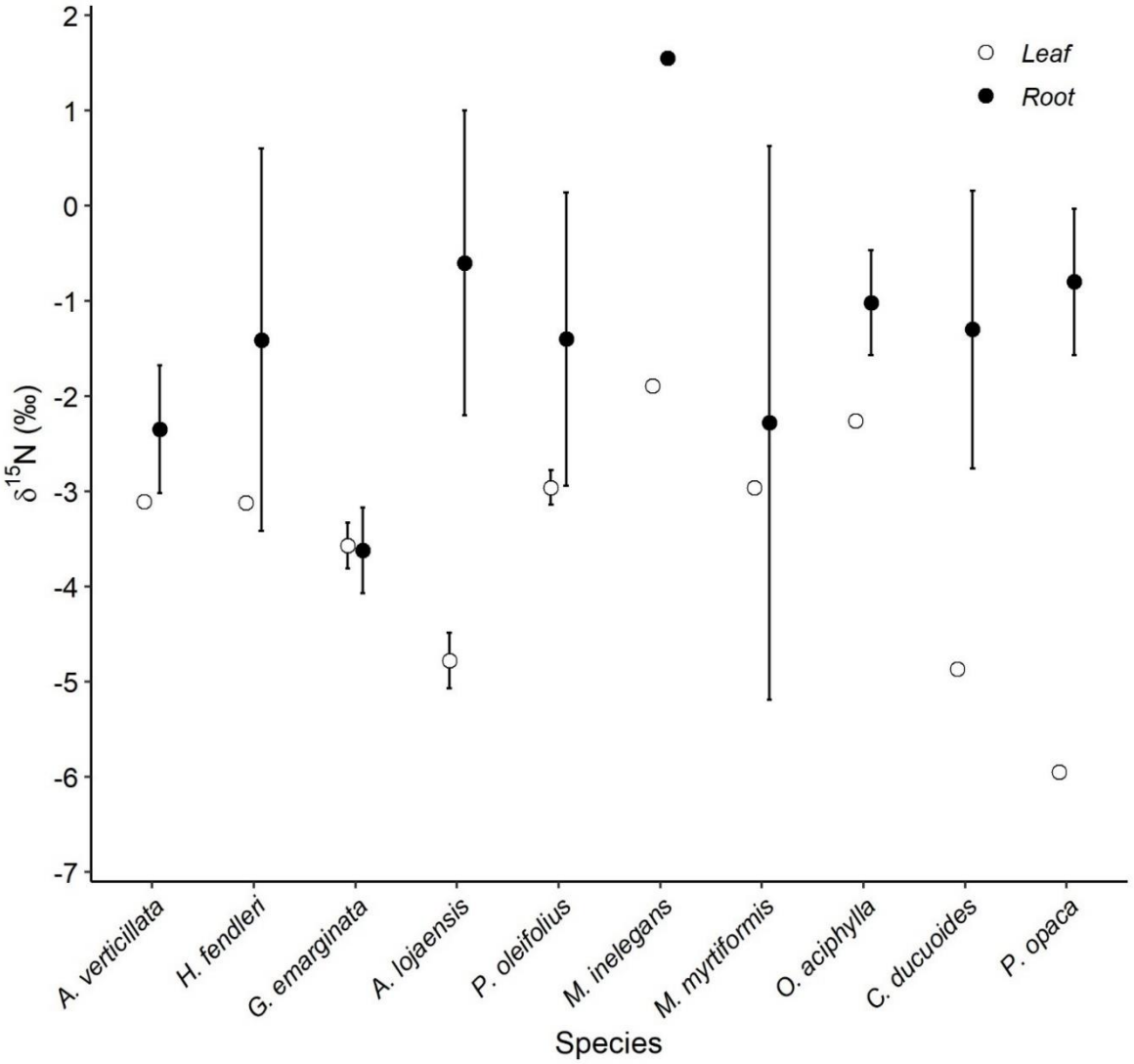


Figure C-S2. Mean $\delta^{15}N$ values of leaves and roots of 10 canopy-forming tree species in the forest of the San Francisco Biological Reserve. Error bars represent standard deviations for leaves (n=1-3 individuals, Table C-S1) and roots (n=3 individuals). The species were ordered from left to right according to their decreasing contribution to the total tree number on the study plots.

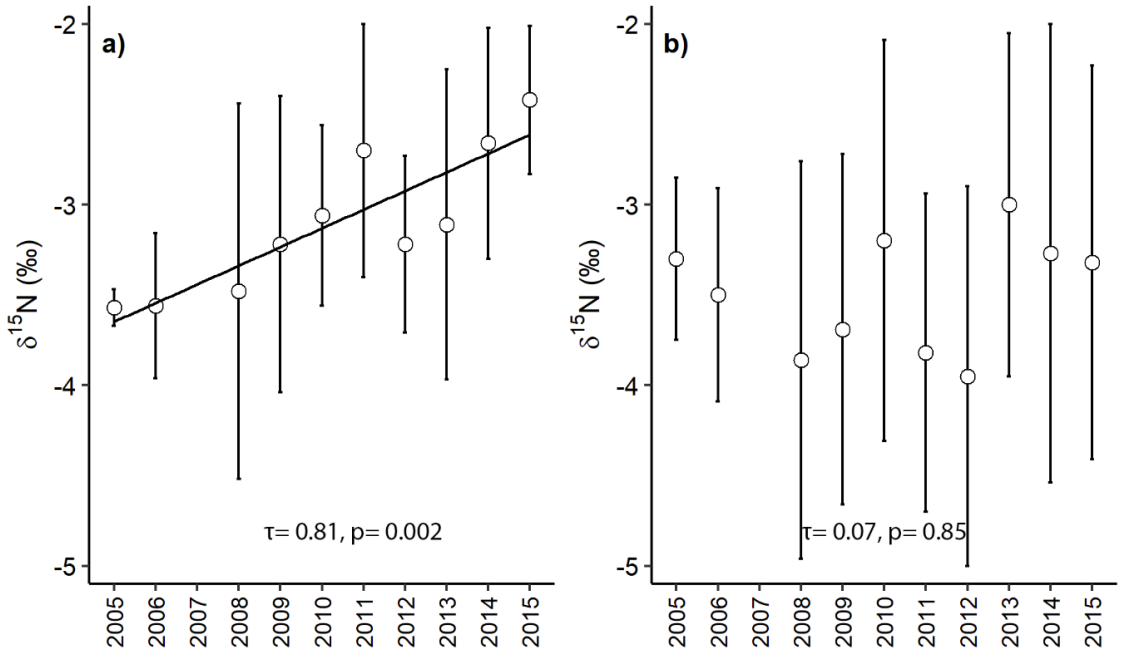


Figure C-S3. Temporal variation of the $\delta^{15}N$ values in leaves of a) *Graffenrieda emarginata* Triana and b) *Myrcia myrtiformis* Naudin in the San Francisco Reserve from 2005 to 2015. Error bars represent standard deviations (n=5 individual trees per species and sampling date). Temporal trends were statistically evaluated with the Mann-Kendall test. Regression lines are shown to illustrate significant trends but do not necessarily imply that the trend is linear.

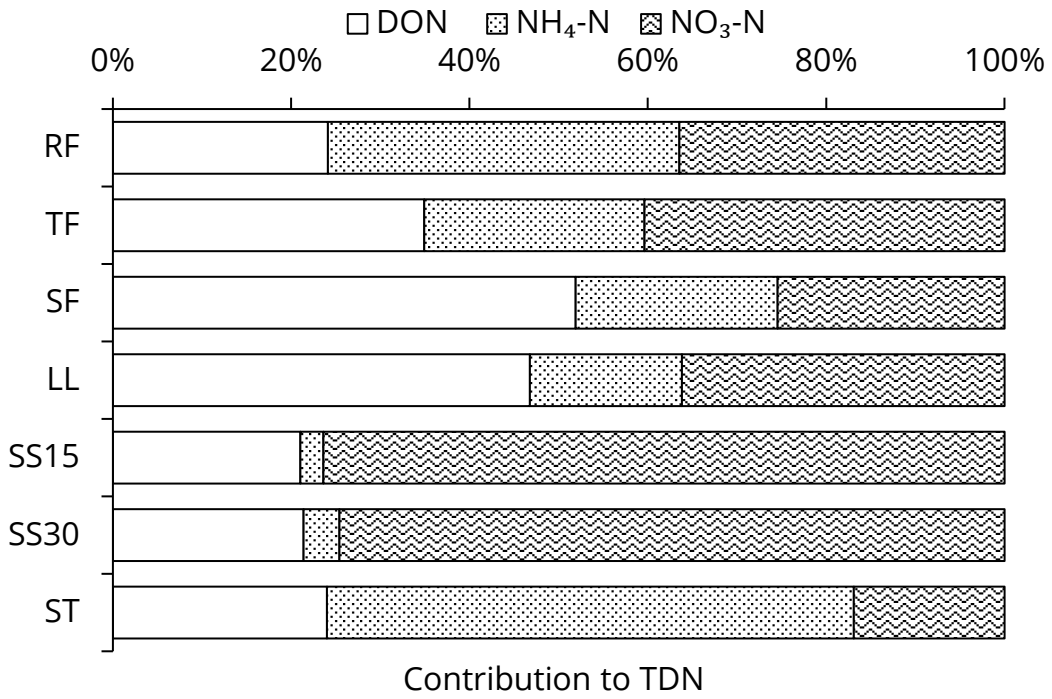


Figure C-S4. Mean contribution of DON, NH_4^+-N, and NO_3^--N to the total dissolved nitrogen (TDN) concentrations in each ecosystem solution, based on monthly mean concentrations from 2013-2016. RF is rainfall, TF throughfall, SF stemflow, LL litter leachate, SS15 and SS30 mineral soil solutions at the 0.15 and 0.30 m mineral soil depths, respectively, and ST streamflow.

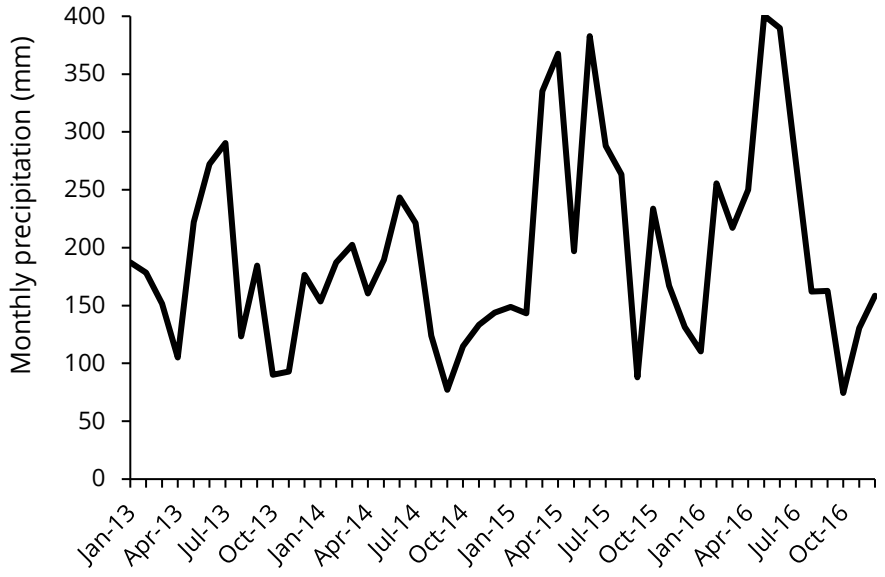


Figure C-S5. Course of the monthly precipitation in the San Francisco Reserve from January 2013 to December 2016 measured at two gaging stations on clear-cut areas.

9. References

Alvarez, P., Velescu, A., Pierick, K., Homeier, J., & Wilcke, W. (2023). Carbon stable isotope ratio of dissolved organic matter as a tool to identify its sources and transformations in a tropical montane forest in Ecuador. *Environmental science & technology*. https://doi.org/10.1021/acs.est.3c01623

Aragão, L. E. O. C., Malhi, Y., Metcalfe, D. B., Silva-Espejo, J. E., Jiménez, E., Navarrete, D., et al. (2009). Above- and below-ground net primary productivity across ten Amazonian forests on contrasting soils. *Biogeosciences, 6*(12), 2759-2778. https://doi.org/10.5194/bg-6-2759-2009

Arango, C. P., & Tank, J. L. (2008). Land use influences the spatiotemporal controls on nitrification and denitrification in headwater streams. *Journal of the North American Benthological Society, 27*(1), 90-107. https://doi.org/10.1899/07-024.1

Barrett, M., Khalil, M. I., Jahangir, M. M. R., Lee, C., Cardenas, L. M., Collins, G., Richards, K. G., & O'Flaherty, V. (2016). Carbon amendment and soil depth affect the distribution and abundance of denitrifiers in agricultural soils. *Environmental Science and Pollution Research, 23*(8), 7899-7910. https://doi.org/10.1007/s11356-015-6030-1

Barthlott, W., Lauer, W., & Placke, A. (1996). Global distribution of species diversity in vascular plants: towards a world map of phytodiversity. *Erdkunde*, 317-327.

Beck, E., Paladines, P., Paladines, R., Matt, F., Farwig, N., & Bendix, J. (2019). Field station profiles – Alexander von Humboldt would have loved it: Estación Científica San Francisco. *Ecotropica, 21*(09).

Bol, R., Julich, D., Brödlin, D., Siemens, J., Kaiser, K., Dippold, M. A., et al. (2016). Dissolved and colloidal phosphorus fluxes in forest ecosystems—an almost blind spot in ecosystem research. *Journal of Plant Nutrition and Soil Science, 179*(4), 425-438. https://doi.org/10.1002/jpln.201600079

Boltersdorf, S. H., Pesch, R., & Werner, W. (2014). Comparative use of lichens, mosses and tree bark to evaluate nitrogen deposition in Germany. *Environmental Pollution, 189*, 43-53. https://doi.org/10.1016/j.envpol.2014.02.017

Bourgeois, I., Clément, J.-C., Caillon, N., & Savarino, J. (2019). Foliar uptake of atmospheric nitrate by two dominant subalpine plants: insights from in situ triple-isotope analysis. *New Phytologist, 223*(4), 1784-1794. https://doi.org/10.1111/nph.15761

Boy, J., Rollenbeck, R., Valarezo, C., & Wilcke, W. (2008a). Amazonian biomass burning-derived acid and nutrient deposition in the north Andean montane forest of Ecuador. *Global Biogeochemical Cycles, 22*, GB4011. https://doi.org/10.1029/2007GB003158

Boy, J., Valarezo, C., & Wilcke, W. (2008b). Water flow paths in soil control element exports in an Andean tropical montane forest. *European Journal of Soil Science, 59*(6), 1209-1227. https://doi.org/10.1111/j.1365-2389.2008.01063.x

Bruijnzeel, L. A., & Hamilton, L. S. (2000). *Decision time for cloud forests. IHP Humid Tropics Programme Series Vol. 13*. Paris, France. IHP-UNESCO, IUCN and WWF. 44 p.

Castellano-Hinojosa, A., González-López, J., & Bedmar, E. J. (2018). Distinct effect of nitrogen fertilisation and soil depth on nitrous oxide emissions and nitrifiers and denitrifiers abundance. *Biology and Fertility of Soils, 54*(7), 829-840. https://doi.org/10.1007/s00374-018-1310-9

Coyle, J. S., Dijkstra, P., Doucett, R. R., Schwartz, E., Hart, S. C., & Hungate, B. A. (2009). Relationships between C and N availability, substrate age, and natural abundance ^{13}C and ^{15}N signatures of soil microbial biomass in a semiarid climate. *Soil Biology and Biochemistry, 41*(8), 1605-1611. https://doi.org/10.1016/j.soilbio.2009.04.022

Craine, J. M., Brookshire, E. N. J., Cramer, M. D., Hasselquist, N. J., Koba, K., Marin-Spiotta, E., & Wang, L. (2015). Ecological interpretations of nitrogen isotope ratios of terrestrial plants and soils. *Plant and Soil, 396*(1), 1-26. https://doi.org/10.1007/s11104-015-2542-1

Craine, J. M., Elmore, A. J., Aidar, M. P. M., Bustamante, M., Dawson, T. E., Hobbie, E. A., et al. (2009). Global patterns of foliar nitrogen isotopes and their relationships with climate, mycorrhizal fungi, foliar nutrient concentrations, and nitrogen availability. *New Phytologist, 183*(4), 980-992. https://doi.org/10.1111/j.1469-8137.2009.02917.x

Craine, J. M., Lee, W. G., Bond, W. J., Williams, R. J., & Johnson, L. C. (2005). Environmental constraints on a global relationship among leaf and root traits of grasses. *Ecology, 86*(1), 12-19. https://doi.org/10.1890/04-1075

Craine, J. M., Towne, E. G., Ocheltree, T. W., & Nippert, J. B. (2012). Community traitscape of foliar nitrogen isotopes reveals N availability patterns in a tallgrass prairie. *Plant and Soil, 356*(1), 395-403. https://doi.org/10.1007/s11104-012-1141-7

Curtin, D., Beare, M. H., & Hernandez-Ramirez, G. (2012). Temperature and Moisture Effects on Microbial Biomass and Soil Organic Matter Mineralization. *Soil Science Society of America Journal, 76*(6), 2055-2067. https://doi.org/10.2136/sssaj2012.0011

Dail, D. B., Hollinger, D. Y., Davidson, E. A., Fernandez, I., Sievering, H. C., Scott, N. A., & Gaige, E. (2009). Distribution of nitrogen-15 tracers applied to the canopy of a mature spruce-hemlock stand, Howland, Maine, USA. *Oecologia, 160*(3), 589-599. https://doi.org/10.1007/s00442-009-1325-x

Dijkstra, P., Ishizu, A., Doucett, R., Hart, S. C., Schwartz, E., Menyailo, O. V., & Hungate, B. A. (2006). ^{13}C and ^{15}N natural abundance of the soil microbial biomass. *Soil Biology and Biochemistry, 38*(11), 3257-3266. https://doi.org/10.1016/j.soilbio.2006.04.005

Dijkstra, P., LaViolette, C. M., Coyle, J. S., Doucett, R. R., Schwartz, E., Hart, S. C., & Hungate, B. A. (2008). ^{15}N enrichment as an integrator of the effects of C and N on microbial metabolism and ecosystem function. *Ecology Letters, 11*(4), 389-397. https://doi.org/10.1111/j.1461-0248.2008.01154.x

Dijkstra, P., Williamson, C., Menyailo, O., Doucett, R., Koch, G., & Hungate, B. A. (2003). Nitrogen stable isotope composition of leaves and roots of plants growing in a forest and a meadow. *Isotopes in Environmental and Health Studies, 39*(1), 29-39. https://doi.org/10.1080/1025601031000102189

DVWK. (1996). *Ermittlung der Verdunstung von Land-und Wasserflächen*. Retrieved from Bonn, Germany:

Federherr, E., Cerli, C., Kirkels, F. M. S. A., Kalbitz, K., Kupka, H. J., Dunsbach, R., Lange, L., & Schmidt, T. C. (2014). A novel high-temperature combustion based system for stable isotope analysis of dissolved organic carbon in aqueous samples. I: development and validation. *Rapid Communications in Mass Spectrometry, 28*(23), 2559-2573. https://doi.org/10.1002/rcm.7052

Federherr, E., Kupka, H. J., Cerli, C., Kalbitz, K., Dunsbach, R., Loos, A., et al. (2016). A novel tool for stable nitrogen isotope analysis in aqueous samples. *Rapid Communications in Mass Spectrometry, 30*(23), 2537-2544. https://doi.org/10.1002/rcm.7740

Felix, J. D., Elliott, E. M., & Gay, D. A. (2017). Spatial and temporal patterns of nitrogen isotopic composition of ammonia at U.S. ammonia monitoring network sites.

Atmospheric Environment, 150, 434-442. https://doi.org/10.1016/j.atmosenv.2016.11.039

Feng, Z., Brumme, R., Xu, Y. J., & Lamersdorf, N. (2008). Tracing the fate of mineral N compounds under high ambient N deposition in a Norway spruce forest at Solling/Germany. *Forest Ecology and Management, 255*(7), 2061-2073. https://doi.org/10.1016/j.foreco.2007.12.049

Fisher, J. B., Malhi, Y., Torres, I. C., Metcalfe, D. B., van de Weg, M. J., Meir, P., Silva-Espejo, J. E., & Huasco, W. H. (2013). Nutrient limitation in rainforests and cloud forests along a 3,000-m elevation gradient in the Peruvian Andes. *Oecologia, 172*(3), 889-902. https://doi.org/10.1007/s00442-012-2522-6

Fleischbein, K., Wilcke, W., Valarezo, C., Zech, W., & Knoblich, K. (2006). Water budgets of three small catchments under montane forest in Ecuador: experimental and modelling approach. *Hydrological processes, 20*(12), 2491-2507. https://doi.org/10.1002/hyp.6212

Galloway, J., Dentener, F., Capone, D., Boyer, E., Howarth, R., Seitzinger, S., et al. (2004). Nitrogen Cycles: Past, Present, and Future. *Biogeochemistry, 70*(2), 153-226. https://doi.org/10.1007/s10533-004-0370-0

Galloway, J., Townsend, A., Erisman, J. W., Bekunda, M., Cai, Z., Freney, J. R., Martinelli, L. A., Seitzinger, S. P., & Sutton, M. A. (2008). Transformation of the Nitrogen Cycle: Recent Trends, Questions, and Potential Solutions. *Science, 320*(5878), 889-892. https://doi.org/10.1126/science.1136674

Garten, C. T. (1996). Stable nitrogen isotope ratios in wet and dry nitrate deposition collected with an artificial tree. *Tellus B: Chemical and Physical Meteorology, 48*(1), 60-64. https://doi.org/10.3402/tellusb.v48i1.15666

Garten, C. T., & Hanson, P. J. (1990). Foliar retention of ^{15}N-nitrate and ^{15}N-ammonium by red maple (*Acer rubrum*) and white oak (*Quercus alba*) leaves from simulated rain. *Environmental and Experimental Botany, 30*(3), 333-342. https://doi.org/10.1016/0098-8472(90)90045-6

Glass, N., de Oliveira, E. D., Molano-Flores, B., Matamala, R., Whelan, C. J., & Gonzalez-Meler, M. A. (2023). Root litter decomposition rates and impacts of drought are regulated by ecosystem legacy. *Applied Soil Ecology, 189*, 104903. https://doi.org/10.1016/j.apsoil.2023.104903

Goller, R., Wilcke, W., Fleischbein, K., Valarezo, C., & Zech, W. (2006). Dissolved nitrogen, phosphorus, and sulfur forms in the ecosystem fluxes of a montane forest

in Ecuador. *Biogeochemistry, 77*(1), 57-89. https://doi.org/10.1007/s10533-005-1061-1

Goller, R., Wilcke, W., Leng, M. J., Tobschall, H. J., Wagner, K., Valarezo, C., & Zech, W. (2005). Tracing water paths through small catchments under a tropical montane rain forest in south Ecuador by an oxygen isotope approach. *Journal of Hydrology, 308*(1), 67-80. https://doi.org/10.1016/j.jhydrol.2004.10.022

Guerrieri, R., Vanguelova, E. I., Michalski, G., Heaton, T. H. E., & Mencuccini, M. (2015). Isotopic evidence for the occurrence of biological nitrification and nitrogen deposition processing in forest canopies. *Global Change Biology, 21*(12), 4613-4626. https://doi.org/10.1111/gcb.13018

Handley, L., Austin, A., Stewart, G., Robinson, D., Scrimgeour, C., Raven, J., & Schmidt, S. (1999). The 15N natural abundance (δ15N) of ecosystem samples reflects measures of water availability. *Functional Plant Biology, 26*(2), 185-199. https://doi.org/10.1071/PP98146

Harrison, A. F., Schulze, E. D., Gebauer, G., & Bruckner, G. (2000). Canopy uptake and utilization of atmospheric pollutant nitrogen. In E.-D. Schulze (Ed.), *Carbon and nitrogen cycling in European forest ecosystems* (pp. 171-188). Germany: Springer. https://doi.org/10.1007/978-3-642-57219-7_8

Hill, A. R. (1990). Ground water flow paths in relation to nitrogen chemistry in the near-stream zone. *Hydrobiologia, 206*(1), 39-52. https://doi.org/10.1007/BF00018968

Högberg, P. (1997). Tansley Review No. 95 ^{15}N natural abundance in soil-plant systems. *New Phytologist, 137*(2), 179-203. https://doi.org/10.1046/j.1469-8137.1997.00808.x

Homeier, J., Hertel, D., Camenzind, T., Cumbicus, N. L., Maraun, M., Martinson, G. O., et al. (2012). Tropical andean forests are highly susceptible to nutrient inputs—rapid effects of experimental N and P addition to an Ecuadorian montane forest. *PLoS One, 7*(10), e47128. https://doi.org/10.1371/journal.pone.0047128

Houle, D., Marty, C., & Duchesne, L. (2015). Response of canopy nitrogen uptake to a rapid decrease in bulk nitrate deposition in two eastern Canadian boreal forests. *Oecologia, 177*(1), 29-37. https://doi.org/10.1007/s00442-014-3118-0

IUSS Working Group WRB. (2014). *World Reference Base for Soil Resources 2014. International soil classification system for naming soils and creating legends for soil maps.* Retrieved from Rome:

Jin, V. L., Haney, R. L., Fay, P. A., & Polley, H. W. (2013). Soil type and moisture regime control microbial C and N mineralization in grassland soils more than atmospheric CO2-induced changes in litter quality. *Soil Biology and Biochemistry, 58*, 172-180. https://doi.org/10.1016/j.soilbio.2012.11.024

Kirkels, F. M. S. A., Cerli, C., Federherr, E., Gao, J., & Kalbitz, K. (2014). A novel high-temperature combustion based system for stable isotope analysis of dissolved organic carbon in aqueous samples. II: optimization and assessment of analytical performance. *Rapid Communications in Mass Spectrometry, 28*(23), 2574-2586. https://doi.org/10.1002/rcm.7053

Knapp, A. N., Hastings, M. G., Sigman, D. M., Lipschultz, F., & Galloway, J. N. (2010). The flux and isotopic composition of reduced and total nitrogen in Bermuda rain. *Marine Chemistry, 120*(1), 83-89. https://doi.org/10.1016/j.marchem.2008.08.007

Koba, K., Fang, Y., Mo, J., Zhang, W., Lu, X., Liu, L., et al. (2012). The 15N natural abundance of the N lost from an N-saturated subtropical forest in southern China. *Journal of Geophysical Research: Biogeosciences, 117*(G2). https://doi.org/10.1029/2010JG001615

Lamarque, J. F., Dentener, F., McConnell, J., Ro, C. U., Shaw, M., Vet, R., et al. (2013). Multi-model mean nitrogen and sulfur deposition from the Atmospheric Chemistry and Climate Model Intercomparison Project (ACCMIP): evaluation of historical and projected future changes. *Atmos. Chem. Phys., 13*(16), 7997-8018. https://doi.org/10.5194/acp-13-7997-2013

Lee, K.-S., Lee, D.-S., Lim, S.-S., Kwak, J.-H., Jeon, B.-J., Lee, S.-I., Lee, S.-M., & Choi, W.-J. (2012). Nitrogen isotope ratios of dissolved organic nitrogen in wet precipitation in a metropolis surrounded by agricultural areas in southern Korea. *Agriculture, Ecosystems & Environment, 159*, 161-169. https://doi.org/10.1016/j.agee.2012.07.010

Lovett, G. M., & Lindberg, S. E. (1993). Atmospheric deposition and canopy interactions of nitrogen in forests. *Canadian Journal of Forest Research, 23*(8), 1603-1616. https://doi.org/10.1139/x93-200

Martinson, G. O., Corre, M. D., & Veldkamp, E. (2013). Responses of nitrous oxide fluxes and soil nitrogen cycling to nutrient additions in montane forests along an elevation gradient in southern Ecuador. *Biogeochemistry, 112*(1), 625-636. https://doi.org/10.1007/s10533-012-9753-9

Michalzik, B., Kalbitz, K., Park, J.-H., Solinger, S., & Matzner, E. (2001). Fluxes and concentrations of dissolved organic carbon and nitrogen – a synthesis for temperate forests. *Biogeochemistry, 52*(2), 173-205. https://doi.org/10.1023/A:1006441620810

Pérez, C. A., Thomas, F. M., Silva, W. A., Aguilera, R., & Armesto, J. J. (2017). Biological nitrogen fixation in a post-volcanic chronosequence from south-central Chile. *Biogeochemistry, 132*(1), 23-36. https://doi.org/10.1007/s10533-016-0285-6

Peters, T., Drobnik, T., Meyer, H., Rankl, M., Richter, M., Rollenbeck, R., Thies, B., & Bendix, J. (2013). Environmental changes affecting the Andes of Ecuador. In J. Bendix, E. Beck, A. Bräuning, F. Makeschin, R. Mosandl, S. Scheu, & W. Wilcke (Eds.), *Ecosystem services, biodiversity and environmental change in a tropical mountain ecosystem of south Ecuador.* (pp. 19-29). Germany: Springer. https://doi.org/10.1007/978-3-642-38137-9_2

Pierick, K., Leuschner, C., & Homeier, J. (2021). Topography as a factor driving small-scale variation in tree fine root traits and root functional diversity in a species-rich tropical montane forest. *New Phytologist, 230*(1), 129-138. https://doi.org/10.1111/nph.17136

Potapov, A. M., Korotkevich, A. Y., & Tiunov, A. V. (2018). Non-vascular plants as a food source for litter-dwelling Collembola: Field evidence. *Pedobiologia, 66*, 11-17. https://doi.org/10.1016/j.pedobi.2017.12.005

Qualls, R. G., & Haines, B. L. (1991). Geochemistry of dissolved organic nutrients in water percolating through a forest ecosystem. *Soil Science Society of America Journal, 55*(4), 1112-1123. https://doi.org/10.2136/sssaj1991.03615995005500040036x

Qualls, R. G., & Haines, B. L. (1992). Biodegradability of dissolved organic matter in forest throughfall, soil solution, and stream water. *Soil Science Society of America Journal, 56*(2), 578-586. https://doi.org/10.2136/sssaj1992.03615995005600020038x

R Core Team. (2025). R: A language and environment for statistical computing. R Foundation for Statistical Computing. Vienna, Austria. Retrieved from https://www.r-project.org/

Roa-Fuentes, L. L., Templer, P. H., & Campo, J. (2015). Effects of precipitation regime and soil nitrogen on leaf traits in seasonally dry tropical forests of the Yucatan Peninsula, Mexico. *Oecologia, 179*(2), 585-597. https://doi.org/10.1007/s00442-015-3354-y

Rolff, C., Elmgren, R., & Voss, M. (2008). Deposition of nitrogen and phosphorus on the Baltic Sea: seasonal patterns and nitrogen isotope composition. *Biogeosciences, 5*(6), 1657-1667. https://doi.org/10.5194/bg-5-1657-2008

Sala, O. E., Stuart Chapin, F., Armesto, J. J., Berlow, E., Bloomfield, J., Dirzo, R., et al. (2000). Global Biodiversity Scenarios for the Year 2100. *Science, 287*(5459), 1770-1774. https://doi.org/10.1126/science.287.5459.1770

Schrumpf, M., Guggenberger, G., Valarezo, C., & Zech, W. (2001). Tropical montane rain forest soils: development and nutrient status along altitudinal gradient in the South Ecuadorian Andes. *Erde, 132*(1), 43-59.

Schwarz, M. T., Bischoff, S., Blaser, S., Boch, S., Grassein, F., Klarner, B., et al. (2016). Drivers of nitrogen leaching from organic layers in Central European beech forests. *Plant and Soil, 403*(1), 343-360. https://doi.org/10.1007/s11104-016-2798-0

Schwarz, M. T., Bischoff, S., Blaser, S., Boch, S., Schmitt, B., Thieme, L., et al. (2014). More efficient aboveground nitrogen use in more diverse Central European forest canopies. *Forest Ecology and Management, 313*, 274-282. https://doi.org/10.1016/j.foreco.2013.11.021

Schwarz, M. T., Oelmann, Y., & Wilcke, W. (2011). Stable N isotope composition of nitrate reflects N transformations during the passage of water through a montane rain forest in Ecuador. *Biogeochemistry, 102*(1), 195-208. https://doi.org/10.1007/s10533-010-9434-5

Smith, S. J., Power, J. F., & Keper, W. D. (1994). Fixed ammonium and nitrogen availability indexes. *Soil Science, 158*(2), 132-140.

Soethe, N., Lehmann, J., & Engels, C. (2007). Carbon and nutrient stocks in roots of forests at different altitudes in the Ecuadorian Andes. *Journal of Tropical Ecology, 23*(3), 319-328. https://doi.org/10.1017/S0266467407004002

Sohrt, J., Lang, F., & Weiler, M. (2017). Quantifying components of the phosphorus cycle in temperate forests. *WIREs Water, 4*(6), e1243. https://doi.org/10.1002/wat2.1243

Solinger, S., Kalbitz, K., & Matzner, E. (2001). Controls on the dynamics of dissolved organic carbon and nitrogen in a Central European deciduous forest. *Biogeochemistry, 55*(3), 327-349. https://doi.org/10.1023/A:1011848326013

Steffens, D., & Sparks, D. (1997). Kinetics of nonexchangeable ammonium release from soils. *Soil Science Society of America Journal, 61*(2), 455-462. https://doi.org/10.2136/sssaj1997.03615995006100020012x

Tipping, E., Benham, S., Boyle, J. F., Crow, P., Davies, J., Fischer, U., et al. (2014). Atmospheric deposition of phosphorus to land and freshwater. *Environmental Science: Processes & Impacts, 16*(7), 1608-1617. http://dx.doi.org/10.1039/C3EM00641G

Turner, B. L., & Wright, J. S. (2014). The response of microbial biomass and hydrolytic enzymes to a decade of nitrogen, phosphorus, and potassium addition in a lowland tropical rain forest. *Biogeochemistry, 117*(1), 115-130. https://doi.org/10.1007/s10533-013-9848-y

Ulrich, B. (1984). Effects of air pollution on forest ecosystems and waters—the principles demonstrated at a case study in Central Europe. *Atmospheric Environment (1967), 18*(3), 621-628. https://doi.org/10.1016/0004-6981(84)90182-3

Vandenbruwane, J., De Neve, S., Qualls, R. G., Sleutel, S., & Hofman, G. (2007). Comparison of different isotherm models for dissolved organic carbon (DOC) and nitrogen (DON) sorption to mineral soil. *Geoderma, 139*(1), 144-153. https://doi.org/10.1016/j.geoderma.2007.01.012

Velescu, A., Valarezo, C., & Wilcke, W. (2016). Response of dissolved carbon and nitrogen concentrations to moderate nutrient additions in a tropical montane forest of south Ecuador. *Frontiers in Earth Science, 4*, 58. https://doi.org/10.3389/feart.2016.00058

Vitousek, P. M. (1984). Litterfall, Nutrient Cycling, and Nutrient Limitation in Tropical Forests. *Ecology, 65*(1), 285-298. https://doi.org/10.2307/1939481

Vitousek, P. M., Bateman, J. B., & Chadwick, O. A. (2021). A "toy" model of biogeochemical dynamics on climate gradients. *Biogeochemistry, 154*(2), 183-210. https://doi.org/10.1007/s10533-020-00734-y

Wang, A., Zhu, W., Gundersen, P., Phillips, O. L., Chen, D., & Fang, Y. (2018). Fates of atmospheric deposited nitrogen in an Asian tropical primary forest. *Forest Ecology and Management, 411*, 213-222. https://doi.org/10.1016/j.foreco.2018.01.029

Wang, X., Wang, B., Wang, C., Wang, Z., Li, J., Jia, Z., et al. (2021). Canopy processing of N deposition increases short-term leaf N uptake and photosynthesis, but not long-term N retention for aspen seedlings. *New Phytologist, 229*(5), 2601-2610. https://doi.org/10.1111/nph.17041

Wassen, M. J., Venterink, H. O., Lapshina, E. D., & Tanneberger, F. (2005). Endangered plants persist under phosphorus limitation. *Nature, 437*(7058), 547-550. https://doi.org/10.1038/nature03950

Wilcke, W., Leimer, S., Peters, T., Emck, P., Rollenbeck, R., Trachte, K., Valarezo, C., & Bendix, J. (2013). The nitrogen cycle of tropical montane forest in Ecuador turns inorganic under environmental change. *Global Biogeochemical Cycles, 27*(4), 1194-1204. https://doi.org/10.1002/2012GB004471

Wilcke, W., Velescu, A., Leimer, S., Bigalke, M., Boy, J., & Valarezo, C. (2017). Biological versus geochemical control and environmental change drivers of the base metal budgets of a tropical montane forest in Ecuador during 15 years. *Biogeochemistry, 136*(2), 167-189. https://doi.org/10.1007/s10533-017-0386-x

Wilcke, W., Velescu, A., Leimer, S., Bigalke, M., Boy, J., & Valarezo, C. (2019). Temporal trends of phosphorus cycling in a tropical montane forest in Ecuador during 14 years. *Journal of Geophysical Research: Biogeosciences, 124*(5), 1370-1386. https://doi.org/10.1029/2018JG004942

Wilcke, W., Velescu, A., Leimer, S., Blotevogel, S., Alvarez, P., & Valarezo, C. (2020). Total organic carbon concentrations in ecosystem solutions of a remote tropical montane forest respond to global environmental change. *Global Change Biology, 26*(12), 6989-7005. https://doi.org/10.1111/gcb.15351

Wilcke, W., Yasin, S., Abramowski, U., Valarezo, C., & Zech, W. (2002). Nutrient storage and turnover in organic layers under tropical montane rain forest in Ecuador. *European Journal of Soil Science, 53*(1), 15-27. https://doi.org/10.1046/j.1365-2389.2002.00411.x

Wittich, B., Homeier, J., & Leuschner, C. (2015). Ammonium, nitrate and glycine uptake of six Ecuadorian tropical montane forest tree species: an in situ pot experiment with saplings. *Journal of Tropical Ecology, 31*(2), 139-152. https://doi.org/10.1017/S0266467414000650

Wullaert, H., Homeier, J., Valarezo, C., & Wilcke, W. (2010). Response of the N and P cycles of an old-growth montane forest in Ecuador to experimental low-level N and P amendments. *Forest Ecology and Management, 260*(9), 1434-1445. https://doi.org/10.1016/j.foreco.2010.07.021

Young, E. O., & Briggs, R. D. (2005). Shallow ground water nitrate-N and ammonium-N in cropland and riparian buffers. *Agriculture, Ecosystems & Environment, 109*(3), 297-309. https://doi.org/10.1016/j.agee.2005.02.026

D. Long-term trends of DOM and its stoichiometric ratios

Environmental change during 25 years altered dissolved organic matter stoichiometry in a tropical montane forest on the rim of the Amazon basin

Pablo Alvarez[1,2], Andre Velescu[1], Wolfgang Wilcke[1]

[1] Institute of Geography and Geoecology, Karlsruhe Institute of Technology (KIT), Reinhard-Baumeister-Platz 1, 76131 Karlsruhe, Germany

[2] Centro de Investigaciones Tropicales del Ambiente y Biodiversidad (CITIAB), Universidad Nacional de Loja. Reinaldo Espinoza Avenue s/n, 110103 Loja, Ecuador

1. Abstract

Dissolved organic matter (DOM) couples carbon (C), nitrogen (N), and phosphorus (P) cycling in forest ecosystems. We assessed whether the DOM composition of a tropical montane forest responded to rising N and continuous P deposition and increasingly drier conditions from 1998-2023. We determined dissolved organic carbon (DOC), nitrogen (DON) and phosphorus (DOP) concentrations and fluxes in ecosystem solutions from rainfall to streamflow. We used previously measured $\delta^{13}C$ and $\delta^{15}N$ values of soil horizons and solutions. Mean DON concentrations increased from rainfall to litter leachate and decreased to streamflow. DOP concentrations were higher in stemflow than in throughfall and litter leachate and not detected in rainfall, mineral soil solutions, and streamflow. From 1998 to 2023, the DON and DOP concentrations increased significantly in several solutions, while the DOC/DON and DOC/DOP ratios decreased in most solutions reflecting an increasing nutrient richness of DOM. The DON/DOP ratios decreased in throughfall, because DOP was more readily leached from the canopy than DON, but increased in litter leachate because of stronger P than N retention in the organic layer. The $\delta^{13}C$ and $\delta^{15}N$ values of soil horizons correlated, as expected for closely coupled C and N cycles. However, the $\delta^{13}C$ and $\delta^{15}N$ values of solutions formed two clusters, reflecting source mixing and DOM transformations. The $\delta^{15}N$ values of total dissolved N did not correlate with the DOC/DON ratios. After 25 years of environmental change, the C, N, and P cycles of the forest changed significantly, with N being increasingly exported but P retained.

Keywords: C:N:P stoichiometry; dissolved organic nitrogen; dissolved organic phosphorus; stable C and N isotope ratios; nitrogen deposition; ecosystem solutions

2. Introduction

Dissolved organic matter (DOM) contains carbon (C), nitrogen (N), and phosphorus (P) and thus contributes to their cycling in forest ecosystems. The DOM fluxes through forests along the water path reflect organic matter production and processing in the forest canopy, on bark surfaces, in the organic layer, and the mineral soil, which in turn regulates nutrient availability and export to downstream aquatic ecosystems (Kalbitz et al., 2000; Michalzik et al., 2001; Qualls et al., 1991). The concentrations and fluxes of dissolved organic nitrogen (DON) and dissolved organic phosphorus (DOP) in ecosystem solutions typically increase along the water flow path through the aboveground ecosystem, from rainfall via throughfall and stemflow to litter leachate, and then decrease through the mineral soil as organic forms are sorbed, mineralized, or transformed into inorganic species (Goller et al., 2006; Michalzik et al., 2001; Schrumpf et al., 2006). The stoichiometric ratios of DOM, i.e., DOC/DON, DOC/DOP, and DON/DOP are indicators of DOM quality, particularly of its nutrient richness, and of the balance between the N and P cycles. They provide complementary signals of the biological and chemical processes governing organic matter production, transformation, and retention in different ecosystem compartments (Cleveland & Liptzin, 2007; Neff et al., 2000; Saunders et al., 2006). The highly biodiverse humid tropical montane forests in south Ecuador harbor huge stocks of C and are important regulators of regional water and nutrient cycles, yet they remain understudied relative to temperate and tropical lowland forests, particularly with regard to the long-term dynamics of DON, DOP, and DOM stoichiometry under ongoing global environmental change (Lange et al., 2024; Leuschner et al., 2013; Wilcke et al., 2020; Wilcke et al., 2002).

In temperate forests, the soil organic layer is the primary source of DON and DOP. In the mineral soil, sorption is the dominant retention mechanism (Kalbitz et al., 2000; Michalzik et al., 2001; Qualls et al., 1991). Goller et al. (2006) reported that organic forms contributed on average 55 and 66%, to total dissolved N and P concentrations, respectively, across all ecosystem fluxes through the same tropical montane forest from which we report our results, in line with findings of Qualls et al. (1991) for temperate forests. However, the data of Goller et al. (2006) were limited to three years, preventing time series analysis. The C/N and C/P stoichiometry of DOM are governed by element-specific mechanisms, with DOC/DON ratios reflecting long-term changes in soil organic matter stoichiometry rather than short-term microbial demand, while DOC/DOP ratios and DOP fluxes respond directly

to P availability (Neff et al., 2000). Interestingly, along a chronosequence of tropical montane forests, DON and DOP losses were shown to occur independently of ecosystem N or P status, with forests developing increasingly higher N/P loss ratios with time as a result of efficient P recycling and high N throughputs from atmospheric deposition (Hedin et al., 2003).

Complementing element stoichiometry, the stable isotope ratios of C ($\delta^{13}C$ values) in DOM and of N ($\delta^{15}N$ values) in total dissolved N (TDN) offer further information about DOM sources and transformation processes, because fractionation during transformation processes such as mixing of different sources, microbial decomposition or sorption to soil surfaces, alter isotope signatures of C and N along the water flow path (Alvarez et al., 2023, 2024c). While the $\delta^{13}C$ values of DOM at our study site were used to identify DOM sources and transformation processes (Alvarez et al., 2023), the $\delta^{15}N$ values of TDN provided a tracer of N sources and sinks along the water flow path (Alvarez et al., 2024c). In contrast to DOM, the $\delta^{13}C$ values of soil organic matter and the $\delta^{15}N$ values of total N in the soil solid phase are known to increase concurrently with soil depth and decomposition, because microbial processing preferentially removes isotopically light C and N, so that the residual organic matter becomes progressively enriched in ^{13}C and ^{15}N (Gerschlauer et al., 2019; Lorenz et al., 2020; Nel et al., 2018). Whether the same coupling holds for DOM along the water flow path has, however, to the best of our knowledge never been studied.

Our study site in the tropical montane forest in south Ecuador underwent environmental changes from 1998 to 2023. Atmospheric N deposition increased substantially, driven primarily by Amazonian biomass burning to the forests on the rim of the Amazon basin (Boy et al., 2008a; Wilcke et al., 2013). Simultaneously, there was a steady low-level input of P, likely because of long-range transport from Africa with the trade winds (Barkley et al., 2019; Van Langenhove et al., 2020; Wilcke et al., 2019). Nitrogen and P inputs have resulted in a progressive shift of the N cycle in the Ecuadorian tropical montane forest toward increasing inorganic N concentrations and decreasing DON contributions to TDN (Wilcke et al., 2013) and in a positive P budget over 14 years (Wilcke et al., 2019). Increasing N deposition has been shown to increase C:P and N:P stoichiometric ratios in plants, soils, and microbial biomass across forest ecosystems globally, thereby progressively pushing the ecosystems toward or enhancing existing P limitation (Jiang et al., 2024; Wang et al., 2017). Long-term N inputs have been reported to alter the molecular composition of soil DOM in a tropical forest, increasing the proportion of recalcitrant aromatic compounds and reducing the bioavailable fraction (Niu et al., 2022). Simultaneously, more frequent

temperatures above 25°C, more frequent and longer dry spells, and decreasing soil water contents have enhanced microbial decomposition and altered the release and transformation of DOM in the organic layer and mineral soil at the study site (Wilcke et al., 2020). The TOC/DON ratios in ecosystem solutions decreased during the first 15 years in most ecosystem solutions, consistent with an accelerated turnover of DOM under increasing N availability and changing climatic conditions (Velescu et al., 2016; Wilcke et al., 2020). Experimental nutrient additions have shown that the organic layer of the study site is co-limited by N and P, and that concurrent N and P inputs accelerate TOC and DON turnover (Homeier et al., 2012; Velescu et al., 2016). Together, these environmental drivers provide the mechanistic basis for expecting progressive and compartment-specific shifts in the concentrations and stoichiometric ratios of DON and DOP in ecosystem solutions, with the direction of change depending on the sizes of N and P enrichment in each compartment along the vertical water flow path. No study has yet examined the long-term temporal trends of DON and DOP concentrations together with their stoichiometric ratios and the relationship between $\delta^{13}C$ and $\delta^{15}N$ values across solid phases and ecosystem solutions during an observation period of more than 20 yr in a tropical forest. This gap limits our understanding of how global environmental change is reorganizing the C, N, and P cycles of tropical montane forests.

Our overall objective was to detect global change effects on the organically bound C, N, and P cycling in a tropical montane forest in Ecuador. We assessed the temporal course of the DON and DOP concentrations and fluxes and the C/N, C/P, and N/P ratios in DOM of ecosystem solutions along the water path through a tropical montane forest (i.e., in rainfall, throughfall, stemflow, litter leachate, mineral soil solutions, and streamflow) during 25 years (1998–2023). Moreover, we studied the relationship among stable C and N isotope ratios and C/N ratios in the soil solid phase and ecosystem solutions. We hypothesized that (i) DON and DOP concentrations and fluxes in the ecosystem solutions increased and DOC/DON and DOC/DOP ratios decreased during the observation period because of the increasing N richness and the continuous P accumulation in the ecosystem from deposition, (ii) the DON/DOP ratios in the ecosystem solutions increased during the observation period because the ecosystem transitions from a N and P colimitation to a pure P limitation of plant growth, and (iii) stable C and N isotope ratios of plant and soil solid phases and ecosystem solutions correlate with each other and the $\delta^{15}N$ values of the ecosystem solutions correlate with the DOC/DON ratios because of the close coupling of the C and N cycles.

3. Materials and methods

3.1. Study site

We studied the DOM properties in a 9.1-ha catchment at 1850-2150 m above sea level (a.s.l.) under evergreen lower tropical montane forest (Bruijnzeel & Hamilton, 2000). The study site is located in the San Francisco Biological Reserve on the east-exposed slope of the Andean cordillera in south Ecuador (Beck et al., 2008). This undisturbed catchment is coded as Microcatchment 2 (MC2), where several previous studies have been conducted (e.g., Alvarez et al., 2023; Boy et al., 2008b; Wilcke et al., 2020). The annual rainfall from April 1998 to March 2023 was 2340 ± SD 235 mm and the mean annual temperature was 15.1 ± 1.0 °C (Bendix, 2020; Bendix et al., 2018, updated in May 2026). The study ecosystem is perhumid with more than 100 mm of precipitation per month. October and November had the lowest monthly precipitation with frequent dry spells of up to six weeks, whereas June had the highest precipitation (>200 mm). Throughfall fluxes, relative humidity, and the soil moisture content decreased, while interception loss from the forest canopy increased in the first 15 years (Wilcke et al., 2020). Soils are shallow, with a depth <0.7 m, loamy Folic Dystric Cambisols (IUSS Working Group WRB, 2022) developed from phyllite with some interlayering of metasandstone. The soil has three organic horizons (Oi, Oe, Oa) that sum up to a mean organic layer thickness of 0.18 m (Wilcke et al., 2002). The dominant phyllosilicates in the mineral soil are illite, vermiculite, and kaolinite (Schrumpf et al., 2001). The mean pH of the A horizon is 4.4, the mean effective cation-exchange capacity 63 ± 26 $mmol_c\ kg^{-1}$, the mean organic carbon concentration 32 ± 19 g kg^{-1}, and the mean C/N ratio 11 ± 2.8 (Wilcke et al., 2017). The N and P availability co-limited the vegetation growth (Homeier et al., 2012).

3.2. Field sampling

The long-term experimental area was set up in April 1998 and since then we have been running the same field sampling methods. Here, we considered weekly ecosystem solutions from April 1998 to March 2023. Rainfall (RF) was collected from one to four gauging stations, each consisting of five Hellmann-type collectors, placed on clear-cut areas. The collectors were permanently open and sampled bulk deposition, i.e., wet deposition and the soluble part of dry deposition (Wilcke et al., 2013; Wilcke et al., 2020). Throughfall (TF)

was sampled using 20 funnel collectors at fixed positions, randomly distributed along three 20-m transects at 1900, 1950, and 2000 m a.s.l. Throughfall was combined into one sample per transect and collection date in the field. Stemflow (SF) was sampled using polyurethane collars installed on five trees in the lower part of the catchment, and the individual samples were combined into one sample per collection date. Litter leachate (LL) was sampled with three zero-tension lysimeters per transect, installed laterally below the organic layer. Mineral soil solutions at the 0.15 (SS15) and 0.30 m depths (SS30) were obtained with three suction cups per depth, each with a pore size of 1 ± 0.1 µm (Wilcke et al., 2020). Like the throughfall samples, LL, SS15, and SS30 were combined to one sample per transect and sampling date. A single instantaneous streamflow (ST) sample was collected weekly from the center of the flowing stream above a weir (Fleischbein et al., 2006).

Water volumes of rainfall, throughfall, and stemflow were measured in the field and converted to water fluxes using the collection area of the samplers for rainfall and throughfall, or extrapolated based on tree density per hectare for stemflow assuming 1,000 trees with a diameter at breast height (dbh) >0.1 m and 4,000 trees with a dbh <0.1 m yielding only 50% of the stemflow of the large trees (Wilcke et al., 2017). Water fluxes of litter leachate and mineral soil solutions were derived from the Soil Water Balance Model (DVWK, 1996), calibrated with data from 1999 to 2003, and extended to the full study period through regression equations described in Wilcke et al. (2020) and (Schwarz et al., 2011), respectively. All ecosystem solutions were filtered in the field laboratory with ashless folded filters of 4–7 µm pore size, Type 392 (Sartorius-Stedim GmbH, Göttingen, Germany), except the mineral soil solutions that passed a ceramic cup with a pore size of 1 µm. Alvarez et al. (2023) reported no detectable difference between TOC concentrations and dissolved organic carbon (DOC) obtained by conventional filtration to <0.45 µm for samples of all ecosystem solutions at the study site so that we stick to the term DOC in this paper.

3.3. Chemical analyses

TOC concentrations were determined with an automatic TOC analyzer (TOC 5050, Shimadzu, Duisburg, Germany) until 2004 and thereafter with a TOC analyzer (varioTOC, Elementar Analysensysteme, Langenselbold, Germany) as non-purgeable organic carbon. Total dissolved nitrogen (TDN), total dissolved phosphorus (TDP), dissolved inorganic nitrogen (DIN = NH_4-N+NO_3-N), and phosphate (PO4-P) concentrations were measured with high-resolution colorimetry and photometric detection using a continuous flow analyzer (CFA San++, Skalar, Breda, The Netherlands from 1998-2003 and from 2015-2023 or

AutoAnalyzer 3 HR; Seal Analytical, Norderstedt, Germany from 2004-2014). Dissolved organic nitrogen (DON) concentrations were calculated as the difference between TDN and DIN concentrations and dissolved organic phosphorus (DOP) concentrations as the difference between TDP and PO_4-P concentrations. The TDN and thus also the DON data are only available from March 1999 onward, i.e. for a period of 24 years and the TDP and DOP data from March 2003 onward, i.e., for a period of 20 years. When the P concentrations were near to the detection limits, PO_4-P concentrations were sometimes measured higher than TDP concentrations, which is physically impossible. In such cases, DOP concentrations were set to zero. Because this was frequently the case in rainfall, mineral soil solutions, and streamflow we refrained from quantifying DOP concentration in these solutions and defined them to be not detected with our method. For N, the measured DIN concentrations were rarely higher than the TDN concentrations and thus DON concentrations set to zero (<5% of all samples).

3.4. Stable isotope ratios

All stable isotope ratios of C and N were taken from previous work (Alvarez et al., 2023, 2024c). From January 2013 to December 2016, the $\delta^{13}C$ values of DOM in monthly resolution and the $\delta^{15}N$ values of TDN in quarterly resolution were obtained by direct measurement in solution with a Total Organic Carbon Analyser coupled to an Isotope Ratio Mass Spectrometer (TOC-IRMS; Elementar Analysensysteme, Langenselbold, Germany). The $\delta^{13}C$ and $\delta^{15}N$ values of litterfall were measured in monthly composite samples collected between 2013 and 2016, while the C and N isotope ratios of the organic layer and the mineral soil were measured in samples from 21 soil profiles collected in December 2016 with an Elemental Analyzer-IRMS (Delta V Advantage, ThermoFisher, Bremen Germany). These data were reanalysed together with the long-term concentration and stoichiometric ratio measurements to investigate relationships between isotopic composition and DOM stoichiometry.

3.5. Calculations and statistical evaluation

We calculated monthly mean concentrations of all element concentrations by averaging 4-5 weekly measurements. To compare annual mean concentrations and stoichiometric ratios among ecosystem solutions, homoscedasticity was first assessed with Levene's test and normality of residuals was checked by visual inspection. Where these assumptions were met, we applied bifactorial ANOVA with year before solution type as

factors, followed by Tukey's Honest Significant Difference (HSD) post hoc test implemented with the emmeans (Lenth & Piaskowski, 2026) and multcomp (Hothorn et al., 2008) packages in R 4.5.1 (R Core Team, 2025).

Temporal trends in monthly mean concentrations, fluxes, and stoichiometric ratios of DON, DOP, DOC/DON, DOC/DOP, and DON/DOP, as well as in the contributions of DON to TDN and DOP to TDP, were assessed with the seasonal Mann-Kendall trend test (Hirsch et al., 1982), implemented in the function kendallSeasonalTrendTest of the EnvStats package (Millard, 2013), which accounts for seasonal autocorrelation by comparing observations only within the same calendar month across years. Missing data were excluded from the corresponding pairwise comparisons, without imputation. Kendall's τ is the rank correlation coefficient which is a measure for the strength of the trend, and does not necessarily have to be linear. To assess the size of significant trends, we additionally report the seasonal Sen's slope (Hirsch et al., 1982), the median of all pairwise rates of change pooled across months, expressed both in the original units of each variable and as a percentage of its median value per year and for the full study period. The level of significance was set at $p < .05$ for all tests. The p values are the error probabilities of two-sided tests. All data handling, statistical analyses, and figures of temporal trends were performed in R, version 4.5.1 (R Core Team, 2025).

4. Results

The annual mean DON concentrations and fluxes increased from rainfall via throughfall and stemflow to litter leachate, and decreased from litter leachate via the mineral soil solutions at the 0.15 m and 0.30 m depths to streamflow (**Table D-S1**). The DON contributions to the TDN concentrations were smallest in the mineral soil solutions, rainfall, and streamflow (**Figure D-S1a**). The DON contributions increased from rainfall via throughfall and litter leachate to stemflow, which showed the largest DON contributions (**Figure D-S1a**). The DOP concentrations were highest in stemflow and similar in throughfall and litter leachate (**Table D-S1**). The DOP contribution to TDP increased from throughfall via stemflow to litter leachate (**Figure D-S1b**). The highest DOC/DON concentrations ratios occurred in rainfall and streamflow and the lowest in throughfall (**Table D-S1**). The DOC/DOP ratios increased from throughfall via stemflow to litter leachate (**Table D-S1**).

The mean monthly DOC concentrations and fluxes decreased significantly during the observation period of 25 years (1998-2023) in all ecosystem solutions except stemflow and litter leachate in which they increased significantly (**Figures D-S2 and D-S3**). The mean annual change rates of the DOC concentrations measured as seasonal Sen's slope in the ecosystem solutions ranged from -4.8% (mineral soil solution at the 0.15 m depth) to +3.2% (stemflow) of the median concentrations during the whole observation period (**Table D-S2**). The mean annual change rates of the DOC fluxes were similar (**Table D-S2**). Thus, the trends reported by Wilcke et al. (2020) for the first 15 years continued. The only exception was litter leachate, for which Wilcke et al. (2020) did not report a significant trend.

The mean monthly DON concentrations and fluxes increased significantly in stemflow, litter leachate, and streamflow and decreased significantly in the two mineral soil solutions from April 1999 to March 2023 (**Figures D-1 and D-S4**). The mean annual change rate of the DON concentrations ranged from -2.9% of the median concentrations (mineral soil solution at the 0.15 m depth) to +3.6% (stemflow, **Table D-S3**). The mean annual change rates of the DON fluxes were similar (**Table D-S3**). The DON contributions to TDN decreased significantly in most ecosystem solutions during the observation period of 24 years except in stemflow and litter leachate which did not show temporal trends (**Figure D-S5**). The contributions of DON to TDN decreased annually by 1.2-5.3% of the median contribution (**Table D-S4**). The decreasing DON contributions to TDN continue the findings for the first 12 years of this time series (Wilcke et al., 2013). The mean monthly DOC/DON ratios decreased significantly in all ecosystem solutions by annually 0.5-6.5% (streamflow) of the median ratio (**Table D-S2**) during the observation period of 24 years (**Figure D-S6**), consistent with the findings of Wilcke et al. (2020) for the first 15 years of the time series, with the decreasing trend now extending also to litter leachate and stemflow.

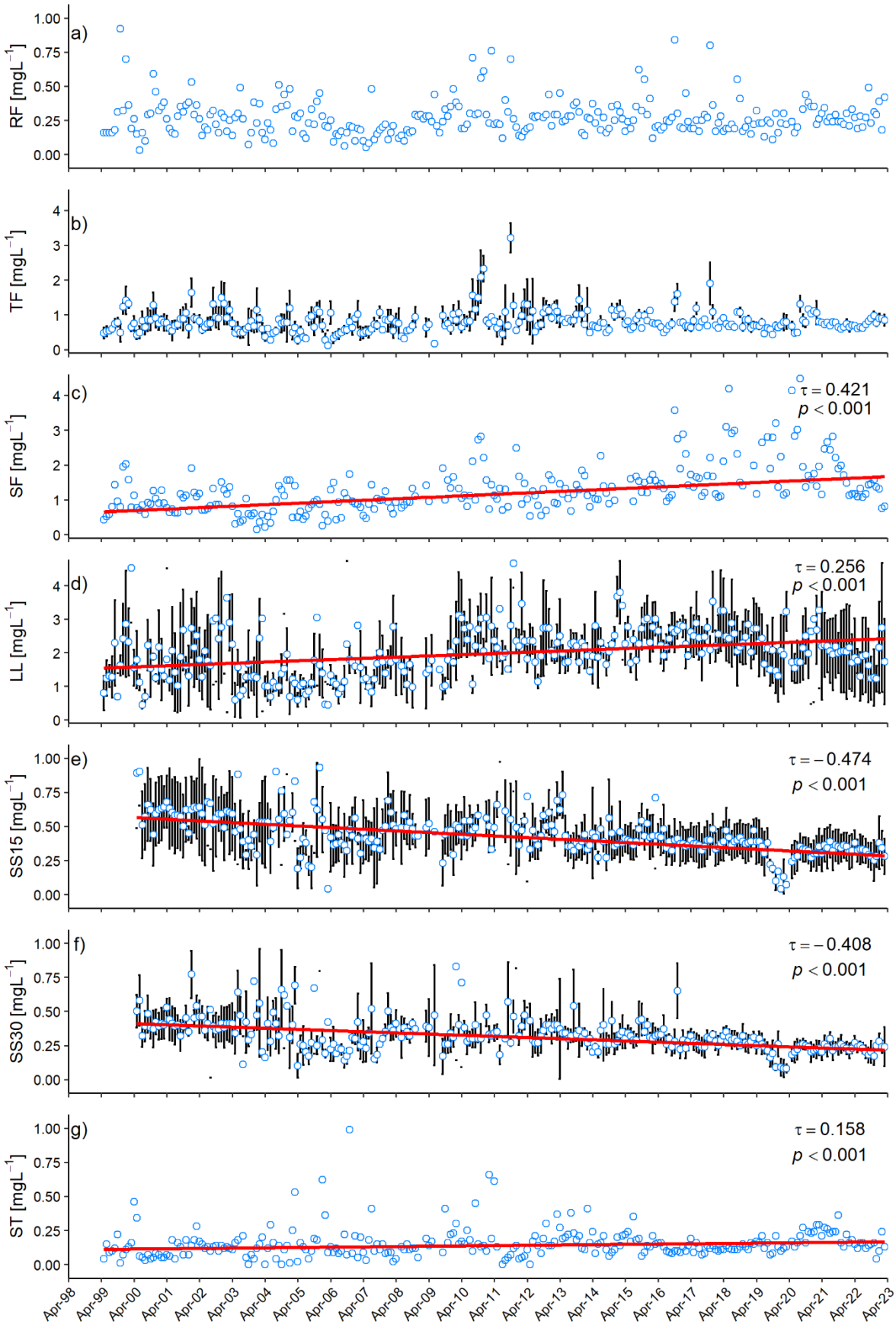

a)
RF [mgL^{-1}]
1.00
0.75
0.50
0.25
0.00
b)
TF [mgL^{-1}]
4
3
2
1
0
c)
SF [mgL^{-1}]
τ = 0.421
p < 0.001
d)
LL [mgL^{-1}]
τ = 0.256
p < 0.001
e)
SS15 [mgL^{-1}]
τ = −0.474
p < 0.001
f)
SS30 [mgL^{-1}]
τ = −0.408
p < 0.001
g)
ST [mgL^{-1}]
τ = 0.158
p < 0.001
Apr-98
Apr-99
Apr-00
Apr-01
Apr-02
Apr-03
Apr-04
Apr-05
Apr-06
Apr-07
Apr-08
Apr-09
Apr-10
Apr-11
Apr-12
Apr-13
Apr-14
Apr-15
Apr-16
Apr-17
Apr-18
Apr-19
Apr-20
Apr-21
Apr-22
Apr-23

Figure D-1. Temporal course of the mean monthly dissolved organic nitrogen (DON) concentrations in ecosystem solutions from April 1998 to March 2023. RF is rainfall, TF throughfall, SF stemflow, LL litter leachate, SS15 and SS30 mineral soil solutions at the 0.15 and 0.30 m depths, respectively, and ST streamflow. Error bars represent the standard deviations among one to four gauging stations for RF and three study transects for TF, LL, SS15, and SS30; there was only one measurement station for each of SF and ST. Temporal trends in monthly data were statistically evaluated with the Seasonal Mann-Kendall test (Hirsch et al., 1982). Regression lines are shown when there was a significant temporal trend for illustration purposes.

The DOP concentrations in throughfall, stemflow, and litter leachates and fluxes in throughfall and litter leachate increased significantly during the observation period (**Figures D-2 and D-S7**). The mean annual change rates of the DOP concentrations ranged from 1.6 to 5.0% of the median concentrations, while the fluxes increased annually by approximately 2% in both, throughfall and litter leachate (**Table D-S3**). Mind that DOP data were only available since 2003, i.e. for a period of 20 years. The contribution of DOP to TDP concentrations increased during the observation period in TF and SF by annually 2.2-2.3% of the median contribution, while there was no significant trend in LL (**Table D-S4**, **Figure D-S8**).

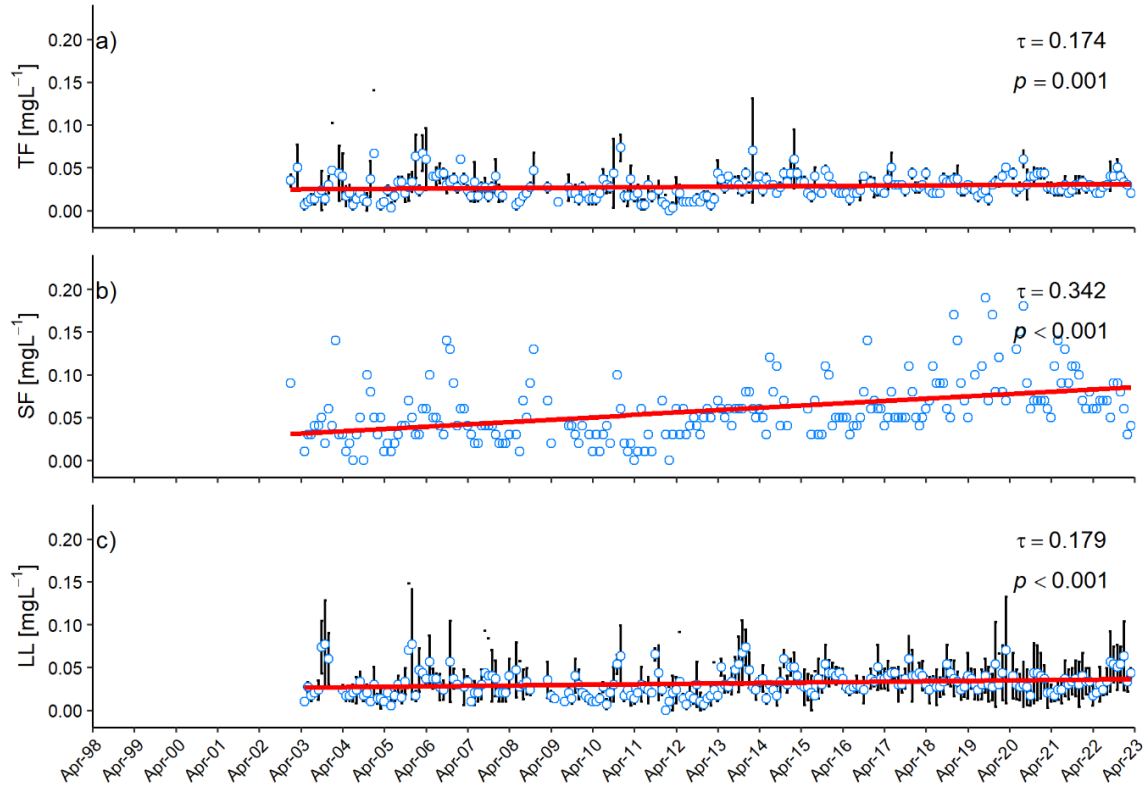


Figure D-2. Temporal course of the dissolved organic phosphorus (DOP) concentrations in throughfall (TF), stemflow (SF) and litter leachate (LL) from April 2003 to March 2023. Error bars represent the standard deviations among three study transects. There was only one measurement station for SF. Temporal trends in monthly data were statistically evaluated with the Seasonal Mann-Kendall test (Hirsch et al., 1982). Regression lines are shown when there was a significant temporal trend for illustration purposes.

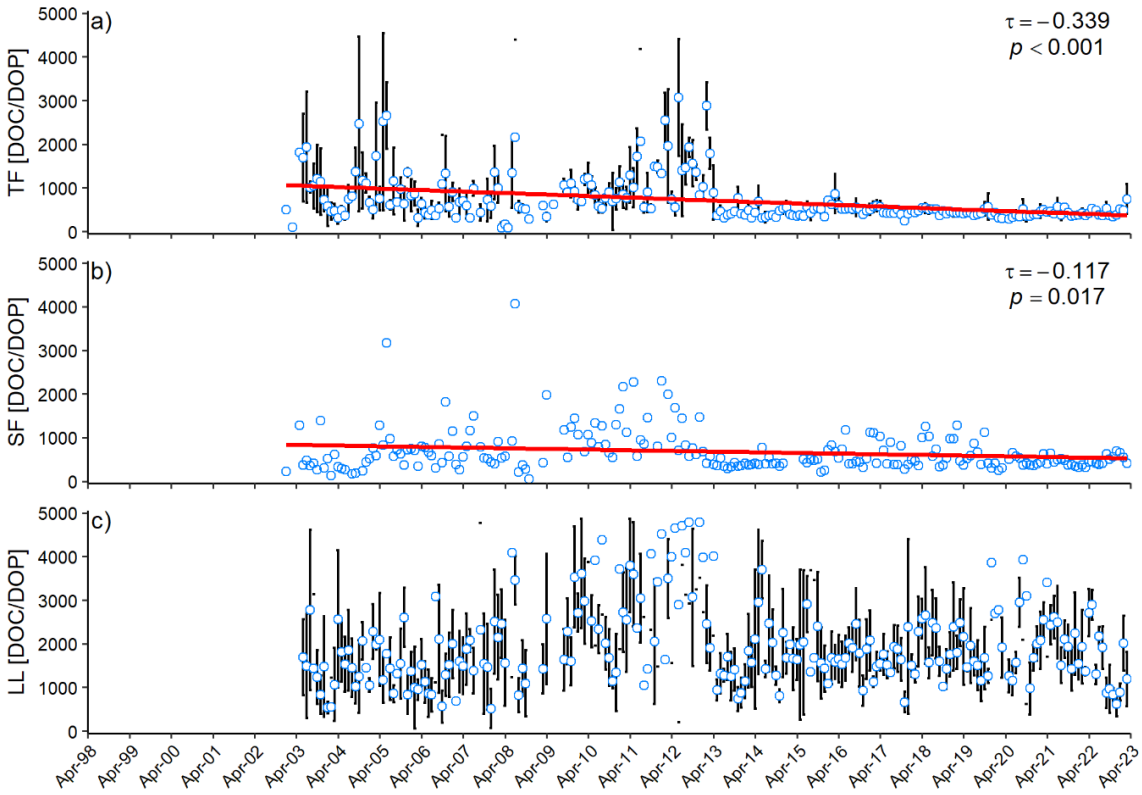


Figure D-3. Temporal course of the dissolved organic carbon to phosphorus concentrations ratio (DOC/DOP) in throughfall (TF), stemflow (SF) and litter leachate (LL) from April 2003 to March 2023. Error bars represent the standard deviations among three study transects. There was only one measurement station for SF. Temporal trends in monthly data were statistically evaluated with the Seasonal Mann-Kendall test (Hirsch et al., 1982). Regression lines are shown when there was a significant temporal trend for illustration purposes.

The mean monthly DOC/DOP ratios decreased significantly from April 2003 to March 2023 in TF and SF at an annual trend of -4.3 and -1.4% of the median DOC/DOP ratio and showed no trend in LL (**Table D-S3**, **Figure D-3**). The mean monthly DON/DOP ratios decreased significantly in TF by annually -1.1% of the median DON/DOP ratio but increased in LL by annually 1.5% (**Figure D-4**, **Table D-S3**). At the same time, LL showed a considerably higher DON/DOP ratio (82 ± 47, n = 240 months) than TF (34 ± 21).

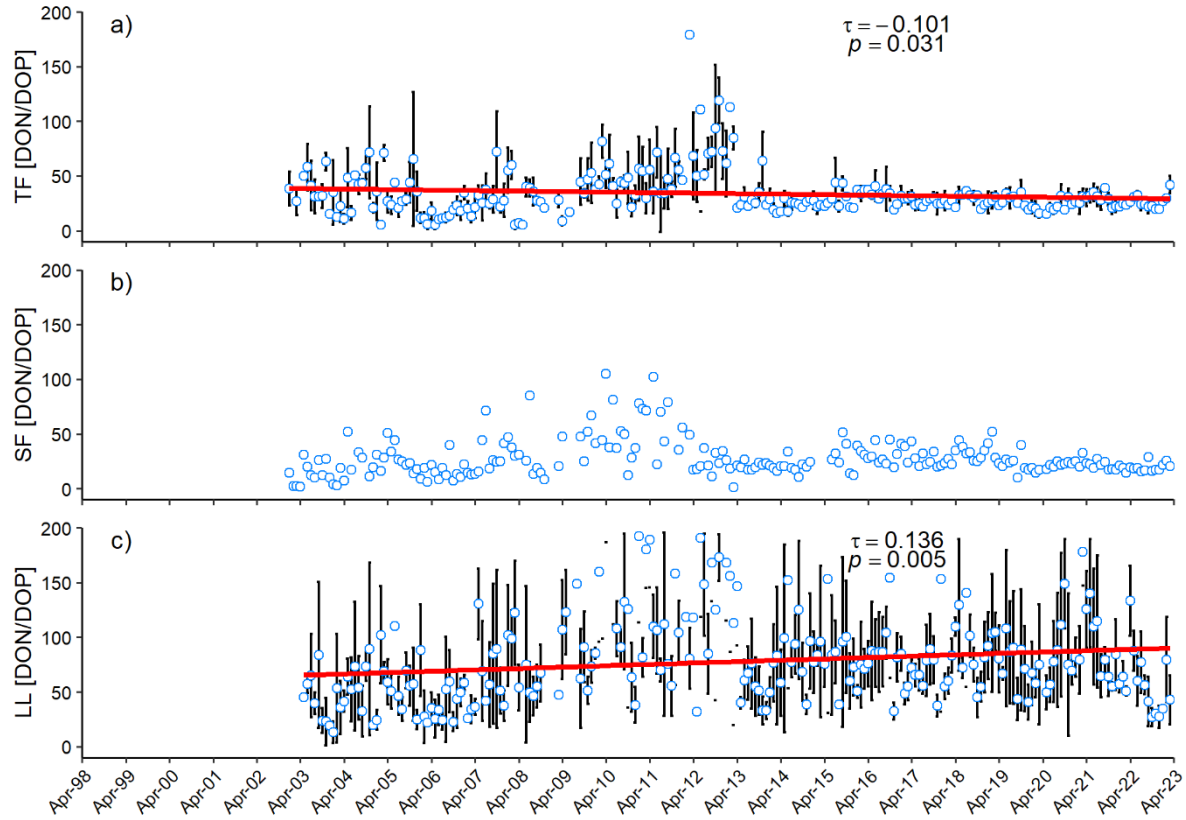


Figure D-4. Temporal course of dissolved organic nitrogen to dissolved organic phosphorus concentrations ratio (DON/DOP) in ecosystem solutions from April 2003 to March 2023. TF is throughfall, SF stemflow and LL litter leachate. Error bars represent the standard deviations from three study transects for TF and LL. There was only one measurement station for SF. Temporal trends in monthly data were statistically evaluated with the Seasonal Mann-Kendall test (Hirsch et al., 1982). Regression lines are shown when there was a significant temporal trend for illustration purposes.

Carbon and nitrogen stable isotope ratios ($\delta^{13}C$ and $\delta^{15}N$ values) showed a strong positive linear relationship across the solid samples, with C and N becoming isotopically heavier from litterfall via the organic layers to mineral soil horizons (**Figure D-5a**). The organic horizons exhibited increasing $\delta^{13}C$ and $\delta^{15}N$ values in the order Oi < Oe < Oa horizons, following the decomposition gradient of the organic matter. The mineral soil horizons A and B had the highest $\delta^{13}C$ and $\delta^{15}N$ values (**Figure D-5a**). In contrast, $\delta^{13}C$ and $\delta^{15}N$ values in ecosystem solutions formed two clusters consisting of the aboveground ecosystem solutions (rainfall, throughfall, stemflow) and the belowground ecosystem solutions (mineral soil solutions and streamflow), while rainfall deviated from all other solutions (**Figure D-5b**). Cluster 1 (left) has lower $\delta^{13}C$ values than Cluster 2 (right), while

the $\delta^{15}N$ values increased along the water paths in both clusters, i.e., throughfall < stemflow < litter leachate and soil solution at the 0.15 m depth < soil solution at the 0.3 m depth < streamflow. Rainfall showed both the highest $\delta^{13}C$ and $\delta^{15}N$ values of all solutions. The lack of a clear relationship between $\delta^{15}N$ values and C/N ratios of DOM in ecosystem solutions, similar to that reported for the relationship between $\delta^{13}C$ and C/N ratios values by (Alvarez et al., 2023), suggested that $\delta^{13}C$ and $\delta^{15}N$ values and C/N ratios of DOM carry different information (**Figure D-6**).

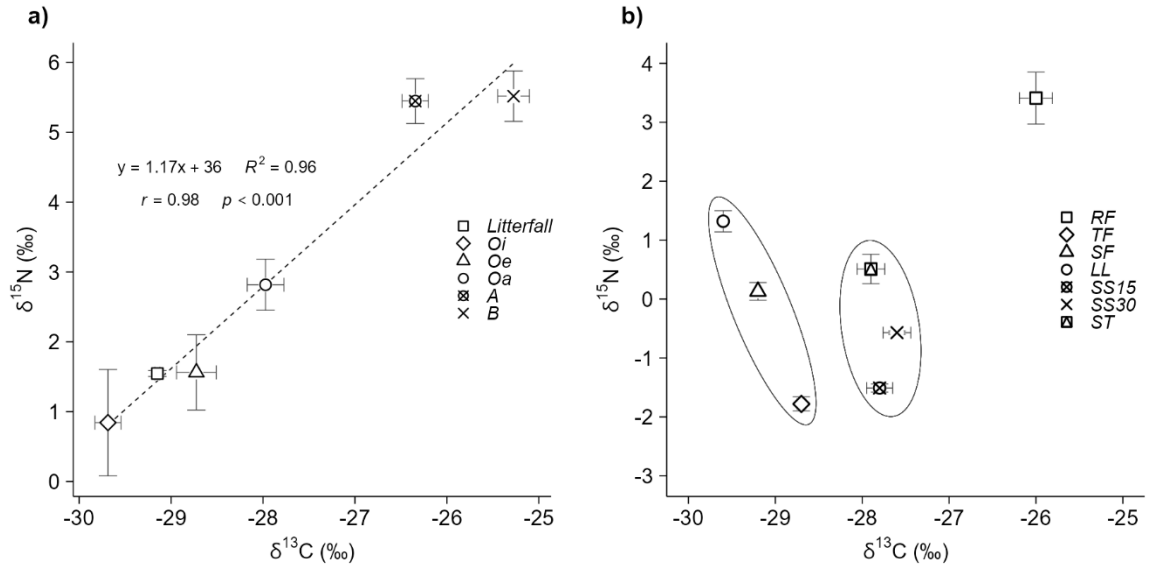


Figure D-5. Relationship between a) C and N stable isotope ratios ($\delta^{13}C$ and $\delta^{15}N$ values) in litterfall (n=48), organic and mineral soil horizons (n=21 soil profiles) from Microcatchment (MC) 2. Oi, Oe, and Oa are the three increasingly decomposed organic horizons, and A and B are the mineral soil horizons; and b) relationship between $\delta^{13}C$ and $\delta^{15}N$ values in dissolved organic matter. RF is rainfall, TF throughfall, SF stemflow, LL litter leachate, SS15 and SS30 mineral soil solutions at the 0.15 and 0.30 m depths, respectively, and ST streamflow (n = 48 monthly values for $\delta^{13}C$ and n = 16 quarterly values for $\delta^{15}N$). Error bars indicate the standard error. The $\delta^{13}C$ values are taken from Alvarez et al. (2023) and the $\delta^{15}N$ values from Alvarez et al. (2024a, 2024b).

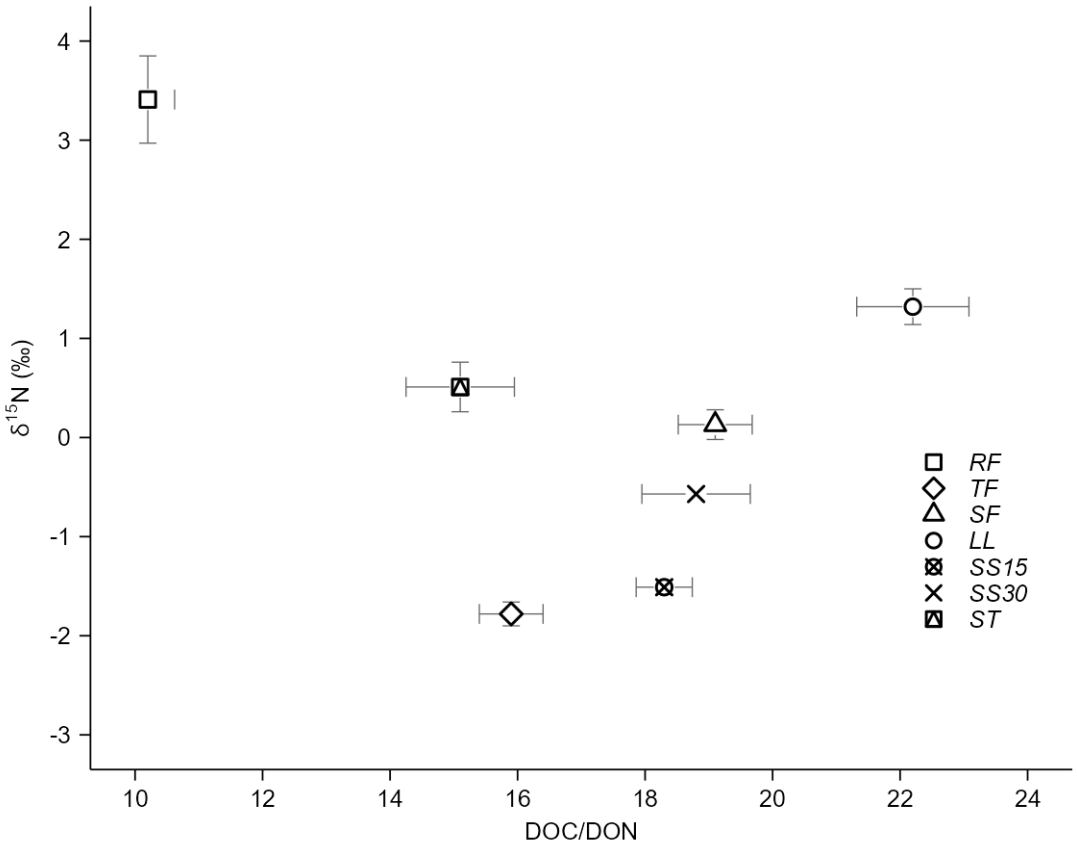


Figure D-6. Relationship between the mean DOC/DON ratios and the $\delta^{15}N$ values of DOM in ecosystem solutions, n = 48 monthly values for DOC and DON concentrations, n = 16 quarterly values for $\delta^{15}N$ values. RF is rainfall, TF throughfall, SF stemflow, LL litter leachate, SS15 and SS30 mineral soil solutions at the 0.15 and 0.30 m depths, respectively and ST streamflow. The error bars indicate standard errors. The $\delta^{15}N$ values of DOM are taken from Alvarez et al. (2024a).

5. Discussion

5.1. Temporal trends in DON and DOP concentrations and fluxes and DOC/DON and DOC/DOP ratios of DOM

The lack of a significant trend in the DON concentrations and fluxes in rainfall during the observation period (**Figures D-1 and D-S4**) is in line with the findings of Wilcke et al. (2013) for the first 11 years of the observation period who reported that the N cycle in the study area turns increasingly inorganic because dissolved inorganic N concentrations increased significantly in rainfall while those of DON remained stable. Although the DON concentrations and fluxes of the throughfall did not change significantly during the observation period (**Figure D-1**), the contribution of DON to TDN decreased significantly (**Table D-S4**, **Figure D-S5**), again in line with the previous report of Wilcke et al. (2013). Stemflow exhibited the strongest positive trend in DON concentrations and second strongest in DON fluxes of all solutions (**Table D-S3**, **Figures D-1 and D-S4**), reflecting the progressive enrichment of organic N during water contact with bark surfaces, bark-associated epiphytes, and accumulated dry-deposited material on tree stems (Van Stan & Pypker, 2015; Van Stan & Stubbins, 2018). Epiphytes, which are particularly abundant in this tropical montane forest (Werner et al., 2012), likely cycle increasingly more N from atmospheric deposition, foliar leachates, and bark substrates (Inselsbacher et al., 2007; Song et al., 2016; Umana & Wanek, 2010) which could have contributed to an increasing DON release into the stemflow under increasing atmospheric N inputs (Boy et al., 2008a). The DON concentrations and fluxes in litter leachate also showed a significant positive trend from 1999 to 2023, likely attributable to the progressive increase in N availability in the organic layer through sustained atmospheric N deposition. Together with a reduction of waterlogging periods and thus enhanced organic matter mineralization because of drier soil conditions (Wilcke et al., 2013), the improved nutrient availability likely stimulated microbial activity and promoted the release of organic N from the decomposing organic horizons (Kalbitz et al., 2000; Silver et al., 1999; Velescu et al., 2016). Conversely, DON concentrations and fluxes in both mineral soil solutions showed strong negative trends. This indicated that in contrast to the organic layer, where DON production was stimulated, in the much nutrient-poorer mineral soil, the DON served as nutrient source for the microorganisms (Schwarz et al., 2011; Wilcke et al., 2020). Alternatively, increasing sorption of DON to the mineral surface could have contributed to the decreasing DON concentrations during the observation period (Alvarez et al., 2024c; Michalzik et al., 2001).

There might have been an increasing formation of Fe(III) oxides and thus more DON sorption because of the reduction in waterlogging periods (Wilcke et al., 2013), which could have resulted in more oxidative conditions (Hall & Silver, 2013). In contrast to the mineral soil solutions and similar to the aboveground ecosystem solutions, DON concentrations and fluxes in streamflow showed a positive trend, illustrating an increase of DON export from the catchment in spite of decreasing DON concentrations and fluxes in the mineral soil solutions. We attribute this finding to a higher frequency of strong rain events which likely resulted in more frequent surface-near lateral flow through the DON-rich organic layer into the stream (Boy et al., 2008b; Goller et al., 2005; Raymond & Saiers, 2010).

The fact that the highest DOP concentrations were found in throughfall, stemflow, and litter leachate, while we were unable to quantify the DOP concentrations in rainfall, mineral soil solutions, and streamflow throughout the entire observation period (**Figure D-2**; **Table D-S1**), indicated that DOP cycling at this site was primarily governed by processes occurring in the forest canopy, on bark surfaces, and in the organic layer with negligible transfer of DOP to deeper soil horizons or to stream water during the observation period of 20 years (2003-2023). This is in agreement with previous observations at the study site and elsewhere (Goller et al., 2006; Kalbitz et al., 2000; Wilcke et al., 2019). The reason is likely that microbial decomposition, litter inputs, and phosphatase activity, which are the primary DOP-generating processes (Bol et al., 2016; Kalbitz et al., 2000; Schaap et al., 2021), are elevated in the aboveground part of the ecosystem. Moreover, DOP is strongly sorbed to the mineral soil (Kalbitz et al., 2000; Qualls et al., 2002). All three ecosystem solutions in which DOP could be reliably determined (throughfall, stemflow, and litter leachate) showed significant positive trends in DOP concentrations and in throughfall and litter leachate also in DOP fluxes (**Table D-S3**, **Figure D-2**), while at the same time the contributions of DOP to TDP increased significantly in throughfall and stemflow (**Table D-S4**, **Figure D-S8**), suggesting enhanced DOP production and release over time. The increasing DOP concentrations and fluxes were likely driven by the cumulative enrichment of the canopy P pool through atmospheric P deposition, including Saharan dust and fire-derived P inputs from Amazonian biomass burning (Bauters et al., 2021; Wilcke et al., 2019; Yu et al., 2015), enhancing biological P cycling (Goller et al., 2006; Van Langenhove et al., 2020; Van Stan & Stubbins, 2018). A similar progressive accumulation of atmospheric P in the canopy was observed by Runyan et al. (2013) in southern Mexico. Increasing DOP concentrations and fluxes in litter leachate could be attributed to enhanced microbial activity in the organic layer under greater

N and P availability, which has been observed in our study area (Dietrich et al., 2017; Velescu et al., 2016) and in tropical forest soils of the Central Amazon (Schaap et al., 2021). The lack of a significant trend in the DOP fluxes with stemflow from 2003-2023 in spite of a significant increase in DOP concentrations is attributable to decreasing water fluxes with stemflow (Kendall's τ=-0.142, $p < .001$).

Similar to the DOC/DON ratios that decreased in all ecosystem solutions significantly from 1998-2023 in line with the previous findings of Wilcke et al. (2020; **Figure D-S6**), the DOC/DOP ratio showed significant negative trends from 2003-2023 in throughfall and stemflow (**Figure D-3**), reflecting a progressive enrichment of organic P relative to C in the canopy-derived DOM. This pattern is consistent with the increasing accumulation of P from atmospheric deposition (Bauters et al., 2021; Wilcke et al., 2019). It also agrees with reports that an increasing P availability enriches canopy and bark leachates in organic P relative to C in tropical forests (Runyan et al., 2013; Van Langenhove et al., 2020; Van Stan & Stubbins, 2018). Overall, the first part of our first hypothesis is only partly supported, because rainfall and throughfall did not show temporal trends in DON concentrations and fluxes while the mineral soil solutions even showed negative trends in DON concentrations. The second part of our first hypothesis is largely supported because DOC/DON and DOC/DOP ratios consistently decreased in all ecosystem solutions with the only exception that the DOC/DOP ratio in litter leachate did not show a significant trend.

5.2. Temporal trend in DON/DOP ratios of DOM in ecosystem solutions

The finding that the DON/DOP ratios in throughfall showed a significant negative trend from 2003 to 2023 (**Table D-S3**, **Figure D-4**) is in contrast to the expectation of an increasing N/P ratio in the leaves in response to increasing P limitation (Ostertag & DiManno, 2016). The reason for this result may be that P can generally be more readily leached from the canopy than N as indicated by the results of a N and P fertilization experiment in the San Francisco Biological Reserve near to our study site, in which N was still retained in the canopy after five years, while P was leached in all treatments (amendment of N, N+P, P, and Ca twice yearly) and in the control (Velescu et al., 2026). Our assumption of a stronger DOP than DON leaching from the canopy is supported by Qualls (2000) and Fetzer et al. (2022), who showed that DOP is generally more soluble than DON. We suggest that the sustained atmospheric P deposition and consequent P accumulation in the canopy of our study forest (Wilcke et al., 2019) progressively increased leachable DOP concentrations.

In contrast, the significant positive trend in the DON/DOP ratios in litter leachate (**Table D-S3**, **Figure D-4**) agrees with the assumption of an increasingly tighter P than N cycling by the ecosystem (Lang et al., 2017), because litter leachate represents a loss from the main root zone (Moser et al., 2011; Soethe et al., 2006). This finding is consistent with reports that N/P ratios in ecosystem fluxes of tropical forests increased with sustained atmospheric N deposition (Jiang et al., 2024; Zhou et al., 2018) and supports our second hypothesis. This assumption is further corroborated by the higher DON/DOP ratio in litter leachate than in throughfall and stemflow likely reflecting a stronger P than N retention in the soil organic layer (Fetzer et al., 2022; Wilcke et al., 2019).

5.3. Relationship between the $\delta^{13}C$ and $\delta^{15}N$ values in solid phases of the ecosystem and dissolved organic matter

The $\delta^{13}C$ and $\delta^{15}N$ values in the solid phases of the ecosystem correlated closely with each other across all sampled materials (**Figure D-5a**), with both elements becoming progressively isotopically heavier in the order, litterfall < Oi < Oe < Oa < A < B horizons. This coupled increase of the $\delta^{13}C$ and $\delta^{15}N$ values with increasing degree of decomposition is consistent with the well-established fractionation of both isotopes during microbial processing of organic matter, whereby isotopically light compounds are preferentially mineralized and respired, leaving behind an increasingly ^{13}C- and ^{15}N-enriched residual organic matter pool (Boström et al., 2007; Lorenz et al., 2020; Soldatova et al., 2024). The strong co-variation of $\delta^{13}C$ and $\delta^{15}N$ along the decomposition gradient from litterfall to the mineral soil horizons indicates that the isotopic enrichment was primarily governed by coupled C and N transformation processes as had been reported earlier (Nel et al., 2018). Our finding is also consistent with the significant relationships among the $\delta^{13}C$ values, $\delta^{15}N$ values, C/N, and O/C ratios reported for other forest soils (Gerschlauer et al., 2019; Lorenz et al., 2020).

The absence of an overall linear correlation between the $\delta^{13}C$ and $\delta^{15}N$ values in DOM of the ecosystem solutions indicates that the relationship between the $\delta^{13}C$ and $\delta^{15}N$ values is not only driven by the coupled C and N turnover (**Figure D-5b**). Instead, we suggest that the observed clustering reflects the combination of source mixing and transformation of DOM rather than a single controlling process (Alvarez et al., 2023; Schwarz et al., 2011). The higher $\delta^{13}C$ values in the mineral soil solutions and streamflow relative to the aboveground solutions are likely attributable to the preferential sorption of ^{13}C-depleted

hydrophobic DOM components onto mineral surfaces and to the preferential mineralization of isotopically light compounds during passage through the mineral soil. Moreover, root exudates and root litter likely contributed ^{13}C-enriched DOM in the mineral soil (Alvarez et al., 2023; Kalbitz et al., 2000; Wilcke et al., 2020). The increase in the $\delta^{15}N$ values along the water path within both clusters can be explained by the N transformation processes identified earlier (Alvarez et al., 2024c). In the aboveground cluster, the canopy retained isotopically heavy N and leached isotopically lighter N. From throughfall via stemflow to litter leachate the $\delta^{15}N$ values increased again because of the progressive contribution of N-isotopically heavier DON. In the belowground cluster, the increase in $\delta^{15}N$ values from the mineral soil solutions to streamflow reflected the loss of isotopically light gaseous N by increasing denitrification (Alvarez et al., 2024c). Thus, N-specific processes, rather than the coupled C and N fractionation during organic matter turnover that governed the solid phases, controlled the $\delta^{15}N$ values of the ecosystem solutions (Alvarez et al., 2024c). Our results therefore support our third hypothesis only for the solid phases but not for the ecosystem solutions.

The absence of a clear relationship between DOC/DON ratios and $\delta^{15}N$ values across ecosystem solutions (**Figure D-6**) indicated that the C:N stoichiometry and the N isotope composition of DOM carry different and complementary information about DOM sources and transformations along the water flow path, in line with the previous report of Alvarez et al. (2023) that $\delta^{13}C$ values of DOM provide an additional and largely independent tool to assess DOM dynamics in this tropical montane forest ecosystem, so that the part of our third hypothesis referring to the $\delta^{15}N$-DOC/DON relationship must be rejected.

6. Conclusions

During our 25-yr observation period, DON and DOP concentrations and fluxes increased in most ecosystem solutions, while those of DOC decreased, likely reflecting a generally increasing nutrient richness in the studied forest because of N and P deposition from the atmosphere. However, DON concentrations and fluxes decreased in the mineral soil solutions during the observations period presumably because of increasing retention and decomposition so that the first part of our first hypothesis is only partly supported. The likely increasing nutrient richness could also explain consistently decreasing DOC/DON and DOC/DOP ratios in all ecosystem solutions during the observation period with the only exception of the DOC/DOP ratios in litter leachate showing no trend. Thus, the second part

of our first hypothesis is largely supported. We were, however, unable to reliably quantify the DOP concentrations in rainfall, the mineral soil solutions, and streamflow.

Our results revealed contrasting temporal trends in the DON/DOP ratios among the three aboveground ecosystem solutions in which we were able to quantify DOP concentrations from 2003 to 2023 so that our second hypothesis is only partly supported. We attribute decreasing DON/DOP ratios in throughfall against our expectations to a stronger retention of N than P in the canopy. The increasing DON/DOP ratios in the litter leachate, however, agree with the assumption of a stronger P than N retention in the forest supporting a possible shift from the current N+P colimitation of plant growth to a pure P limitation.

Our results only confirmed the first part of our third hypothesis for the solid phases, as $\delta^{13}C$ and $\delta^{15}N$ values of organic matter showed a strong positive linear correlation across all sampled materials. Both elements became progressively isotopically heavier from litterfall through the organic to the mineral soil horizons, because of the coupling of the C and N cycles via organic matter turnover. In contrast, the second part of the third hypothesis must be rejected because the relationship between $\delta^{13}C$ and $\delta^{15}N$ values of DOM reflected the combined influence of source mixing and DOM transformation rather than a single controlling process. Finally, the $\delta^{15}N$ values of the ecosystem solutions did not correlate with the DOC/DON ratios illustrating that $\delta^{15}N$ values and DOC/DON ratios of DOM carry different information.

Overall, our study emphasizes that the C, N, and P cycling of the humid tropical montane forests on the rim of the Amazon basin underwent significant changes during the 25-yr observation period with unknown consequences for the plant species richness, the C storage, and the nutrient concentrations in the headwater streams.

7. Acknowledgments

We thank the German Research Foundation (DFG) for funding our research in Ecuador (FOR 402, FOR 816, PAK 823-825, FOR 2730), Naturaleza y Cultura Internacional (NCI) in Loja for providing access to the study area and to the research station, and the Ecuadorian Ministry of Environment for the research permits. We thank Felix Matt and Jörg Zeilinger for their support at the research station, J. Boy, K. Fleischbein, R. Goller, M. Meyer-Grünefeldt, A. Rehmus, M. Sequeira, H. Wullaert, S. Yasin and numerous undergraduate students for data acquisition during parts of the observation period, José Luis Peña

Caivinagua and Jimmy Alexander Villalta Vaca for their dedicated assistance as field technicians, and Tobias Fabian for his valuable contribution to the field and laboratory analyses. Pablo Alvarez received a four-year scholarship from the Secretary of Higher Education, Science, Technology and Innovation of Ecuador (SENESCYT), Grant No. CA07-000439-2018.

8. Supporting information

Table D-S1. Mean (± standard deviation, n = 20 yr for DOP, n = 24 yr for DON and n = 25 yr for DOC) annual dissolved organic carbon (DOC), nitrogen (DON), and phosphorus (DOP) concentrations, and DOC/DON and DOC/DOP ratios in dissolved organic matter of ecosystem solutions along the water path through the ecosystem. Lowercase letters indicate significant differences ($p < .05$) among the ecosystem solutions according to a Tukey's HSD post hoc test following two-factor analysis of variance (ANOVA) with year and solution type as fixed factors and sequential (Type I) sum of squares. n.d., not detected with our method.

Ecosystem solutions	DOC mg L^{-1}	DON mg L^{-1}	DOP mg L^{-1}	DOC/DON	DOC/DOP
Rainfall	3.8 (±2.0) a	0.28 (±0.17) b	n.d.	31.4 (±13.6) c	-
Throughfall	13.8 (±4.6) c	0.81 (±0.32) e	0.032 (±0.007) a	21.7 (±11.2) a	710 (±509) a
Stemflow	30.1 (±28.8) d	1.40 (±1.01) f	0.067 (±0.033) b	24.6 (±12.5) ab	720 (±702) a
Litter leachate	44.6 (±12.5) e	2.00 (±0.75) g	0.032 (±0.009) a	26.3 (±9.7) b	2025 (±1016) b
Soil solution at 0.15 m	10.4 (±4.1) b	0.45 (±0.16) d	n.d.	26.8 (±14.3) b	-
Soil solution at 0.30 m	7.1 (±2.7) ab	0.34 (±0.15) c	n.d.	26.4 (±14.8) b	-
Streamflow	3.4 (±2.4) a	0.16 (±0.12) a	n.d.	29.7 (±28.3) c	-

Table D-S2. Kendall's τ, p values, and Sen's slopes of the seasonal Mann-Kendall trend test for the mean monthly dissolved organic carbon (DOC) concentrations and fluxes from April 1998 to March 2023 and DOC/DON ratios in dissolved organic matter (DOM) from April 1999 to March 2023 in ecosystem solutions (related to Figures D-S2, D-S3, and D-S6). Trends were assessed with the seasonal Mann-Kendall test (Hirsch et al., 1982), implemented in the function kendallSeasonalTrendTest of the EnvStats package (Millard, 2013). Significant trends are shown in bold. The seasonal Sen's slopes are referred to the overall median concentrations of the whole observation period. RF, rainfall; TF, throughfall; SF, stemflow; LL, litter leachate; SS15 and SS30, soil solution at the 0.15 and 0.3 m mineral soil depth, respectively; ST, streamflow.

Solution	τ	p	Seasonal Sen's slope	Slope (%/year)	Slope (% over period)
			DOC concentrations		
RF	**−0.350**	**<0.001**	**−0.11**	**−3.2%**	**−80%**
TF	**−0.292**	**<0.001**	**−0.14**	**−1.2%**	**−29%**
SF	**0.364**	**<0.001**	**0.74**	**+3.2%**	**+81%**
LL	**0.209**	**<0.001**	**0.47**	**+1.1%**	**+27%**
SS15	**−0.666**	**<0.001**	**−0.43**	**−4.8%**	**−120%**
SS30	**−0.676**	**<0.001**	**−0.28**	**−4.3%**	**−107%**
ST	**−0.357**	**<0.001**	**−0.09**	**−3.3%**	**−82%**
			DOC fluxes		
RF	**−0.325**	**<0.001**	**−19**	**−3.4%**	**−86%**
TF	**−0.170**	**<0.001**	**−19**	**−1.3%**	**−34%**
SF	**0.156**	**<0.001**	**0.94**	**+2.1%**	**+51%**
LL	**0.156**	**<0.001**	**52**	**+1.3%**	**+33%**
SS15	**−0.480**	**<0.001**	**−36**	**−4.5%**	**−113%**
SS30	**−0.514**	**<0.001**	**−23**	**−4.3%**	**−107%**
ST	**−0.151**	**<0.001**	**−3.4**	**−1.6%**	**−40%**
			DOC/DON ratios in DOM		
RF	**−0.499**	**<0.001**	**−1.2**	**−4.7%**	**−113%**
TF	**−0.334**	**<0.001**	**−0.36**	**−2.1%**	**−50%**
SF	**−0.102**	**0.023**	**−0.11**	**−0.5%**	**−12%**
LL	**−0.231**	**<0.001**	**−0.27**	**−1.2%**	**−28%**
SS15	**−0.285**	**<0.001**	**−0.36**	**−1.7%**	**−40%**
SS30	**−0.302**	**<0.001**	**−0.39**	**−1.8%**	**−43%**
ST	**−0.483**	**<0.001**	**−1.2**	**−6.5%**	**−156%**

Table D-S3. Kendall's τ, p values, and Sen's slopes of the seasonal Mann-Kendall trend test for the mean monthly dissolved organic nitrogen (DON) and dissolved organic phosphorus (DOP) concentrations and fluxes and DOC/DOP and DON/DOP ratios in dissolved organic matter (DOM) in ecosystem solutions from April 1999 for DON and April 2003 for DOP to March 2023 (related to Figures D-1 to D-4, D-S4, and D-S7). Trends were assessed with the seasonal Mann-Kendall test (Hirsch et al., 1982), implemented in the function kendallSeasonalTrendTest of the EnvStats package (Millard, 2013). Significant trends are shown in bold. The seasonal Sen's slopes are referred to the overall median concentrations of the whole observation period. RF, rainfall; TF, throughfall; SF, stemflow; LL, litter leachate; SS15 and SS30, soil solution at the 0.15 and 0.3 m mineral soil depth, respectively; ST, streamflow; n.a. is not applicable, because if the trend was not significant, we did not calculate a seasonal Sen's slope.

Ecosystem solution	τ	p	Seasonal Sen's slope	Slope (%/year)	Slope (% total period)
			DON concentrations		
RF	0.051	0.234	n.a.	n.a.	n.a.
TF	0.041	0.336	n.a.	n.a.	n.a.
SF	**0.421**	**<0.001**	**0.042**	**+3.6%**	**+87%**
LL	**0.256**	**<0.001**	**0.037**	**+1.8%**	**+44%**
SS15	**−0.474**	**<0.001**	**−0.012**	**−2.9%**	**−70%**
SS30	**−0.408**	**<0.001**	**−0.0085**	**−2.7%**	**−65%**
ST	**0.158**	**<0.001**	**0.0023**	**+1.6%**	**+39%**
			DON fluxes		
RF	0.080	0.056	n.a.	n.a.	n.a.
TF	0.048	0.257	n.a.	n.a.	n.a.
SF	**0.201**	**<0.001**	**0.061**	**+2.7%**	**+65%**
LL	**0.251**	**<0.001**	**4.441**	**+2.6%**	**+62%**
SS15	**−0.308**	**<0.001**	**−0.974**	**−2.7%**	**−65%**
SS30	**−0.286**	**<0.001**	**−0.687**	**−2.6%**	**−62%**
ST	**0.249**	**<0.001**	**0.341**	**+3.0%**	**+72%**
			DOP concentrations		
TF	**0.175**	**<0.001**	**0.00042**	**+1.6%**	**+31%**
SF	**0.342**	**<0.001**	**0.0025**	**+5.0%**	**+100%**
LL	**0.179**	**<0.001**	**0.00049**	**+1.6%**	**+32%**
			DOP fluxes		
TF	**0.157**	**0.001**	**0.059**	**+2.1%**	**+41%**
SF	0.048	0.361	n.a.	n.a.	n.a.
LL	**0.151**	**0.002**	**0.050**	**+1.9%**	**+38%**
			DOC/DOP ratios in DOM		
TF	**−0.339**	**<0.001**	**−22.0**	**−4.3%**	**−86%**

Ecosystem solution	τ	p	Seasonal Sen's slope	Slope (%/year)	Slope (% total period)
SF	**−0.117**	**0.017**	**−7.4**	**−1.4%**	**−28%**
LL	0.047	0.339	n.a.	n.a.	n.a.
			DON/DOP ratios in DOM		
TF	**−0.101**	**0.031**	**−0.33**	**−1.1%**	**−23%**
SF	0.024	0.668	n.a.	n.a.	n.a.
LL	**0.136**	**0.005**	**1.1**	**+1.5%**	**+30%**

Table D-S4. Kendall's τ, p-values, and Sen's slopes of the seasonal Mann-Kendall trend test for the dissolved organic nitrogen (DON) contribution to total dissolved nitrogen (TDN) in ecosystem solutions from April 1999 to March 2023 (related to Figure D-S5) and dissolved organic phosphorus (DOP) contributions to total dissolved P (TDP) from April 2003 to March 2023. DOP was not detected in rainfall, the mineral soil solutions, and streamflow. Trends were assessed with the seasonal Mann-Kendall test (Hirsch et al., 1982), implemented in the function kendallSeasonalTrendTest of the EnvStats package (Millard, 2013). Significant trends are shown in bold. The seasonal Sen's slopes are referred to the overall median concentrations of the whole observation period. RF, rainfall; TF, throughfall; SF, stemflow; LL, litter leachate; SS15 and SS30, soil solution at the 0.15 and 0.3 m mineral soil depth, respectively; ST, streamflow; n.a. is not applicable, because if the trend was not significant, we did not calculate a seasonal Sen's slope.

Solution	τ	p	Seasonal Sen's slope	Slope (%/year)	Slope (% over period)
			DON contribution to TDN		
RF	**−0.502**	**<0.001**	**−1.278**	**−4.8%**	**−115%**
TF	**−0.197**	**<0.001**	**−0.432**	**−1.2%**	**−29%**
SF	0.052	0.264	n.a.	n.a.	n.a.
LL	−0.029	0.476	n.a.	n.a.	n.a.
SS15	**−0.335**	**<0.001**	**−0.871**	**−2.2%**	**−53%**
SS30	**−0.274**	**<0.001**	**−0.680**	**−1.8%**	**−43%**
ST	**−0.389**	**<0.001**	**−1.358**	**−5.3%**	**−128%**
			DOP contribution to TDP		
TF	**0.163**	**<0.001**	**0.272**	**+2.2%**	**+43%**
SF	**0.129**	**0.009**	**0.333**	**+2.3%**	**+46%**
LL	0.014	0.796	n/a	n/a	n/a

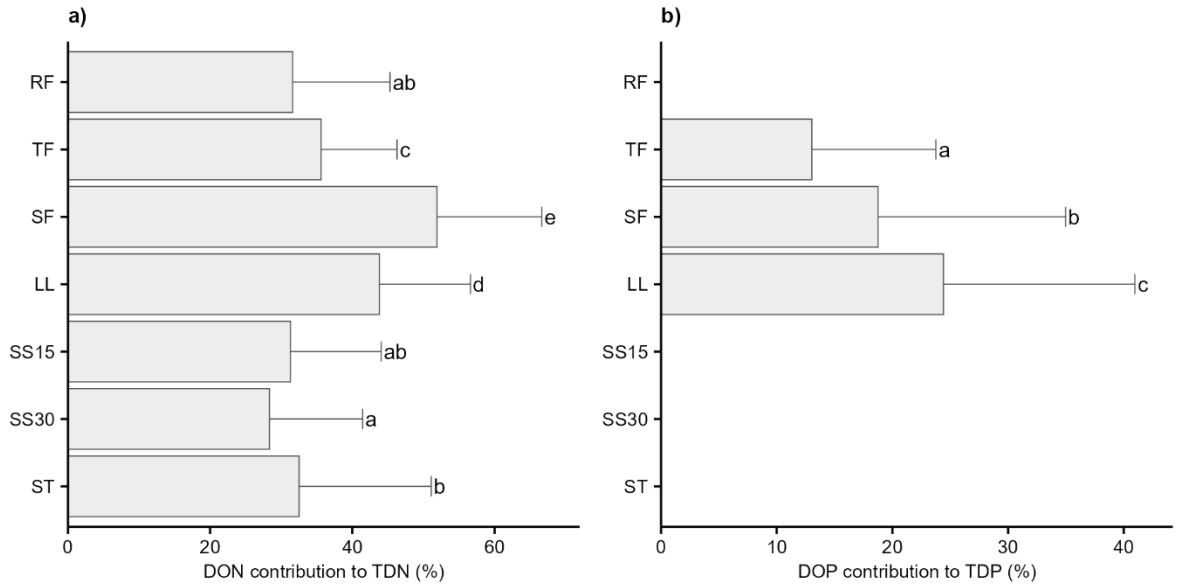


Figure D-S1. Vertical distribution of the a) dissolved organic nitrogen (DON) contribution to the total dissolved nitrogen (TDN) concentrations and b) dissolved organic phosphorus (DOP) contribution to total dissolved phosphorus (TDP) concentrations, based on mean monthly concentrations from April 1999 to March 2023 for DON and April 2003 to March 2023 for DOP. RF is rainfall, TF throughfall, SF stemflow, LL litter leachate, SS15 and SS30 mineral soil solutions at the 0.15 and 0.30 m depths, respectively, and ST streamflow. Error bars represent the standard deviations among 24 years for DON (1999-2023) and 20 years for DOP (2003-2023). Lower case letters indicate significant differences ($p < .05$) among the ecosystem solutions according to a Tukey's HSD post hoc test following two-factor analysis of variance (ANOVA) with year and solution type as fixed factors.

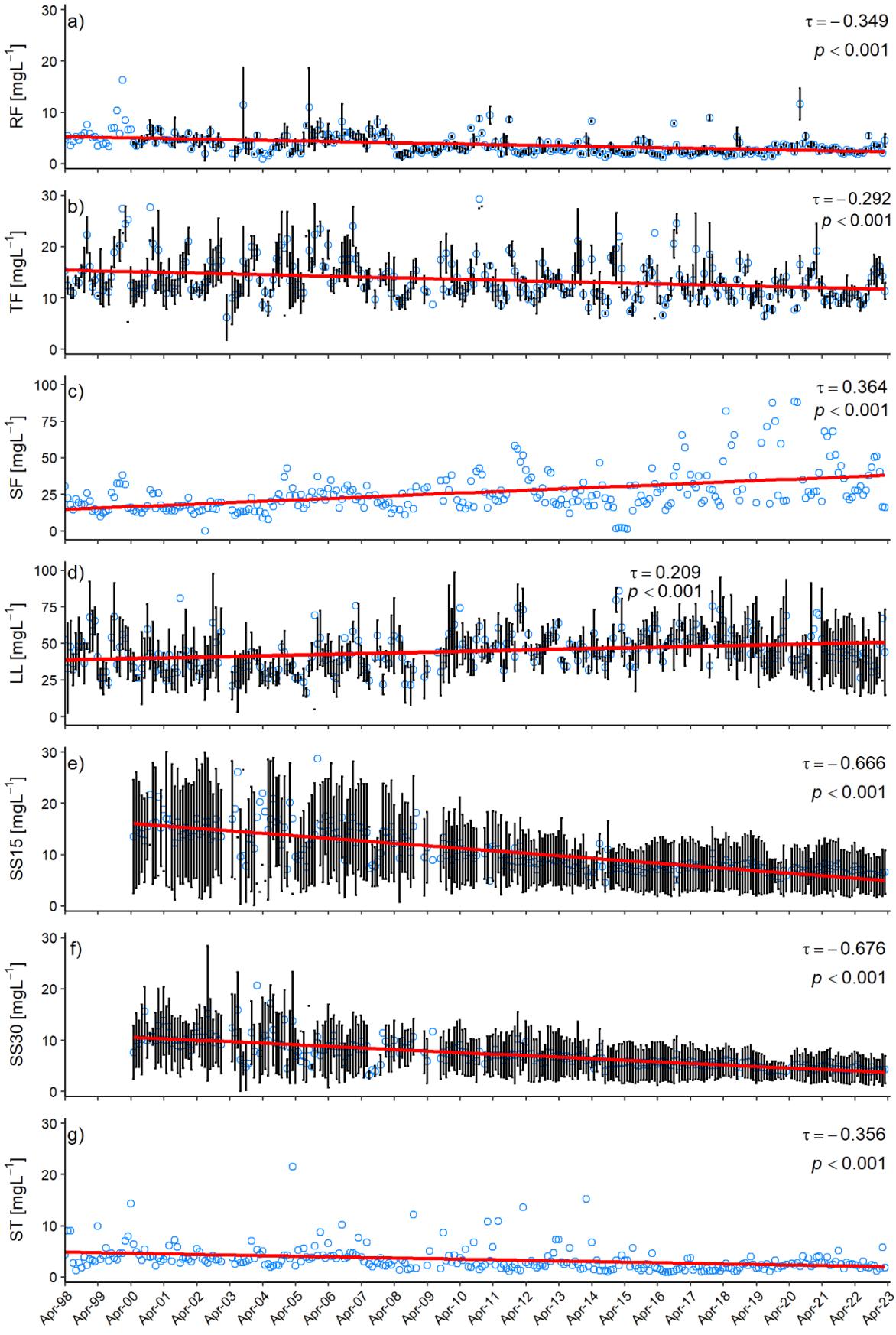

a)
τ = −0.349
p < 0.001
RF [mgL−1]
b)
τ = −0.292
p < 0.001
TF [mgL−1]
c)
τ = 0.364
p < 0.001
SF [mgL−1]
d)
τ = 0.209
p < 0.001
LL [mgL−1]
e)
τ = −0.666
p < 0.001
SS15 [mgL−1]
f)
τ = −0.676
p < 0.001
SS30 [mgL−1]
g)
τ = −0.356
p < 0.001
ST [mgL−1]
Apr-98
Apr-99
Apr-00
Apr-01
Apr-02
Apr-03
Apr-04
Apr-05
Apr-06
Apr-07
Apr-08
Apr-09
Apr-10
Apr-11
Apr-12
Apr-13
Apr-14
Apr-15
Apr-16
Apr-17
Apr-18
Apr-19
Apr-20
Apr-21
Apr-22
Apr-23

Figure D-S2. Course of mean monthly dissolved organic carbon (DOC) concentrations in ecosystem solutions from April 1998 to March 2023. RF is rainfall, TF throughfall, SF stemflow, LL litter leachate, SS15 and SS30 mineral soil solutions at the 0.15 and 0.30 m depths, respectively, and ST streamflow. Error bars represent the standard deviations from two to four gauging stations for RF and from three study transects for TF, LL, SS15, and SS30, whereas there was only one measurement station for each of SF and ST. The regression lines are shown only to illustrate significant trends. Please note the different y-axis scaling for SF, ST and LL. Temporal trends in monthly data were statistically evaluated with the Seasonal Mann-Kendall test (Hirsch et al., 1982). Regression lines are shown when there was a significant temporal trend for illustration purposes.

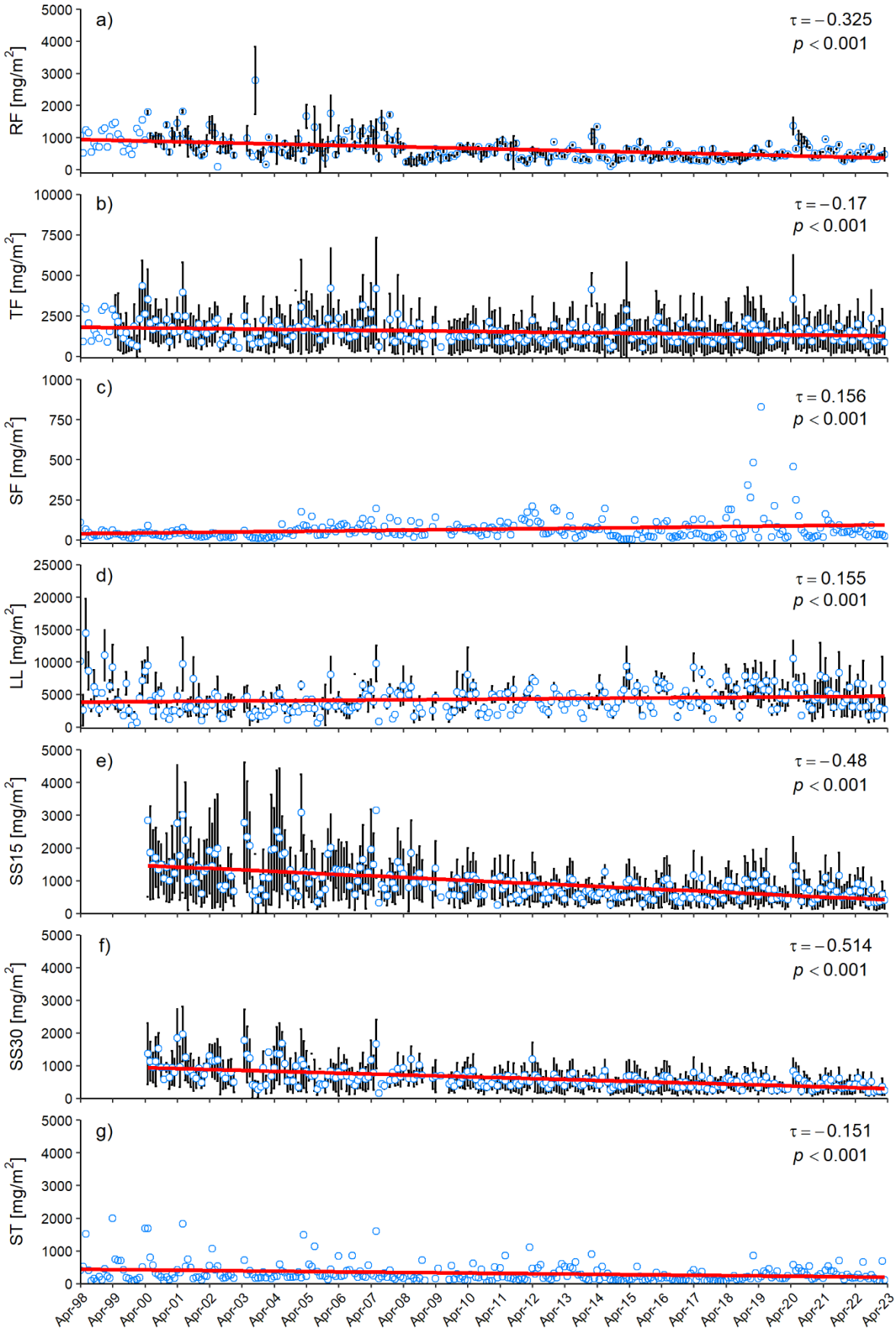

a)
τ = −0.325
p < 0.001
RF [mg/m²]
b)
τ = −0.17
p < 0.001
TF [mg/m²]
c)
τ = 0.156
p < 0.001
SF [mg/m²]
d)
τ = 0.155
p < 0.001
LL [mg/m²]
e)
τ = −0.48
p < 0.001
SS15 [mg/m²]
f)
τ = −0.514
p < 0.001
SS30 [mg/m²]
g)
τ = −0.151
p < 0.001
ST [mg/m²]
Apr-98
Apr-99
Apr-00
Apr-01
Apr-02
Apr-03
Apr-04
Apr-05
Apr-06
Apr-07
Apr-08
Apr-09
Apr-10
Apr-11
Apr-12
Apr-13
Apr-14
Apr-15
Apr-16
Apr-17
Apr-18
Apr-19
Apr-20
Apr-21
Apr-22
Apr-23

Figure D-S3. Course of mean monthly dissolved organic carbon (DOC) fluxes in ecosystem solutions from April 1998 to March 2023. RF is rainfall, TF throughfall, SF stemflow, LL litter leachate, SS15 and SS30 mineral soil solutions at the 0.15 and 0.30 m depths, respectively, and ST streamflow. Error bars represent the standard deviations from two to four gauging stations for RF and from three study transects for TF, LL, SS15, and SS30, whereas there was only one measurement station for each of SF and ST. The regression lines are shown only to illustrate significant trends. Please note the different y-axis scaling for SF, ST and LL. Temporal trends in monthly data were statistically evaluated with the Seasonal Mann-Kendall test (Hirsch et al., 1982). Regression lines are shown when there was a significant temporal trend for illustration purposes.

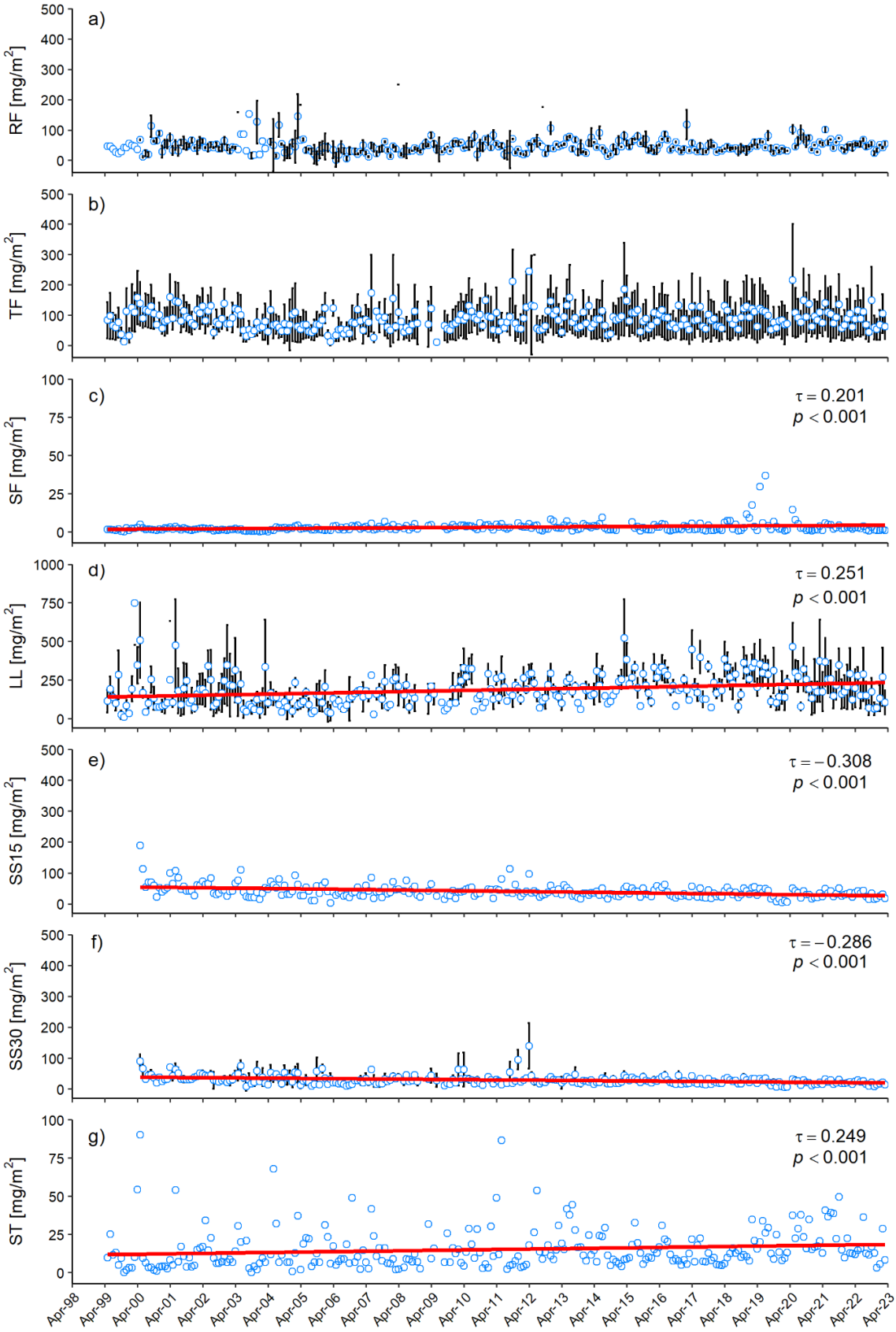

a)
RF [mg/m²]
b)
TF [mg/m²]
c)
SF [mg/m²]
τ = 0.201
p < 0.001
d)
LL [mg/m²]
τ = 0.251
p < 0.001
e)
SS15 [mg/m²]
τ = −0.308
p < 0.001
f)
SS30 [mg/m²]
τ = −0.286
p < 0.001
g)
ST [mg/m²]
τ = 0.249
p < 0.001
Apr-98
Apr-99
Apr-00
Apr-01
Apr-02
Apr-03
Apr-04
Apr-05
Apr-06
Apr-07
Apr-08
Apr-09
Apr-10
Apr-11
Apr-12
Apr-13
Apr-14
Apr-15
Apr-16
Apr-17
Apr-18
Apr-19
Apr-20
Apr-21
Apr-22
Apr-23

Figure D-S4. Course of mean monthly dissolved organic nitrogen (DON) fluxes in ecosystem solutions from April 1999 to March 2023. RF is rainfall, TF throughfall, SF stemflow, LL litter leachate, SS15 and SS30 mineral soil solutions at the 0.15 and 0.30 m depths, respectively, and ST streamflow. Error bars represent the standard deviations from two to four gauging stations for RF and from three study transects for TF, LL, SS15, and SS30, whereas there was only one measurement station for each of SF and ST. The regression lines are shown only to illustrate significant trends. Temporal trends in monthly data were statistically evaluated with the Seasonal Mann-Kendall test (Hirsch et al., 1982). Regression lines are shown when there was a significant temporal trend for illustration purposes. Please note the different y-axis scaling for SF, LL and ST.

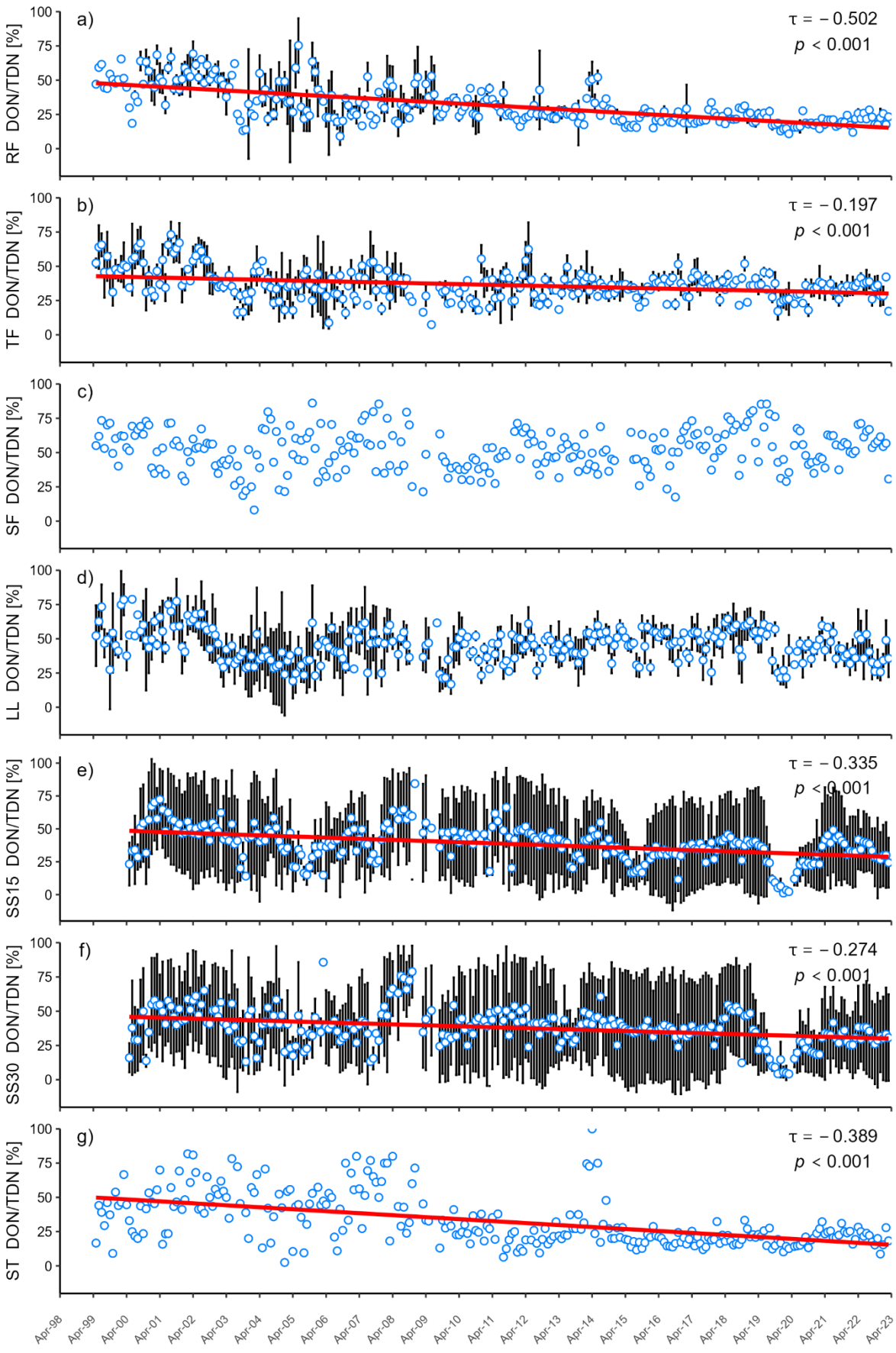

a)
τ = – 0.502
p < 0.001
RF DON/TDN [%]
b)
τ = – 0.197
p < 0.001
TF DON/TDN [%]
c)
SF DON/TDN [%]
d)
LL DON/TDN [%]
e)
τ = – 0.335
p < 0.001
SS15 DON/TDN [%]
f)
τ = – 0.274
p < 0.001
SS30 DON/TDN [%]
g)
τ = – 0.389
p < 0.001
ST DON/TDN [%]
0
25
50
75
100
Apr-98
Apr-99
Apr-00
Apr-01
Apr-02
Apr-03
Apr-04
Apr-05
Apr-06
Apr-07
Apr-08
Apr-09
Apr-10
Apr-11
Apr-12
Apr-13
Apr-14
Apr-15
Apr-16
Apr-17
Apr-18
Apr-19
Apr-20
Apr-21
Apr-22
Apr-23

Figure D-S5. Temporal course of dissolved organic nitrogen (DON) contributions to total dissolved nitrogen (TDN) in ecosystem solutions from April 1999 to March 2023. RF is rainfall, TF throughfall, SF stemflow, LL litter leachate, SS15 and SS30 mineral soil solutions at the 0.15 and 0.30 m depths, respectively, and ST streamflow. Error bars represent the standard deviations from two to four gauging stations for RF and from three study transects for TF, LL, SS15, and SS30, whereas there was only one measurement station for each of SF and ST. The regression lines are shown only to illustrate significant trends. Temporal trends in monthly data were statistically evaluated with the Seasonal Mann-Kendall test (Hirsch et al., 1982). Regression lines are shown when there was a significant temporal trend for illustration purposes. Mean monthly trends of the relative DON contributions to TDN from 1998 to 2013 (Wilcke et al. (2013) were extended and evaluated until March 2023.

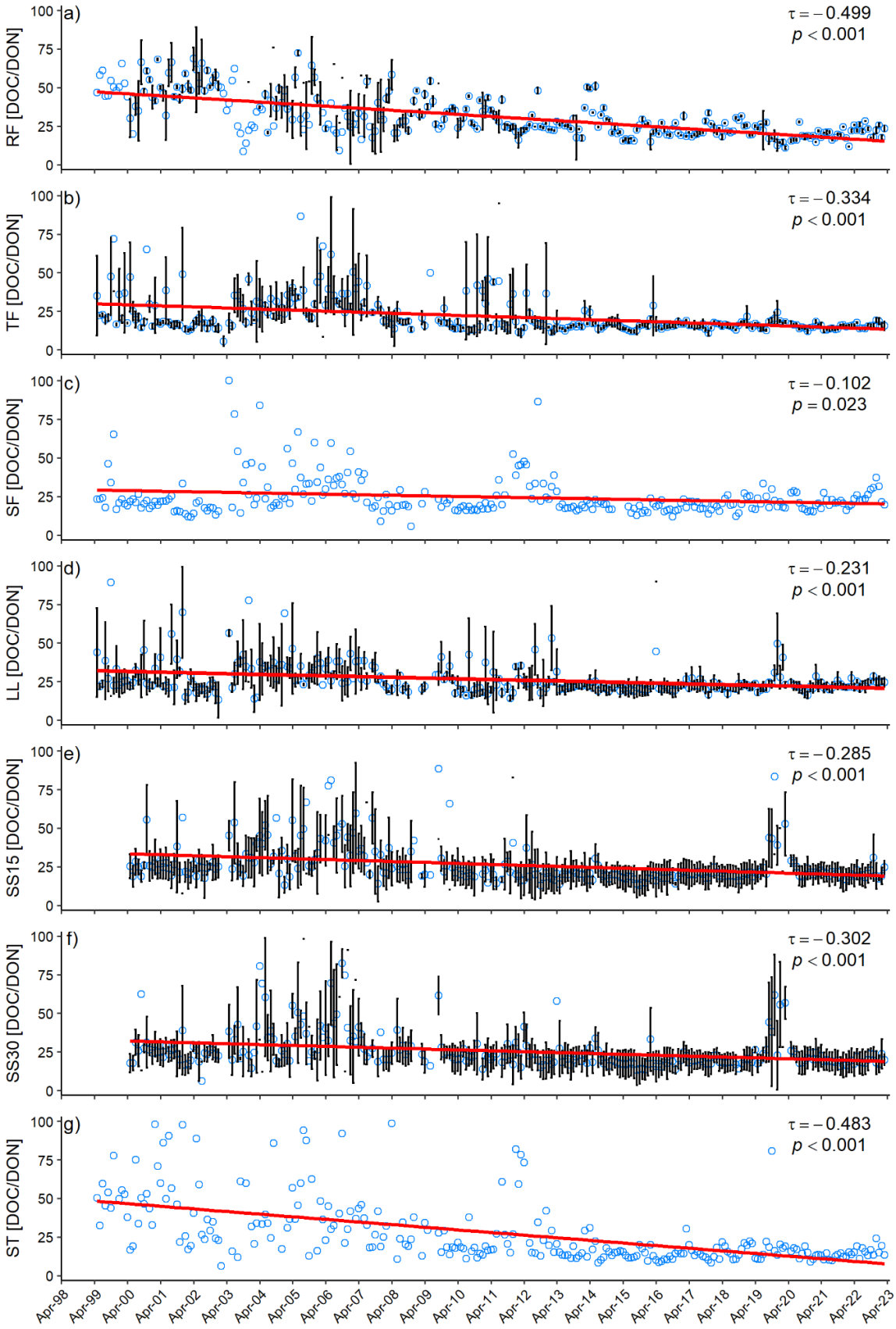

a)
τ = −0.499
p < 0.001
RF [DOC/DON]
b)
τ = −0.334
p < 0.001
TF [DOC/DON]
c)
τ = −0.102
p = 0.023
SF [DOC/DON]
d)
τ = −0.231
p < 0.001
LL [DOC/DON]
e)
τ = −0.285
p < 0.001
SS15 [DOC/DON]
f)
τ = −0.302
p < 0.001
SS30 [DOC/DON]
g)
τ = −0.483
p < 0.001
ST [DOC/DON]
0
25
50
75
100
Apr-98
Apr-99
Apr-00
Apr-01
Apr-02
Apr-03
Apr-04
Apr-05
Apr-06
Apr-07
Apr-08
Apr-09
Apr-10
Apr-11
Apr-12
Apr-13
Apr-14
Apr-15
Apr-16
Apr-17
Apr-18
Apr-19
Apr-20
Apr-21
Apr-22
Apr-23

Figure D-S6. Course of mean monthly dissolved organic carbon (DOC) to dissolved organic nitrogen (DON) ratios in ecosystem solutions from April 1999 to March 2023. RF is rainfall, TF throughfall, SF stemflow, LL litter leachate, SS15 and SS30 mineral soil solutions at the 0.15 and 0.30 m depths, respectively, and ST streamflow. Error bars represent the standard deviations from two to four gauging stations for RF and from three study transects for TF, LL, SS15, and SS30, whereas one weekly sample was collected for SF and ST. The regression lines are shown only to illustrate significant trends. Temporal trends in monthly data were statistically evaluated with the Seasonal Mann-Kendall test (Hirsch et al., 1982). Regression lines are shown when there was a significant temporal trend for illustration purposes. Please note the different y-axis scaling for SF, ST and LL.

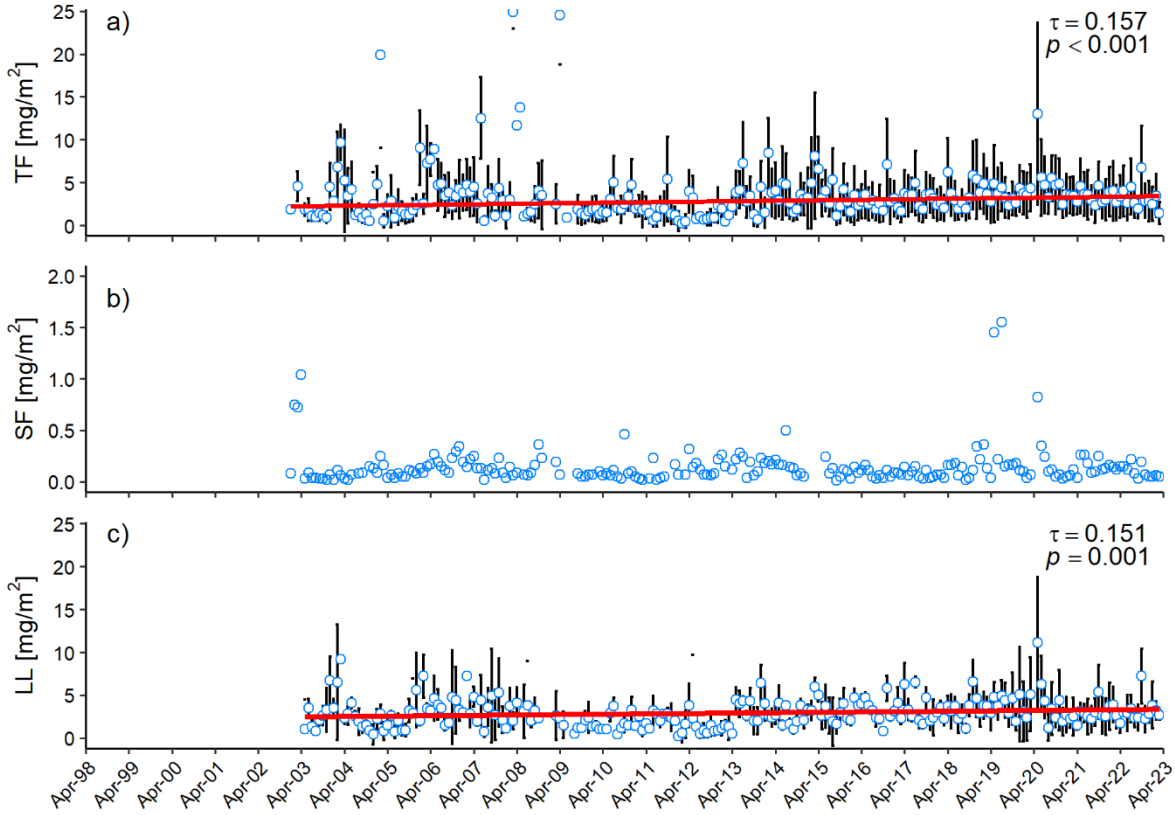


Figure D-S7. Course of the mean dissolved organic phosphorus (DOP) fluxes in ecosystem solutions from April 2003 to March 2023. TF throughfall, SF stemflow, and LL litter leachate. Error bars represent the standard deviations of three study transects for TF and LL. There was only one measurement station for SF. Temporal trends in monthly data were statistically evaluated with the Seasonal Mann-Kendall test (Hirsch et al., 1982). Regression

lines are shown when there was a significant temporal trend for illustration purposes. Please note the different y-axis scaling for SF.

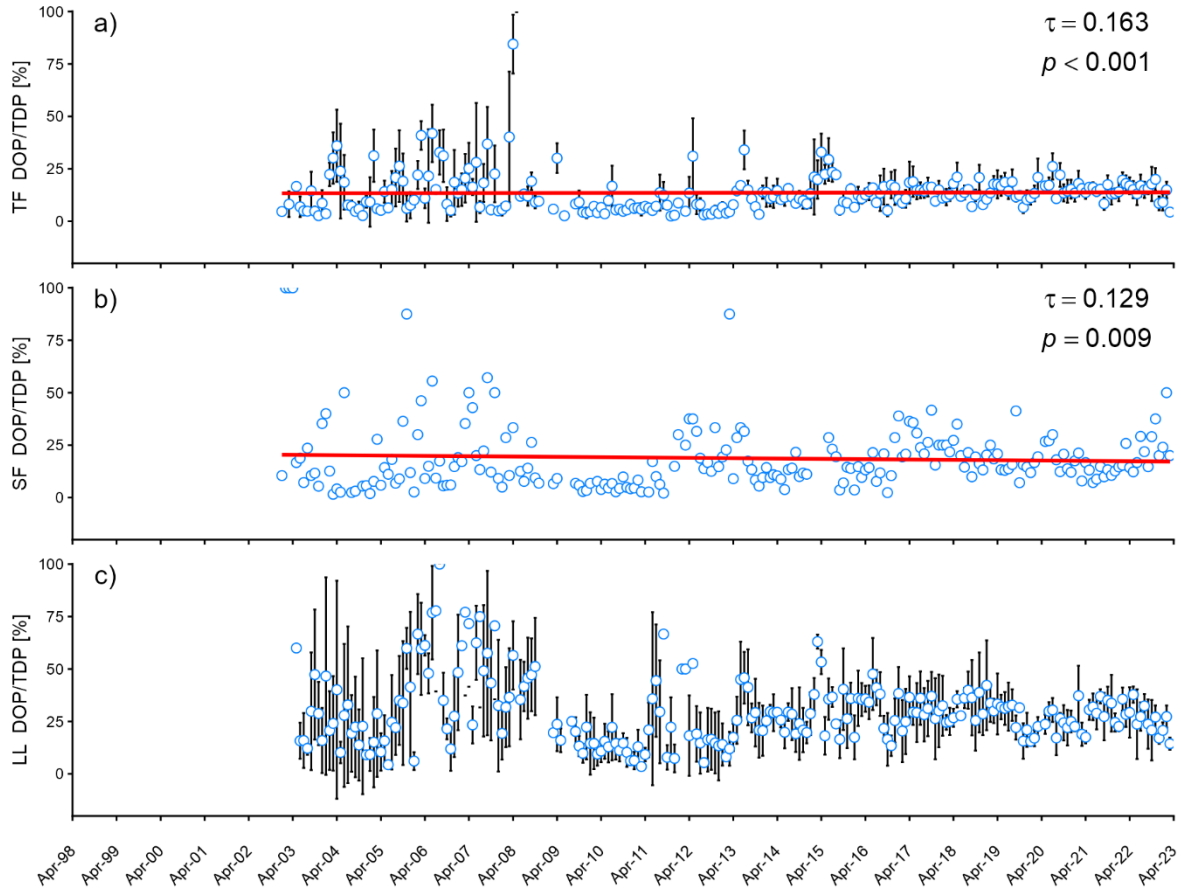


Figure D-S8. Temporal course of dissolved organic phosphorus (DOP) contribution to total dissolved phosphorus (TDP) in ecosystem solutions from April 2003 to March 2023. TF throughfall, SF stemflow and LL litter leachate. Error bars represent the standard deviations from three study transects for TF and LL, whereas there was only one measurement station for SF. Temporal trends in monthly data were statistically evaluated with the Seasonal Mann-Kendall test (Hirsch et al., 1982). Regression lines are shown when there was a significant temporal trend for illustration purposes.

9. References

Alvarez, P., Velescu, A., Pierick, K., Homeier, J., & Wilcke, W. (2023). Carbon stable isotope ratio of dissolved organic matter as a tool to identify its sources and transformations in a tropical montane forest in Ecuador. *Environmental science & technology*. https://doi.org/10.1021/acs.est.3c01623

Alvarez, P., Velescu, A., Pierick, K., Homeier, J., & Wilcke, W. (2024a). Concentrations of total organic carbon, dissolved organic nitrogen, TOC/DON ratios, ammonium-nitrogen, nitrate-nitrogen, ammonium-N/nitrate-N ratios, and δ15N values of solution samples from a tropical montane forest in south Ecuador. Retrieved from: https://doi.org/10.1594/PANGAEA.968797

Alvarez, P., Velescu, A., Pierick, K., Homeier, J., & Wilcke, W. (2024b). pH, total organic carbon concentrations, total nitrogen concentrations, TC/TN concentration ratios, and $\delta^{15}N$ values of solid phase samples from a tropical montane forest in south Ecuador. Retrieved from: https://doi.org/10.1594/PANGAEA.968791

Alvarez, P., Velescu, A., Pierick, K., Homeier, J., & Wilcke, W. (2024c). Sources and sinks of N in ecosystem solutions along the water path through a tropical montane forest in Ecuador assessed with $\delta^{15}N$ values of total dissolved nitrogen. *Journal of Geophysical Research: Biogeosciences, 129*(10), e2024JG008043. https://doi.org/10.1029/2024JG008043

Barkley, A. E., Prospero, J. M., Mahowald, N., Hamilton, D. S., Popendorf, K. J., Oehlert, A. M., et al. (2019). African biomass burning is a substantial source of phosphorus deposition to the Amazon, Tropical Atlantic Ocean, and Southern Ocean. *Proceedings of the National Academy of Sciences, 116*(33), 16216-16221. https://doi.org/10.1073/pnas.1906091116

Bauters, M., Drake, T. W., Wagner, S., Baumgartner, S., Makelele, I. A., Bodé, S., et al. (2021). Fire-derived phosphorus fertilization of African tropical forests. *Nature Communications, 12*, 5129. https://doi.org/10.1038/s41467-021-25428-3

Beck, E., Bendix, J., Kottke, I., Makeschin, F., & Mosandl, R. (2008). *Gradients in a tropical mountain ecosystem of Ecuador* (Vol. 198). Berlin, Heidelberg. Springer.p. https://doi.org/10.1007/978-3-540-73526-7

Bendix, J. (2020). ECSF climate station best estimate Ver. 3 1998-2020. Retrieved from: http://www.tropicalmountainforest.org/data_pre.do?citid=1876

Bendix, J., Dobbermann, M., & Werner, N. (2018). Climate station data from ECSF Thies station. Updated on 2026-05-22. Retrieved from: http://www.tropicalmountainforest.org/data_pre.do?citid=1713

Bol, R., Julich, D., Brödlin, D., Siemens, J., Kaiser, K., Dippold, M. A., et al. (2016). Dissolved and colloidal phosphorus fluxes in forest ecosystems—an almost blind spot in ecosystem research. *Journal of Plant Nutrition and Soil Science, 179*(4), 425-438. https://doi.org/10.1002/jpln.201600079

Boström, B., Comstedt, D., & Ekblad, A. (2007). Isotope fractionation and ^{13}C enrichment in soil profiles during the decomposition of soil organic matter. *Oecologia, 153*(1), 89-98. https://doi.org/10.1007/s00442-007-0700-8

Boy, J., Rollenbeck, R., Valarezo, C., & Wilcke, W. (2008a). Amazonian biomass burning-derived acid and nutrient deposition in the north Andean montane forest of Ecuador. *Global Biogeochemical Cycles, 22*, GB4011. https://doi.org/10.1029/2007GB003158

Boy, J., Valarezo, C., & Wilcke, W. (2008b). Water flow paths in soil control element exports in an Andean tropical montane forest. *European Journal of Soil Science, 59*(6), 1209-1227. https://doi.org/10.1111/j.1365-2389.2008.01063.x

Bruijnzeel, L. A., & Hamilton, L. S. (2000). *Decision time for cloud forests. IHP Humid Tropics Programme Series Vol. 13*. Paris, France. IHP-UNESCO, IUCN and WWF. 44 p.

Cleveland, C. C., & Liptzin, D. (2007). C:N:P stoichiometry in soil: is there a "Redfield ratio" for the microbial biomass? *Biogeochemistry, 85*(3), 235-252. https://doi.org/10.1007/s10533-007-9132-0

Dietrich, K., Spohn, M., Villamagua, M., & Oelmann, Y. (2017). Nutrient addition affects net and gross mineralization of phosphorus in the organic layer of a tropical montane forest. *Biogeochemistry, 136*(2), 223-236. https://doi.org/10.1007/s10533-017-0392-z

DVWK. (1996). *Ermittlung der Verdunstung von Land-und Wasserflächen*. Retrieved from Bonn, Germany:

Fetzer, J., Frossard, E., Kaiser, K., & Hagedorn, F. (2022). Leaching of inorganic and organic phosphorus and nitrogen in contrasting beech forest soils – seasonal patterns and effects of fertilization. *Biogeosciences, 19*(5), 1527-1546. https://doi.org/10.5194/bg-19-1527-2022

Fleischbein, K., Wilcke, W., Valarezo, C., Zech, W., & Knoblich, K. (2006). Water budgets of three small catchments under montane forest in Ecuador: experimental and modelling approach. *Hydrological processes, 20*(12), 2491-2507. https://doi.org/10.1002/hyp.6212

Gerschlauer, F., Saiz, G., Schellenberger Costa, D., Kleyer, M., Dannenmann, M., & Kiese, R. (2019). Stable carbon and nitrogen isotopic composition of leaves, litter, and soils of various ecosystems along an elevational and land-use gradient at Mount Kilimanjaro, Tanzania. *Biogeosciences, 16*(2), 409-424. https://doi.org/10.5194/bg-16-409-2019

Goller, R., Wilcke, W., Fleischbein, K., Valarezo, C., & Zech, W. (2006). Dissolved nitrogen, phosphorus, and sulfur forms in the ecosystem fluxes of a montane forest in Ecuador. *Biogeochemistry, 77*(1), 57-89. https://doi.org/10.1007/s10533-005-1061-1

Goller, R., Wilcke, W., Leng, M. J., Tobschall, H. J., Wagner, K., Valarezo, C., & Zech, W. (2005). Tracing water paths through small catchments under a tropical montane rain forest in south Ecuador by an oxygen isotope approach. *Journal of Hydrology, 308*(1), 67-80. https://doi.org/10.1016/j.jhydrol.2004.10.022

Hall, S. J., & Silver, W. L. (2013). Iron oxidation stimulates organic matter decomposition in humid tropical forest soils. *Global Change Biology, 19*(9), 2804-2813. https://doi.org/10.1111/gcb.12229

Hedin, L. O., Vitousek, P. M., & Matson, P. A. (2003). Nutrient losses over four million years of tropical forest development. *Ecology, 84*(9), 2231-2255. https://doi.org/10.1890/02-4066

Hirsch, R. M., Slack, J. R., & Smith, R. A. (1982). Techniques of trend analysis for monthly water quality data. *Water Resources Research, 18*(1), 107-121. https://doi.org/10.1029/WR018i001p00107

Homeier, J., Hertel, D., Camenzind, T., Cumbicus, N. L., Maraun, M., Martinson, G. O., et al. (2012). Tropical Andean forests are highly susceptible to nutrient inputs—rapid effects of experimental N and P addition to an Ecuadorian montane forest. *PLoS One, 7*(10), e47128. https://doi.org/10.1371/journal.pone.0047128

Hothorn, T., Bretz, F., & Westfall, P. (2008). Simultaneous Inference in General Parametric Models. John Wiley & Sons, Ltd. Retrieved from https://doi.org/10.1002/bimj.200810425

Inselsbacher, E., Cambui, C. A., Richter, A., Stange, C. F., Mercier, H., & Wanek, W. (2007). Microbial activities and foliar uptake of nitrogen in the epiphytic bromeliad Vriesea

gigantea. *New Phytologist, 175*(2), 311-320. https://doi.org/10.1111/j.1469-8137.2007.02098.x

IUSS Working Group WRB. (2022). *World Reference Base for Soil Resources. International soil classification system for naming soils and creating legends for soil maps* (4th ed.). Vienna, Austria. International Union of Soil Sciences (IUSS). 236 p.

Jiang, X., Wang, X., Qiao, Y., Cao, Y., Jiao, Y., Yang, A., et al. (2024). Atmospheric nitrogen deposition affects forest plant and soil system carbon:nitrogen:phosphorus stoichiometric flexibility: A meta-analysis. *Forest Ecosystems, 11*, 100192. https://doi.org/10.1016/j.fecs.2024.100192

Kalbitz, K., Solinger, S., Park, J.-H., Michalzik, B., & Matzner, E. (2000). Controls on the dynamics of dissolved organic matter in soils: a review. *Soil Science, 165*(4), 277-304. https://doi.org/10.1097/00010694-200004000-00001

Lang, F., Krüger, J., Amelung, W., Willbold, S., Frossard, E., Bünemann, E. K., et al. (2017). Soil phosphorus supply controls P nutrition strategies of beech forest ecosystems in Central Europe. *Biogeochemistry, 136*(1), 5-29. https://doi.org/10.1007/s10533-017-0375-0

Lange, D. F., Schröter, S. A., da Luz, F. M., Pires, E., Santos, Y. R., da Silva, J. S., et al. (2024). Cycling of dissolved organic nutrients and indications for nutrient limitations in contrasting Amazon rainforest ecosystems. *Biogeochemistry, 167*(12), 1567-1588. https://doi.org/10.1007/s10533-024-01187-3

Lenth, R. V., & Piaskowski, J. (2026). emmeans: Estimated marginal means, aka least-squares means [R package]. Comprehensive R Archive Network (CRAN). Retrieved from https://doi.org/10.32614/CRAN.package.emmeans

Leuschner, C., Zach, A., Moser, G., Homeier, J., Graefe, S., Hertel, D., et al. (2013). The carbon balance of tropical mountain forests along an altitudinal transect. In J. Bendix, E. Beck, A. Bräuning, F. Makeschin, R. Mosandl, S. Scheu, & W. Wilcke (Eds.), *Ecosystem Services, Biodiversity and Environmental Change in a Tropical Mountain Ecosystem of South Ecuador* (pp. 117-139). Berlin, Heidelberg: Springer Berlin Heidelberg. https://doi.org/10.1007/978-3-642-38137-9_10

Lorenz, M., Derrien, D., Zeller, B., Udelhoven, T., Werner, W., & Thiele-Bruhn, S. (2020). The linkage of ^{13}C and ^{15}N soil depth gradients with C:N and O:C stoichiometry reveals tree species effects on organic matter turnover in soil. *Biogeochemistry, 151*(2), 203-220. https://doi.org/10.1007/s10533-020-00721-3

Michalzik, B., Kalbitz, K., Park, J.-H., Solinger, S., & Matzner, E. (2001). Fluxes and concentrations of dissolved organic carbon and nitrogen – a synthesis for temperate forests. *Biogeochemistry, 52*(2), 173-205. https://doi.org/10.1023/A:1006441620810

Millard, S. P. (2013). *EnvStats: An R package for environmental statistics* (2nd ed.). Springer. https://doi.org/10.1007/978-1-4614-8456-1

Moser, G., Leuschner, C., Hertel, D., Graefe, S., Soethe, N., & Iost, S. (2011). Elevation effects on the carbon budget of tropical mountain forests (S Ecuador): the role of the belowground compartment. *Global Change Biology, 17*(6), 2211-2226. https://doi.org/10.1111/j.1365-2486.2010.02367.x

Neff, J. C., Hobbie, S. E., & Vitousek, P. M. (2000). Nutrient and mineralogical control on dissolved organic C, N and P fluxes and stoichiometry in Hawaiian soils. *Biogeochemistry, 51*(3), 283-302. https://doi.org/10.1023/A:1006414517212

Nel, J. A., Craine, J. M., & Cramer, M. D. (2018). Correspondence between $\delta^{13}C$ and $\delta^{15}N$ in soils suggests coordinated fractionation processes for soil C and N. *Plant and Soil, 423*(1), 257-271. https://doi.org/10.1007/s11104-017-3500-x

Niu, G., Yin, G., Mo, X., Mao, Q., Mo, J., Wang, J., & Lu, X. (2022). Do long-term high nitrogen inputs change the composition of soil dissolved organic matter in a primary tropical forest? *Environmental Research Letters, 17*(9), 095015. https://doi.org/10.1088/1748-9326/ac8e87

Ostertag, R., & DiManno, N. M. (2016). Detecting terrestrial nutrient limitation: A global meta-analysis of foliar nutrient concentrations after fertilization. *Frontiers in Earth Science, 4*, 23. https://doi.org/10.3389/feart.2016.00023

Qualls, R. G. (2000). Comparison of the behavior of soluble organic and inorganic nutrients in forest soils. *Forest Ecology and Management, 138*(1), 29-50. https://doi.org/10.1016/S0378-1127(00)00410-2

Qualls, R. G., Haines, B. L., & Swank, W. T. (1991). Fluxes of dissolved organic nutrients and humic substances in a deciduous forest. *Ecology, 72*(1), 254-266. https://doi.org/10.2307/1938919

Qualls, R. G., Haines, B. L., Swank, W. T., & Tyler, S. W. (2002). Retention of soluble organic nutrients by a forested ecosystem. *Biogeochemistry, 61*, 135-171. https://doi.org/10.1023/A:1020239112586

R Core Team. (2025). R: A language and environment for statistical computing. R Foundation for Statistical Computing. Vienna, Austria. Retrieved from https://www.r-project.org/

Raymond, P. A., & Saiers, J. E. (2010). Event controlled DOC export from forested watersheds. *Biogeochemistry, 100*(1), 197-209. https://doi.org/10.1007/s10533-010-9416-7

Runyan, C. W., D'Odorico, P., Vandecar, K. L., Das, R., Schmook, B., & Lawrence, D. (2013). Positive feedbacks between phosphorus deposition and forest canopy trapping, evidence from Southern Mexico. *Journal of Geophysical Research: Biogeosciences, 118*(4), 1521-1531. https://doi.org/10.1002/2013JG002384

Saunders, T. J., McClain, M. E., & Llerena, C. A. (2006). The biogeochemistry of dissolved nitrogen, phosphorus, and organic carbon along terrestrial-aquatic flowpaths of a montane headwater catchment in the Peruvian Amazon. *Hydrological processes, 20*(12), 2549-2562. https://doi.org/10.1002/hyp.6215

Schaap, K. J., Fuchslueger, L., Hoosbeek, M. R., Hofhansl, F., Martins, N. P., Valverde-Barrantes, O. J., Hartley, I. P., Lugli, L. F., & Quesada, C. A. (2021). Litter inputs and phosphatase activity affect the temporal variability of organic phosphorus in a tropical forest soil in the Central Amazon. *Plant and Soil, 469*(1), 423-441. https://doi.org/10.1007/s11104-021-05146-x

Schrumpf, M., Guggenberger, G., Valarezo, C., & Zech, W. (2001). Tropical montane rain forest soils: development and nutrient status along altitudinal gradient in the South Ecuadorian Andes. *Erde, 132*(1), 43-59.

Schrumpf, M., Zech, W., Lehmann, J., & Lyaruu, H. V. C. (2006). TOC, TON, TOS and TOP in rainfall, throughfall, litter percolate and soil solution of a montane rainforest succession at Mt. Kilimanjaro, Tanzania. *Biogeochemistry, 78*(3), 361-387. https://doi.org/10.1007/s10533-005-4428-4

Schwarz, M. T., Oelmann, Y., & Wilcke, W. (2011). Stable N isotope composition of nitrate reflects N transformations during the passage of water through a montane rain forest in Ecuador. *Biogeochemistry, 102*(1), 195-208. https://doi.org/10.1007/s10533-010-9434-5

Silver, W. L., Lugo, A. E., & Keller, M. (1999). Soil oxygen availability and biogeochemistry along rainfall and topographic gradients in upland wet tropical forest soils. *Biogeochemistry, 44*(3), 301-328. https://doi.org/10.1023/A:1006034126698

Soethe, N., Lehmann, J., & Engels, C. (2006). The vertical pattern of rooting and nutrient uptake at different altitudes of a south Ecuadorian montane forest. *Plant and Soil, 286*(1), 287-299. https://doi.org/10.1007/s11104-006-9044-0

Soldatova, E., Krasilnikov, S., & Kuzyakov, Y. (2024). Soil organic matter turnover: Global implications from $\delta^{13}C$ and $\delta^{15}N$ signatures. *Science of The Total Environment, 912*, 169423. https://doi.org/10.1016/j.scitotenv.2023.169423

Song, L., Lu, H.-Z., Xu, X.-L., Li, S., Shi, X.-M., Chen, X., et al. (2016). Organic nitrogen uptake is a significant contributor to nitrogen economy of subtropical epiphytic bryophytes. *Scientific Reports, 6*, 30408. https://doi.org/10.1038/srep30408

Umana, N. H. N., & Wanek, W. (2010). Large canopy exchange fluxes of inorganic and organic nitrogen and preferential retention of nitrogen by epiphytes in a tropical lowland rainforest. *Ecosystems, 13*(3), 367-381. https://doi.org/10.1007/s10021-010-9324-7

Van Langenhove, L., Verryckt, L. T., Bréchet, L., Courtois, E. A., Stahl, C., Hofhansl, F., et al. (2020). Atmospheric deposition of elements and its relevance for nutrient budgets of tropical forests. *Biogeochemistry, 149*(2), 175-193. https://doi.org/10.1007/s10533-020-00673-8

Van Stan, J. T., II, & Pypker, T. G. (2015). A review and evaluation of forest canopy epiphyte roles in the partitioning and chemical alteration of precipitation. *Science of The Total Environment, 536*, 813-824. https://doi.org/10.1016/j.scitotenv.2015.07.134

Van Stan, J. T., II, & Stubbins, A. (2018). Tree-DOM: Dissolved organic matter in throughfall and stemflow. *Limnology and Oceanography Letters, 3*(3), 199-214. https://doi.org/10.1002/lol2.10059

Velescu, A., Homeier, J., Espinosa, C. I., & Wilcke, W. (2026). Response of element cycling and budgets to nutrient additions in a tropical montane forest of Ecuador. *Geoderma, 466*, 117698. https://doi.org/10.1016/j.geoderma.2026.117698

Velescu, A., Valarezo, C., & Wilcke, W. (2016). Response of Dissolved Carbon and Nitrogen Concentrations to Moderate Nutrient Additions in a Tropical Montane Forest of South Ecuador. *Frontiers in Earth Science, 4*(58). https://doi.org/10.3389/feart.2016.00058

Wang, R., Goll, D., Balkanski, Y., Hauglustaine, D., Boucher, O., Ciais, P., et al. (2017). Global forest carbon uptake due to nitrogen and phosphorus deposition from 1850 to 2100. *Global Change Biology, 23*(11), 4854-4872. https://doi.org/10.1111/gcb.13766

Werner, F. A., Homeier, J., Oesker, M., & Boy, J. (2012). Epiphytic biomass of a tropical montane forest varies with topography. *Journal of Tropical Ecology, 28*(1), 23-31. https://doi.org/10.1017/S0266467411000526

Wilcke, W., Leimer, S., Peters, T., Emck, P., Rollenbeck, R., Trachte, K., Valarezo, C., & Bendix, J. (2013). The nitrogen cycle of tropical montane forest in Ecuador turns inorganic under environmental change. *Global Biogeochemical Cycles, 27*(4), 1194-1204. https://doi.org/10.1002/2012GB004471

Wilcke, W., Velescu, A., Leimer, S., Bigalke, M., Boy, J., & Valarezo, C. (2017). Biological versus geochemical control and environmental change drivers of the base metal budgets of a tropical montane forest in Ecuador during 15 years. *Biogeochemistry, 136*(2), 167-189. https://doi.org/10.1007/s10533-017-0386-x

Wilcke, W., Velescu, A., Leimer, S., Bigalke, M., Boy, J., & Valarezo, C. (2019). Temporal trends of phosphorus cycling in a tropical montane forest in Ecuador during 14 years. *Journal of Geophysical Research: Biogeosciences, 124*(5), 1370-1386. https://doi.org/10.1029/2018JG004942

Wilcke, W., Velescu, A., Leimer, S., Blotevogel, S., Alvarez, P., & Valarezo, C. (2020). Total organic carbon concentrations in ecosystem solutions of a remote tropical montane forest respond to global environmental change. *Global Change Biology, 26*(12), 6989-7005. https://doi.org/10.1111/gcb.15351

Wilcke, W., Yasin, S., Abramowski, U., Valarezo, C., & Zech, W. (2002). Nutrient storage and turnover in organic layers under tropical montane rain forest in Ecuador. *European Journal of Soil Science, 53*(1), 15-27. https://doi.org/10.1046/j.1365-2389.2002.00411.x

Yu, H., Chin, M., Yuan, T., Bian, H., Remer, L. A., Prospero, J. M., et al. (2015). The fertilizing role of African dust in the Amazon rainforest: A first multiyear assessment based on data from Cloud-Aerosol Lidar and Infrared Pathfinder Satellite Observations. *Geophysical Research Letters, 42*(6), 1984-1991. https://doi.org/10.1002/2015GL063040

Zhou, K., Lu, X., Mori, T., Mao, Q., Wang, C., Zheng, M., Mo, H., Hou, E., & Mo, J. (2018). Effects of long-term nitrogen deposition on phosphorus leaching dynamics in a mature tropical forest. *Biogeochemistry, 138*(2), 215-224. https://doi.org/10.1007/s10533-018-0442-1

E. Appendix

The appendix is attached on an USB stick containing the following files:

Tables_1 and_2_DOM properties_paper1.xlsx: Underlying data of Tables B-1 and B-S1 of Section B, in separate sheets. Table B-1 contains the means, standard deviations, and interquartile ranges of the pH, the electrical conductivity, and the concentrations of TOC, dissolved organic N (DON), total N (TN), ammonium, and nitrate, together with the TOC/DON and TOC/TN ratios, in the ecosystem solutions, that is, rainfall, throughfall, stemflow, litter leachate, mineral soil solutions at the 0.15 and 0.30 m depths, and streamflow. Table B-S1 contains the solid-phase properties of the organic layer horizons and the mineral soil, that is, the horizon thickness, the pH, the organic C and total N concentrations, and the C/N ratio, along with additional soil properties such as the exchangeable Al and the oxalate-extractable Fe concentrations, and the effective and potential cation exchange capacities. Concentrations are given in mg L^{-1} for the solutions, in g kg^{-1} for the solid phase, the electrical conductivity is in µS cm^{-1}, and the thickness in m (**Section B**).

C_N_d13C_d15N_soil_profiles_MC2_paper1.xlsx: Solid-phase data of the soil profiles from Microcatchment 2 (MC2) used in Section B. For each sample, identified by profile and horizon, the file contains the sample type, that is, the organic layer horizons and the mineral soil horizons, the $\delta^{13}C$ and $\delta^{15}N$ values, the organic C and total N concentrations, and the C/N ratio. The $\delta^{13}C$ and $\delta^{15}N$ values are given in ‰, and the C and N concentrations in g kg^{-1} (**Section B**).

d13C_leaves_and_roots_paper1.xlsx: $\delta^{13}C$ values of the leaves and the roots of the sampled tree species of Section B. For each species, the file contains the mean $\delta^{13}C$ value and its standard deviation, separately for leaves and roots. The $\delta^{13}C$ values are given in ‰ (**Section B**).

d13Cvalues_replicates_temporal_course_paper1.xlsx: Temporal course of the $\delta^{13}C$ values of DOM in the ecosystem solutions along the water path (Section B). The file contains the monthly $\delta^{13}C$ values according to the experimental design. The $\delta^{13}C$ values are given in ‰ (**Section B**).

Data_figures_d15N-TDN_paper2.xlsx: data of Table C-1 and figures of Section C, organized in separate sheets. It contains the monthly TC/TN ratios of the solid phase (leaves,

roots, and soil horizons) and TOC/DON, and nitrate/ammonium ratios of the ecosystem solutions, that is, rainfall, throughfall, stemflow, litter leachate, mineral soil solutions at the 0.15 and 0.30 m depths, and streamflow, from 2013 to 2016 (Table C-1); the mean concentrations of dissolved organic N (DON), ammonium, nitrate, and total dissolved N (TDN) and the contribution of each N form to TDN in these solutions (Figures C-1 and C-S4); the DON and total N concentrations and fluxes used for the canopy budget (Figure C-2); the quarterly $\delta^{15}N$ values of TDN in the ecosystem solutions over time (Figure C-3); the $\delta^{15}N$ values of the potential N sources, that is, leaves, bark, and organic layer horizons, and of DOM in the solutions (Figure C-4); the $\delta^{15}N$ values and the C and N concentrations of the leaves and roots of the dominant tree species (Figure C-S2); the $\delta^{15}N$ values of the leaves of *Graffenrieda emarginata* and *Myrcia myrtiformis* over the years (Figure C-S3); and the monthly precipitation from 1998 onward (Figure C-S5). Concentrations are given in mg L^{-1}, fluxes in mg m^{-2} $month^{-1}$, and the stable isotope ratios as $\delta^{13}C$ and $\delta^{15}N$ values in ‰ (**Section C**).

Two datasets of section C have been published:

Alvarez, P., Velescu, A., Pierick, K., Homeier, J., & Wilcke, W. (2024). pH, total organic carbon concentrations, total nitrogen concentrations, TC/TN concentration ratios, and $\delta^{15}N$ values of solid phase samples from a tropical montane forest in south Ecuador. Retrieved from: https://doi.org/10.1594/PANGAEA.968791

Alvarez, P., Velescu, A., Pierick, K., Homeier, J., & Wilcke, W. (2024). Concentrations of total organic carbon, dissolved organic nitrogen, TOC/DON ratios, ammonium-nitrogen, nitrate-nitrogen, ammonium-N/nitrate-N ratios, and $\delta^{15}N$ values of solution samples from a tropical montane forest in south Ecuador. Retrieved from: https://doi.org/10.1594/PANGAEA.968797

DOM_composition_temporal_course_1998-2023_paper3.xlsx: Temporal course of the DOM composition in the ecosystem solutions along the water path through the forest, from rainfall to streamflow, from April 1998 to March 2023. The file contains the TOC, DON, and DOP concentrations and fluxes and the DOC/DON, DOC/DOP, and DON/DOP concentration ratios, as well as the contributions of DON to the total dissolved N (TDN) and of DOP to the total dissolved P (TDP) over time. Concentrations are given in mg L^{-1} and fluxes in mg m^{-2} $month^{-1}$ (**Section D**).

One dataset of section D has been published:

Alvarez, P., Velescu, A., & Wilcke, W. (2026). Monthly concentrations, fluxes, and stoichiometric ratios of dissolved organic carbon, nitrogen, and phosphorus in ecosystem solutions of a tropical montane forest in south Ecuador from 1998 to 2023 [dataset]. PANGAEA. Retrieved from: https://doi.org/10.1594/PANGAEA.998037